Genetic strategies to manipulate meiotic recombination in *Arabidopsis thaliana*

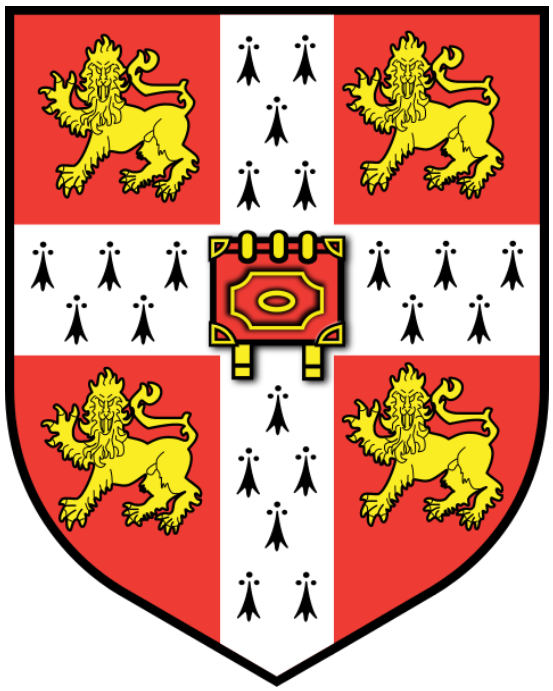

A dissertation submitted to the University of Cambridge for the degree of Doctor of Philosophy

by

Patrick L Diaz

of

Gonville and Caius College

in

May 2017

Preface

This dissertation is the result of my own work and includes nothing which is the outcome of work done in collaboration except as declared in the Preface and specified in the text. It is not substantially the same as any that I have submitted, or, is being concurrently submitted for a degree or diploma or other qualification at the University of Cambridge or any other University or similar institution except as declared in the Preface and specified in the text. I further state that no substantial part of my dissertation has already been submitted, or, is being concurrently submitted for any such degree, diploma or other qualification at the University of Cambridge or any other University or similar institution except as declared in the Preface and specified in the text.

Dedicated to my father, Bernard Maitland Diaz, who taught me many things.

Serius est quam cogitas.

"It's later than you think" – Common sundial inscription
(and personal realisation during the drafting of this thesis).

Acknowledgements

I owe a great debt to the following people, without whom this work would not have been created:

Dr Ian Henderson; a truly great supervisor, scientist and friend. I always left my meetings with Ian feeling a little more assured and enlightened than when I entered.

Dr Natasha Elina (Nataliya Yelina); who dedicated a a great deal of time to training me in various scientific techniques as well as helping me to refine the focus of my work through many helpful discussions.

Dr Charlie Underwood; a friend who always had time for me.

Catherine Griffin; a friend whose work ethic was an inspiration.

Alex Blackwell; who was always good for an interesting chat.

Alex Canto-Pastor; who, I think, shared my sense of humour.

Dr Natasha Latysheva; a friend who helped me through a difficult time and with whom I shared many good times.

Angela (Bo) Wan; who sees something in me that I do not see myself.

Caroline, Diz, Izzi and John; who I will love forever.

I would also like to thank Rijk Zwaan for sponsoring my PhD studentship.

Table of Contents

Table of figures

Abstract

Genetic strategies to manipulate meiotic recombination in *Arabidopsis thaliana*

by

Patrick L Diaz

During meiosis eukaryotes produce four haploid gametes from a single diploid parental cell. In meiotic S-phase homologous chromosomes, which were inherited from maternal and paternal parents, are replicated. Homologous chromosomes then pair and undergo reciprocal crossover, which generates new mosaics of maternal and paternal sequences. Meiosis also involves two rounds of chromosome segregation, meaning that only one copy of each chromosome is finally packaged into the resulting haploid gametes. In this work I sought to genetically engineer two elements of meiosis, in order to generate tools which may be useful for plant breeding. The first project sought to generate a second division restitution (SDR) population, where the second meiotic division is skipped. This is created by crossing an SDR mutant, *omission of second division1*, which produces diploid pollen due to a defective meiosis-II, to a haploid inducer line, whose chromosomes are lost from the zygote post-fertilisation. This was intended to give rise to diploid plants possessing chromosomes from just the SDR parent. Importantly, the SDR parent used was heterozygous, meaning that SDR progeny should show mostly homozygous chromosomes, but with regions of residual heterozygosity, determined by crossover locations. This project succeeded in creating a small number of plants with the predicted SDR genotype, although a range of aberrant genotypes were also observed. I present several hypotheses that could account for the observed progeny genotypes. In a second project I attempted to direct meiotic recombination using DNA double strand breaks targeted to specific sites. This project used a *spo11-1* mutant, which is unable to produce the endogenous meiotic DNA DSBs that normally mature into crossovers. Instead, TAL-*FokI* nucleases (TALENs) were expressed from meiotic promoters in order to generate exogenous DSBs at sites determined by the DNA binding specificity of the TAL repeat domains. The project succeeded in transforming TALENs into *spo11-1* mutants and confirming their expression. However, this was not sufficient to recover the *spo11-1* mutant infertility or direct crossovers. Potential reasons for this non-complementation are discussed, as well as their implications for control of meiotic recombination in plant genomes.

1 Chapter 1: Introduction

1.1 Overview of meiosis

Meiosis is a central feature of the life-cycle of sexually-reproducing eukaryotic organisms. During meiosis the diploid complement of two homologs of each chromosome are first replicated, generating a total of four chromatids. Chromatids are identical to one another, unless mutations occur, and are termed sister chromatids. As opposed to mitosis, during meiosis the four chromatids undergo two rounds of chromosome segregation. The first of these divisions is termed meiosis-I and serves to separate homologous chromosomes from one another. The two daughter cells (or in plants, the two daughter nuclei in one cell) thus created then undergo a second division termed meiosis-II. During meiosis-II sister chromatid cohesion is lost and each sister segregates to an opposite pole of the cell. Thus the outcome of a single meiosis is the production of four haploid sister-gametes. Haploid gametes produced by meiosis may then go on to combine with one another during fertilisation, regenerating organisms with the diploid chromosome complement of the parent cell (Figure 1.1). The halving of ploidy during meiosis, therefore, ensures that a constant ploidy is maintained throughout generations (Weismann 1893). Importantly, during prophase of meiosis-I homologous chromosomes physically interact and recombine with one another. Recombination can involve the reciprocal exchange of some portion of a chromosome arm with the corresponding portion from a homologous chromosome. As the homologous chromosomes in a diploid organism originate from the maternal and paternal parents of the organism, this generates chromosomes which are mosaics of maternal and paternal sequence. These recombined chromosomes undergo random segregation in meiosis-I and meiosis-II meaning the resulting gametes have the potential to possess chromosomes with novel allele combinations not present in the parental cell. The ability to generate chromosomes with alleles originating from two separate individuals confers a large benefit to sexually reproducing organisms, as it allows organisms to spread beneficial alleles through a population in less generations than asexual organisms, where beneficial mutations arising in separate organisms may compete with one another (Muller 1932; Smith & Maynard-Smith 1978). Sexual reproduction may also allow more effective purging of deleterious mutations from populations (Kondrashov 1988; Keightley & Eyre-Walker 2000). In addition to its importance for patterns of natural genetic variation and genome evolution, recombination is also important in agriculture, as

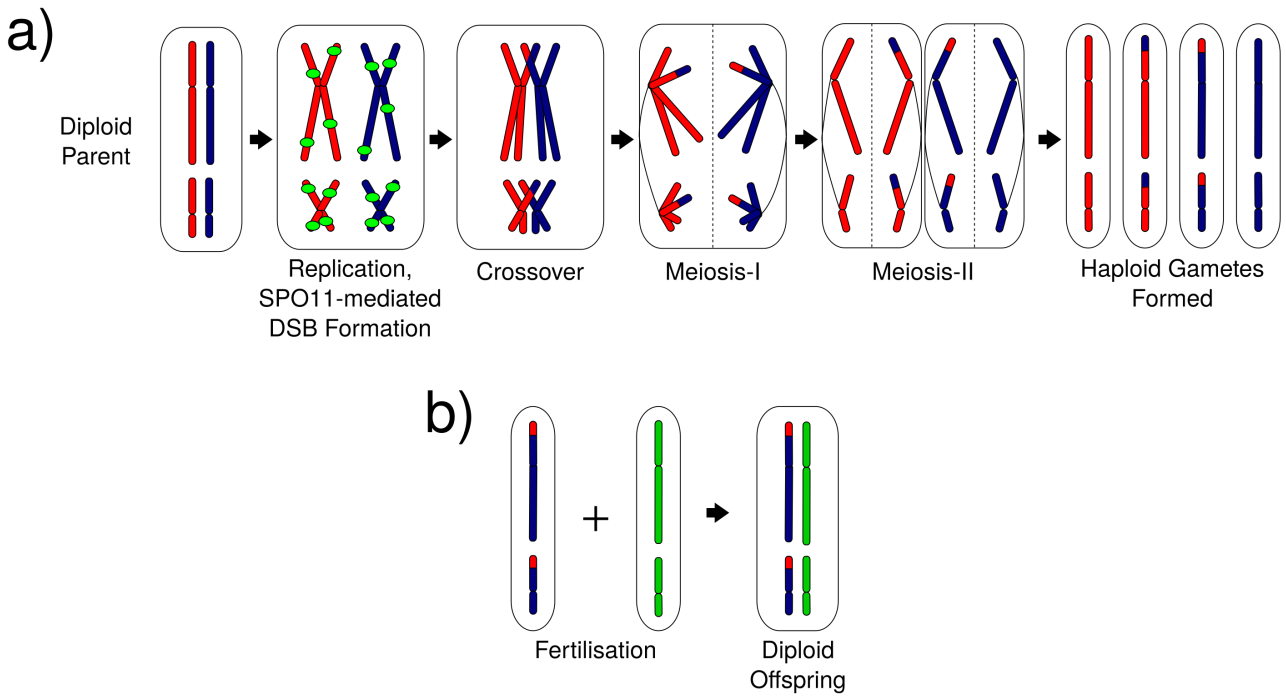

Figure 1.1: Meiosis and fertilisation*: Schematic of* ***a)*** *meiosis with homologous chromosomes (blue and red bars) replicating to form sister chromatids, being cut by SPO11 (green ovals) to form DNA double strand breaks (DSBs), undergoing crossover and both divisions of meiosis to form haploid gametes.* ***b)*** *Fertilisation, one gamete from a) containing a recombined chromosome fertilises another gamete to generate diploid offspring, thereby reconstituting the parental ploidy.*

it allows the combination of desirable traits in animal and plant crop species.

1.2 Stages of meiosis

Meiosis follows a typical progression of stages in most eukaryotes. As the work described here occurs in *Arabidopsis thaliana*, these stages will be described relative to this species. Meiosis proceeds via three main stages; first meiotic interphase, which is followed by two rounds of chromosome segregation called meiosis-I and meiosis-II. Meiosis-I and -II are further subdivided into four stages; prophase, metaphase, anaphase and telophase (Ross *et al.* 1996). These stages are suffixed with either -I or -II to indicate which stage of meiosis they belong to. A short interkinesis stage separates meiosis-I from meiosis-II (Wijnker & Schnittger 2013). One full round of meiosis from meiotic S-phase to tetrad formation takes approximately 33 hours (Armstrong *et al.* 2003). The prophase-I stage of meiosis is of particular interest, as it is in this stage that homologous chromosomes pair, synapse and undergo recombination, taking around 21.5 hours (Armstrong *et al.* 2003). For this reason, prophase-I is subdivided into 5 cytologically determined sub-stages; leptotene, zygotene, pachytene, diplotene and diakinesis, which are associated with different recombination events and chromosome morphologies (Ross *et al.* 1996; Armstrong *et al.* 2003).

1.2.1 Meiotic interphase

Meiotic interphase is comprised of three stages G1, S and G2 (Ross *et al.* 1996; Armstrong *et al.* 2003). Cells in these stages are larger than the somatic cells that surround them and also display larger nucleoli (Armstrong *et al.* 2003). Meiotic interphase cells of different stages display subtle differences in appearance. For example, G1 cells have more condensed pericentromeric heterochromatin, while G2 cells possess short stretches of chromatin threads, which may correspond to the formation of the meiotic chromosome axis, a structure which serves to hold sister chromatids and homologous chromosomes together during meiosis (Armstrong *et al.* 2003). S-phase begins when DNA initiates replication, ultimately producing chromosomes comprised of two sister chromatids. Sister chromatid cohesion is also established during this phase (Armstrong *et al.* 2003). G2 phase begins when DNA replication is complete and concludes when chromosomes condense into thin threads, marking entry into leptotene (Ross *et al.* 1996). It is

estimated via BrdU pulse-labelling of nuclear DNA that both S and G2 phase take around 5-9 hours to complete in *Arabidopsis* (Armstrong *et al.* 2003).

1.2.1.1 Meiosis-I

1.2.1.1.1 Prophase-I

Prophase-I is the longest stage of *Arabidopsis* meiosis taking around 21 hours to complete. Its long duration is believed to reflect the complex series of chromosome pairing and recombination events that occur (Ross *et al.* 1996; Armstrong *et al.* 2003).

1.2.1.1.1.1 Leptotene

In the earliest stages of leptotene (from leptonema *i.e.* thin threads) chromosomes, consisting of two sister chromatids, appear as thin, unsynapsed threads (Ross *et al.* 1996). Leptotene is characterised by the gradual extension of the chromosome axes, which will ultimately occupy the entire length of the chromosomes (Sanchez-moran *et al.* 2007). During this stage the telomeres of chromosomes gradually associate with the nucleolus, which moves from the centre of the cell to associate with the nuclear periphery, giving rise to a ‘chromosome bouquet’ (Ross *et al.* 1996; Armstrong *et al.* 2001; Armstrong *et al.* 2003).

1.2.1.1.1.2 Zygotene

Zygotene (from zygonema, paired threads) begins with chromosomes concentrated at one end of the nucleus. Formation of the synaptonemal complex (SC) begins, which holds homologous chromosomes in close proximity to one another (Higgins *et al.* 2005). Telomeres also lose their nucleolar association at this stage (Armstrong *et al.* 2001; Armstrong *et al.* 2003).

1.2.1.1.1.3 Pachytene

Pachytene (from pachynema, thick threads) is characterised by the continued full assembly of SC culminating in condensed, fully synapsed homologous chromosomes (Higgins *et al.* 2005). The structure of four chromatids, organised as two paired homologous chromosomes, held together by

SC is known as a bivalent (Ross *et al.* 1996). It is during pachytene that non-sister chromatids of homologous chromosomes mature as crossover recombination events and exchange portions of their chromosome arms with one another (Ross *et al.* 1996; Hunter & Kleckner 2001; Armstrong *et al.* 2003).

1.2.1.1.1.4 Diplotene

During diplotene (from diplonema, two threads) the SC degrades, ending the close association of homologous chromosomes (Ross *et al.* 1996). At the same time the chromosomes of the bivalent condense (Ross *et al.* 1996; Armstrong *et al.* 2003). At this stage the bivalent has the appearance of two threads held together at discrete points. These points are the sites where crossover has taken place between homologous chromosomes and are termed ‘chiasma’ (Ross *et al.* 1996). Chiasma are the physical manifestation of crossovers which link together homologous chromosomes and ensure correct segregation during anaphase-I (Lacefield & Murray 2007).

1.2.1.1.1.5 Diakinesis

During diakinesis (i.e. ‘moving through’) chromosomes condense further, nucleoli disappear (Ross *et al.* 1996), the nuclear membrane dissipates and spindle fibres assemble ready to segregate homologous chromosomes to opposite poles of the cell (Niu *et al.* 2015).

1.2.1.1.2 Metaphase-I

At metaphase-I the chromosomes are maximally condensed and are co-oriented on the spindle with homologous centromeres facing opposite poles of the cell, in anticipation of segregation. Bivalents with chiasmata in both arms are discernible as ‘ring’ bivalents while those with chiasmata in one arm form ‘rod’ bivalents (Darlington 1937; Ross *et al.* 1996).

1.2.1.1.3 Anaphase-I

During anaphase-I sister chromatids organised in chromosomes lose arm cohesion with their homologous partners and are drawn to opposite poles of the cell. Centromeric cohesin remains

and ensures sister chromatid cohesion (Ross *et al.* 1996; Armstrong *et al.* 2003).

1.2.1.1.4 Telophase-I

At telophase-I two groups of chromosomes are clustered at opposite poles of the cell and begin to slightly decondense. This is known as the 'dyad' stage. It is important to note that partitioning of the cytoplasm (cytokinesis) does not occur at this stage but upon the completion of the second division (Ross *et al.* 1996; Armstrong *et al.* 2003).

1.2.1.2 Interkinesis

Interkinesis is the short period between the first and second division of meiosis. Unlike meiotic interphase no DNA replication takes place during this stage (Riehs *et al.* 2008).

1.2.1.3 Meiosis-II

During meiosis-II the sister chromatids segregate. During prophase-II chromosomes condense, reaching their maximum condensation at metaphase-II. At this point chromosomes are aligned on the metaphase-II spindle. During anaphase-II sister chromatid cohesion at centromeres is finally lost and individual chromatids move to opposite poles of the cell. At telophase-II four groups of five chromatids are spread throughout a common cytoplasm. Finally cytokinesis occurs and the cytoplasm becomes partitioned, producing a tetrad of four haploid gametes (Ross *et al.* 1996; Armstrong *et al.* 2003).

1.3 Chromosome cohesion during meiosis

A critical element to the events that take place during meiosis is chromosome cohesion which is mediated by the protein complex cohesin. Cohesin is a complex of four proteins (Haering *et al.* 2008) in *Saccharomyces cerevisiae*, the mitotic cohesin contains two members of the structural maintenance of chromosomes (SMC) family; SMC1 and SMC3 and two members of the sister chromatid cohesion family; the α-kleisin RAD21/SCC1 and SCC3 (Stoop-Myer & Amon 1999; Watanabe & Nurse 1999). SMC1 and SMC3 form a V-shape complex consisting of a globular

'head' domain, corresponding to the vertex of the V connected to two globular 'hinge' domains by two anti-parallel coiled-coils, corresponding to the arms of the V. Both the N- and C-terminals of SMC1 and SMC3 reside in the hinge domains (Gruber *et al.* 2003). The 'embrace' model of cohesin function posits that chromatids are held together inside a loop formed when the V-shape consisting of SMC1 and SMC3 is closed by the α-kleisin subunit RAD21/SCC1 binding to the C-terminal domain of SMC1 and the N-terminal domain of SMC3 (Figure 1.2). This structure is stabilised by the recruitment of SCC3 to RAD21/SCC1 (Gruber *et al.* 2003). The meiotic cohesin complex is broadly similar, but with Rec8 replacing RAD21/SCC1 (Stoop-Myer & Amon 1999; Watanabe & Nurse 1999). In *Arabidopsis* the homologue of Rec8 is named SYN1/REC8 and is required for sister chromatid cohesion during meiosis (Bhatt *et al.* 1999; Chelysheva *et al.* 2005).

Sister chromatids are held together by cohesin during meiosis from replication until anaphase-II (Haering *et al.* 2008). This cohesion ensures correct attachment of chromosomes to the meiotic spindle and accurate segregation of chromosomes into daughter cells. Initially cohesion is established along the entire length of the chromatids and is then removed in a stepwise manner (Figure 1.2). At anaphase-I cohesion at chromosome arms is released while cohesion at centromeres is maintained, this allows homologous chromosomes (which may have undergone recombination) to separate, except at sites of crossover, which form chiasmata at this stage (Cooper & Strich 2011). At anaphase-II centromeric cohesion is released allowing sister chromatids to segregate into separate daughter cells (Cooper & Strich 2011). The progressive release of cohesion through meiosis is controlled by cyclin-CDK complexes, the APC/C and the spindle assembly checkpoint (discussed below).

In *Arabidopsis* SMC1 and SMC3 homologs are both present in single copies. Mutation of either gene causes seedling lethality, making attempts at genetic characterisation difficult (Liu *et al.* 2002). However, localisation studies using antibodies against SMC3 have shown that it is present in both the cytoplasm and nucleus of mitotic and meiotic cells, suggesting that the protein functions in both types of cell division (Lam *et al.* 2005). During *S. cerevisiae* meiotic prophase SMC3 and REC8 localise along sister chromatids to axial and lateral elements, which are precursors to the synaptonemal complex, and *smc3* and *rec8* mutants show defective SC formation suggesting that cohesins plays a role in SC formation (Klein *et al.* 1999). In *Arabidopsis* SMC3 is found at chromosome centromeres and on the spindle at metaphase-I and

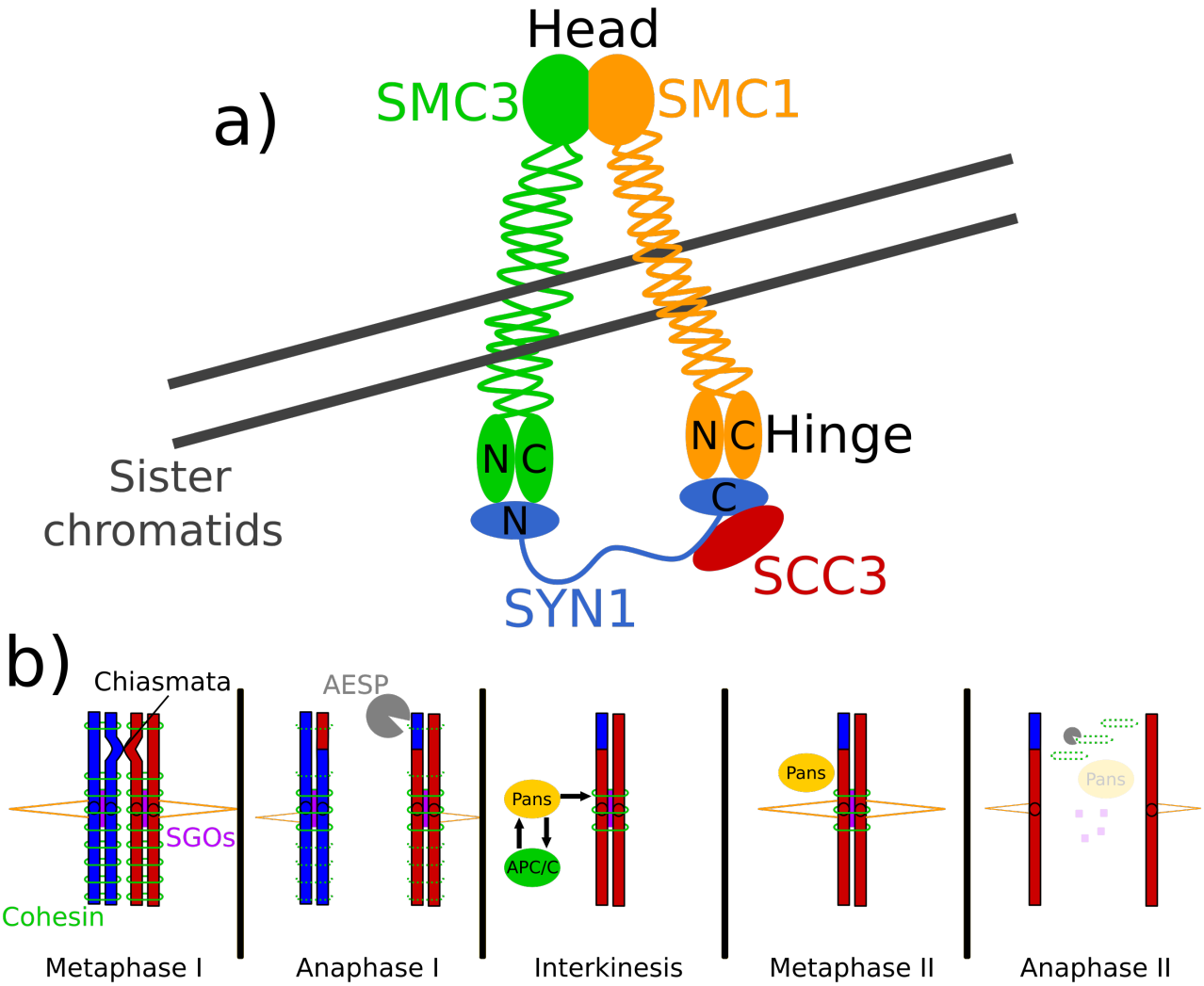

Figure 1.2: Chromosome cohesion during meiosis: a) *The components and structure of cohesin bound around sister chromatids according to the 'embrace' model. The head and hinge domains of SMC1 and SMC3 are shown, as well as the N- and C-terminals of the proteins involved.* ***b)*** *Schematic of cohesin removal during meiosis. At metaphase-I sister chromatids are held together by cohesin (green circles) along their entire length. At anaphase-I cohesin present at arm regions of chromatids is degraded by AESP (Grey circle), while centromeric cohesin is protected by shugoshin (purple rectangle). During interkinesis, interaction between the APC/C (green oval) and patronus (yellow oval) serves to reinforce protection of centromeric cohesion which continues into metaphase-II. At anaphase-II both patronus and shugoshin are degraded, allowing the remaining centromeric cohesin to be removed and sister chromatids to separate. (Diagram adapted from (Zamariola, Tiang, et al. 2014))*

this association persists until anaphase-II (Lam *et al.* 2005). Intriguingly, the spindle association is independent of the presence of SYN1 supporting roles for SMC3 outside of cohesion, as without SYN1 the cohesin complex is unable to form (Lam *et al.* 2005). In tomato SMC1 and SMC3 are present on the axial elements of the SC during prophase-I and give a weak signal on chromatin from metaphase-I to telophase-II. However, no spindle association was observed suggesting SMC3 dynamics in *Arabidopsis* are not conserved throughout plants (Lhuissier *et al.* 2007).

In *Arabidopsis* the α-kleisin subunit SYN1 is required for sister chromatid cohesion in meiosis (Chelysheva *et al.* 2005). SYN1 fully co-localises with SCC3 at pachytene and is necessary for the correct loading of SCC3 onto sister chromatids, providing strong support for the idea that they act as part of a complex (Chelysheva *et al.* 2005). In *syn1* mutants chromatid arm and centromere cohesion as detected by FISH are defective (Cai *et al.* 2003). SYN1 is also necessary for SC polymerisation and elongation. In *syn1* mutants synapsis during meiosis is blocked, leading to an absence of chromosome condensation and paring and the presence of univalents at metaphase-I. Localisation of the axis-associated ASY1 is impaired although not completely absent in *syn1* mutants, suggesting a role for SYN1 in axis polymerisation and elongation, but not initial deposition (Chelysheva *et al.* 2005). In addition, *syn1* mutants display chromatin bridges and chromosome fragmentation, which is characteristic of unrepaired DNA DSBs (Bhatt *et al.* 1999; Chelysheva *et al.* 2005). These defects are corrected in a *syn1 spo11* mutant, confirming a role for SYN1 in repairing the meiotic DNA DSBs formed by SPO11 (Chelysheva *et al.* 2005). In yeast and *Arabidopsis* mutation of REC8/SYN1 leads to loss of the monopolar orientation of chromosomes at meiosis-I and the same defect is observed in *scc3* mutants suggesting that the cohesin complex is responsible for ensuring correct kinetochore geometry in meiosis-I (Yokobayashi *et al.* 2003; Chelysheva *et al.* 2005; Watanabe 2012).

There are three SYN1 paralogs in *Arabidopsis* named SYN2, SYN3 and SYN4 (Schubert *et al.* 2009). SYN2 has been hypothesised to be involved with DNA repair in somatic cells, SYN3 is required for plant viability and known to localise to the nucleolus and SYN4 is required for centromere cohesion during mitosis (Schubert *et al.* 2009). The fact that SYN1 is not observed at the centromere cores at metaphase-I and metaphase-II, even though cohesion is present at these sites, combined with the fact that in *syn1* mutants chromosome cohesion is maintained until

anaphase-I, suggests that the paralogs of SYN1 may play a role in meiotic chromosome cohesion (Chelysheva *et al.* 2005).

Chromosome cohesion is released in a stepwise manner. In *S. cerevisiae* the first step is the cleavage of REC8 leading to the removal of cohesin at chromosome arms at anaphase-I. During anaphase-II cohesin at the centromeres is released, enabling sister chromatids to separate. The cleavage of REC8 is performed by the cysteine protease separase which is broadly conserved in yeast, plants and animals (Kitajima *et al.* 2003; Kudo *et al.* 2009). Separase function is inhibited by securin which is degraded at the onset of anaphase-I by ubiquination by the anaphase promoting complex/cyclosome (APC/C), an E3 ubiquitin ligase that marks proteins for degradation. The *Arabidopsis* homologue of separase is named AESP, which is an essential protein, meaning that mutant studies are not possible. However, RNAi lines under the control of the meiotic *DMC1* promoter (Liu & Makaroff 2006) and the temperature sensitive mutant *rsw4* (Wu *et al.* 2010; Yang *et al.* 2011), have allowed the meiotic function of AESP to be determined. In *aesp* and *rsw4* mutants chromosome segregation at meiosis-I is defective leading to entangled chromosomes and chromosome fragments becoming visible at this stage (Liu & Makaroff 2006; Wu *et al.* 2010; Yang *et al.* 2011). In meiosis-II bivalents are still present in these mutants, indicating that chromosome cohesion has not been lost (Liu & Makaroff 2006; Wu *et al.* 2010; Yang *et al.* 2011). SYN1 and SMC3 signals persist on *aesp* and *rsw4* chromatin past metaphase-I when they usually disappear, indicating that AESP is responsible for the removal of cohesin from chromosomes at anaphase-I (Liu & Makaroff 2006; Wu *et al.* 2010; Yang *et al.* 2011). Additionally, in an *aesp ask1* double mutants where disrupted SC formation means that homologous chromosomes prematurely separate at meiosis-I, sister chromatids do not separate at meiosis-II, indicating that *aesp* is also responsible for removal of cohesin at meiosis-II (Yang *et al.* 2009). In addition to its main role, periphery phenotypes of *aesp* mutants suggest further roles in meiosis. For example, non-homologous centromere associations at zygotene and disturbed microtubule arrays at teleophase-II in *aesp* mutants suggest a role for the protein in the control and release of transient centromere associations at zygotene and in microtubule organisation during meiosis (Armstrong *et al.* 2001; Yang *et al.* 2009; Yang *et al.* 2011).

During meiosis sister chromatid cohesion is protected from degradation by Shugoshin (Sgo) a protein first discovered in *Drosophila* and successively found in yeast, mammals and plants

(Kerrebrock *et al.* 1995; Yao & Dai 2012). In *Drosophila melanogaster* and *S. cerevisiae* SGO is present in a single copy, whereas mammals and plants possess two Sgo paralogs SGO1 and SGO2. Whereas in Drosophila, *S. cerevisiae* and plants Sgo1 is responsible for protection of centromere-specific sister chromatid cohesion, in mammals SGOL2 plays this role (Gutiérrez-Caballero *et al.* 2017). In yeast and vertebrates Sgo is recruited to pericentromeric heterochromatic regions, where it associates with the phosphatase PP2A to dephosphorylate Rec8 and prevent its cleavage in meiosis-I (Lee *et al.* 2008; Xu *et al.* 2010). In *S. cerevisiae* Sgo1 localises to centromeres until the end of anaphase-I, while in animals SGOL2 persists on the chromosomes into meiosis-II (Kitajima *et al.* 2004; Lee *et al.* 2008). In plants, SGO1's role in protecting cohesion has been demonstrated in *Arabidopsis* maize and rice (Hamant *et al.* 2005; Wang *et al.* 2011; Cromer *et al.* 2013). In *Arabidopsis* FISH analysis of *sgo1* mutants showed premature release of sister-chromatid centromere cohesion at anaphase-I resulting in random chromosome segregation (Cromer *et al.* 2013; Zamariola *et al.* 2014). Only *sgo1* mutants show a meiotic phenotype in *Arabidopsis*, meaning that the role of SGO2 is currently unclear (Cromer *et al.* 2013; Zamariola *et al.* 2014). Another protein responsible for chromosome cohesion protection is the plant-specific PATRONUS1 (PANS1), which was first discovered in *Arabidopsis* (Cromer *et al.* 2013; Zamariola *et al.* 2014). In *pans1* mutants meiocytes show a premature release of sister chromatid cohesion at metaphase-II, but not in meiosis-I (Zamariola *et al.* 2014). This suggests the protein in required for the maintenance of cohesion during interkinesis.

1.4 Meiotic cell cycle control

The mitotic cell-cycle is commonly divided into 4 phases named gap-1 (G1), synthesis (S), gap-2 (G2) and mitosis (M) (Howard & Pelc 1953). During G1 phase the cell has recently divided and resumes the biosynthetic activities that were suspended during mitosis. During G1 the cell grows in size and increases the levels of protein and organelles present in the cell. Next the cell enters S-phase and initiates DNA synthesis to replicate each chromosome present in the cell once. After S-phase the cell enters G2, a further period of cell growth and protein synthesis in preparation for mitosis. Following G2 the cell enters mitosis and the cell undergoes nuclear division producing two daughter cells, which may then re-enter G1 (Nasmyth 2001). Meiosis is sometimes similarly split into 5 phases; gap-1 (G1), synthesis (S), meiosis-I (MI), interkinesis (I) and meiosis-II (MII). Meiotic G1- and S-phase proceed in a broadly analogous way to G1- and S-phase in the mitotic

cell cycle. However, during MI homologous chromosomes are segregated into two cells in a reductional division. Following this there is a brief interkinesis-phase before MII where the two cells produced at the end of MI undergo a further equational division, with segregation of sister chromatids to form four haploid gametes (Nasmyth 2001).

Progression through mitosis and meiosis are controlled by three main inter-related factors, i) cyclin-dependant kinase-cyclin (CDK-cyclin) complexes , ii) the anaphase-promoting complex/cyclosome (APC/C), which regulates CDK-cyclin levels and marks proteins for degradation by the proteasome and iii) meiotic checkpoint pathways, which control entry into new phases of meiosis, dependant on certain conditions being met. The current model of cell cycle control posits that during the mitotic cell-cycle in budding yeast, cyclin-CDK activity is lowest during G1, but slowly increases through the S- and G2-phases and reaches a maximum at the beginning of mitosis (Nasmyth 1996). Cyclin-CDK activity then rapidly decreases due to the action of the APC/C causing cells to complete mitosis and reenter G1 phase (Nasmyth 1996; Stern & Nurse 1996). This is in contrast to the meiotic programme of one round of chromosome replication, followed by two rounds of cell division. This requires cyclin-CDK activity to build to a maximum at the beginning of MI (as in M-phase in mitosis), cyclin-CDK activity then dips slightly, moving the cell through MI and into interkinesis. Cyclin-CDK activity then builds again triggering meiosis-II (See Fig 1.3) (Wijnker & Schnittger 2013). Following meiosis-II cyclin-CDK activity drops to a minimum, ending meiosis and leaving the resulting gametes with the cyclin-CDK activity level of a G1-phase cell (Wijnker & Schnittger 2013).

1.4.1 CDK-cyclins

In *S. cerevisiae* mitosis a threshold level of cyclin-CDK activity is required for a cell to progress from G1-phase to S-phase, and a higher threshold must be achieved in order to move the cells from G2-phase to M-phase (i.e. mitosis) (Nasmyth 1996; Stern & Nurse 1996). After M-phase the cyclin-CDK activity drops allowing replication origins to be licensed in preparation for a new S-phase (Nasmyth 1996; Stern & Nurse 1996). These cyclin-CDK activity oscillations coordinate the various cell cycle events involved in mitosis and ensure the unidirectional progression of cells through the cell division programme (Nasmyth 1996; Stern & Nurse 1996). The regulation of cyclin-CDK occurs at many levels. One of the major determinants of cyclin-CDK activity is the

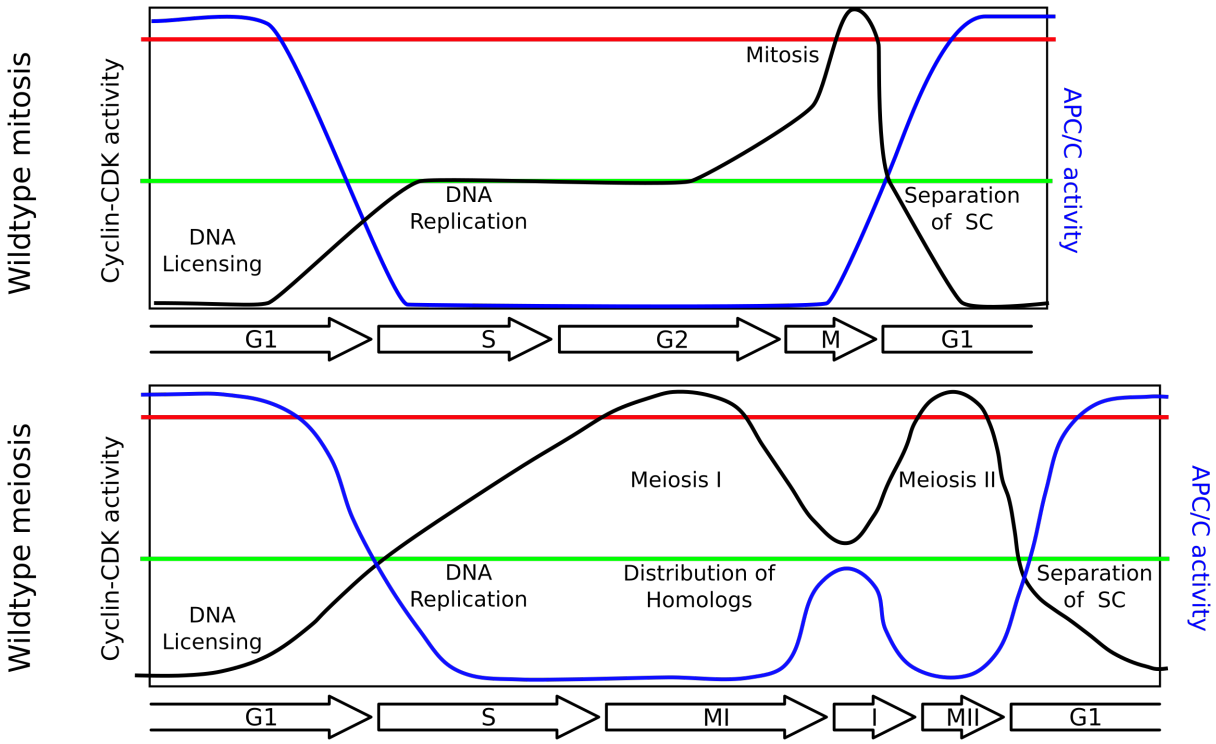

Figure 1.3: Cyclin-CDK and APC/C activity during mitosis and meiosis. *(Diagram adapted from (Wijnker & Schnittger 2013))*

type and quantity of cyclin partners available (Pines 1995). In animals, D-type and E-type cyclins are responsible for entry into S-phase, while cyclin-A controls S-phase and early M-phase events. B-type cyclins control the rest of M-phase (Pines 1995). In plants homologs of the A- and B- type cyclins are known and a third group of cyclins named D-type show an intermediate similarity between animal D- and E-type cyclins (Wang *et al.* 2004). In addition to the direct control of the cell-cycle exercised by cyclin-CDK complexes through their control of the kinase levels, many proteins involved in meiotic recombination possess CDK-phosphorylation or cyclin-binding domains including SPO11, DMC1 and REC8 (Esposito & Esposito 1969; Ponticelli & Smith 1989; Bishop *et al.* 1992). This suggests that not only general progression through meiosis, but also more local meiotic events such as recombination may be coordinated or influenced by cyclin-CDK complexes.

In *Arabidopsis* there are five central cell-cycle CDKs (CDKA;1, CDKB1;1, CDKB1;2, CDKB2;1 and CDKB2;2) and thirty cyclins (Vandepoele *et al.* 2002). CDKA;1 is thought to be the homologue of animal CDK1 and CDK2 based on sequence similarity (Nowack *et al.* 2012). CDKA;1 is responsible for controlling S-phase entry into mitosis and null mutants are not viable (Dissmeyer *et al.* 2007). However, in *cdka;1* loss-of-function mutants plants are sterile, suggesting a role for CDKA;1 in meiosis, which is supported by the fact that CDKA;1 has been found localising to meiocytes in both immunolocalisation and YFP-tagging studies (Dissmeyer *et al.* 2007). The B1-type CDKs appear to function mostly in mitotic entry and double *cdkb1;1 cdkb1;2* mutants remain fertile suggesting a minor role, if any, in meiosis (Nowack *et al.* 2012).

In *Arabidopsis* three meiotic cyclins have been discovered; TARDY ASYNCHRONUS MEIOSIS (TAM), SOLO DANCERS (SDS) and CYCB3;1 (Magnard *et al.* 2001; Azumi *et al.* 2002; Bulankova *et al.* 2013). TAM is an A1-type cyclin and the only type of its class to be expressed during meiosis. In *tam* mutants progression through meiosis is slowed and meiosis is abandoned after the first meiotic division, giving rise to diploid gametes (Magnard *et al.* 2001). This suggests TAM controls the pace of progression through meiosis. SDS is specifically expressed during meiosis and *sds* mutants display defects in homologue pairing and crossover formation during meiosis-I, suggesting that this cyclin plays a role in regulating these events (Azumi *et al.* 2002). SDS is also a requisite for DMC1 recruitment to chromosomes (De Muyt *et al.* 2009). CYCB3;1 is the only meiotically expressed B-type cyclin and is also implicated in mitotic cell-cycle control.

In *cycb3;1* mutants cell wall-like structures begin to from from prophase-I onwards, a phenotype that is also observed to a less dramatic extent in *sds* mutants (Bulankova *et al.* 2013). It therefore seems likely that CYCB3;1 plays a role in preventing premature cytokinesis.

1.4.2 The APC/C

The APC/C is a large multi-subunit complex which performs two roles during meiosis. The first is to mediate the turnover of cyclins, thus progressing the cell through meiosis (Kitajima *et al.* 2004). The second is to mediate the turnover of securin, an inhibitor of separase that cleaves centromeric cohesion of sister chromatids and promotes the progression of anaphase (see above). The current model of mitotic progression holds that high cyclin-CDK activity promotes APC/C activity via phosphorylation of several proteins which interact with the APC/C (Pesin & Orr-Weaver 2008). One of the central proteins in this process is CDC20 which forms an APC/C^{CDC20} complex. Due to the action of the spindle checkpoint (see below), APC/C activity is low during S- and G2-phase until all sister chromatids attach to the mitotic spindle and come under tension (Lara-Gonzalez *et al.* 2012; Jia *et al.* 2013). The checkpoint activates the APC/C which inhibits cyclin-CDK activity by targeting cyclins for degradation. This in turn suppresses APC/C^{CDC20} activity (Lara-Gonzalez *et al.* 2012). This interplay of regulating factors ensures that APC/C activity is low during S- and G2-phase and increases rapidly at anaphase of mitosis. High anaphase levels of activity are maintained until the next S-phase when APC/C activity decreases and CDK-cyclin activity increases (Lara-Gonzalez *et al.* 2012; Jia *et al.* 2013).

In animals and yeast, the APC/C is also required during meiosis-I and -II (Cooper & Strich 2011). The APC/C degrades the separase inhibitor securin at metaphase-I, which leads to the cleavage of meiotic cohesin REC8 along chromosome arms. REC8 protected by shugoshin at centromeric regions is not destroyed at this stage. However, cyclin-CDK activity is kept high during meiosis-I, via increased synthesis of meiotic cyclins (Kitajima *et al.* 2004). In *tam* and hypomorphic *cycb3;1* mutants where this high level of cyclin-CDK activity is not maintained, premature meiotic exit and cell wall synthesis begins (Magnard *et al.* 2001; Bulankova *et al.* 2013).

1.4.3 Meiotic checkpoints

Progression through the mitotic cell-cycle is controlled by several checkpoints. The G1-S checkpoint prevents entry into S-phase, unless cyclin-CDK activity meets a certain threshold level (Nurse 2000). The G2-M checkpoint prevents entry into mitosis unless there is M-phase specific cyclin-CDK activity and the spindle checkpoint controls the activity of the APC/C, which prevents entry into anaphase unless all chromosome are aligned on the equatorial plate and attached to the mitotic spindle (Nurse 2000). In *S. cerevisiae* and animals there are at least three meiotic checkpoints. However, the stringency of these checkpoints seems weaker in plants (Brownfield & Köhler 2011; De Storme & Geelen 2013). In *S. cerevisiae* the first meiotic checkpoint is at the entry into meiotic S-phase, which depends on the metabolic state of the cell (Nurse 2000). In animals and yeast a meiosis-specific checkpoint termed the meiotic recombination checkpoint is present at the end of pachytene, which only permits entry into diplotene if recombination has completed successfully, as determined by the strength of tension that the meiotic spindles are under (Roeder & Bailis 2000). This checkpoint appears to be more relaxed, if present at all, in *Arabidopsis* (and plants more generally) as *dmc1* mutants are capable of completing meiosis, even though recombination and thus spindle tension is not present (Couteau *et al.* 1999; De Muyt *et al.* 2009).

The next meiotic checkpoints are at the transitions from metaphase-I to anaphase-I, and from metaphase-II to anaphase-II. The metaphase-I to anaphase-I checkpoint again seems attenuated in plants, as *Arabidopsis spo11* mutants, which cannot undergo recombination, still progress through meiosis, giving rise to aneuploid gametes (Couteau *et al.* 1999; Hartung *et al.* 2007). There is little evidence for the second checkpoint in plants either, however, in *smg7* mutants (an EST1 domain-containing protein whose homologues in humans are implicated in nonsense-mediated RNA decay and telomere metabolism) cells become arrested at anaphase II and cannot decondense chromosomes or reorganise the meiosis-II spindle (Riehs *et al.* 2008). However, it is unclear whether this is a true checkpoint.

1.5 Recombination during meiosis

A concept of meiotic crossover was conceived early in the 20th century by Thomas Hunt Morgan (Morgan 1916). Morgan was aware of cytological work by Frans Alfons Janssens (Janssens 1909) describing chiasma and drew a link between Janssens' observations and trait inheritance data

from his own work on Drosophila. He hypothesised that homologous chromosomes were capable of exchanging portions of their arms during meiosis in order to generate hybrid chromosomes, which were then passed on to offspring via fertilisation (Morgan 1916). This model was experimentally confirmed by Creighton and McClintock who used morphological features of *Zea mays* chromosomes to confirm a correlation between cytological and genetic crossover (Creighton & McClintock 1931). Subsequent work on recombination has revealed large numbers of proteins that are involved in the initiation, resolution and regulation of meiotic recombination and crossover formation.

1.5.1 DNA double stand break formation

Early models of crossover formation hypothesised that recombination between the chromosomes was initiated by a single-strand nick in the double-stranded structure of DNA (Holliday 1964; Meselson & Radding 1975). However, a variety of experimental evidence accumulated which could not be explained by either the Holliday or Meselson-Radding single-strand break models. This led to the proposition of a new ‘double-strand-break repair’ model (Szostak *et al.* 1983). Under this model crossovers were hypothesised to initiate from a DNA double-stand break (DSB). Both sides of the DSB would then be resected by exonucleases to create 3' single-stranded overhangs on either side of the break. One of these 3' ends would then invade a homologous chromosome forming a displacement loop (D-loop). The D-loop would then be enlarged by template-driven repair synthesis, leading to the 3' end containing sequence from its homologous partner. The other 3' end produced by resection would anneal to the DNA strand displaced from the D-loop and a second round of DNA synthesis would be initiated from this. Following these steps, branch migration would then lead to the creation of a double-Holliday junction, which could be resolved to give either a non-crossover, with local regions of gene conversion that can be detected by 3:1 inheritance patterns through meiosis, or a crossover (Szostak *et al.* 1983).

The discovery of the SPO11 transesterase in budding yeast lent support to the DSB repair model (Esposito & Esposito 1969; Bergerat *et al.* 1997; Keeney *et al.* 1997). SPO11 was first identified in a mutant screen that identified genes required for sporulation (i.e. fertility) in yeast (Esposito & Esposito 1969). SPO11 shows some similarity to the ‘A’ catalytic subunit of the type II DNA topoisomerase VI (TopoVIA). Type II topoisomerases catalyse the formation of DSBs and the

subsequent migration of a DNA duplex through this break before resealing the original DSB in an ATP-dependant reaction, usually for the purposes of decatenating DNA rings or relaxing supercoiled DNA (Bergerat *et al.* 1997). SPO11 homologs have been found in diverse eukaryotes, which suggests a conserved mechanism for recombination initiation throughout sexually reproducing organisms (de Massy 2013). Mutant *spo11* phenotypes are similar across many species and are characterised by a lack of meiotic DSBs (Keeney *et al.* 1997; Dernburg *et al.* 1998; Baudat *et al.* 2000; McKim *et al.* 1998; Grelon *et al.* 2001; An *et al.* 2011). Mutants also display other phenotypes which can be regarded as downstream effects of the loss of meiotic DSBs, for example, loss of chromosome pairing and meiotic recombination, defects in chromosome segregation and loss of fertility. Lack of chromosome synapsis is often observed in *spo11* mutants, due to a requirement for recombination to initiate pairing . However in at least two organisms, *D. melanogaster* (McKim *et al.* 1998) and *C. elegans* (Dernburg *et al.* 1998; Macqueen 2002), loss of synapsis does not occur in *spo11* mutants, due to the presence of additional chromosome pairing mechanisms (MacQueen *et al.* 2005; Martinez-Perez & Villeneuve 2005).

Mutational analysis has identified a catalytic tyrosine residue in SPO11 which, when mutated, causes loss of DSBs in *S. cerevisiae* (Bergerat *et al.* 1997), *S. pombe* (Cervantes *et al.* 2000), mouse (Boateng *et al.* 2013), *S. macrospora* (Storlazzi *et al.* 2003) and *Arabidopsis* (Hartung *et al.* 2007). In *Arabidopsis* there are three SPO11 paralogues, called SPO11-1, SPO11-2 and SPO11-3 (Hartung & Puchta 2000; Hartung & Puchta 2001). SPO11-3 has been found to have a non-meiotic role decatenating chromosomes during endoreduplication cycles (Hartung *et al.* 2002; Sugimoto-Shirasu *et al.* 2002). Both SPO11-1 and -2 are required non-redundantly for DSB formation, suggesting that in plants SPO11-1/SPO11-2 acts as a heterodimer to generate DSBs (Grelon *et al.* 2001; Stacey *et al.* 2006) (Figure 1.4). Following DSB creation SPO11 remains covalently bound to DNA and requires a resection reaction to remove it (Garcia *et al.* 2011). This creates a complex of SPO11 bound to a short stretch of DNA (an oligonucleotide). SPO11-oligonucleotide complexes have been isolated in many species including mouse (Neale *et al.* 2005; Lange *et al.* 2011), *S. cerevisiae* (Neale *et al.* 2005), *S. pombe* (Milman *et al.* 2009; Rothenberg *et al.* 2009) and *Arabidopsis* (Choi and Henderson, unpublished), and sequencing SPO11-oligonucleotides reveals information about preferred DSB sites, which varies between species (Choi & Henderson 2015). In *S. macrospora* GFP-tagged SPO11 forms multiple foci

associated with chromatin at early leptotene. As chromosomes align, before synapsis, SPO11 appears as foci along the chromosome axes, where these foci remain until the end of pachytene when the SPO11 signal becomes diffuse, disappearing before the onset of diplotene (Storlazzi *et al.* 2003). In *S. cerevisiae* Myc-tagged SPO11 foci appear at early zygotene, concomitant with DNA DSBs. By pachytene, SPO11 foci occur in proximity to the chromosome axes and disappear before diplotene (Prieler *et al.* 2005). Intriguingly, this study also showed that SPO11 colocalises with the Rec8 cohesin on chromosome axes and this localisation was dependant on three other proteins, REC102, REC104 and REC114. SPO11 has also been found to localise to the linear elements (analogous to the chromosome axes) of *Schizosaccharomyces pombe* (Lorenz *et al.* 2006). This was unexpected, as while there is strong evidence SPO11 that localises to the chromosome axes, DSBs are preferentially formed on chromatin loops (Panizza *et al.* 2011). This has led to the hypothesis that DSB machinery occupies sites on the chromosome axes, while DSB sites are transiently recruited to the axes to allow DSB formation. In *S. cerevisiae* this is mediated by the axis-located factor Mer2 and Spp1, which is a component of the Set1 histone methyltransferase complex that reads $H3K4^{me3}$ chromatin marks. This demonstrates how an epigenetic modification can tether hotspot sequences to meiotic axes components and promote recombination (Sommermeyer *et al.* 2013; Acquaviva *et al.* 2013).

As noted above, in *S. cerevisiae* three accessory proteins (REC102, REC104 and REC114) were discovered, which were essential for SPO11 DSB formation (Prieler *et al.* 2005). Elimination of any of these proteins destroyed the interaction of the remaining proteins with the chromosome axes, suggesting they function together in a complex that forms prior to axis binding (Prieler *et al.* 2005). This suggests that SPO11 functions as part of a ‘DSB complex’. A mutant screen in plants recently identified a structural homolog of archeal topoisomerase VIB (TopoVIB), the complementary subunit to TopoVIA of which SPO11 is a homologue (Vrielynck *et al.* 2016). The protein was named meiotic TopoVIB-like (MTOPVIB/TOPOVIBL). Bioinformatics approaches found structural homologues of MTOPVIB in animals and the essential role of this subunit in DSB formation has been demonstrated in mice. Rec102 and Rec6 from *S. cerevisiae* and *S. pombe* respectively show similarity to parts of MTOPVIB, but lack some domains (Robert *et al.* 2016). In *D. melanogaster* Mei-P22 also shows similarity to MTOPVIB and is required for DSB formation (Liu *et al.* 2002). Although MTOPVIB displays a high level of sequence divergence from TopoVIB, it has high structural similarity. These similarities include the presence of a

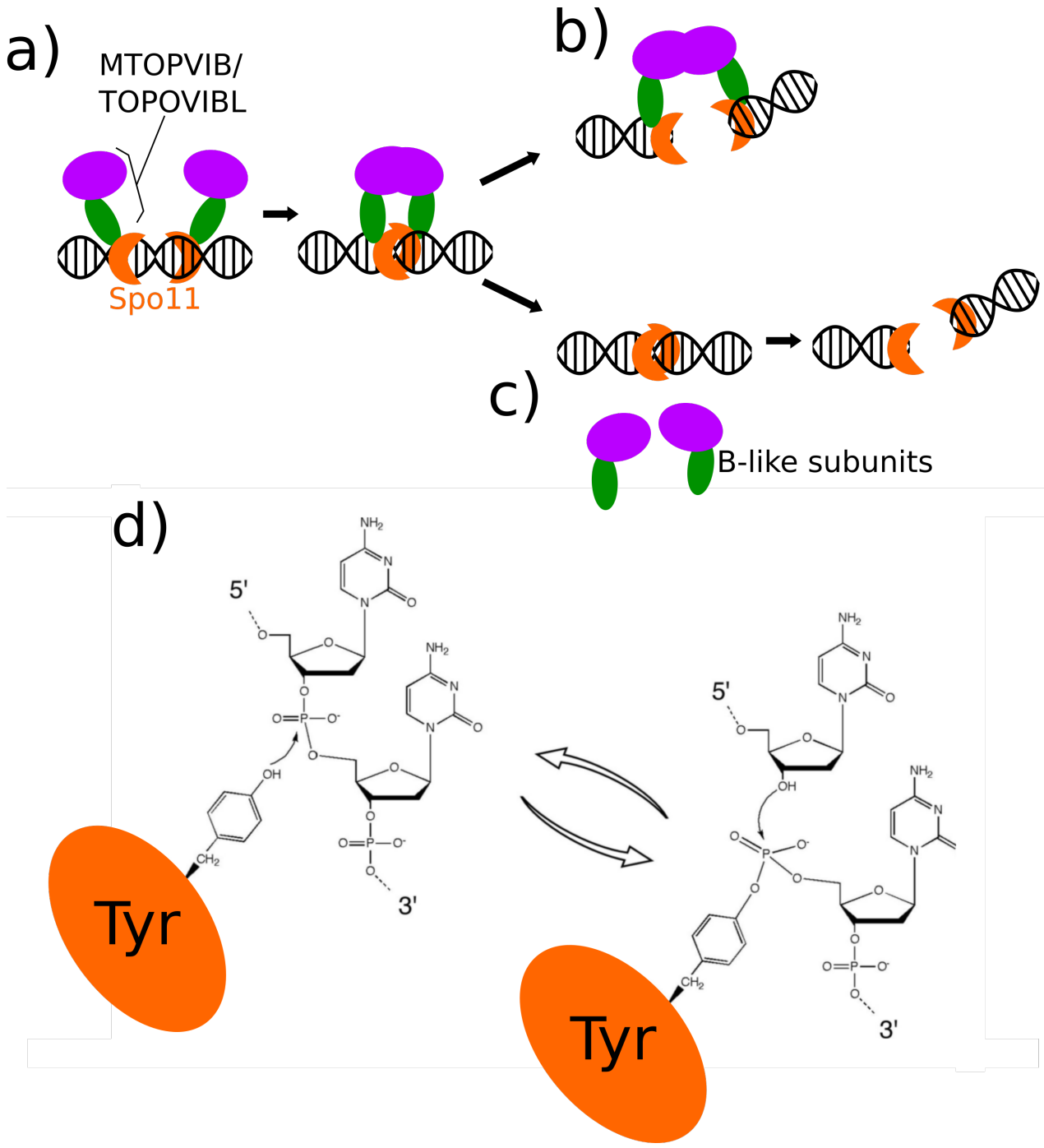
a)
MTOPVIB/
TOPOVIBL
Spo11
b)
c)
B-like subunits
d)
5'
3'
Tyr
Tyr

Figure 1.4: Catalytic mechanism of SPO11 transesterases. a) *Schematic of possible DSB-creation mechanisms by the meiotic SPO11 complex. The TOPOVIB-like subunits (purple and green ovals) complex with SPO11 (orange circle) and bind DNA then either* ***b)*** *the complex generates a DSB or* ***c)*** *the B-like subunits detach from the SPO11 dimer, which goes on to form a DSB.* ***d)*** *The catalytic mechanism of type-II topoisomerases, which is also the mechanism of SPO11-mediated DSB formation. A catalytic tyrosine residue performs a nucleophilic attack on the phosphodiester backbone of DNA. To form a DSB two monomers must perform the same reaction on opposite strands of the DNA (Diagram adapted from (Robert et al. 2016; Keeney 2008)).*

Bergerat fold GHKL domain and a transducer region (Vrielynck *et al.* 2016). The ATP-binding pocket consisting of β-sheets and α-helices is also conserved. One difference is in the ATP-lid loop which suggests distinct mechanisms in ATP capture and/or hydrolysis between TopoVIB and MTOPVIB (Vrielynck *et al.* 2016; Robert *et al.* 2016). Revealingly, the most highly conserved part of MTOPVIB corresponds to a region of interaction between A and B subunits heavily suggesting an interaction between MTOPVIB and SPO11 (Vrielynck *et al.* 2016). In plants MTOPVIB was found to be expressed during meiosis and disruption causes the same meiotic phenotypes as *spo11* mutants, its physical interaction with SPO11 was confirmed by yeast two-hybrid assays (Vrielynck *et al.* 2016). The mouse MTOPVIB homologue can only interact with the DSB creating SPO11-β splice variant and not with the SPO11-α variant, which plays no role in DSB formation (Robert *et al.* 2016). In *Arabidopsis*, MTOPVIB mediates the formation of SPO11-1/SPO11-2 heterodimers, further supporting the idea that such a heterodimer is responsible for DSBs in *Arabidopsis* (Vrielynck *et al.* 2016).

1.5.1.1 Control of the distribution and quantity of DSBs

As noted above, the formation of DSBs is limited temporally to specific substages of prophase-I. In addition to this temporal limitation, the distribution and number of DSBs are also tightly regulated. DSB distributions can be determined by a range of factors including DNA base composition, local chromatin modifications, chromosome structure and regulatory kinase activity (Cooper *et al.* 2016). DSB hotspots, sites that are much more likely to be cut by SPO11 than expected by chance, have been identified in numerous plants, animal and fungi (Blitzblau *et al.* 2007; Cromie *et al.* 2007; Smagulova *et al.* 2011; Fowler *et al.* 2014). In *S. cerevisiae*, mice and humans hotspots occur in chromatin regions associated with the histone H3 trimethylated on lysine 4 ($H3K4^{me3}$). In mice and humans this mark is deposited by PRDM9, a zinc-finger DNA-binding methytransferase. PRDM9 binds to DNA motifs via its zinc-finger domain and then methylates proximal histones, which promotes recombination (Baudat *et al.* 2010; Myers *et al.* 2010; Parvanov *et al.* 2010). In *S cerevisiae* the SET1 complex deposits $H3K4^{me3}$ at future meiotic DSB sites (Sommermeyer *et al.* 2013). In plants PRDM9-like genes have not been observed and crossover hotspots tend to localise in promoters and terminators of genes associated with chromatin marks that promote RNA pol II transcription, for example, low nucleosome density, $H3K4^{me3}$, the histone variant H2A.Z and hypomethylated DNA (Choi *et al.* 2013a). A-rich, CCN

and CTT motifs enriched in hotspot regions are likely to contribute to the chromatin organisation of these regions, putatively leading to increased DSB and crossover formation (Horton *et al.* 2012; Choi *et al.* 2013; Shilo *et al.* 2015). Thus, at the level of chromatin, plant recombination hotspots resemble those observed in yeast.

In *S. cerevisiae*, *D. melanogaster* and mice the ATM (Tel1) and ATR (Mec1) kinases have been found to control DSB numbers through both negative and positive feedback mechanisms (Cooper *et al.* 2014). In *S. cerevisiae* DSB formation leads to the activation of ATM and ATR which phosphorylate Rec144. Rec114 associates with the chromosomes axes and promotes DSB formation. Phosphorylation of Rec114 reduces its interaction with DSB hotspots and so downregulates DSB formation (Carballo *et al.* 2013). ATM and ATR also provide *trans* negative feedback loops, which ensure that only one DSB arises at any given chromosomal locus per chromatid quartet (Kleckner *et al.* 2012). Intriguingly, ATR kinase can also provide positive feedback. In *S. cerevisiae* strains with hypomorphic *spo11* alleles, the loss of ATR led to a reduction in DSBs (Gray *et al.* 2013). This suggests that ATR monitors global DSB levels and can delay or promote exit from prophase-I accordingly.

ATM has a similarly complex role in DSB formation. In *S. cerevisiae* ATM can negatively influence DSB formation in *cis*, inhibiting the clustering of DSBs along a chromosome. This phenomena is known as DSB interference. Mutating ATM causes loss of DSB interference 20 – 100 kilobases away from a hotspot (Garcia *et al.* 2015). Indeed, negative interference (i.e. more DSBs than expected by chance, not less) was observed in 0–7.5 kilobase regions surrounding a hotspot. This second phenomena is only seen in DSB hotspots estimated to reside within the same chromosomal loop, reinforcing the importance of chromosome structure to DSB placement (Garcia *et al.* 2015). The overall effect of ATM and ATR DSB regulation is to create an environment where DSBs are relatively evenly distributed and made in sufficient numbers to ensure efficient recombination during meiosis (Figure 1.5). Further evidence of DSB homeostasis was obtained in *S. cerevisiae*, when a novel hotspot was inserting next to a high frequency DSB site (*HIS4::LEU2*), which suppressed local DSBs in an ATM/ATR-independent manner (Fan *et al.* 1997; Robine *et al.* 2007; Fukuda *et al.* 2008). This is termed DSB competition and is hypothesised to occur due to competition within a loop cluster for the pro-recombination factors

Rec114, Mer2 and Mei4.

1.5.2 DSB Processing

Following DSB formation SPO11 remains covalently bound to the 5' ends of the DNA. The MRX/MRN complex (Mre11/Rad50/Xrs or Mre11/Rad50/Nbs2), together with Com1/Sae1 creates a single-strand nick that releases SPO11 attached to a short DNA oligomer (Neale *et al.* 2005). In plants, *mre11, rad50* and *com1* mutants show chromosome fragmentation at anaphase-I and this fragmentation is SPO11-dependant, supporting the hypothesis they play a role downstream of DSB formation (Puizina *et al.* 2004; Uanschou *et al.* 2007). In *S. cerevisiae* 5' ends exposed by nucleolytic release of SPO11 are then further resected, which creates long 3' ssDNA ends (Wold 1997; Fanning *et al.* 2006). These are bound by the RPA proteins, which protect the single-strand DNA from nucleolytic degradation and hairpin formation (Wold 1997; Fanning *et al.* 2006). In plants, there are multiple paralogs of the RPA proteins (RPA1, RPA2 and RPA3) with five RPA1, two RPA2 and two RPA3 paralogs discovered in *Arabidopsis* (Aklilu *et al.* 2014). The resected ssDNA ends are then loaded with the RecA-related recombinases RAD51 and DMC1 (Bishop *et al.* 1992; Shinohara *et al.* 1992; Bishop 1994). The ssDNA strands can then invade the DNA heteroduplex of a homologous chromosome until they locate complementary sequence, a process termed ‘homology search’ (Figure 1.6). Therefore, RAD51 and DMC1 loading onto ssDNA forms nucleofilaments competent for homology search and heteroduplex formation. Expression of DMC1 is meiosis specific, while RAD51 is not (Klimyuk & Jones 1997; Da Ines, Degroote, Goubely, *et al.* 2013). In *Arabidopsis* there is some evidence that RAD51 and DMC1 localise to opposite strands of the DSB (Kurzbauer *et al.* 2012). In *S. cerevisiae* and Arabidopsis separation of function mutants have shown that RAD51 strand exchange activity is not necessary for meiosis, but DMC1 activity is (Cloud *et al.* 2012; Da Ines *et al.* 2013; Pradillo *et al.* 2014). In the absence of DMC1, RAD51 is capable of compensating, likely directing DNA to invade sister chromatids instead of homologous chromosome. Therefore synapsis and bivalent formation fails in *dmc1* mutants, but DSB repair takes place (Couteau *et al.* 1999; Deng & Wang 2007). RAD51 therefore appears to play a backup function, allowing repair from a sister chromatid instead of a homologous partner. RAD51 and DMC1 display 54% amino acid identity in humans and 45% in yeast (Masson & West 2001). In addition, there are limited structural differences between RAD51 and DMC1, suggesting that differences in their meiotic activities

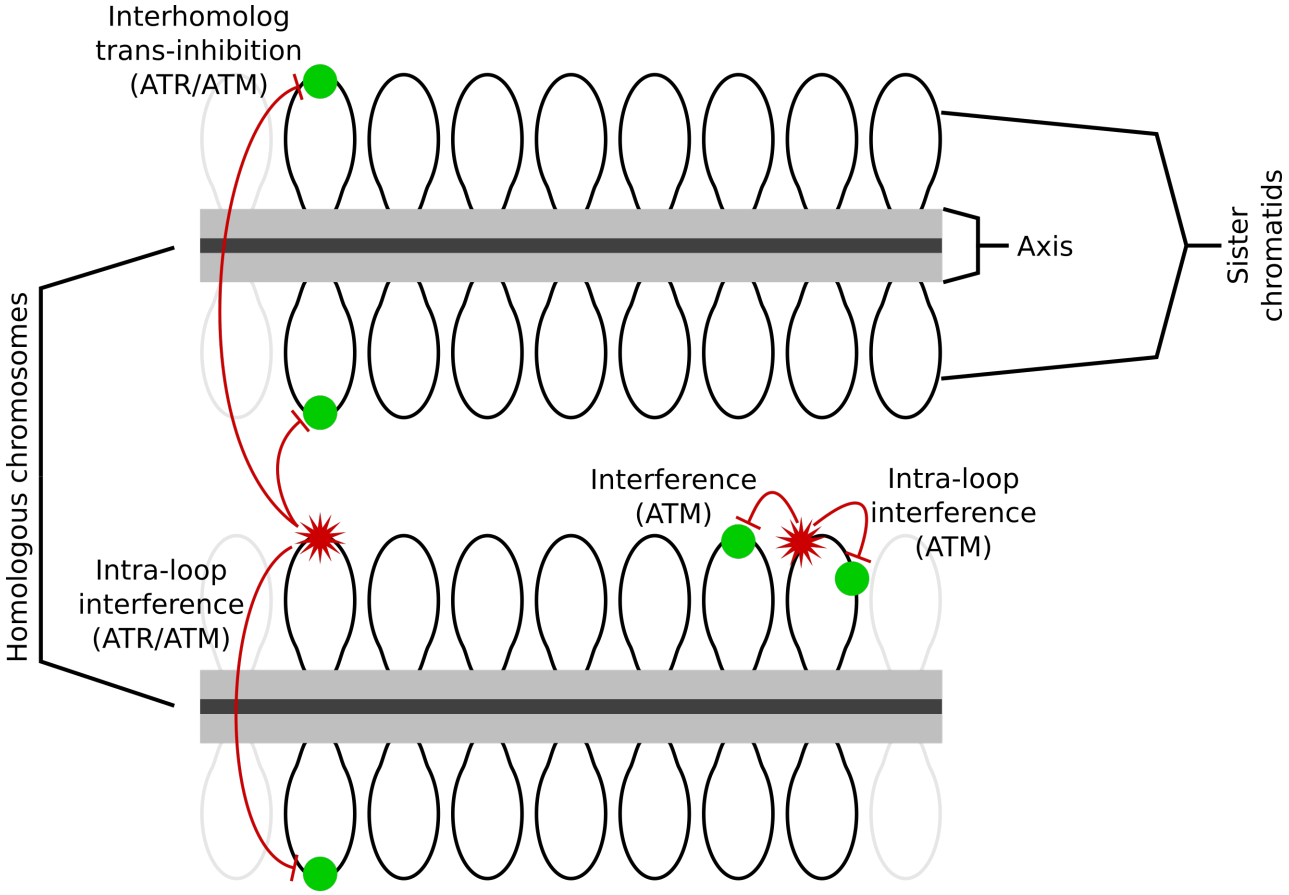

Figure 1.5: ATM- and ATR-mediated regulation of crossovers. *During meiosis chromosomes are organised along the meiotic axis (grey rectangles) into chromosomal loops (black ovals). DSBs (red stars) inhibit further DSB formation via a number of mechanisms mediated by the ATM and ATR kinases. DSBs at a hotspot on a chromatid inhibit further DSBs at the corresponding hotspot location on a sister chromatid and homologous chromosomes via intra-loop interference and interhomolog trans-inhibition respectively (left side of diagram). In addition, DSBs can inhibit further DSBs at hotspots on nearby loops via interference and within the same loop via intra-loop interference (right side of diagram) (Diagram adapted from (Cooper et al. 2014)).*

may also be via accessory factors (Sheridan *et al.* 2008). The axial protein ASY1 stabilises DMC1 during meiosis and allows proper interhomolog repair (Sanchez-moran *et al.* 2007). SDS, the plant specific cyclin-D-like protein is also required for DMC1 for loading (De Muyt *et al.* 2009). ATR also negatively regulates DMC1 loading at DSB sites (Kurzbauer *et al.* 2012). Other proteins which regulate RAD51 and DMC1 are HOP2/MND, which promotes interhomolog repair at the expense of intersister repair (Uanschou *et al.* 2013), FIGL1, an unfoldase which limits crossovers (Mercier *et al.* 2015), BRCA2, which interacts with the meiotic proteins RAD51, DMC1, and DSS1, (Siaud *et al.* 2004; Dray *et al.* 2006) and the RAD51 paralogs XRCC3, RAD51B, C and D (Mercier *et al.* 2015).

1.5.2.1 Non-crossover repair

As mentioned above, following double Holliday junction formation the alternate resolution of the junction may lead to either a crossover or non-crossover event (Nishino *et al.* 2005) (Figure 1.7). In *Arabidopsis* there are several genes known to control this process. In addition to crossover promoting factors (discussed below), there are many proteins which act to repress crossovers and three independent anti-crossover pathways have been identified. One pathway includes the helicase FANCM (Crismani *et al.* 2012) and its cofactors MHF1 and MHF2, which act in concert to prevent crossover formation. The conclusion that these factors act in the same pathway is based on the fact that in both *fancm* mutants and *fancm mhf2* double mutants genetic distance increases three-fold, showing epistasis (Girard *et al.* 2014). The BLOOM/Sgs1 homologs RECQ4A, RECQ4B, TOP3α and RMI1 also act in a parallel pathway to suppress crossovers (Séguéla-Arnaud *et al.* 2015). In *C. elegans* the helicase RTEL1 was found to limit meiotic crossover. However, the *Arabidopsis* homologue of RTEL1 has been found to limit somatic homologous recombination in a pathway parallel to FANCM, while also playing a role in telomere maintenance (Recker *et al.* 2014). Finally, the AAA-ATPase FIDGITIN-LIKE1 also limits crossover formation, independently of FANCM, by regulating early interhomolog invasion steps catalysed by RAD51 and DMC1 (Girard *et al.* 2015). There is some evidence to suggest the RAD51 paralogs XRCC2 and RAD51D also act in concert with FIDGITIN-L1 during this regulation (Da Ines *et al.* 2013).

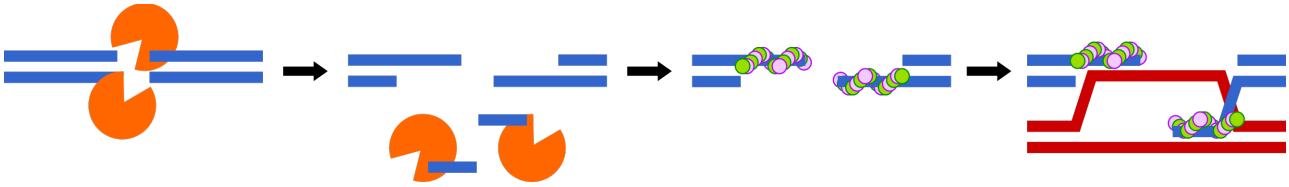

Figure 1.6: Heteroduplex formation. During meiosis SPO11 (orange circles) forms DNA DSBs which become resected to form ssDNA. This ssDNA is then bound by DMC1 and RAD51 (green and purple circles) generating a nucleofilament capable of homologue invasion. On this diagram RAD51 and DMC1 are shown binding both sides of the DSB however, the exact orientation of RAD51 and DMC1 binding is debated (Diagram adapted from (Robert et al. 2016)).

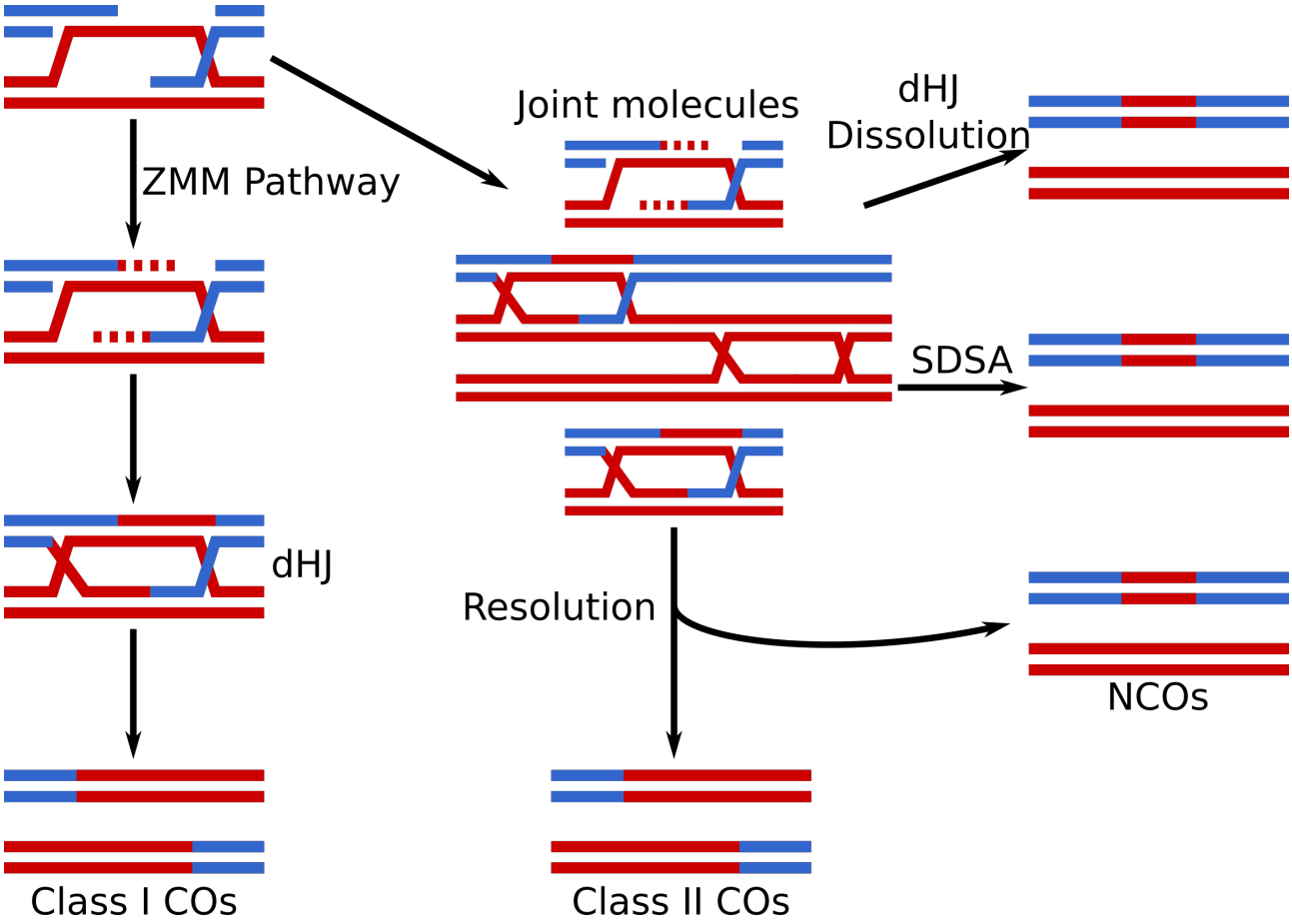

Figure 1.7: Crossover and non-crossover pathways. *Following inter-homologue invasion there are numerous paths that can lead to crossover resolution. The ZMM pathway gives rise to interfering class I crossovers, alternatively double Holliday junctions can also be resolved via the class II crossover pathway, or resolved as a non-crossover. Other joint molecules formed during homologue invasion can be resolved to non-crossovers via dHJ dissolution or synthesis-dependant strand annealing (Diagram adapted from (Mercier et al. 2015)).*

1.5.2.2 Crossover repair

There are two characterised crossover pathways termed ‘Class I’ and ‘Class II’ (Berchowitz & Copenhaver 2010). In addition, chiasmata are still observed in class I and II double mutants, implying the existence of additional repair pathways (Berchowitz *et al.* 2007). The major difference between the two crossover classes is that class I crossovers display interference while class II crossovers do not (Copenhaver *et al.* 2002; De los Santos *et al.* 2003). Crossover interference is the phenomena whereby crossovers appear to inhibit the formation of other crossovers near to them on the same chromosome. It was discovered when observations of crossovers between genetic markers revealed that double crossovers in adjacent intervals were less common than expected, based on the independent frequency of crossover in both intervals (Sturtevant 1915). The strength of this inhibition decreases with physical distance from a crossover and leads to crossovers being more evenly spread along a chromosome than expected by chance. Class I crossovers are dependent on a group of proteins known as the ZMM pathway, due to the *S. cerevisiae* names of the genes comprising the group (ZIP1, ZIP2, ZIP3, ZIP4, Mer3, MSH4, MSH5) (Börner *et al.* 2004). When the *Arabidopsis* homologues of these genes are mutated, disabling the class I crossover pathway, the crossover number drops to ~15% of the wild-type value, suggesting that the class I pathway account for 85% of crossovers in normal plants (Higgins *et al.* 2004; Chelysheva *et al.* 2007; Macaisne *et al.* 2008; Macaisne *et al.* 2011). Many of the ZMM proteins localise to chromatin during lepototene/zygotene and are thought to promote crossovers by counteracting the anti-recombinase activities of non-crossover helicases (Crismani *et al.* 2012; Knoll *et al.* 2012). The plant specific PARTING DANCERS is thought to be a plant-specific ZMM pathway protein, due to the fact it shows an 85% drop in crossover number when mutated, similar to the drop seem in other ZMM mutants, but does not possess animal homologs (Wijeratne *et al.* 2005). MLH1 and MLH3 are also thought to act in the *Arabidopsis* ZMM pathway at a late stage involved with crossover resolution (Jackson *et al.* 2006). In yeast a heterodimer formed by MLH1 and MLH3 is responsible for resolving dHJs into crossovers (Wang *et al.* 1999). *Arabidopsis* MLH3 is specifically expressed during meiosis and localises to foci associated with the chromosome axes during prophase-I. In *mlh3* mutants prophase is extended and recombination is reduced, suggesting that MLH3 plays a similar dHJ resolving role in plants (Jackson *et al.* 2006).

In plants, ZMM proteins such as MSH4, MSH5, ZIP4 and MER3 form numerous foci (typically 100-200) at leptotene, which coincide with RAD51/DMC1 foci. Over the course of prophase-I many of these foci disappear or become restricted to a smaller number of foci (Higgins *et al.* 2004; Wang *et al.* 2009; Shen *et al.* 2012; Luo *et al.* 2013). For example, the ZMM proteins MLH1, MLH3 and HEI10 mark foci at late prophase that are believed to represent the sites of class I crossovers (Chelysheva *et al.* 2010; Chelysheva *et al.* 2012; Wang *et al.* 2012). The number and spacing of MLH1 foci is the same as the number of chiasmata and genetically measured crossovers. Hence, the ZMM components show persistent association with meiotic chromosomes and are required for efficient repair of DSBs as crossovers.

Less is known about the non-ZMM class II pathway. However, one component which has been characterised is MUS81, which forms a nuclease complex with EME1 in yeast capable of cleaving nicked and intact Holliday junctions (Geuting *et al.* 2009). Mutating *Arabidopsis MUS81* reduces crossovers by ~10% compared with wild-type and reduces crossovers by a third in *mus81*-ZMM double mutants (e.g. *mus81 msh4*) (Berchowitz *et al.* 2007). The observation of residual crossovers in *mus81 msh4* double mutants has led to the hypothesis that a third crossover pathway exists, which remains intact after class I and class II inactivation (Berchowitz *et al.* 2007). Along with MUS81, YEN1 and SLX1 are required for resolution of double Holliday junctions in *S. cerevisiae* (Zakharyevich *et al.* 2012). The homologue of YEN1 in plants is GEN1, though whether it plays a role in crossover formation is unknown (Bauknecht & Kobbe 2014). It is thought that these nucleases cleave double Holliday junctions both symmetrically and asymmetrically, leading to equal numbers of non-crossover and crossover events (Nishino *et al.* 2005).

A study in tomato which visualised Class I crossovers using MLH1 immunofluorescence and Class II crossovers by detecting late recombination nodules (characteristic of all crossovers), showed that class II crossovers were higher in the pericentromeric heterochromatin than in the rest of the chromosome (Anderson *et al.* 2014). This study also showed that class I crossovers interfere with class II crossovers, although class II crossovers do not interfere with one another. The strength of Class I-Class II interference was weaker than Class I-Class I interference, spreading over ~8 μm of synaptonemal complex as compared to 13μm (Anderson *et al.* 2014). This suggests the existence of some form of communication between class I and class II crossover

sites.

1.5.2.3 Crossover interference

The mechanism through which crossover interference establishes itself is currently unknown (Mercier *et al.* 2015). A number of models have been proposed which fall into three general categories, based on the nature of the underlying mechanism through which interference is proposed to be established. The three categories are: (i) models which posit a molecular signal spreading along chromosomes (e.g. the polymerisation model and the counting model), (ii) models which posit a biochemical reaction/diffusion process that moves along chromosomes (e.g. the reaction/diffusion model) and (iii) models which posit that interference is established by intrinsic mechanical forces acting on chromosomes (e.g. the chromosome oscillatory movement model and the beam-film model).

The first model proposed to explain crossover interference was the 'polymerisation model', which proposed that a factor would spread bi-directionally from a crossover designated site along chromosomes, inhibiting other DSB sites from becoming designated as crossovers and continuing until it met a similar signal coming from the other direction (King & Mortimer 1990). A similar 'counting model' hypothesised that some molecular entity moved along a chromosome, initially designating a DSB site as a crossover site and then designating a certain number of DSB sites as non-crossover sites, before designating a new crossover site after a certain set number of intervening non-crossover sites had been 'counted' (Foss *et al.* 1993). While both of these models were able to describe certain crossover data sets well, the counting model prediction that tetrads with close double crossovers should be enriched for conversion events that themselves are not associated with crossing over proved to be false when tested in *S. cerevisiae* (Foss & Stahl 1995). In addition to this, there are no obvious candidates for the molecular factor which could perform the roles required in either model, although this does not necessarily invalidate the models.

More recently, the reaction-diffusion model was proposed which envisions the formation of 'contact points' between homologous chromosomes before and during prophase, which are free to undertake random walks along the chromosome, and either mature into crossovers or cancel one another out when two points of contact meet (Fujitani *et al.* 2002). This model is given some

support by the discovery of similar processes in bacterial systems (Han & Mizuuchi 2010; Vecchiarelli *et al.* 2013), although no specific meiotic mechanism has been proposed.

The chromosome oscillatory movement (COM) model proposed that waves set up along a chromosome by oscillation of the telomere bouquet and centromere encourage crossover at nodal sites where homologous chromosomes are in close proximity to one another (Hultén 2011). While this model made a set of predictions about crossover placement and how it would be influenced by mitotic karyotype, bivalent length and frequency of oscillatory movement, it remains currently untested. Another model which relies on the mechanical properties of chromosomes to explain crossover interference is the beam-film model. This model proposes that chromosomes are populated with a certain number of precursor crossover sites and are under stress along their length (Kleckner *et al.* 2004; Börner *et al.* 2004). When crossovers occur they alleviate this stress locally and this alleviation is spread outwards with magnitude of alleviation decreasing with distance (Kleckner *et al.* 2004; Börner *et al.* 2004; Zhang *et al.* 2014). The creators of this model see its most attractive feature as the fact that the redistribution of stress provides an intrinsic way to pattern crossovers as opposed to other models, which require an as yet unidentified signal to be sent along chromosomes (Zhang *et al.* 2014).

1.6 Engineering meiosis

Both research scientists and plant breeders have attempted to manipulate the mechanisms and parameters of meiosis in order to maximise generation of novel or useful outcomes. The most obvious trait over which greater control would be desirable is crossover placement and number. There are a number of approaches plant scientists have discovered capable of modifying the number and/or placement of crossovers which fall into three broad categories; i) exploiting the natural properties of meiosis, ii) using meiotic mutants for their desirable phenotypes and iii) using multiple mutants in combination to engineer novel plant behaviour (Crismani *et al.* 2012). Some examples of these approaches are detailed below.

There are various ways in which our understanding of meiosis suggests ways to manipulate plant material, in order to generate desirable outcomes. For example, in *Arabidopsis* crossover frequency is increased in flowers formed on non-primary branches as well as in plants grown at elevated temperatures (Francis *et al.* 2007). Additionally male crossover rate is 67% higher than

female (Francis *et al.* 2007). These properties could be exploited during crossing, depending on whether a higher or lower number of recombinants was desired. In many plant species including *Arabidopsis*, rice, barley and maize there is also natural variation in crossover rate (Yandeau-Nelson *et al.* 2006; Esch *et al.* 2007; Bovill *et al.* 2009). Discovering the responsible allelles and combining them in a single individual could presumably create a plant with a higher crossover rate than would be expected from a wild-type plant selected at random. Alternatively, low crossover rate alleles could also be stacked to achieve the opposite effect.

Meiotic mutants can be used to manipulate crossover numbers and distribution. In *Arabidopsis msh2* mutants the crossover rate as measured in one interval increased by 40% in a heterozygous situation, consistent with the function of MSH2 as an anti-crossover factor that is dependent on heterology (Emmanuel *et al.* 2006). Additionally, *met1* mutants have been found to remodel the distribution of crossovers from chromosome arms to centromeres (Yelina *et al.* 2012). Perhaps the most striking single mutant is *fancm* which is capable of tripling the crossover rate (Crismani *et al.* 2012). One well characterised mutant that has been used in in plant breeding is the wheat *Ph1* locus. *Ph1* prevents homeologous chromosomes from associating and undergoing crossover (as *Triticum aestivum* is a hexaploid species (Riley & Chapman 1958)). Plant breeders have used the *ph1* mutant to induce homeologous recombination and break linkage between a stem rust resistance gene and secalin, a seed storage protein that leads to quality defects, in a cross between rye and wheat (Anugrahwati *et al.* 2008).

Another approach to engineering meiosis involves combining mutants in order to fundamentally alter the meiotic process. An example of this approach is the ‘mitosis instead of meiosis’ (MiMe) phenotype which was first generated in *Arabidopsis* and has since been transferred to rice and maize (d’Erfurth *et al.* 2009; Mieulet *et al.* 2016; Ronceret & Vielle-Calzada 2015). MiMe plants combine the *spo11-1* mutant, where meiotic DSBs are eliminated, with the *rec8* mutant, in which sister chromatid cohesion is lost, and the *tam* or *osd1* mutants, where the second division of meiosis is skipped (d’Erfurth *et al.* 2009). The combination of these mutants produces plants which produce diploid gametes that are genetically identical to the parent plant. These gametes can then be crossed to haploid inducer lines whose genetic material is lost after fertilisation in order to generate an apomictic population (Britt & Kuppu 2016).

1.7 Project Aims

The following work describes the development of two procedures that alter the natural course of meiosis in ways that could potentially be useful in plant breeding. The first is the generation of SDR plants. These are individuals generated by crossing the diploid gametes of an SDR-mutant with a haploid inducer. This results in the genetic material of the haploid-inducer being lost post-fertilisation, thereby generating plants which contain nuclear genetic material solely from the SDR-mutant parent. The ultimate goal of generating SDR populations is that in a single generation plants could be generated which are mostly genetically homozygous but which retain small regions of heterozygosity. Such individuals would be useful for dissecting epistatic traits in addition to having plant breeding applications (See sections 3.2.2, 3.2.3 and 5.1.4 for details). Two approaches were taken to generating an SDR population. The first approach involved creating an *OSD1* RNAi line in the Columbia accession. In such a line the activity of OSD1 would be reduced, leading to the creation of diploid gametes. It was expected that the penetrance of this phenotype would not be complete and that *OSD1* RNAi plants would also produce some 'normal' haploid pollen. The plan was to use haploid *OSD1* RNAi Col pollen in a cross to a Ler accession plant creating an *OSD1* RNAi Col/Ler hybrid. Diploid pollen from this hybrid could then be crossed to a haploid-inducer plant to create an SDR population. However the first cross of this plan could not be attempted due to the high penetrance of the *OSD1* RNAi construct (See Section 3.3.1 for full details). The second (ultimately successful) approach to generating an SDR population involved backcrossing the *osd1-3* mutation from Col background into a Ler background then crossing *osd1-3* Col and *osd1-3* Ler to generate an *osd 1-3* Col/Ler hybrid. This SDR mutant was then crossed to the GEM haploid-inducer line to generate an SDR population. Of the 169 plants generated via this method, 3 were confirmed as 'true' SDR individuals via conventional genotyping and genotyping by sequencing (GBS) methods (See Sections 3.3.2 and 3.3.3 for full details). In addition to the true SDR individuals a number of other plants were generated with unexpected ploidies and/or genotypes.

The second project described in this work is the targeting of meiotic recombination. This was an effort to direct the location of meiotic crossovers in a *spo11* mutant by using a TALEN to generate exogenous meiotic DNA DSBs. The ability to direct crossover may be useful for determining the mechanisms of crossover interference and homeostasis as well as breaking up linkage groups

during plant breeding. TALENs are artificial proteins comprising a DNA targeting domain and an endonuclease domain making them capable of recognising and binding defined DNA sequences then generating a DSB close to their recognition site. The attempt to direct meiotic crossover involved creating a variety of TALENs which had different numbers of target sites in the *Arabidopsis* genome ranging from tens to millions and transforming these TALENs into *spo11* mutants which are unable to create meiotic DNA DSBs, leading to infertility. It was expected that the DSBs created by the TALENs would compensate for the lack of endogenous DSBs in the *spo11* mutants and restore the fertility of TALEN *spo11* plants. Although fertility was not restored, PCR analysis and western blots confirm that the TALEN constructs were expressed (See section 4.3.3 for details). Additionally the abberant growth displayed by some *spo11* plants transformed with TALENs suggests that TALENs were capable of generating DSBs during meiosis but that these breaks went on to be repaired by mechanisms other than crossover (See Section 4.4 for details).

2. Chapter 2: Materials and Methods

2.1. Arabidopsis Cultivation

2.1.1. *Arabidopsis thaliana* lines

Plant Line	**Source**	**Reference**
Col-0	N/A	(Weigel & Mott 2009)
Ler-0	Franklin Lab, University of Birmingham	(Weigel & Mott 2009)
spo11-1-3 (Col-0 Background)	Franklin Lab	(Alonso *et al.* 2003) (Stacey *et al.* 2006)
osd1-3 (Col-0 Background)	Mercier Lab, IJPB INRA,Versailles, France	(Koncz *et al.* 1992) (Heyman *et al.* 2011)
GFP-Tailswap (Col-0 Background)	Simon Chan and Luca Comai , University of California, Davis, USA	(Ravi & Chan 2010a)
Genome Elimination Line (GEM) (*GFP-Tailswap + GFP-CENH3,* Col-0 Background)	Mercier Lab	(Marimuthu *et al.* 2011)

2.1.2. Growth conditions

2.1.2.1. Growth on soil

Seeds were sown on a soil mix of 5 parts John Innes No. 1 compost to 1 part medium vermiculite. Once sown, seeds were stratified at 4°C in the dark for three nights. After stratification plants were transferred to a growth room and grown at 18°C with a 16-hour light cycle under artificial white light.

2.1.2.2. Growth on agar plates

Seeds were sown on 0.8% MS-agar plates (see appendix for recipe). Seeds were stratified as above and then transferred to Percival growth chambers at 20°C with a 16-hour light cycle.

2.1.2.3. Growth on Liquid Media

Seeds were stratified and grown on agar plates as above. After two weeks they were transferred to small plastic growth chambers with reservoirs. ~50 ml of plant liquid growth media (see appendix) was added to each reservoir. These chambers were then moved to growth rooms with the same conditions as for soil-grown plants above.

2.1.3. Sterilisation of seed

Seeds were placed in 1.5 ml micro-centrifuge tubes and washed in 0.5 ml of 100% ethanol (Sigma) for 2 minutes with occasional mixing. Tubes were then pulse-centrifuged and the ethanol pipetted off. Seeds were then washed in 1 ml dH_2O for 1 minute, spun down and water removed. This wash was repeated a second time. Seeds were then dried for sowing on soil or resuspended in a small amount of dH_2O for sowing on plates.

2.1.4. Crossing *A. thaliana* plants

Plants were crossed at around 5-6 weeks old. Flowers, open buds, immature buds and siliques were removed from the mother plant. Buds of the appropriate size (~1mm) were opened using watchmaker's forceps and immature anthers removed. Following emasculation a flower from the father plant was taken and anthers were applied on the newly exposed stigma of the mother plant until it was covered with pollen. The mother plant was then allowed to generate seeds, which were harvested 2-3 weeks after crossing.

2.1.5. Arabidopsis transformation by Agrobacterium floral dip

A. tumefaciens cells containing binary vectors were generated by electroporation (see protocol below). A single colony was selected and used to inoculate 5 ml of Luria broth (LB, see appendix) with rifampicin (25 µg/ml) and other vector-specific antibiotics. This culture was incubated under agitation in an Infors Multitron shaker (28°C, 200 rpm) overnight. The overnight culture was than transferred to 500 ml of LB broth with rifampicin (12.5 µg/ml) and other vector-specific antibiotics and returned to the incubator for another 24 hours. The resulting culture was then centrifuged at 4°C for 15 minutes at 4000 rpm. The supernatant was discarded and the pellet resuspended in 200 ml of dipping solution (see appendix).

Before dipping, 100 µl of Silwet L-77 was added to the sucrose solution. The inflorescences of plants aged ~6 weeks were then dipped into the solution for 30 seconds. Excess liquid was removed by dripping and the plants were wrapped in cling-film and a bin-bag and left overnight in the dark. The next day the bin-bag was removed and the day following the cling-film was removed and the plants grown under normal growth-room conditions.

2.2. DNA and RNA Protocols

2.2.1. Plant DNA extraction

2.2.1.1. Small scale

Leaf tissue was placed in a 1.5 ml micro-centrifuge tube and ground in 50 µl of extraction buffer (see appendix). More extraction buffer was added to a final volume of 300 µl. The sample was centrifuged for 1 minute at 13,000 rpm and 250 µl of supernatant transferred to a new tube. 250 µl of ethanol was added and the sample was then briefly vortexed. The sample was then centrifuged for 5 minutes at 13,000 rpm. The supernatant was then removed and the DNA pellet allowed to air-dry. DNA was subsequently resuspended in 100 µl of dH_20.

2.2.1.2. Bulk extraction

Plant tissue was collected in 12-row racks of 8 x 1.2 ml microtube strips (Alpha laboratories), 96 samples per rack. A 3 mm glass ball (Sigma) and 300 µl of extraction buffer without SDS (as above, without SDS) was added to each tube. The tissue samples were then disrupted in a TissueLyser II (Qiagen) at 20,000 Hz for 2 minutes. The plates were then pulsed centrifuged to remove liquid from the top of the tubes and 300 µl of extraction buffer with SDS (as above) was added to each well. The racks were then centrifuged at 3000 g for 7 minutes. 200 µl of the resulting supernatant was pipetted off and added to 200 µl of isopropanol in a 96-well, 0.8 ml storage plate (ABGene). The plates were then incubated at room temperature for 10 minutes. Next the plates were centrifuged at 3000 g for 35 minutes. The supernatant from each well was poured off and the plates were blotted on paper towels. The DNA pellets were washed with 70% EtOH which was then poured off and the pellet was allowed to air dry. The dried pellet was resuspended in 150 µl dH_2O.

2.2.2. Plant RNA extraction

RNA was extracted from *Arabidopsis* buds using TRIzol® reagent (Ambion). Frozen bud samples had 1 3mm glass bead added to them and were disrupted in a TissueLyser II (Qiagen) at 20,000Hz for 2 mintues. 1ml of TRIzol was added to the resulting powder and the sample was incubated at room temperature for 5 minutes. Next 0.2ml of chloroform was added and the tube was vortexed for 15 seconds and incubated at room temperature for 3 minutes. The

sample was then centrifuged at 12,000g for 15 minutes at 4°C. The resulting aqueous phase of the sample was transferred to a new tube. 0.5ml of isopropanol was added to the supernatant and it was incubated at room temperature for 10 minutes. The sample was then centrifuged at 12,000g for 10 minutes at 4°C. The supernatant was removed and the pellet washed with 1ml of 75% EtOH. The sample was briefly vortexed and then centrifuged at 7500g for 5 minutes at 4°C. The pellet was then left to air dry and resuspended in 50 µl dH_2O.

2.2.3. cDNA synthesis

0.2 µl of TURBO DNase buffer and 1 µl of TURBO DNase (Thermo) was added to 20 µl of 0.25 µg/µl RNA. The sample was incubated at 37°C for 30 minutes. 0.2 µl DNase inactivation buffer was then added and the sample was incubated at room temperature for 10 minutes. The sample was then centrifuged at 10,000g for 90 seconds. The RNA-containing supernatant was then transferred to a new tube.

cDNA was synthesised using the SuperScript® III First-Strand Synthesis System for RT-PCR (Invitrogen). 10 µl of RNA, 3 µl of dNTPs (10 mM) and 1.5 µl random hexamers (10 mM) were mixed and the sample was made up to 30 µl with dH_2O. The sample was incubated at 65°C for 5 minutes then put on ice. The sample was then split into two 14 µl samples (+RT and -RT control). To each sample was added 4 µl 5X RT buffer, 1 µl DTT (0.1 M) and 1 µl RNase inhibitor. 1 µl reverse transcriptase was also added to the +RT tube. Each sample was made up to 20 µl then incubated at 25°C for 10 minutes (Annealing), 50°C for 50 minutes (cDNA synthesis) then 85°C for 5 minutes (Terminate reaction). Next, 1 µl of RNase H was added to each sample and they were incubated at 37°C for 20 minutes.

2.2.4. Agarose gel DNA electrophoresis

Various concentrations of agarose gel were used depending on the length of DNA that was to be separated. Unless otherwise stated 1% gels were used. Agarose was dissolved in 0.5X TBE buffer (see appendix) in a microwave. The molten solution was then cooled and ethidium bromide added to a final concentration of 0.5 µg/ml or SYBR® Safe DNA Gel Stain (Thermo) added to a concentration of 100 µl/l. The solution was then poured into gel casts and allowed to solidify

DNA samples were mixed with 5X Orange G (See appendix) prior to loading. A 100 bp or 1 kb DNA Ladder (New England BioLabs) was also loaded into a separate well. Gels were run at 100V-250V until the Orange G reached the bottom of the gel. Gels were imaged using a G:BOX gel documentation system (Syngene).

2.2.5. Recovery of DNA from agarose gel

Gels were lit with a UV transilluminator and the desired bands were cut out using razor blades.

2.2.6. Agarose gel RNA electrophoresis

RNA gels were prepared and run identically to DNA gels with the exception that all pipettes, measuring cylinders and casts were first treated with RNaseZap® (Thermo) to prevent contaminating RNase activity destroying the samples.

2.2.7. PCR Protocols

Different PCR systems were used for different tasks.

2.2.7.1. PCR using PCRBIO Taq polymerase

PCRBIO Taq DNA Polymerase (PCRBIOSystems) was used for Col/Ler genotyping of the SDR population. See reaction mix and PCR conditions below.

2.2.7.2. PCR using GoTaq® polymerase

GoTaq® Polymerase with Green Master Mix (Promega) was used for *osd1-3*, *spo11-1-3*, GFP-Tailswap and GEM genotyping reactions. See reaction mix and PCR conditions below.

2.2.7.3. PCR using Phusion® polymerase.

Phusion High-Fidelity DNA Polymerase (Thermo) was used for PCR reactions whose products would be used in cloning. See reaction mix and PCR conditions below.

2.2.7.4. Polymerase reaction mixes and PCR conditions

Polymerase Type	PCRBIO	GoTaq	Phusion High-Fidelity
Buffer Vol. (µl)	2	2	4
Forward Primer (10 µM) Vol. (µl)	0.4	0.4	1
Reverse Primer (10 µM) Vol. (µl)	0.4	0.4	1
DNTPs (10 µM) Vol. (µl)	N/A	1	0.4
Template DNA Vol. (µl)	2	2	1
Polymerase Vol. (µl)	0.05	0.25	0.2
Final Volume (µl)	10	10	20
Denaturation Temp. (°C)	95	95	98
Extension Temp. (°C)	72	72	72

2.2.8. Digestion of DNA by restriction enzymes

Unless otherwise stated all restriction enzymes were sourced from New England BioLabs. All digestions were run in 20 µl volumes containing 2 µl of 10X enzyme-specific buffer, 1 µl of restriction enzyme, varying amounts of DNA and dH_2O to 20 µl.

2.2.9. Purification of amplified and digested DNA

DNA was purified from gels using the QIAquick Gel Extraction Kit (Qiagen).

2.3. Bacterial strains and growth conditions

2.3.1. *E. coli* DH5α

To prepare competent DH5α, *E. coli* a glycerol stock was streaked on an LB agar plate and incubated overnight at 37°C. The next day 5 ml of LB was inoculated with a single colony and allowed to grow for ~16 hours at 37°C with shaking (200 rpm). The following day 200 µl of culture was used to inoculate 100 ml of LB and it was allowed to grow until it reached an OD_{550} of ~0.35. The culture was then cooled on ice for 15 minutes and centrifuged at 3000 rpm for 5 minutes at 4°C. Supernatant was poured off and cells were resuspended in 20 ml of TFB1 (see appendix) and left on ice for 2 hours. The cells were then centrifuged at 2000 rpm at 4°C for 10 minutes. The supernatant was poured off and resuspended in 4 ml TFBII (see

appendix). Cells were then aliquoted into micro-centrifuge tubes and snap-frozen in liquid nitrogen and stored at -80°C.

2.3.2. *E. coli* ccdB Survival

One Shot® *ccd*B Survival™ 2 T1^{R} Competent Cells (Thermo) were used for propagating the pJawohl Gateway® destination vector.

2.3.3. A. tumefaciens

The GV3101 strain was used for all *A. tumefaciens* binary vector transformations.

2.4. Cloning Protocols

2.4.1. Quantification of DNA

2.4.1.1. By NanoDrop®

For estimations of miniprep plasmid DNA concentrations a NanoDrop ND1000 spectrophotometer (Thermo) on 'DNA-50' setting was used.

2.4.1.2. By Qubit®

For precise quantification of DNA a Qubit 1.0® fluorometer was used.

2.4.2. Quantification of RNA

For precise quantification of RNA a Qubit 1.0® fluorometer was used.

2.4.3. Cloning vectors

2.4.3.1. pJawohl

pJawohl:ACT2pro#8 is a 9.8 kb Gateway compatible destination vector used for generating inverted-repeat RNAi constructs. The plasmid contains two attR1 and attR2 recombination sites arranged in an inverted order (i.e. –attR1– attR2–attR2–attR1–). These sites allow an entry vector containing arbitrary sequence between single attL1 and attL2 sites to be recombined into the destination vector twice in an inverted repeat. The plasmid contains an

ampicillin resistance site and also contains ccdB genes between its two attR1-attR2 sites. Normally the ccdB genes produce a topoisomerase II inhibitor that is lethal to the cell however after cloning into these sites the gene is removed giving a way to select for successful recombinants.

To produce final expression vectors the *ACTIN2* promoter was replaced with *35S* and *DMC1* promoters using conventional cloning (See below). Subsequently a 501 bp sequence from the *Arabidopsis OSD1* gene was cloned in as an inverted repeat using the Gateway recombination sites.

2.4.3.2. pBIN GFP4

pBIN GFP4 is a plasmid containing a CaMV 2x35S promoter. It was used as a PCR template to generate *35S* promoter sequence for cloning into pJawohl.

2.4.3.3. pZHY013 (151 and 161)

pZHY013 is an entry vector which allows two TAL arrays to be cloned in front of two *Fok*I heterodimeric nuclease sequences to create a T2A-linked polycistronic message for expression in plants. The left and right TAL arrays are added in by conventional cloning using the *Bam*HI and *Xba*I, and *Nhe*I and *Bgl*II restriction sites respectively. pZHY013 contains a spectinomycin resistance gene for selection. Dr. Natasha Elina modified pZHY013 to generate pZHY013 151 and pZHY013 161. These vectors contain HA or Myc tags respectively upstream of the left TAL-array insertion site in addition to retaining the FLAG tags upstream of the right TAL-array insertion site.

2.4.3.4. pMDC32-HPB

pMDC32-HPB is a Gateway destination binary vector for plant expression. pMDC032-HPB can accept the polycistronic message constructed in pZHY013 and be used for transformation into *Agrobacterium* and subsequent plant transformation. The vector contains the ccdB gene between its gateway recombination sites to allow for selection of successful recombinants. The vector also contains kanamycin and hygromycin resistance genes for selection in bacteria and plants respectively.

Dr. Natasha Elina generated a series of pMDC32-HPB vectors with modified promoters as listed below.

pMDC32-1 *DMC1* promoter.

pMDC32-19 *SPO11-1* promoter.

pMDC32-101 *SPO11-1* promoter with translational fusion (promoter includes translation start site and first three SPO11 amino acids).

pMDC3-112 *DMC1* promoter with translational fusion (promoter includes translation start site and first two DMC1 exons).

2.4.4. Conventional cloning

2.4.4.1. Ligation reactions

All ligation reactions were performed using T4 DNA ligase (Roche). 1 µg of digested DNA (insert and vector) were added to 3 µl of 10X ligation buffer, 1 µl of T4 DNA Ligase and made up to 30 µl with dH_2O. The sample was then incubated at 4°C overnight. The next day the ligase was heat-inactivated by incubation at 65°C for 10 minutes. The sample was then used for transformation.

2.4.4.1.1. Ligation of *35S* promoter into pJawohl

A 2x35S promoter was amplified by PCR from pBIN GFP4 using the primers PLD101 and PLD102 (see appendix). These primers added *Asc*I and *Xho*I restriction sites to the amplified product. Both the *2x35S* amplification product and pJawohl plasmid were digested with *Asc*I and *Xho*I (this removed the *ACTIN2* promoter from pJawohl) and PCR purified. The *2x35S* promoter was then ligated into pJawohl.

2.4.4.1.2. Ligation of TAL arrays into pZHY013

TAL arrays assembled in the pZHY500 destination vector (see below) were digested using *Bam*HI and ligated into pZHY013.

2.4.5. Golden Gate cloning

The ‘Golden Gate TALEN and TAL Effector Kit 2.0’ developed by the Voytas lab, University of Minnesota (Cermak *et al.* 2011) and sourced from the Addgene plasmid repository

(https://www.addgene.org/taleffector/goldengatev2/#kit-details) was used to generate TAL arrays.

2.4.5.1. pNS plasmid

The pNS plasmid which allows construction of TAL arrays with the 'degenerate' NS repeat variable di-residue (RVD) is not part of the standard kit and was obtained from the Voytas lab and created by A.J. Bogdanove (Cornell University) and C. Schmidt (Iowa State University).

2.4.5.2. Cloning TAL arrays

The desired TAL array sequence was decided and plasmids for the first 10 RVDs were combined by golden gate cloning into the pFUS_A plasmid. The RVDs from position 11 to N-1 (where N is total number of RVDs in the array) were combined into pFUS_B#N-1 (e.g. if final TAL array was 15 RVDs long pFUS_B14 would be used) also by golden gate cloning. The reaction mix for this golden gate step was as follows. 150 ng of each RVD vector, 150 ng of pFUS vector, 1 µl *Bsa*I, 1 µl T4 DNA ligase, 2 µl 10X T4 DNA ligase buffer, dH_2O to 20 µl. The samples were then incubated in a PCR cycler on this cycle; 10x(37°C/5 min + 16°C/10 min) + 50°C/5 min + 80°C/5 min. Following cycling, 1 µl ATP (10 mM) and 1 µl Plasmid-safe nuclease (Epicentre) were added to each sample. The samples were then incubated at 37°C for 1 hour. The samples were then transformed into DH5α *E. coli* and plated on Spec (50 µg/ml) IPTG (0.5 mM) X-gal (80 µg/ml) plates.

The following day, white colonies were checked by colony PCR using the primers pCR8_F1 and pCR8_R1 (see appendix). Correct clones were inoculated in 5 ml LB media with spectinomycin and grown overnight. The next day pFUS_A(+10RVDs) and pFUS_B(+11-(N-1) RVDs) were mini-prepped and combined with pLR-XX (Where XX= the last RVD of the TAL array) into the destination vector pZHY500. The reaction mix for this step was as follows. 150 ng of each pFUS vector, 150 ng of pLR-XX vector, 75 ng of pZHY500 vector, 1 µl Esp3I, 1 µl T4 DNA ligase, 2 µl 10X T4 DNA ligase buffer, dH_2O to 20 µl. The samples were then incubated in a PCR cycler on this cycle; 37°C/10 min + 16°C/15 min + 37°C/15 min + 80°C/5 min. The samples were then transformed into DH5α *E. coli* and plated on Carb (50 µg/ml), IPTG (0.5 mM), X-gal (80 µg/ml) plates.

The following day, white colonies were checked by colony PCR using the primers TAL_F1 and TAL_F2 (see appendix). Correct clones harbouring vectors with complete TAL arrays were inoculated in 5 ml LB media with carbomycin, incubated overnight at 37°C and the vector isolated via miniprep.

2.4.5.3. Cloning TAL arrays into entry vector

TAL arrays in pZHY500 were cloned into the pZHY013 entry vector by conventional cloning. Left and right arrays were cut from pZHY500 using *Xba*I and *Bam*HI. Right arrays were ligated into pZHY013 which had been digested with *Nhe*I and *Bgl*II. pZHY013 with the right array ligated was then digested with *Xba*I and *Bam*HI and the left array ligated into the vector.

2.4.6. Gateway® cloning

2.4.6.1. Cloning TAL arrays into binary vector

pZHY013 containing left and right TAL arrays upstream of *FokI* heterodimeric nucleases was cloned into the pMDC32 binary vector using Gateway® LR Clonase® II Enzyme Mix (Thermo). 150 ng of entry clone (pZHY013) and destination vector (pMDC32) were combined and made up to 8 µl with TE buffer (see appendix). Gateway® LR Clonase® II Enzyme Mix was thawed on ice for two minutes and briefly vortexed. 2 µl of Clonase mix was added to the sample and it was incubated at 25°C for 1 hour. Next, 1 µl of Proteinase K solution was added to the sample and it was incubated at 37°C for 1 hour. The sample was then used to transform DH5α *E. coli.*

2.4.6.2. Cloning of 501bp *OSD1* fragment into pJawohl

A 501 bp section of the *A. thaliana OSD1* gene was amplified using the primers PLD103 and PLD104 (see appendix). The amplified fragment has CACC sequences at both ends which allow for it to be cloned into the pENTR™ vector using the pENTR™ directional TOPO® Cloning Kit (Invitrogen). 2 µl of fresh PCR product was mixed with 1 µl of pENTR mix and incubated at room temperature for 5 minutes. The sample was then used to transform DH5α *E. coli.* Once the *OSD1* fragment was cloned into pENTR it could be recombined into pJawohl to generate an inverted repeat using Gateway® LR Clonase® II Enzyme Mix as above.

2.4.7. Heat-shock transformation of competent *E. coli* cells

5 µl of plasmid DNA was added to 50 µl of *E. coli* cells (DH5α or ccdB survival) and incubated on ice for 10 minutes. Cells were then heat-shocked at 42° for 1 minute then returned to ice for 5 minutes. 500 µl of LB were then added to the sample which was then incubated with shaking at 37° and 200 rpm for 1h. Cells were plated on agar plates containing the relevant compounds for antibiotic and blue/white colony selection if required.

2.4.8. Electroporation of electro-competent *A. tumefaciens* cells

50 µl of *A. tumefaciens* GV3101 was thawed on ice for 10 minutes. Binary vector solutions were diluted 20-100X then 1 µl of solution was added to the cells. The sample was then transferred to an electroporation cuvette with a 0.1 cm gap (BioRad) and electroporated using a Gene Pulser Xcell (BioRad) at settings 2.5 kV, 25 µFD, 400 Ω. 500 µl of SOC (see appendix) was then added to the sample and it was transferred to an micro-centrifuge tube. The sample was then incubated at 28°C for 1 hour. 10 µl of sample was then spread on an agar plate containing rifamycin (50 µg/ml), gentamicin (25 µg/ml) and the relevant selective antibiotics for the binary vector and the plate was incubated at 28°C for 2-3 days.

2.4.9. Bacterial growth media

All media was prepared using dH_2O and sterilised by autoclave. Recipes for SOC and LB media and plates can be found in the appendix. Agar plates were poured to a depth of ~5 mm and stored at 4°C prior to use. All inoculations and plating was performed under aseptic conditions in a laminar flow hood.

Liquid *E. coli* cultures were grown in an Infors Multitron shaking incubator at 37°C, 200 rpm for ~16 hours. Liquid *A. tumefaciens* cultures were grown at 28°C, 200 rpm for ~40 hours. Plated *E. coli* cultures were grown in an incubator at 37°C for ~16 hours. Plated *A. tumefaciens* cultures were grown at 28°C for ~40 hours.

2.4.10. Colony PCR

Colony PCR was used to test the correct assembly of TAL arrays. Sterile pipette filter tips were used to transfer a small amount of cells from a single colony into a micro-centrifuge

tube containing 100 µl of dH_2O. The sample was then incubated at 95°C for 10 minutes. The resulting solution was then used as a template DNA sample for PCR reactions.

2.4.11. Purification of plasmid DNA

Plasmid DNA was purified from *E. coli.* and *A. tumefaciens* liquid cultures using the QIAprep Spin Miniprep Kit (Qiagen) and other similar kits.

2.4.12. DNA sequencing

Sanger sequencing of plasmid DNA was performed by Source BioScience and Beckman Coulter Genomics. For each sequencing reaction, 2 µl of primer at 5 mM and 5 µl of plasmid at 100 ng/µl was supplied.

2.4.13. Sequence analysis

Sequencing results and plasmid maps were analysed using A Plasmid Editor (ApE) software (www./biologylabs.utah.edu/jorgensen/wayned/ape/). Vector map graphics were generated using the Benchling suite (www.benchling.com). The *Arabidopsis* information resource (TAIR) website was used as a source of various genetic and molecular biology data from *Arabidopsis* (www.arabidopsis.org). TAIR was also used to perform BLAST searches against the *Arabidopsis* reference genome.

2.5. Flow cytometry protocols

2.5.1. Isolating pollen

1 ml of pollen sorting buffer (see appendix) was added to *Arabidopsis* flowers. The sample was incubated at room temperature for 5 minutes. The sample was then vortexed and the liquid removed using a pipette. The liquid was then passed through a 70 µm strain (Fisher) then centrifuged at 450g for 2 minutes. The supernatant was removed and the pellet resuspended in 15-30 ml of pollen sorting buffer without triton. The sample was then centrifuged at 450g for 2 minutes. The majority of the supernatant was then poured off leaving ~1 ml of buffer left in which the pellet was then resuspended.

2.5.2. Isolating plant nuclei

Plant nuclei for use in ploidy analysis were isolated from *Arabidopsis* leaf tissue. Leaf tissue was placed in a Petri dish and covered in 0.5 ml Galbraith buffer (see appendix). A razor blade was then used to repeatedly cut the leaf until it was reduced to a pulp. The pulp was then strained through a 40 µm filter (Fisher).

2.5.3. Propidium iodide staining of nuclei

Propidium iodide was added to isolated nuclei in Galbraith buffer to a final concentration of 20 µg/ml. The samples were then vortexed and incubated on ice for five minutes.

2.5.4. Measuring ploidy of propidium iodine stained nuclei

Nuclei were assayed using an Accuri C6 flow cytometer (Beckson Dickson) equipped with a 488 nm laser and a 585/40 filter (FL-2). Data was analysed using BD Accuri C6 software. A gate was set up with the following boundaries; SSC-H 10^2 – $10^{6.5}$, FL2-H 10^4 – $10^{5.6}$. This gate captured all stained nuclei while excluding noise. Each sample was run until 30,000 events were captured within this gate. Count vs. FL2-H (logarithmic) was plotted for each sample which gives several peaks which correspond to the ploidy level of the cell. In a wild-type sample the smallest peak will correspond to cells with 2n ploidy with the next peak being 4n and the next 8n. These higher ploidy peaks are the result of endoreduplication within cells.

2.6. Protein Protocols

2.6.1. Protein extraction from bud tissue

Buds were harvested from *Arabidopsis* and flash frozen in liquid nitrogen. 100 µl of protein extraction buffer (see appendix) was added and the sample was ground with a pestle. The sample was vortexed then centrifuged at 13,000 rpm for 5 minutes. The supernatant was then transferred to a 1.5 ml micro-centrifuge tube.

2.6.2. SDS-PAGE gel electrophoresis

An equal volume of SDS-PAGE sampling buffer (see appendix) was added to the protein sample isolated above. The sample was then boiled for 5 minutes. Precast TBE gels (Invitrogen) were used for electrophoresis. The gel was submerged in 500 ml of running

buffer (NuPage® MES SDS Running Buffer) and 5 µl of pre-stained protein ladder (NEB) was loaded in the first well. The gel was run at 180V for 90 minutes.

2.6.3. Western blotting

Gels were released from their casing and the stacking gel removed. A transfer tank apparatus was then assembled (BioRad). A PVDF membrane was cut to the size of the gel and activated by dipping in 100% methanol for 1 minute. The SDS-PAGE gel was rinsed in transfer buffer (1X Buffer stock solution, 20% (v/v) methanol). A stack was created consisting of a sponge pre-soaked in transfer buffer, a layer of 3 mm blotting paper soaked in transfer buffer, the activated PVDF membrane, the SDS-PAGE gel, another paper layer and a final sponge layer. This stack was placed in the transfer tank holder and placed inside the western blot apparatus. An ice-block was added to the tank and it was run at 100V for 1 hour in a 4°C fridge.

After transfer, the membrane was incubated for 60 minutes in 5% milk TBS-T (see appendix). The membrane was then washed three times in TBS-T and incubated in 5% milk TBS-T with primary antibodies (6000x dilution) overnight at 4°C. The membrane was then triple washed in TBS-T then incubated with secondary antibodies (8000x dilution) in 5% milk TBS-T for 60 minutes. The membrane was then triple washed with TBS-T, dried and used for imaging.

2.6.4. Imaging

Proteins were imaged using Amersham ECL Prime Western Blotting Detection Reagent (GE Healthcare) according to the manufacturer's instructions. Blots were exposed on Amersham Hyperfilm ECL (GE) and developed using an X-OMAT 1000 (Kodak).

2.7. Irradiation protocols

X-ray irradiation of plants was performed using a CellRad (Faxitron) machine as an X-ray source.

2.8. Toluidine blue staining

To prepare toluidine blue stained meiotic tetrads *Arabidopsis* buds of ~0.5 mm were harvested and opened with a pair of watchmaker’s forceps. All primordial sepals were removed and the anthers were isolated. A small drop of 0.1% w/v toluidine was added and the anthers were

squashed between two microscope slides. Tetrads were then visualised using a light microscope.

Appendix 1: Growth media and buffer recipes

Agar plates
0.8% Agar
0.44g/l Murashige & Skoog medium inc. vitamins (Duchefa Biochemie)
pH 5.7 (adjust with KOH)

Dipping solution
5% sucrose
0.5g/l MES
pH 5.5

Extraction buffer
200 mM Tris-HCL
25 mM EDTA
250 mM NaCl
0.5% (w/v) SDS

Galbraith buffer
45 mM MgCl
20 mM MOPS
30 mM Sodium citrate
0.1% (v/v) Triton

Orange G
2 g/l Orange G
400 g/l Sucrose

Plant liquid growth media
0.44 g/l MS Media inc. vitamins
3.5 mM MES
pH 5.7 (KOH)

Pollen sorting buffer
10 mM CaCl
1 mM KCl
2 mM MES
5% (w/v) Sucrose
0.1% (v/v) Triton
pH 6.5 (adjust with NaOH)

Protein extraction buffer
50 mM Tris-Cl
100 mM NaCl
10 mM $MgCl_2$
1 mM EDTA
10% (w/v) glycerol
1 mM PMSF
1 mM DTT
1X Complete protease inhibitor (Roche)

SDS-PAGE sampling buffer
0.08 mM Tris-Cl
2% (w/v) SDS
10% (v/v/) glycerol
0.01% (w/v) bromophenol blue

SOC
0.5% (w/v) Yeast extract
2% (w/v) Tryptone
10 mM NaCl
2.5 mM KCl
10 mM $MgCl_2$
10 mM $MgSO_4$
20 mM Glucose

TBE (1X)
90 mM Tris base
90 mM Boric acid
2 mM EDTA

TBS
50 mM Tris-HCl
150 mM NaCl

TBS-T
As above plus;
1 ml/l Tween-20

5% milk TBS-T
As above plus;
50 g/l dried skimmed milk

TE buffer
10 mM Tris-HCl
1 mM EDTA
pH 8.0 (Adjust with HCl)

TFBI
30 mM Potassium acetate
100 mM Rubidium chloride
10 mM Calcium chloride
50 mM Magnesium chloride
15% (v/v) Glycerol
pH 5.8

TFBII
10 mM MOPS
75 mM Calcium chloride
10 mM Rubidium chloride
15% (v/v) Glycerol
pH 6.5

Appendix 2: Primers

PLD 001	gtcggtatccatggcgttccctctagataacgcaggatccatggagggaaaattcgctatttcag
PLD 002	ccctctccgccgccggaccttcaaggagagcttacttcacgacg
PLD 003	tattccttctaagattcgtcgtgaagtaagctctccttgaaggtccggcggcggagagggcaga
PLD 004	agtcctgaactttcctccatagatctaagcttactagctagccggcaccccgtgaatg
PLD 005	ggcattcacggggtgccggctagctagtaagcttagatctatggaggaaagttcaggactatca
PLD 006	ctttgtacaagaaagctgggtcgaattcgcccttctattattatatgtatttgccttgcacgatc
PLD 007	taatagaagggcgaattcgaccca
PLD 008	ggatcctgcgttatctagagggaa
PLD 009	atggagggaaaattcgctatttca
PLD 010	tcaaggagagcttacttcacgacg
PLD 011	atggaggaaagttcaggactatca
PLD 012	ttatatgtatttgccttgcacgat
PLD 013	tatataggatccatggagggaaaattcgctatttca
PLD 014	atatatcggccgtcaaggagagcttacttcacgacg
PLD 015	atatatcggccgaggtccggcggcggagagggcaga
PLD 016	tatatacggccggaaattgatttcaccattgttgaa
PLD 017	taatagctgcagaagggcgaattcgaccca
PLD 018	atatatctgcagctattaaaagtttatctcgccgtt
PLD 019	ttattaagatctatggaggaaagttcaggactatca
PLD 020	ttaattctgcagctattattatatgtatttgccttgcacgat
PLD 021	cttcaccatggattataaggatca
PLD 022	agatcatgacatcgattacaagga
PLD 023	tccttgtaatcgatgtcatgatct
PLD 024	tttattttgactgatagtgacctg
PLD 025	gctcatcaatttgttgcaacgaac
PLD 026	tccgcagtggatggcggcctgaag
PLD 027	tgagcgtcagaccccgtagaaaag
PLD 028	tattaccgcctttgagtgagctga
PLD 029	ttgaaacgatgttgaaaagagggg
PLD 030	cctccacgtcaccgcatgttagaa
PLD 031	actggtaaaagagcggaaattgaa
PLD 032	tgcaacaaattgatgagcaattat
PLD 033	ttatattgatcaatggaggaaagttcaggactatca
PLD 034	aatatatgatcaaagcttactagctagccggcaccc
PLD 035	acggtgaccgtaaggcttgatgaaacaacgcggcgagcttagatcaacgacctttttggaaacttc
PLD 036	gagagagatcggagatagctggat
PLD 037	attttgaactccccagatccagctatctccgatctctctctcatcaataggaagagaagcaatagt
PLD 038	aagctcgccgcgttgtttcatcaa
PLD 039	acggtgaccgtaaggcttgatgaaacaacgcggcgagcttaaatcaacgacctttttggaaacttc
PLD 040	ttaagctcgccgcgttgtttcatcaa
PLD 041	ggtgaccgtaaggcttgatgaaacaacgcggcgagcttaaatcaacgacctttttggaaacttcg
PLD 042	aagctcgccgcgttgtttcatcaa
PLD 043	cctgaatttatggctatggaagctcctggaattagaatggagggaaaattcgctatttcag
PLD 044	tctaattccaggagcttccatagccataaattcaggcaccttcctcttcttcttggggtc
PLD 045	tgtggtctcaattgccggaccgaggagtacggggttttagagctagaaatagcaag
PLD 046	tgtggtctcaattatcacgtcgtgaacacgcacgttttagagctagaaatagcaag

PLD 047	tgtggtctcaattgccttcacctagagttgtgggttttagagctagaaatagcaag
PLD 048	tgtggtctcaattggaggctaatgactgtcaaggttttagagctagaaatagcaag
PLD 049	tgtggtctcaattcgccgataacgtcctcaatggttttagagctagaaatagcaag
PLD 050	tgtggtctcaattctacatcaccgtcagctcgcgttttagagctagaaatagcaag
PLD 051	tgtggtctcaattaagccaagagttgagattgggttttagagctagaaatagcaag
PLD 052	tgtggtctcaattgaatatctctctatctcctcgttttagagctagaaatagcaag
PLD 053	tgtggtctcaatt ggaagtgagtagcatcgaat gttttagagctagaaatagcaag
PLD 054	tgtggtctcaattttgggtcataacgatatctcgttttagagctagaaatagcaag
PLD 055	tgtggtctcaagcgtaatgccaactttgtac
PLD 056	taccagtttgaaccatcagtgaca
PLD 057	atgttcataaatgagaggtcagga
PLD 058	ggtgcgatttctccagcagtaaaaatc
PLD 059	ctgagaagatgaagcaccggcgatat
PLD 060	cacatactcgctactggtcagagaatc
PLD 061	ctgaagctgaaccttcgtctcg
PLD 062	aatccagatcccccgaatta
PLD 063	cagcagaacacccccatc
PLD 064	ctgagaagatgaagcaccggcgatat
PLD 065	cgcagccatcaaacaaagtca
PLD 066	tacgatgtgcctgactacgc
PLD 067	tctggcaacgccgtgattat
1-10655-F	ttgtggtccctggctaatca
1-10655-R	cagtgacgaattccaaaacga
1-16908-F	gcacagaaagacaaacccaaag
1-16908-R	cgaccagcaaggttgttcttag
1-20154-F	tcccaactggtaatgatatttattttc
1-20154-R	ccgaatcaaaatcggaatctt
1-23477-F	tgcttttccttttaatcttttctca
1-23477-R	tgatgatttgttttaatccgctca
1-27077-F	atcggaatgcggaagacact
1-27077-R	ccacccagccttcctcctat
1-30413-F	ccagccacagcttctttctga
1-30413-R	ttgattgaataatggttcttgtgatga
2-132-F	tccaatgggccacaaattaac
2-132-R	tttgtgctttgattactgcaagtg
2-6276-F	tcaagagatttcaaataaaaaccaaa
2-6276-R	aaacctaaaatcaaagcataaacca
2-9391-F	cggtcactgtgaggtcattg
2-9391-R	tttttggtcatcggtacttgg
2-11995-F	tatgtcaagcccgtgggtta
2-11995-R	ccgagccagctcactttagtc
2-15964-F	tgcagcactgtgttttaattttagtc
2-15964-R	tttgagtttgttgaccctgagaa
2-19311-F	tttctgccaatgatttaaagtaacg
2-19311-R	cagcgctgatgcaaaggtaa
2-19554-F	cacacgaatattgattgtctaagga
2-19554-R	aggctactcggtcaaagcaa

3-2718-F	acaactgggcgactcacctt
3-2718-R	cgtaaacacaaactgcgaggt
3-5704-F	tctttggatgcatcatggac
3-5704-R	gacgcgatcccaagaactgt
3-9404-F	aacggtccaggttcctcctc
3-9404-R	ttggttttaaggctctggaatca
3-10695-F	gagggatgcaaggaggatca
3-10695-R	ttcatcacatcaacgctccaa
3-12356-F	ctacgcccggtgtatttgga
3-12356-R	gcttgtgaggctatgtggctta
3-17088-F	gctcttgaggttttagggttgtt
3-17088-R	tgcgttcgcatgattcaaaa
3-19165-F	tacgtcgccctcgaagaaat
3-19165-R	gcgctacatacgcaccacat
3-21008-F	ccgacgttgtgtttctatttcc
3-21008-R	tgagggaacaaggacctaacca
3-23040-F	tgctacgacacgcaaacaca
3-23040-R	cgacttctcctgtggtaagtcttg
4-1313-F	tgcgactaataaccgttgga
4-1313-R	tgatttgtgacgagagtttgct
4-1782-F	tggttgatttcacttgattttga
4-1782-R	cttcccatcacgacttctctct
4-4371-F	atttgccacatccaacaaca
4-4371-R	tcaagtacgttaaaggatcagaaca
4-8358-F	ggattgtgtccccattccta
4-8358-R	gagagtttcgtgtggcatgtt
4-11840-F	atttacggcggttcttgatg
4-11840-R	tttttgggttccaacaatgtaa
4-12848-F	ctccaagctccttgttttgg
4-12848-R	aatcgtccggtcaatctgag
4-18510-F	tgacggcagattcagagaga
4-18510-R	agggaggacgaagaatgagg
5-53-F	tctgcatgggaaatctctgg
5-53-R	ggaaattatagaaagacggaagtgc
5-7064-F	actggcctcgcctttcacta
5-7064-R	aatcacaactgtgccctcgtt
5-10406-F	tgtataattagagccgttcgtcgt
5-10406-R	ttttgaaactatccaaattacccaaa
5-13155-F	gcggacaatgaactgatgga
5-13155-R	ttcgccttagaaattctgccta

3 Chapter 3: Generating an *Arabidopsis thaliana* second division restitution population

3.1 Abstract

Second division restitution (SDR) describes situations where diploid gametes are produced due to omission of the second meiotic division, for example *osd1* in *Arabidopsis*. SDR gametes can be combined with haploid-inducer lines, in order to generate diploid SDR populations, which show unique genetic properties. Arabidopsis haploid-inducer lines are available that have a modified CENH3 gene which causes them to generate haploid gametes that undergo fertilisation normally, however, in the resulting zygote the chromosome set donated by the haploid-inducer is then eliminated. In this study diploid pollen produced by a Col/Ler hybrid *osd1-3* mutant was crossed with a GEM haploid-inducer line, with the aim of producing an SDR population. The resulting population was then characterised using manual and genotyping-by-sequencing (GBS), in addition to ploidy analysis. I observed that SDR individuals were generated at very low efficiency (1.2%) with the remaining members of the population displaying varying haploid, aneuploid and hybrid diploid genotypes. This result confirms that this strategy of SDR production is viable, but will require optimisation in order to generate SDR individuals in sufficient numbers for use in genetic experiments or breeding programs.

3.2 Introduction

3.2.1 Project aim: Combine *osd1* and haploid inducer mutants to generate an SDR population

In this project the properties of *osd1* mutants (also known as second division restitution (SDR) mutants) and haploid inducer lines were combined in order to create a population with a novel genetic structure. The strategy used was as follows; diploid pollen produced by *osd1* mutants was crossed to haploid egg cells from a haploid-inducer line, in order to generate diploid plants whose nuclear genetic material came entirely from one parent, yet which had undergone meiotic recombination (in this case in the paternal parent) (Marimuthu *et al.* 2011;

Mieulet *et al.* 2016). This genetic structure arises as following fertilisation, the single set of chromosomes contributed by the maternal haploid-inducer egg cell, experience anaphase lag and loss due to an altered CENH3 variant present at their centromeres (d'Erfurth *et al.* 2009; Mieulet *et al.* 2016). This causes the haploid-inducer chromosomes to be lost during early embryonic development, reducing zygote ploidy from triploidy (immediately following fertilisation) to diploidy, with only paternally inherited chromosomes remaining in the mature plants (Marimuthu *et al.* 2011; Tan *et al.* 2015; Mieulet *et al.* 2016).

For this project, I created an F_1 Columbia/Landsberg *erecta* (Col/Ler) hybrid with *osd1-3 -/-* genotype, which generates diploid pollen (d'Erfurth *et al.* 2009; d'Erfurth *et al.* 2010). I then crossed this to a GEM haploid-inducer line (Marimuthu *et al.* 2011), to generate an SDR population. Because meiosis-I, and therefore crossover, proceeds as normal in *osd1* SDR mutant plants (d'Erfurth *et al.* 2009), this population is expected to be isogenic for Col or Ler genotyping markers for most of the length of its chromosomes, but to show regions of Col/Ler heterozygosity. The location of heterozygous regions are determined by crossover positions occurring between the homologs during prophase-I of the *osd1* meiosis.

The novel genetic structure of SDR populations, compared to backcross populations, can be visualised graphically (Figure 3.1). In this figure the creation of an SDR individual is contrasted with the creation of an F_1 Col/Ler backcross to Col. The resulting backcross is the closest approximation of the genetic structure of an SDR population it is possible to achieve with conventional breeding approaches (Figure 3.1). It is useful to consider chromosomes as comprising two halves, one from the 'north' telomere of the chromosome to the centromere and another from the centromere to the 'south' telomere of the chromosome (Figure 3.1A). Assuming a single crossover per set of four sister chromatids at meiosis-I, SDR individuals will posses chromosomes where one half is always homozygous for either Col or Ler. The other half will comprise a homozygous stretch continuing from the first half and then a heterozygous stretch, which has been created by the crossover (Figure 3.1G). In contrast, in the conventional backcross a greater variety of homo- and heterozygous stretches will be observed due to the fact that haploid gametes have been generated by the random segregation of sister chromatids (Figure 3.1E). This leads to two main differences in genetic structure between the SDR and backcross populations; (i) not every chromosome pair in a backcross

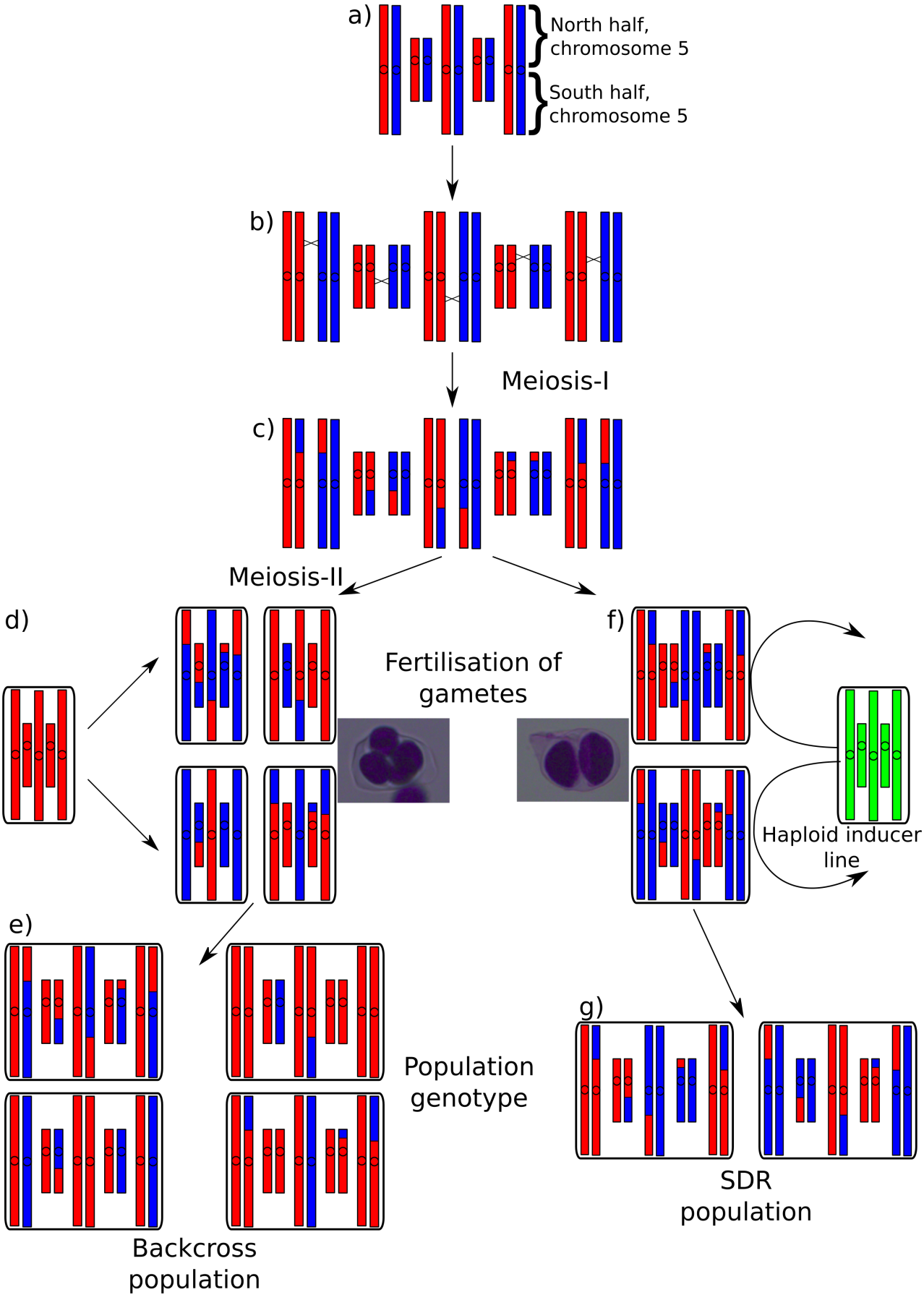
a)
North half, chromosome 5
South half, chromosome 5
b)
Meiosis-I
c)
Meiosis-II
d)
Fertilisation of gametes
f)
Haploid inducer line
e)
Backcross population
Population genotype
g)
SDR population

Figure 3.1: Schematic of backcross and SDR population generation. a) *Genetic structure of the chromosomes of a Col/Ler F_1 hybrid plant with Col sequence shown in red and Ler in blue. The 'north' and 'south' halves of chromosome 5 are also marked. In germ-line cells the plant replicates its chromosomes prior to meiosis.* ***b)*** *After chromosomes are replicated homologous partners undergo recombination and crossover.* ***c)*** *In wild-type plants chromosomes are segregated twice giving rise to haploid gametes (see (d)), whereas in SDR mutants only one division takes place giving rise to diploid gametes (see (f)).* ***d)*** *To produce a backcross population the four haploid gametes produced by a single wild-type meiosis are shown backcrossed to homozygous Col. Inset is shown a toluidine blue stained wild-type tetrad produced by meiosis).* ***e)*** *Genetic structure of a backcross population is shown. Note how some chromosomes are completely homozygous for Col, while some are completely Col/Ler heterozygous and some are majority Col/Ler heterozygous with small regions of homozygosity. These are genotype configurations not seen in an SDR population.* ***f)*** *To produce an SDR population the two diploid gametes produced by a single SDR meiosis are crossed to a haploid inducer. The curly arrow indicates that the haploid-inducer chromosomes are lost from the zygote post-fertilisation. Inset is a picture showing a toluidine blue stained SDR dyad produced by SDR meiosis.* ***g)*** *Genetic structure of an SDR population is shown. Note that every chromosome pair has one 'half' which is homozygous for either Col or Ler, while the other half is partially homozygous with a heterozygous region that varies in size depending on where the site of crossover occurred in the SDR parent.*

would be expected to show a switch from homozygosity to heterozygosity, for example, compare chromosome 1 between the individuals in 3.1E, and (ii) that some chromosomes have the potential of having one of their halves completely heterozygous, while showing a switch to homozygosity in their other half. For example, compare chromosome 4 between the individuals in 3.1E. This last feature is essentially a reversal of what is expected for all chromosomes in an SDR individual (Figure 3.1G). The ability to reliably create SDR populations would have both pure- and applied-science applications. The heterozygous regions present on each chromosome will segregate further in subsequent generations. This would generate recombinant inbred backgrounds with regions of residual heterozygosity, which will allow for the study of complex epistatic and quantitative traits in segregating families. SDR approaches also generate lines with useful combinations of genetic variation in less generations than would be required by conventional breeding approaches, providing a time advantage.

3.2.2 SDR mutants fail to undergo the second division of meiosis

In plants the tight control of cyclin-CDK activity by cyclins is important during meiosis (Wijnker & Schnittger 2013). As discussed, during meiosis a single round of genome duplication is followed by two rounds of cell division (Wang *et al.* 2004; Bulankova *et al.* 2013). This is in contrast to the mitotic programme of one round of duplication followed by one round of cell division. This requires cyclin-CDK activity to build to a maximum at the beginning of MI (as in M-phase in mitosis), cyclin-CDK activity then dips slightly, moving the cell through MI and into interkinesis. Cyclin-CDK activity then builds again triggering meiosis-II (Figure 3.2). Following meiosis-II cyclin-CDK activity drops to a minimum, ending meiosis and leaving the resulting gametes with the cyclin-CDK activity level of a G1-phase cell (Wijnker & Schnittger 2013). *Arabidopsis* possesses five cell-cycle CDKs (CDKA;1, CDKB1;1, CDKB1;2, CDKB2;1 and CDKB2;2) and 30 cyclins (Vandepoele *et al.* 2002; G. Wang *et al.* 2004), making it challenging to determine which combinations of cyclin and CDK are important for meiotic progression. However, there is evidence suggesting CDKA;1, which shows the most similarity to animal CDK1 and CDK2, is involved in meiotic progression due to the fact it localises to meiocytes throughout meiosis (Oa *et al.* 2010; Nowack *et al.* 2012), and that weak loss-of-function alleles are sterile due to a loss of

coordinated chromosome segregation during meiosis (Dissmeyer *et al.* 2007).

Failure to increase cyclin-CDK activity following meiosis-I can lead to premature exit from meiosis in Arabidopsis. Two genes in *Arabidopsis* have been found to give rise to this phenotype when mutated: the cyclin CYCA1;2 (also known as TARDY ASYNCHRONOUS MEIOSIS (TAM)) (d'Erfurth *et al.* 2010) and OMISSION OF SECOND DIVISION 1 (OSD1, also known as GIG1) (d'Erfurth *et al.* 2009; Iwata *et al.* 2011). OSD1 is thought to act as an APC/C inhibitor (Cromer *et al.* 2012). The APC/C is a multi-subunit E3 ubiquitin ligase which marks proteins, including cyclins (King *et al.* 1995; Irniger *et al.* 1995), for degradation by the proteasome in both meiosis and mitosis (Lin *et al.* 2014). In *osd1* mutants meiotic cells progress through meiosis-I normally, undergoing recombination and crossover between homologs, which then segregate to opposite poles of the cell. However, instead of then undergoing meiosis-II and segregating sister chromatids, cells exit meiosis, giving rise to diploid gametes that are capable of fertilisation (d'Erfurth *et al.* 2009). Mutations or conditions that trigger this process are known as second division restitution (SDR). The gametes of SDR mutants contain the centromeres of sister chromatids from the parental meiocyte (Figure 3.1). Therefore the chromosomes in SDR gametes are isogenic, apart from where crossovers with homologous chromosomes occurred. Importantly, the gametes of *Arabidopsis osd1* mutants are viable and give rise to tetraploid progeny upon selfing and triploid progeny upon crossing to wild-type (d'Erfurth *et al.* 2009).

3.2.3 Haploid induction caused by inheritance of modified CENH3

The centromere is important in both mitosis and meiosis, as it is the site on chromosomes where kinetochores assemble during cell division (Liu *et al.* 2006; Régnier *et al.* 2005; Fachinetti *et al.* 2013) *Arabidopsis* possesses regional, monocentric centromeres (Watts *et al.* 2016). This means that its centromeres, which are several Mb in length (Hosouchi *et al.* 2002), occupy discrete, well-defined positions on the chromosome. CENTROMERIC HISTONE H3 (CenH3) is a histone variant with sequence similarity to canonical histone H3 (Palmer *et al.* 1991; Sullivan *et al.* 1994). CenH3 and related histone variants act to epigenetically define the centromere in most eukaryotic organisms (McKinley & Cheeseman 2016). In *Arabidopsis thaliana* the centromeric DNA sequences are largely comprised of

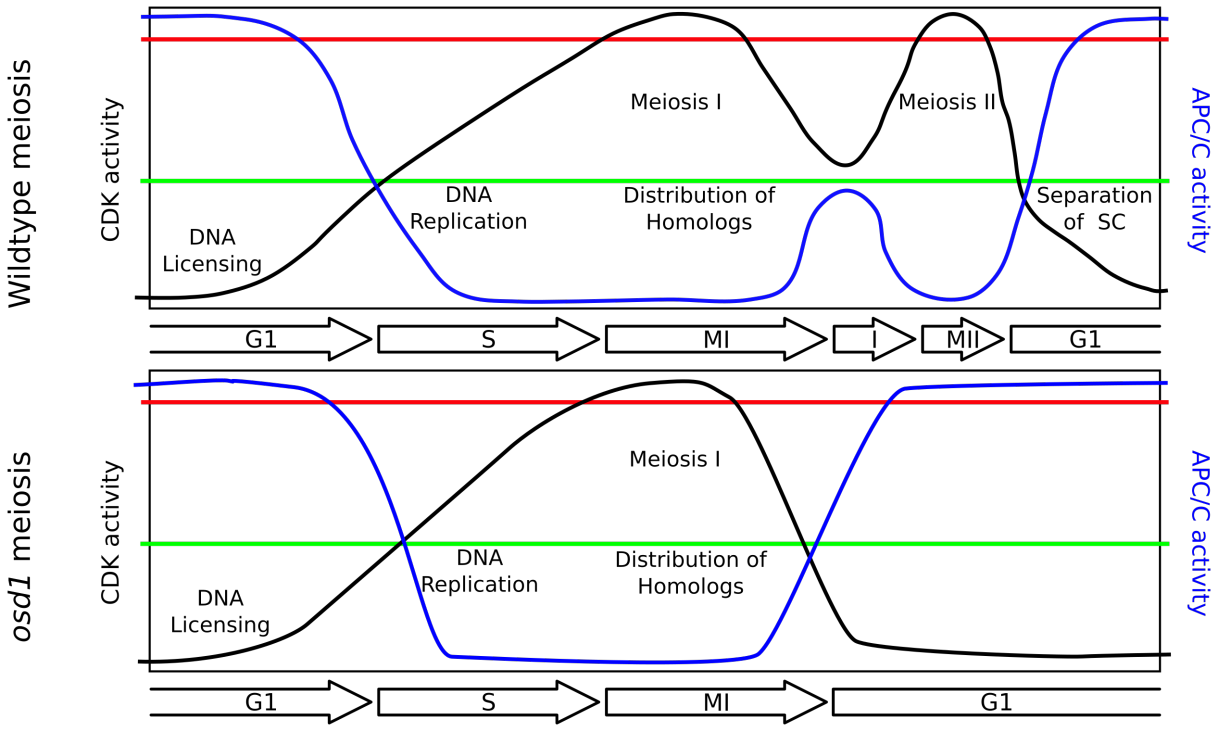

Figure 3.2: Putative cyclin-CDK and APC/C activity during wild-type and osd1 meiosis *(adapted from (Wijnker & Schnittger 2013b)). Increasing cyclin-CDK activity (black line) is thought to drive meiosis, an intermediate level of cyclin-CDK activity (horizontal green line) triggers S-phase while a high level of cyclin-CDK activity (horizontal red line) promotes meiosis-I (MI) and meiosis-II (MII). (N.B. While this schematic presents cyclin-CDK activity as a single line it is likely that in plants there are separate S- and M-phase cyclin-CDK levels). The licensing of replication origins requires low cyclin-CDK activity which is generated by the action of the APC/C (blue line) which mediates the degradation of cyclin-CDK complexes, keeping cyclin-CDK activity low during G1-phase (G1). In wild-type meiosis cyclin-CDK and/or APC/C activity must be carefully modulated at the end of MI to prevent exit from meiosis and establish interkinesis (I). It should be noted that the extent of change in cyclin-CDK and APC/C levels shown at wild-type interkinesis is speculative. In osd1 mutant meiosis the second division of meiosis is skipped. This is presumably because in the absence of inhibition by OSD1 the APC/C becomes fully activated at the end of MI, degrading meiotic cyclins and thereby reducing cyclin-CDK activity in the cell.*

megabase arrays of tandem repeats of a 178-180 bp sequence known as cen180 (Kumekawa *et al.* 2000; Kumekawa *et al.* 2001; Nagaki *et al.* 2003). These repeat stretches vary in length from 0.4 to 3 Mb (Kumekawa *et al.* 2000; Kumekawa *et al.* 2001). Cen180 repeats play an important role in CenH3 deposition and are enriched for binding of CenH3, as shown via immunolocalisation and chromatin immunoprecipitation (Nagaki *et al.* 2003).

Arabidopsis cenh3 mutants were found to be embryo lethal. However, it was discovered that a modified fusion version of CenH3, consisting of the CenH3 C-terminal histone-fold domain (HFD), a truncated tail-domain from regular histone H3 and GFP was able to recover null mutant lethality (Ravi & Chan 2010). This construct was named *GFP-tailswap* and homozygous *GFP-tailswap* lines were observed to grow and self-fertilize normally. However, upon crossing to wild-type it was found to yield haploid progeny (Ravi & Chan 2010; Marimuthu *et al.* 2011; Ravi *et al.* 2014). These progeny were found to possess chromosomes only from its non-*GFP-tailswap* parent (Ravi & Chan 2010). Hence, *GFP-tailswap* lines have the ability to generate haploid offspring and are called haploid inducers. Since the discovery of the haploid-inducing properties of *GFP-tailswap*, more efficient haploid-inducers have been discovered. These include (i) the *cenh3* L130F point mutant (Karimi-Ashtiyani *et al.* 2015), (ii) the SeedGFP-HI line which allows for identification of haploid seed before germination (Ravi *et al.* 2014) and (iii) the Genome Elimination induced by Mix of CENH3 variants (GEM) line which combines the GFP-tailswap and GFP-CENH3 transgenes in a *cenh3-1* mutant plant, which gives an increased number of haploid offspring per cross (Marimuthu *et al.* 2011).

In all these lines the loss of one set of chromosomes post-fertilisation is assumed to proceed via the same mechanism, albeit with different efficiencies (Marimuthu *et al.* 2011; Ravi *et al.* 2014; Karimi-Ashtiyani *et al.* 2015). One intriguing study used RT-PCR and GFP-tagging methods to track CenH3 in both maternal and paternal gametes before and after fertilisation, in an attempt to understand histone dynamics during fertilisation. The study confirmed the presence of CenH3-GFP in male sperm cells, but could not detect either CenH3-GFP or CenH3 transcripts in isolated egg cells (Ingouff *et al.* 2010). After fertilisation the maternal chromosomes in the zygote appeared relatively depleted for CenH3-GFP, while the paternal chromosomes retain the CenH3-GFP deposited onto them in the sperm cell (Ingouff et al.

2010). This residual CenH3-GFP was observed to be removed within a few hours of fertilisation (Ingouff et al. 2010). CenH3-GFP is then reloaded onto both paternal and maternal chromosomes in the zygote at the 16 nuclei stage of endosperm development (Ingouff *et al.* 2010). It is hypothesised that at this point CENH3 loading onto the chromosomes originating from the haploid inducer is impaired or delayed, though the exact cause of this delay is unknown (Karimi-Ashtiyani *et al.* 2015). These findings are difficult to interpret due to the fact they were obtained by using GFP-tagged CenH3, which is known not to behave identically to wild-type CenH3. For example it is incapable of recovering a *cenh3* null mutant (Ravi & Chan 2010). Another study examined the genetic make-up of *Arabidopsis* plants produced by crossing a wild-type plant to a haploid inducer (Tan *et al.* 2015). It found that ~40% of offspring from such a cross were haploid, containing chromosomes from one parent only (i.e. 'true' SDR individuals), 25% were diploid hybrids of maternal and paternal chromosomes (as in a regular F_1 cross) and 37% were aneuploid hybrids. The aneuploid individual's genomes were sequenced and three classes of aneuploid were discovered; i) aneuploids displaying trisomy of an entire chromosome, ii) aneuploids displaying trisomy of a truncated chromosome and iii) aneuploids possessing an extra 'shattered' chromosome, believed to be produced by chromothripsis (localised chromosome shattering and reconstitution), chromoanasynthesis (gene rearrangements resulting from template switching during DNA synthesis) or a combination of both (Tan *et al.* 2015). While the study fails to explain why or how haploid-inducer chromosomes are lost post-fertilisation, it does offer a useful descriptive account of the possible fates of haploid-inducer chromosomes and emphasises the fact that total loss that gives rise to a haploid plant is only as common as the generation of diploid hybrid and aneuploid plants.

3.3 Results

3.3.1 An *OSD1* RNAi construct generates diploid pollen

Two approaches to generating an SDR population were taken (Figure 3.1F+G and Figure 3.8). The first approach involved generating an *OSD1* RNA interference (RNAi) line in the Columbia accession. Our strategy was then to cross to the polymorphic Ler accession, in order to generate an *OSD1* RNAi F_1 Col/Ler hybrid. These F_1 plants could then be crossed to the GEM haploid inducer line to generate an SDR population (Figure 3.1F+G). For this plan to be viable it is necessary that the *OSD1* RNAi line be partially penetrant, as haploid pollen is required for the first cross to Ler, while diploid pollen is required in the cross to GEM.

In order to generate an RNAi construct, a 501 bp fragment of *OSD1* sequence was cloned from *Arabidopsis* cDNA using primers PLD003 and PLD004 (See Chapter 2, Appendix 2), which hybridize in the first and second exon of the *OSD1* gene respectively. In addition to amplifying the fragment the primer also added a 4 bp 'CACC' sequence to both ends of the amplified fragment, allowing it to be cloned into the pENTR™ vector. Two copies of the 501 bp *OSD1* fragment in pENTR™ were then cloned into the pJawohl binary destination vector to generate a hairpin RNAi construct, separated by an intron spacer under the control of a 2XCaMV promoter (Figure 3.3). This was accomplished by performing a Gateway cloning reaction, which makes use of attR1 and attR2 recombination sites, in order to directionally clone a compatible sequence into a vector. The resulting *OSD1* RNAi binary pJawohl vector was then transformed into *Agrobacterium* strain GV3101 and used to transform Col via the floral dip method (Clough & Bent 1998).

Of the 14 *OSD1* RNAi T_1 lines recovered following transformant selection using BASTA, 13 were observed to show increased pollen size, as analysed by light microscopy (Figure 3.4). This is consistent with these lines producing diploid pollen (De Storme & Geelen 2011; Reeder *et al.* 2016). In order to confirm this, the male meiotic products of the *OSD1* RNAi lines were analysed microscopically using toluidine blue staining in an anther squash. Wild-type plants produce four spores arranged in a tetrahedron (called a 'tetrad'), with each spore going on to produce a single pollen grain (Figure 3.4A). In SDR mutants, such as *osd1* and

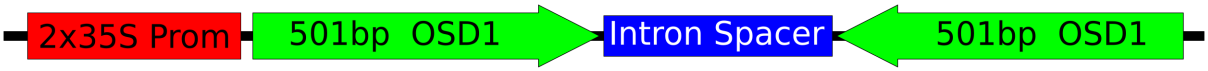

Figure 3.3: Schematic of 35S OSD1 RNAi construct.

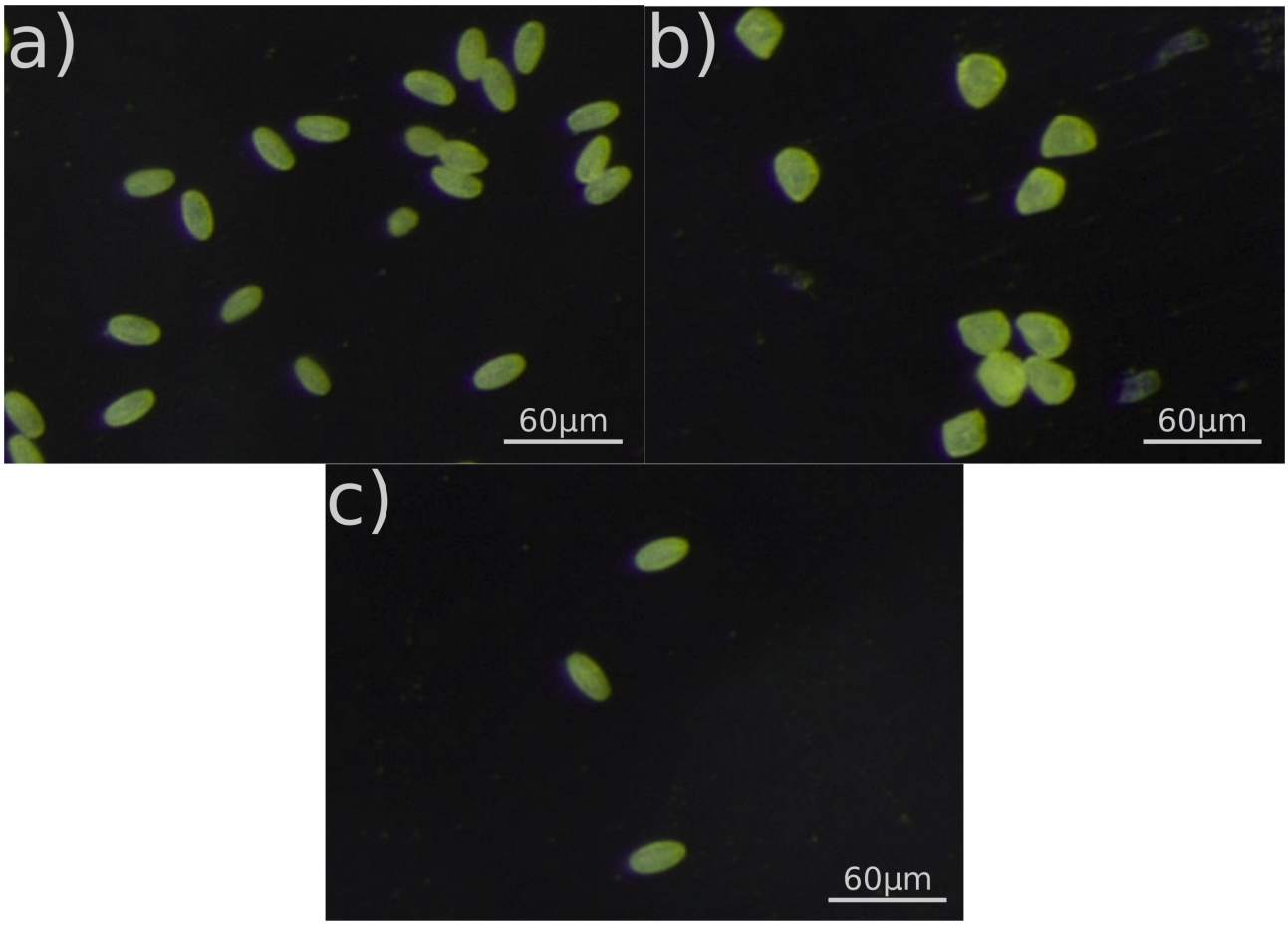

d)

Phenotype	Lines
Wild-type	6 (shown above)
Distorted	1, 2, 3, 4, 5, 7, 8, 9 (shown above), 10, 11, 12, 13, 14

Figure 3.4: Pollen phenotypes in 35S::OSD1 RNAi lines. *Light microscopy images of pollen from,* ***a)*** *Wild-type,* ***b)*** *a 35S::OSD1 RNAi transformant displaying a distorted pollen phenotype (e.g. Line 9) and* ***c)*** *a 35S::OSD1 RNAi transformant displaying wild-type pollen (e.g. Line 6).* ***d)*** *A summary of which lines displayed wild-type and distorted pollen phenotypes.*

tam1, plants instead produce two spores (called a 'dyad'), as they have failed to undergo the second meiotic division which would have produced four daughter cells (d'Erfurth *et al.* 2010). Toluidine blue staining allows the visualisation of tetrads and dyads and therefore provides a way of determining whether the *OSD1* RNAi lines were true SDR plants. Tetrad analysis showed three lines 1, 2 and 13, which were exclusively producing dyads (i.e. diploid) pollen (Figure 3.5).

In order to confirm whether transgenic lines produced a mixture of haploid and diploid pollen, four lines (5, 6, 8 and 10) which had showed enlarged pollen, but had not been confirmed to produce only diploid gametes via toluidine blue staining, were allowed to self-fertilize and ploidy analysed in their offspring via flow cytometry of propidium iodide stained nuclei (Figure 3.6 and 3.7). Propidium iodide stains dsDNA, the majority of which is present in the nucleus. The amount of DNA present in a cell can then be determined using flow cytometry (Durbarry *et al.* 2005; De Storme & Geelen 2011). In wild-type diploid plants this analysis gives rise to a flow cytometry graph with multiple peaks (Figure 3.6A). The first peak is generated by cells with a 2n chromosome count. Further peaks are generated by cells which possess multiplications of this count (4n, 8n etc), due to endoreduplication (Galbraith *et al.* 1991). Tetraploid plants can be identified due to their lack of a 2n peak (Figure 3.6B). Plants producing a mixture of haploid and diploid gametes would produce a mixture of diploid (haploid+haploid), triploid (haploid+diploid) and tetraploid (diploid+diploid) offspring upon selfing, whereas plants only producing diploid pollen would generate tetraploid offspring. All lines analysed produced either solely diploid or solely tetraploid plants (Figure 3.6 and 3.7), suggesting the *OSD1* RNAi SDR phenotype was fully penetrant.

Taken together these results suggest that the *OSD1* RNAi construct was successful at reducing endogenous *OSD1* expression, as the majority of the transformants displayed the expected diploid pollen phenotype. Unfortunately no variability in the penetrance of the constructs was observed, as all successful transformants appeared to be exclusively producing diploid pollen. For this reason the *OSD1* RNAi lines could not be used to generate an SDR population, as haploid pollen is required for the first cross to generate a Col/Ler F_1 population (Figure 3.1F+G).

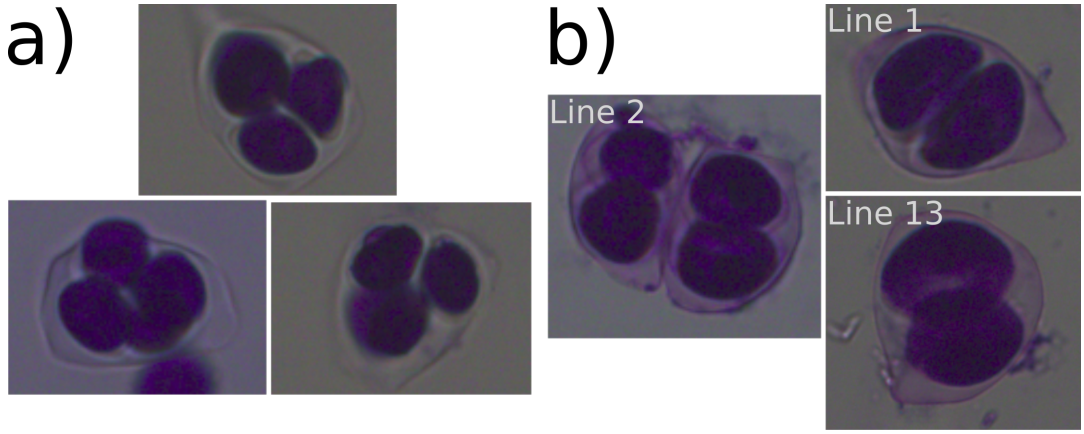

Figure 3.5: Toluidine blue staining of male meiotic products. a) *Wild-type tetrads.* ***b)*** *Representative examples of dyads from the three lines tested (N.B. The Line 2 image shows two dyads close together, not a distorted tetrad).*

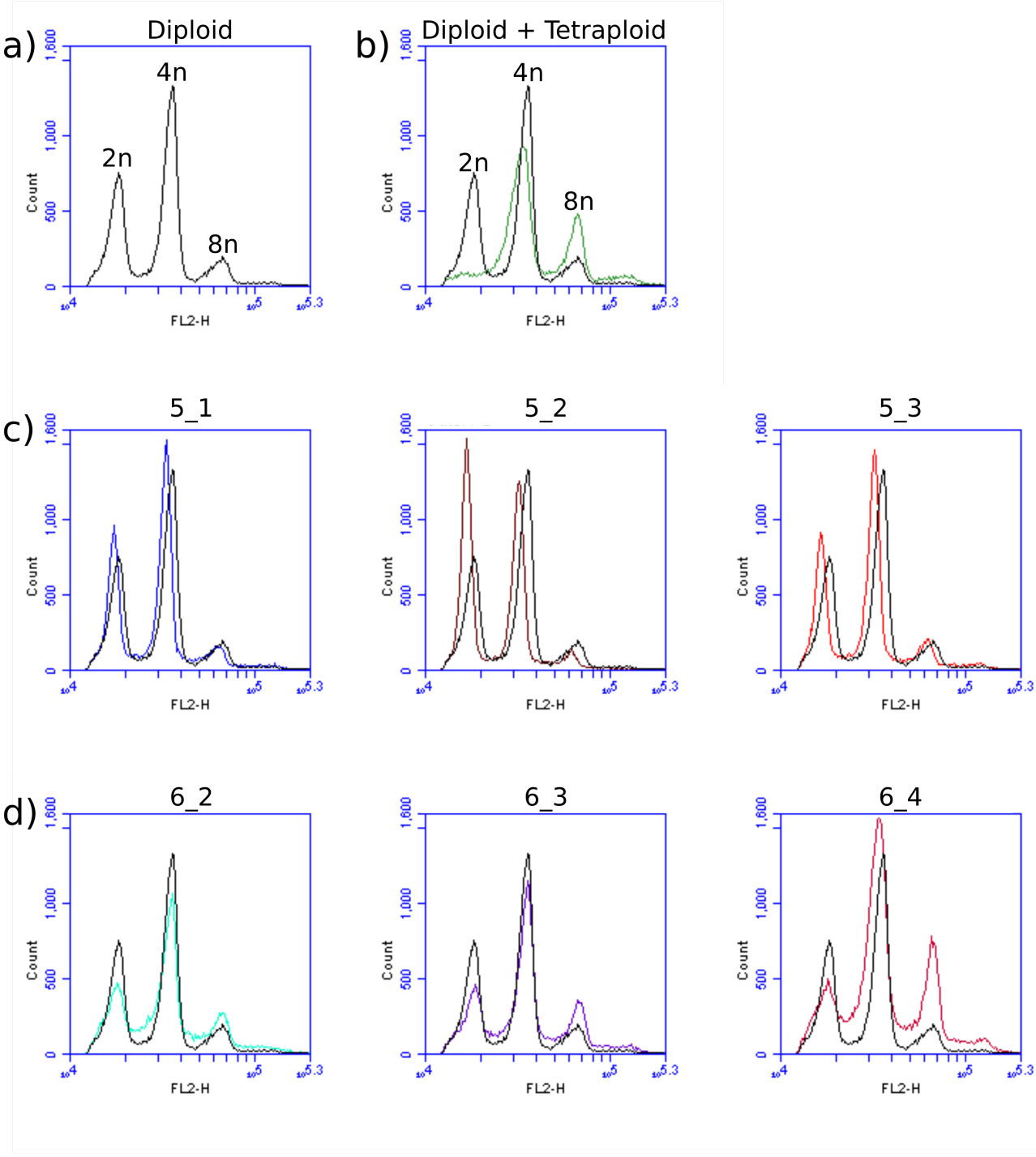

Figure 3.6: OSD1 RNAi lines producing diploid offspring. *Flow cytometry of propidium iodide stained nuclei.* ***a)*** *Wild-type diploid control (black line) with 2n, 4n and 6n peaks labelled (N.B. This curve is reproduced on all subsequent plots as a guide).* ***b)*** *Tetraploid control (green line), note the missing 2n peak.* ***c)*** *Representative offspring from OSD1-RNAi Line 5 (coloured lines). All offspring from this line were diploid.* ***d)*** *Representative offspring from OSD1-RNAi Line 6 (coloured lines). All offspring from this line were diploid.*

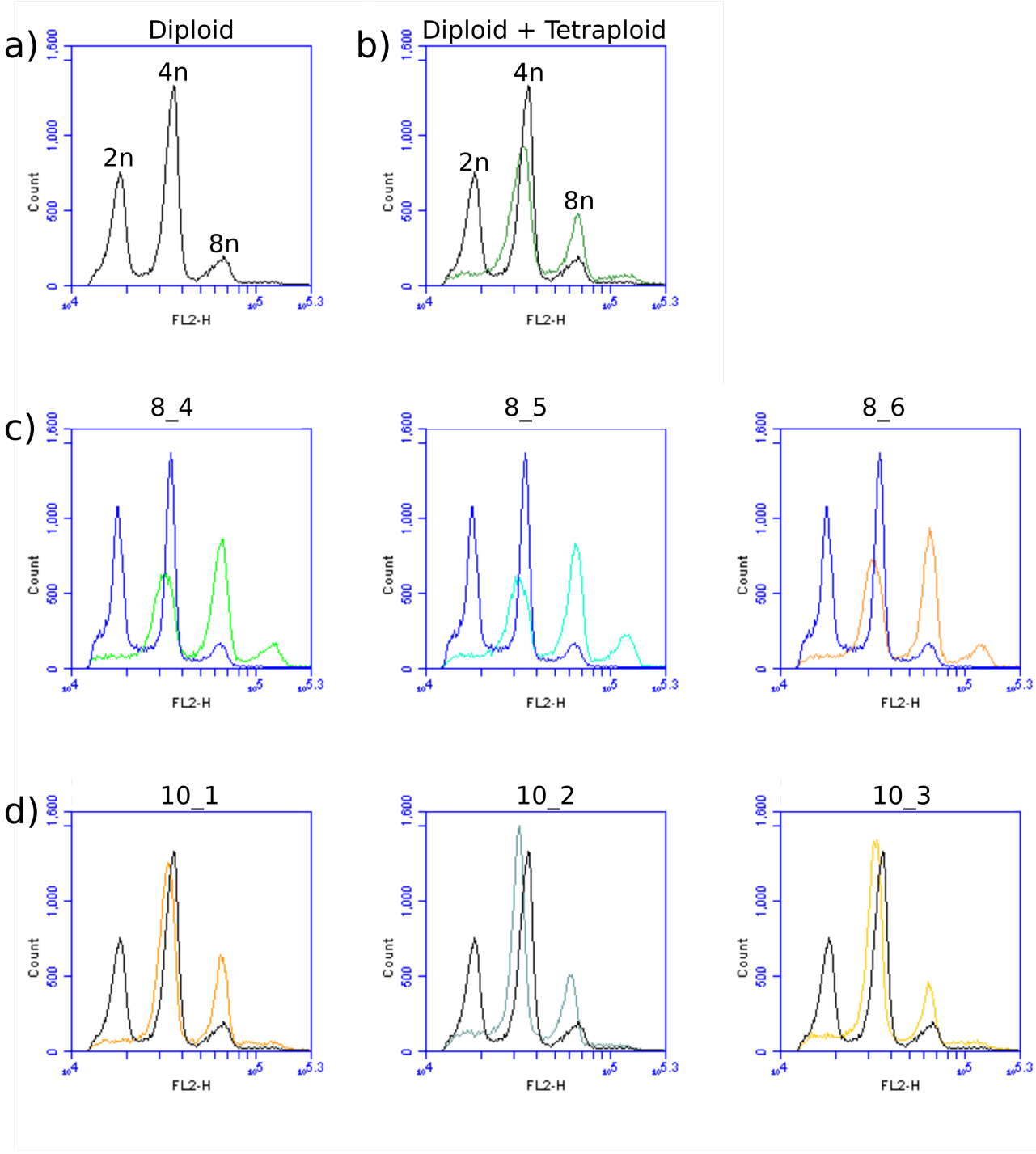
a)
Diploid
4n
2n
8n
Count
FL2-H
b)
Diploid + Tetraploid
4n
2n
8n
Count
FL2-H
c)
8_4
8_5
8_6
Count
FL2-H
d)
10_1
10_2
10_3
Count
FL2-H

Figure 3.7: OSD1-RNAi lines producing tetraploid offspring. *Flow cytometry of propidium iodide stained nuclei.* ***a)*** *Wild-type diploid control (black line) with 2n, 4n and 6n peaks labelled (N.B. This curve is reproduced on all subsequent plots except c), where a different diploid control was used).* ***b)*** *Tetraploid control (green line), note the missing 2n peak.* ***c)*** *Representative offspring from OSD1-RNAi Line 8 (coloured lines). All offspring from this line were tetraploid. (N.B. The dark blue lines on these plots are a diploid control different to one seen in a)).* ***d)*** *Representative offspring from OSD1-RNAi Line 10 (coloured lines). All offspring from this line were tetraploid.*

3.3.2 The *osd1-3* mutant was introgressed into *Landsburg erecta* to allow for generation of an SDR population.

The second approach to creating an SDR population involved first introgressing the *osd1-3* mutant from Col into Ler, then crossing *osd1-3* +/- Col to *osd1-3* +/- Ler to generate an F_1 Col/Ler *osd1-3* hybrid (Figure 3.8). This hybrid could then be crossed to GEM to produce an SDR population. Introgression of *osd1-3* into Ler was accomplished by backcrossing *osd1-3* (Col) to wild-type Ler a total of 6 times. Col/Ler marker analysis was performed on the resulting *osd1-3* Ler lines, which showed that following these backcrosses the majority of the genome was Ler homozygous, except for an approximately 10 Mb region of Col sequence on chromosome 3, surrounding the site of the *osd1-3* mutation, which remained Col homozygous due to linkage drag (Figure 3.9).

3.3.3 Characteristics of SDR population

Col/Ler *osd1-3* mutants generated as described in the above section were crossed as males to GEM line individuals to produce an SDR population. The SDR_0 population that was thus generated comprised 169 individuals which were given names SDR001 to SDR169. All SDR plants were genotyped on each chromosome using PCR markers. While a subset of 16 individuals were genotyped using a genotyping by sequencing (GBS) method, which gives much higher resolution data genome-wide.

Of the 169 plants, PCR genotyping showed 88 to be homozygous for Col sequence along the entire length of every chromosome (Figure 3.10). This group will subsequently be termed the ‘all-Col’ group. Of the 88 individuals in the all-Col group, 5 individuals (SDR005, 006, 009, 036, 121) had their genotypes verified by GBS (Figure 3.11), which confirmed that they were completely isogenic for Col. True SDR individuals should be KO for OSD1 while being wild type for GFP-tailswap and GFP-CenH3. However, none of the all-Col group SDR plants displayed this genotype (Figure 3.10). Only 1 was *osd1-3* KO (SDR121), while 2 were GFP-tailswap WT (SDR031, 079) and 7 were GFP-CenH3 WT (SDR001, 009, 016, 024, 045, 103, 120).

After the all-Col group, the second largest group by genotype in the SDR population was that displaying both Col and heterozygous chromosome stretches according to PCR genotyping. This group will subsequently be termed the Col+Het group. In total 64 individuals displayed the Col+Het genotype (Figure 3.10). Of these, 8 were verified by GBS (SDR002, 017, 021, 052, 053, 075, 135, 146, Figure 3.12). Only 3 individuals in the Col+Het group were *osd3-1* homozygous, while 11 were WT for GFP-tailswap and 22 were WT for GFP-CenH3 (See Fig. 3.10). In addition, one of the plants in this group was aneuploid (SDR146) and one (SDR163) was triploid (Figure 3.13).

The next largest group by genotype was those individuals which displayed Col, Ler and heterozygous genotype markers. This group shall subsequently be termed the Col+Ler+Het group. There were 12 of these individuals overall, however, only 4 displayed each genotype at more than one marker. There were 8 plants which displayed the Ler genotype at only one marker (Figure 3.10) and which therefore might not actually be true Col+Ler+Het individuals as this genotype may be the result of a single faulty genotyping reaction or misinterpretation of the bands seen on the genotyping gel. One Col+Ler+Het individual, SDR153, was verified by GBS and did not show any heterozygous stretches (Figure 3.14). Of this group of Col+Ler+Het plants, 3 individuals showed the correct *OSD1*, CenH3-tailswap and GFP-CenH3 genotypes to qualify as true SDR plants; SDR126, 127 and 153 (Figure 3.10). However SDR153 appears to be haploid (Figure 3.13), and so cannot qualify as a true SDR plant.

The smallest group by genotype was that showing Col and Ler homozygous stretches with no intervening heterozygous stretches. This group will subsequently be termed the Col+Ler group. There were 4 of these individuals (Fig 3.10), of which 2 were verified by GBS and shown to possess only Col and Ler homozygous sequence (Figure 3.15). One of these individuals, SDR167, only displays one Ler marker suggesting it may be an all-Col plant which has been incorrectly genotyped. SDR070, 078 and 101 were tested for ploidy and all individuals appear to be haploid (Figure 3.13).

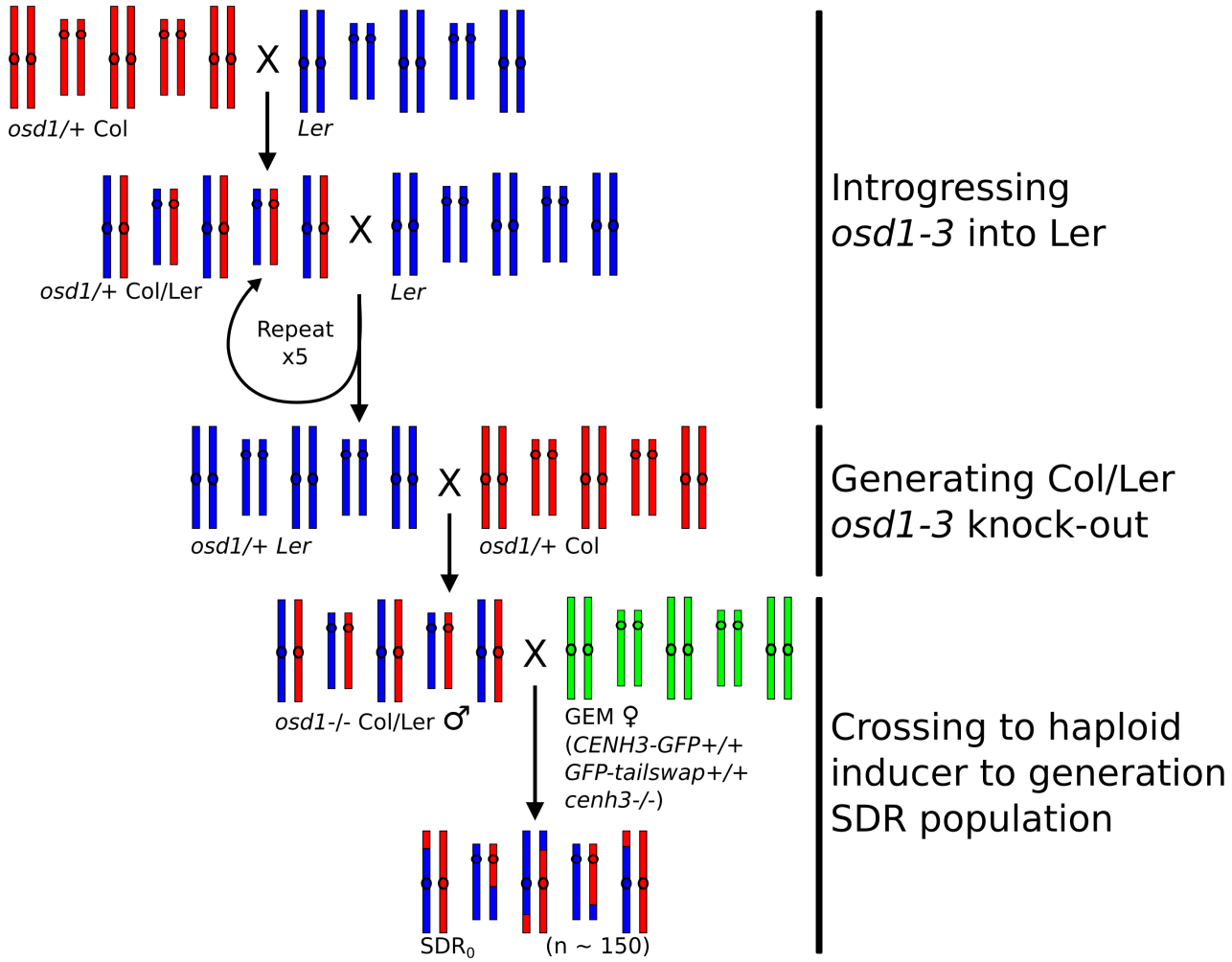

Figure 3.8: Alternative approach to creating an SDR population via backcrossing of osd1-3 from Col into Ler.

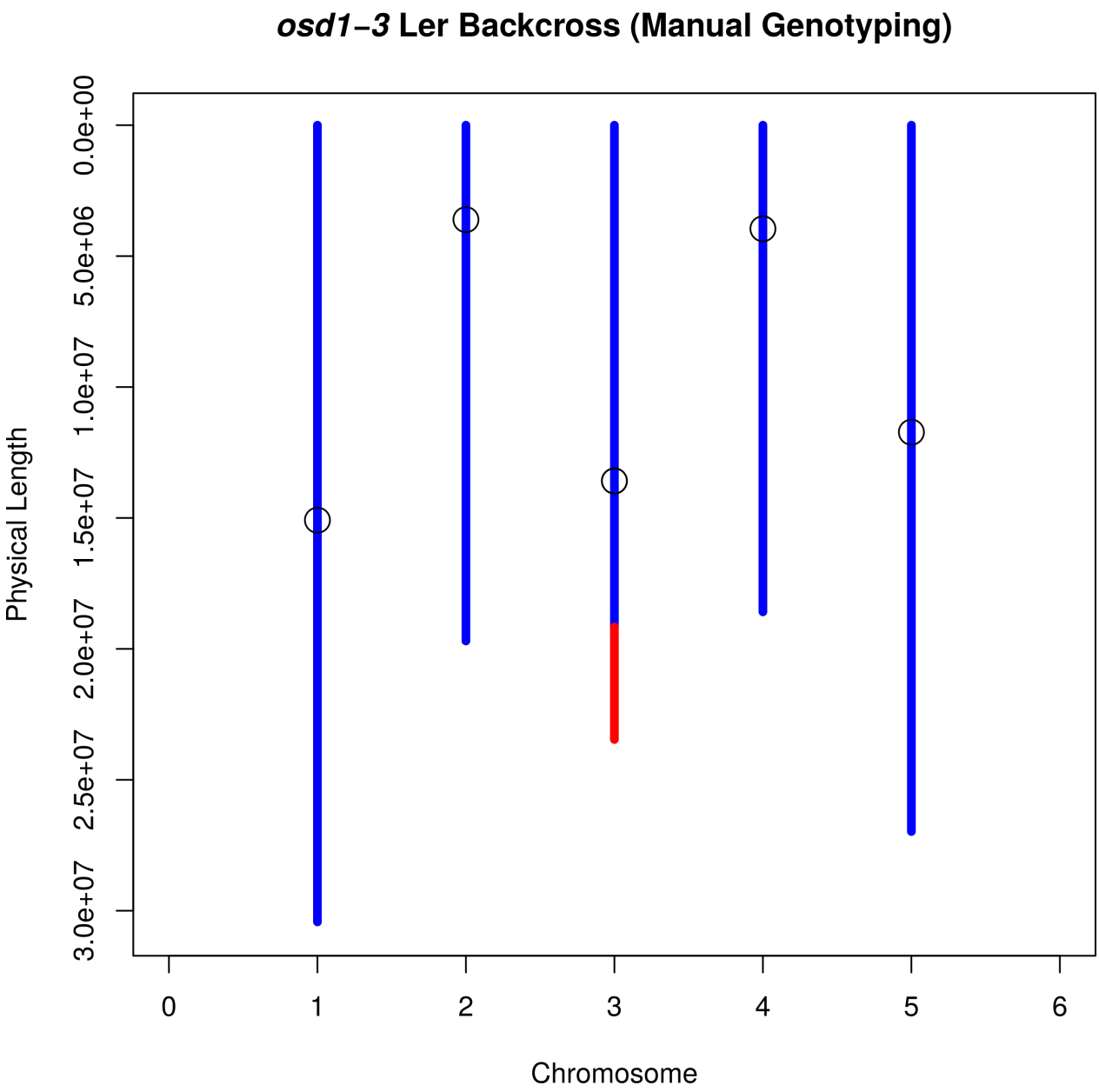

Figure 3.9: Col/Ler marker analysis of osd1-3 (Ler) line generated by introgression. *Each vertical line represents one chromosome. Blue=homozygous Ler sequence Red=homozygous Col sequence. Open circle=approximate location of centromeres.*

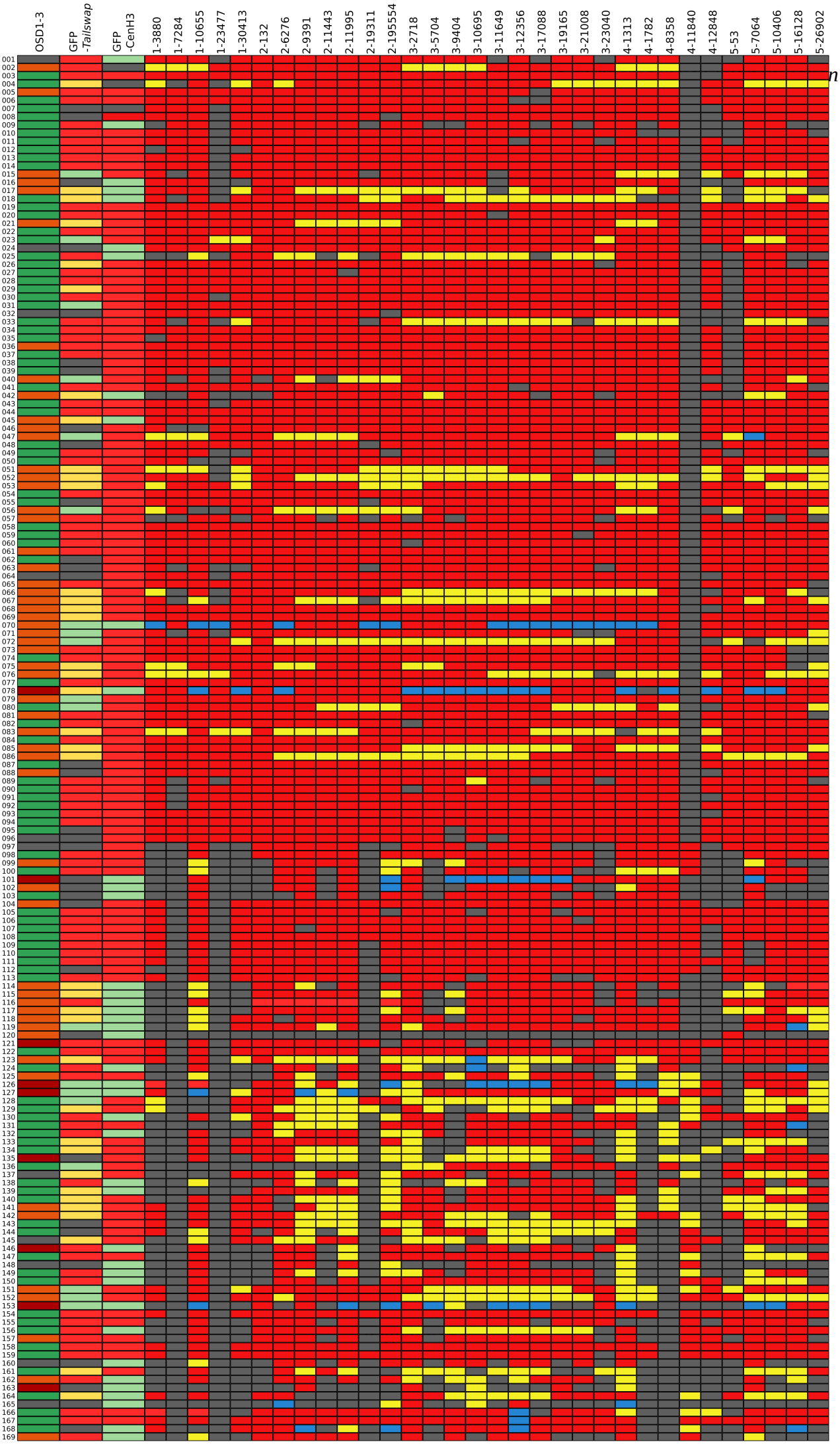
OSD1-3
GFP -Tailswap
GFP -CenH3
1-3880
1-7284
1-10655
1-23477
1-30413
2-132
2-6276
2-9391
2-11443
2-11995
2-19311
2-195554
3-2718
3-5704
3-9404
3-10695
3-11649
3-12356
3-17088
3-19165
3-21008
3-23040
4-1313
4-1782
4-8358
4-11840
4-12848
5-53
5-7064
5-10406
5-16128
5-26902
n

Figure 3.10: PCR genotyping results for SDR population. First column) *OSD1-3 genotype; Green=WT (OSD1-3 +/+), Orange=Heterozygous (OSD1-3/osd1-3+/-), Red=homozygous mutant (osd1-3-/-), Grey=Undetermined.* ***Second column)*** *GFP-Tailswap genotype; Light green= WT (GFP-Tailswap-/-), Yellow=Hemizygous (GFP-Tailswap+/-), Red=Homozygous transgene (GFP-Tailswap+/+), Grey=Undetermined.* ***Third column)*** *GFP-CenH3 genotype; Light green=Wild type (GFP-CenH3 -/-), Red=Homozygous transgene, (GFP-CenH3 +/+) or transgene hemizygous (GFP-CenH3 +/-) Grey=Undetermined.* ***Remaining columns)*** *Col/Ler sequence analysis for specified markers along the chromosomes. Marker position is shown at the top of each column. The first number before the dash indicates chromosome number, the number after the dash represents position (see Chapter 2, Appendix 2 for primer details) Red=Col/Col, Yellow=Col/Ler, Blue=Ler/Ler, Grey=Undetermined.*

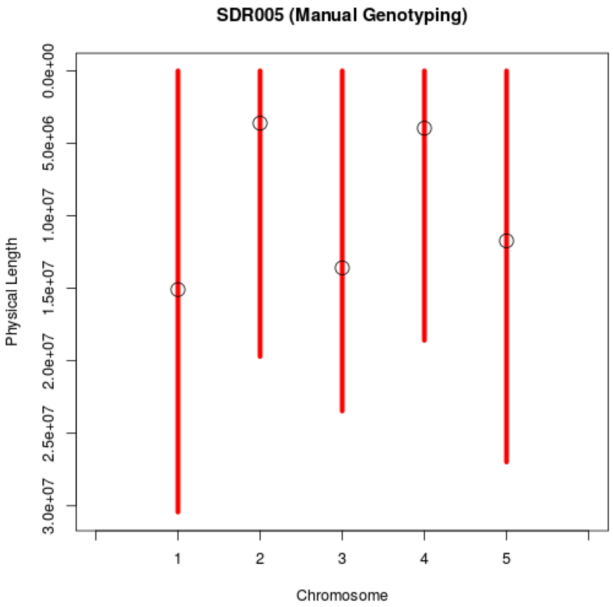
SDR005 (Manual Genotyping)
Physical Length
0.0e+00
5.0e+06
1.0e+07
1.5e+07
2.0e+07
2.5e+07
3.0e+07
1
2
3
4
5
Chromosome

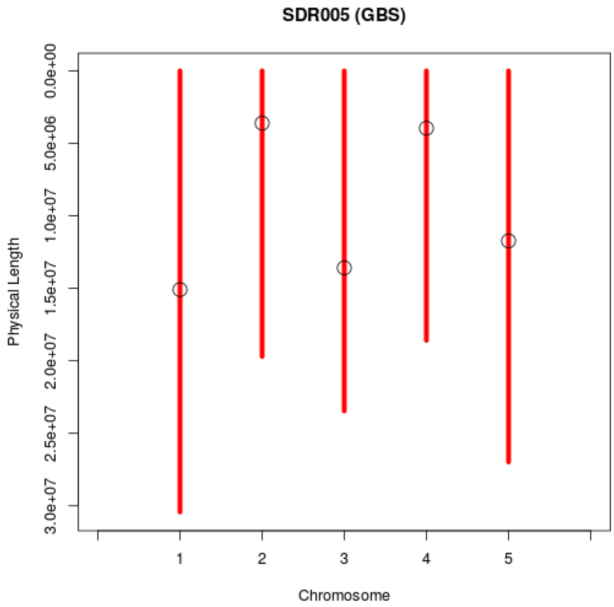
SDR005 (GBS)
Physical Length
0.0e+00
5.0e+06
1.0e+07
1.5e+07
2.0e+07
2.5e+07
3.0e+07
1
2
3
4
5
Chromosome

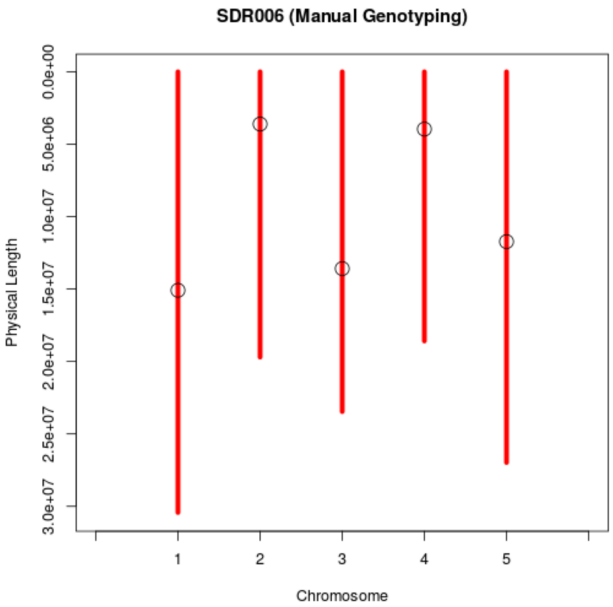
SDR006 (Manual Genotyping)
Physical Length
0.0e+00
5.0e+06
1.0e+07
1.5e+07
2.0e+07
2.5e+07
3.0e+07
1
2
3
4
5
Chromosome

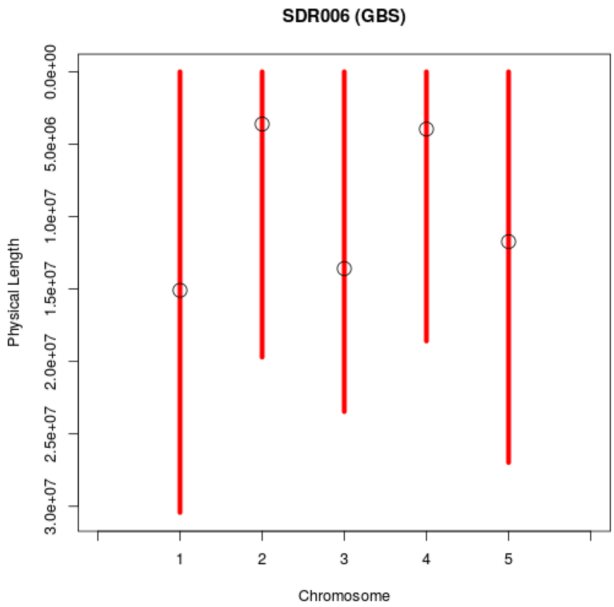
SDR006 (GBS)
Physical Length
0.0e+00
5.0e+06
1.0e+07
1.5e+07
2.0e+07
2.5e+07
3.0e+07
1
2
3
4
5
Chromosome

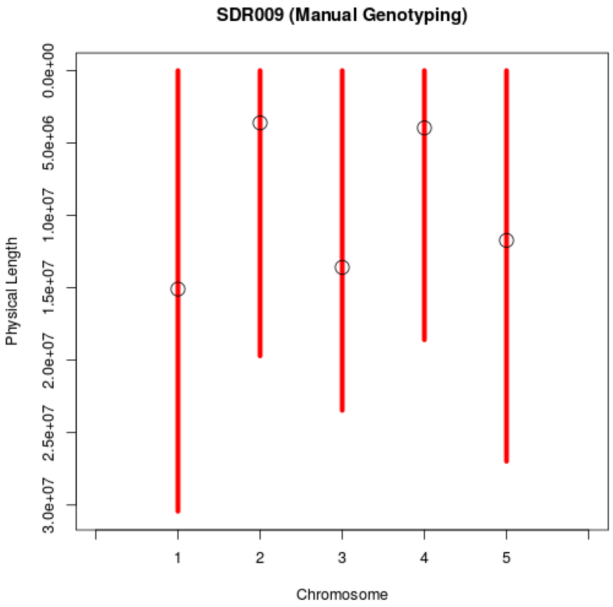
SDR009 (Manual Genotyping)
Physical Length
0.0e+00
5.0e+06
1.0e+07
1.5e+07
2.0e+07
2.5e+07
3.0e+07
1
2
3
4
5
Chromosome

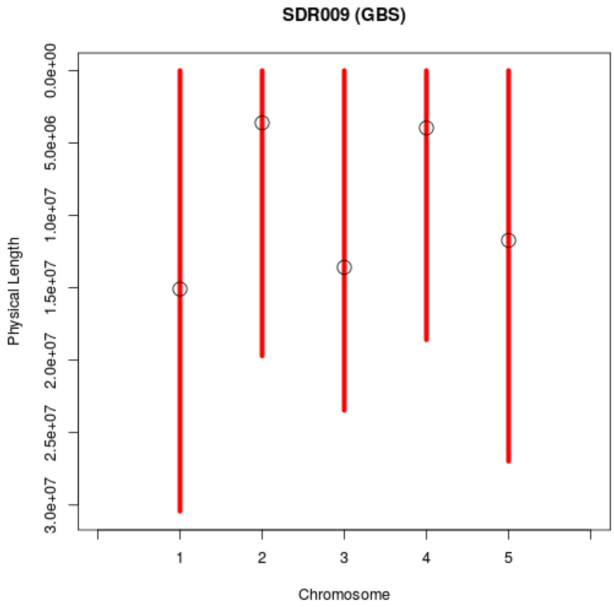
SDR009 (GBS)
Physical Length
0.0e+00
5.0e+06
1.0e+07
1.5e+07
2.0e+07
2.5e+07
3.0e+07
1
2
3
4
5
Chromosome

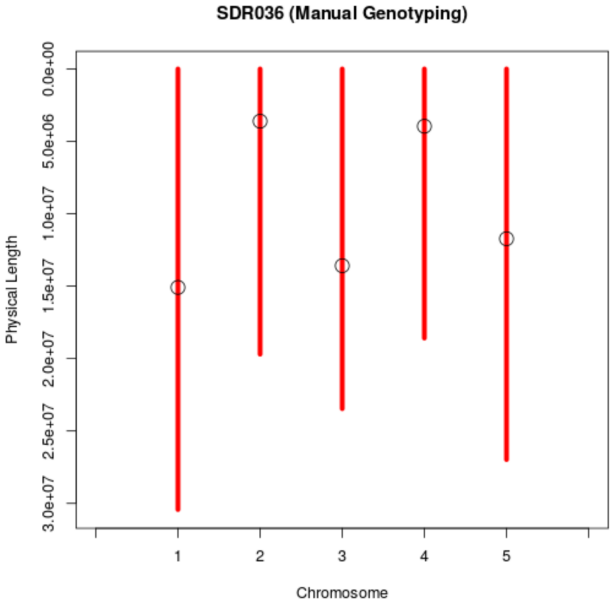
SDR036 (Manual Genotyping)
Physical Length
0.0e+00
5.0e+06
1.0e+07
1.5e+07
2.0e+07
2.5e+07
3.0e+07
1
2
3
4
5
Chromosome

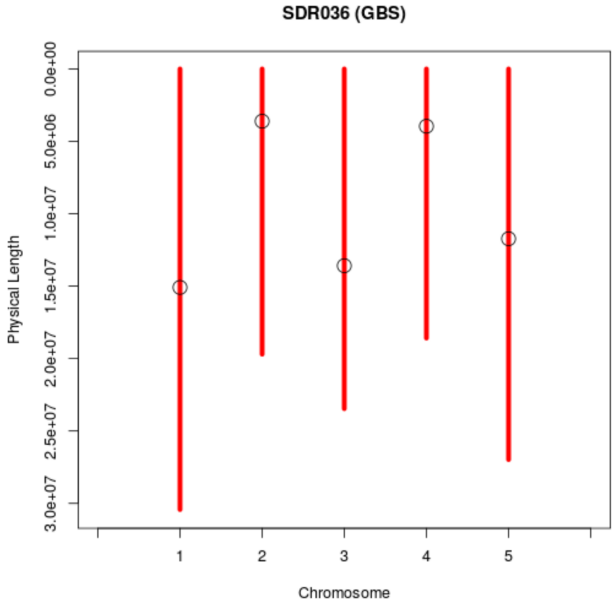
SDR036 (GBS)
Physical Length
0.0e+00
5.0e+06
1.0e+07
1.5e+07
2.0e+07
2.5e+07
3.0e+07
1
2
3
4
5
Chromosome

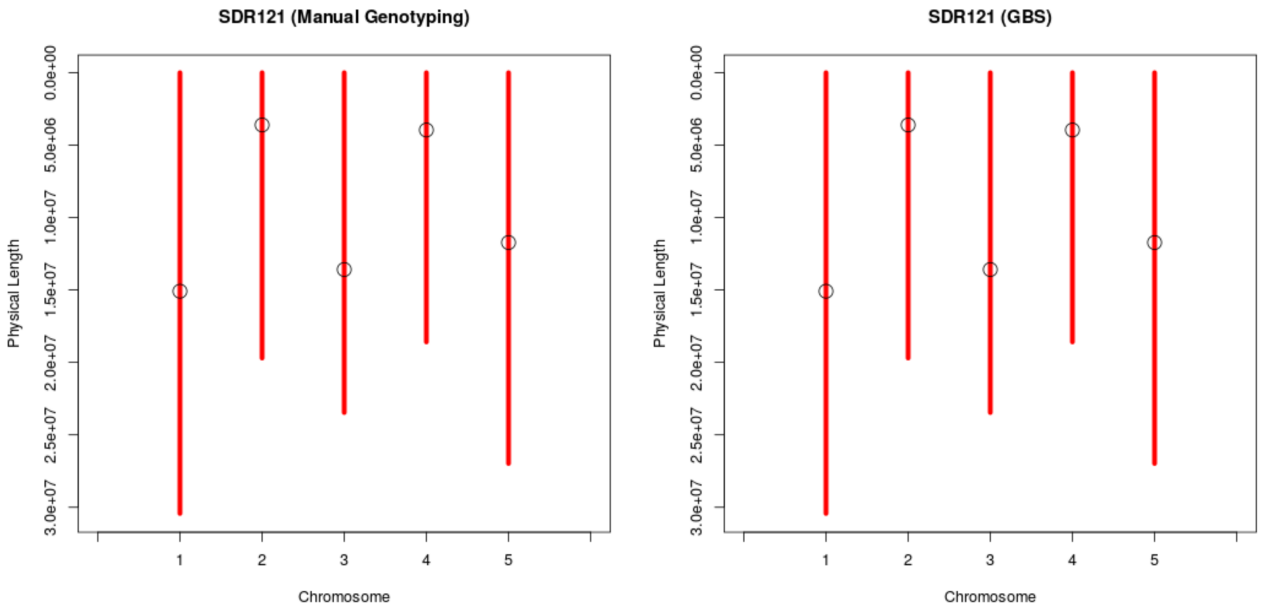

Figure 3.11: Manual and GBS genotyping for the 'all Col' group progeny. Red=Col/Col sequence, Green=Col/Ler sequence, Blue=Ler/Ler sequence.

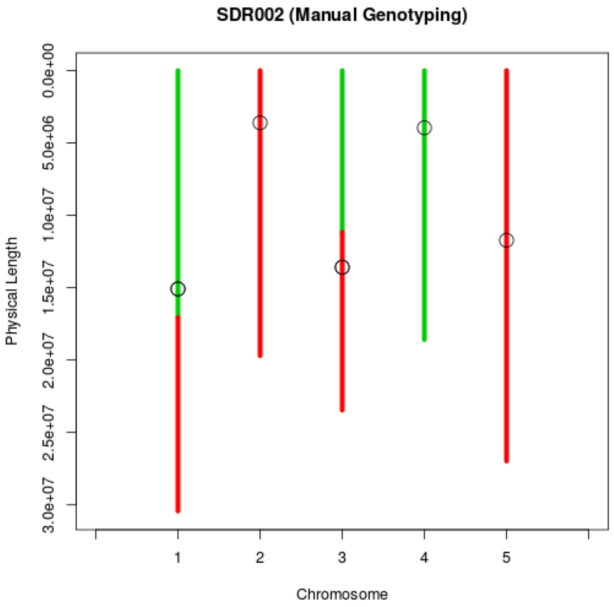
SDR002 (Manual Genotyping)
Physical Length
0.0e+00
5.0e+06
1.0e+07
1.5e+07
2.0e+07
2.5e+07
3.0e+07
1
2
3
4
5
Chromosome

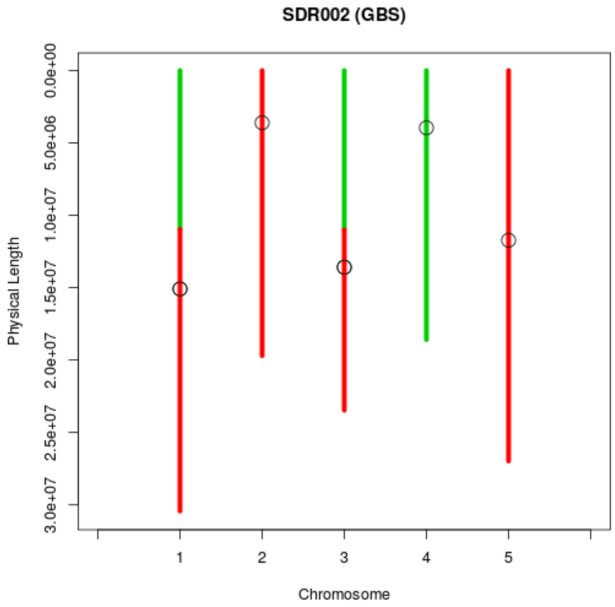
SDR002 (GBS)
Physical Length
0.0e+00
5.0e+06
1.0e+07
1.5e+07
2.0e+07
2.5e+07
3.0e+07
1
2
3
4
5
Chromosome

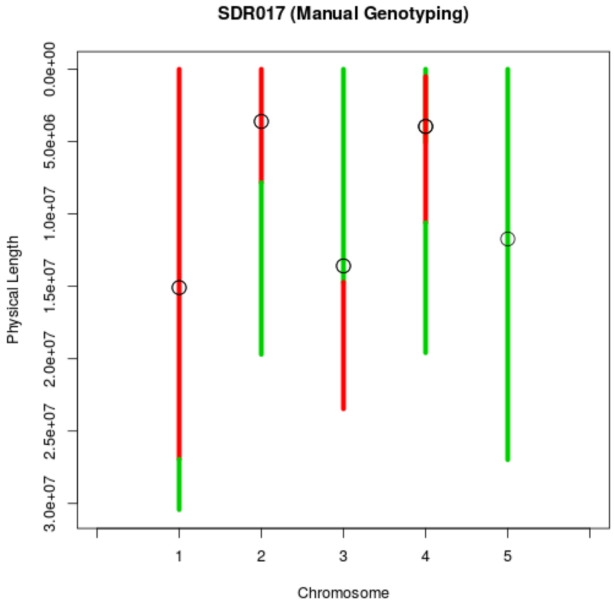
SDR017 (Manual Genotyping)
Physical Length
0.0e+00
5.0e+06
1.0e+07
1.5e+07
2.0e+07
2.5e+07
3.0e+07
1
2
3
4
5
Chromosome

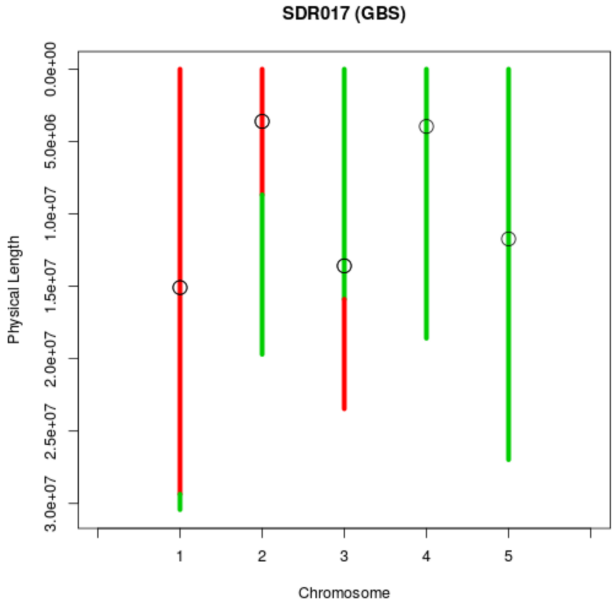
SDR017 (GBS)
Physical Length
0.0e+00
5.0e+06
1.0e+07
1.5e+07
2.0e+07
2.5e+07
3.0e+07
1
2
3
4
5
Chromosome

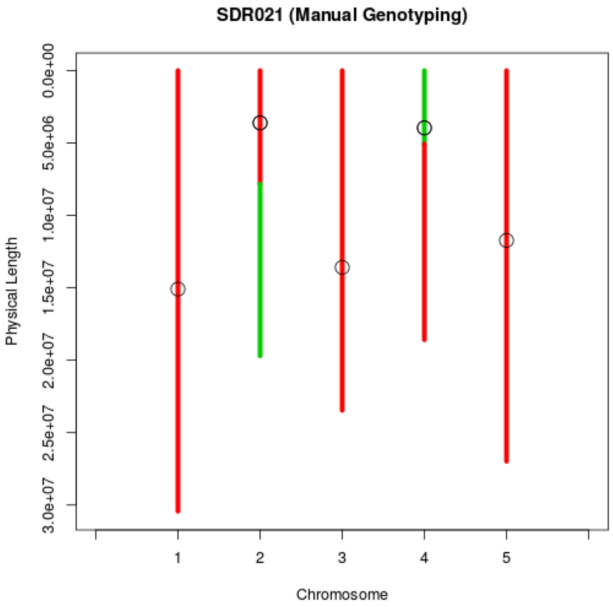
SDR021 (Manual Genotyping)
Physical Length
0.0e+00
5.0e+06
1.0e+07
1.5e+07
2.0e+07
2.5e+07
3.0e+07
1
2
3
4
5
Chromosome

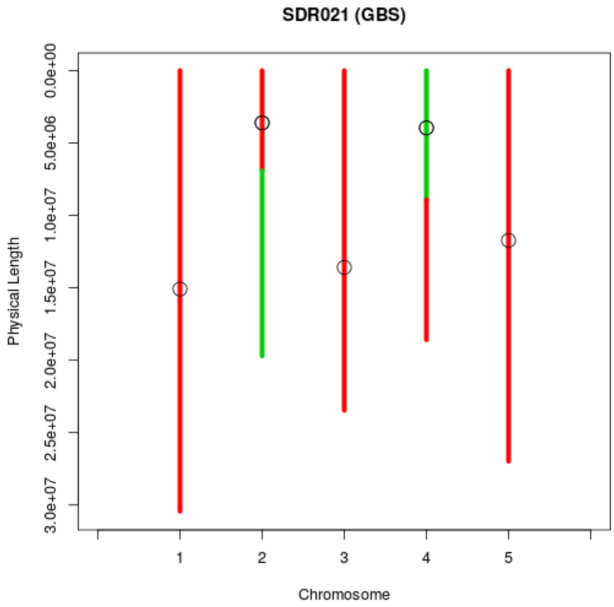
SDR021 (GBS)
Physical Length
0.0e+00
5.0e+06
1.0e+07
1.5e+07
2.0e+07
2.5e+07
3.0e+07
1
2
3
4
5
Chromosome

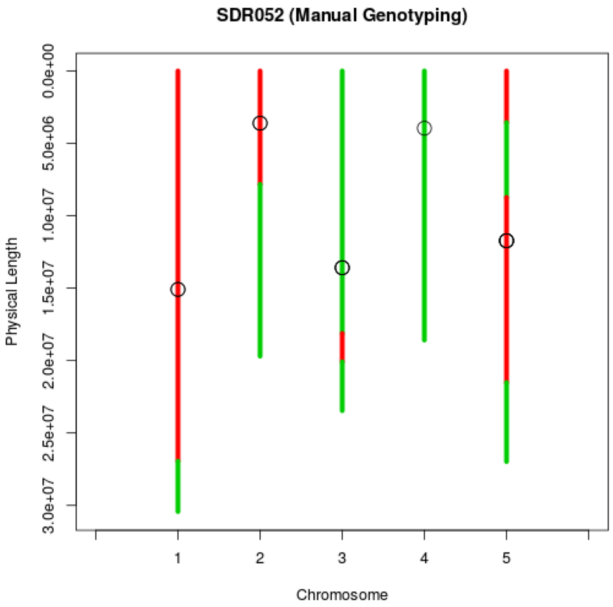
SDR052 (Manual Genotyping)
Physical Length
0.0e+00
5.0e+06
1.0e+07
1.5e+07
2.0e+07
2.5e+07
3.0e+07
1
2
3
4
5
Chromosome

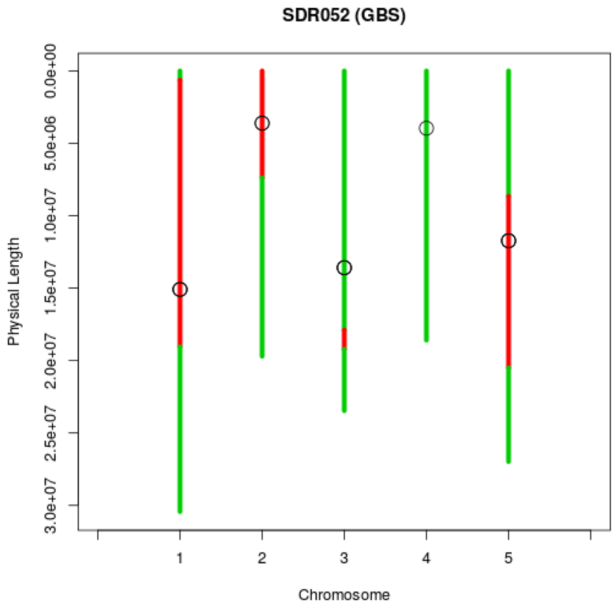
SDR052 (GBS)
Physical Length
0.0e+00
5.0e+06
1.0e+07
1.5e+07
2.0e+07
2.5e+07
3.0e+07
1
2
3
4
5
Chromosome

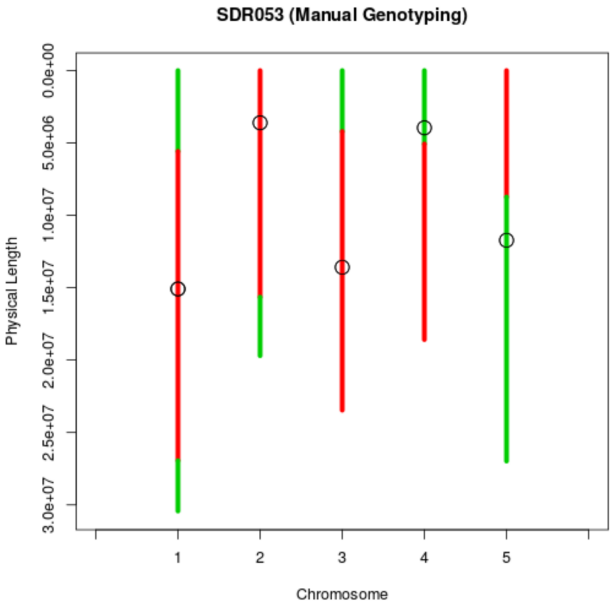
SDR053 (Manual Genotyping)
Physical Length
0.0e+00
5.0e+06
1.0e+07
1.5e+07
2.0e+07
2.5e+07
3.0e+07
1
2
3
4
5
Chromosome

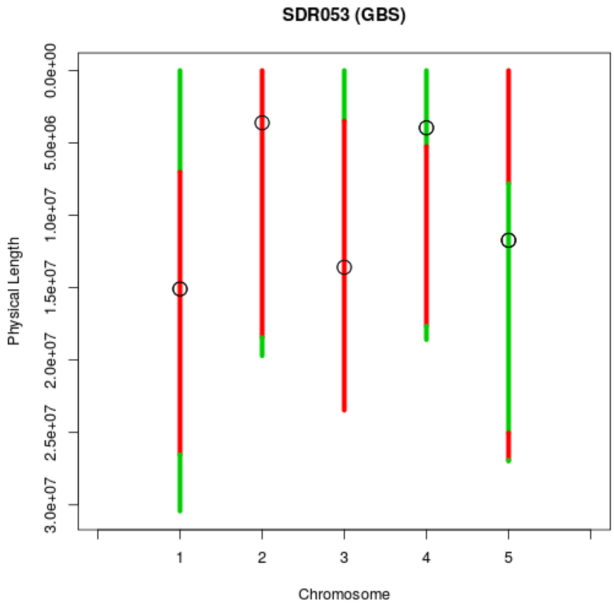
SDR053 (GBS)
Physical Length
0.0e+00
5.0e+06
1.0e+07
1.5e+07
2.0e+07
2.5e+07
3.0e+07
1
2
3
4
5
Chromosome

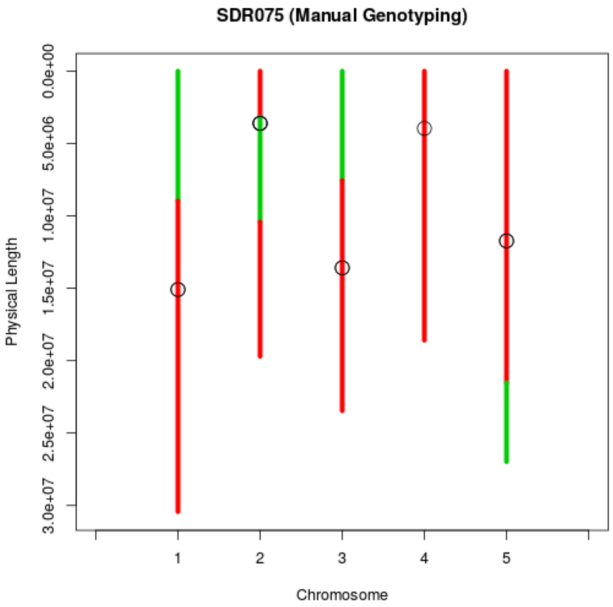
SDR075 (Manual Genotyping)
Physical Length
0.0e+00
5.0e+06
1.0e+07
1.5e+07
2.0e+07
2.5e+07
3.0e+07
1
2
3
4
5
Chromosome

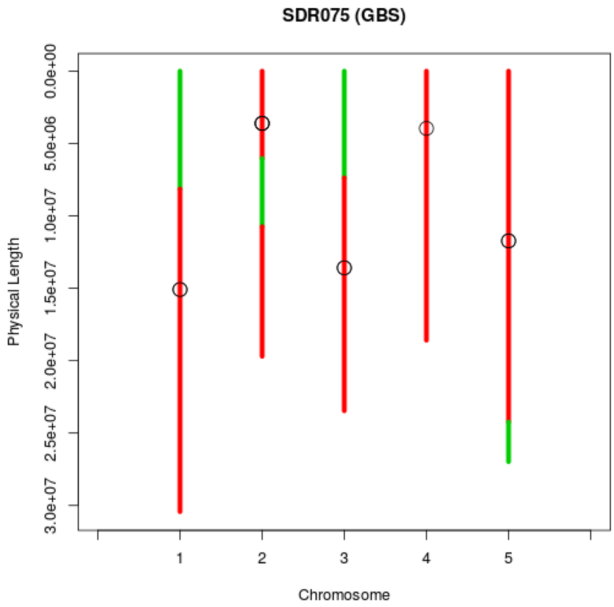
SDR075 (GBS)
Physical Length
0.0e+00
5.0e+06
1.0e+07
1.5e+07
2.0e+07
2.5e+07
3.0e+07
1
2
3
4
5
Chromosome

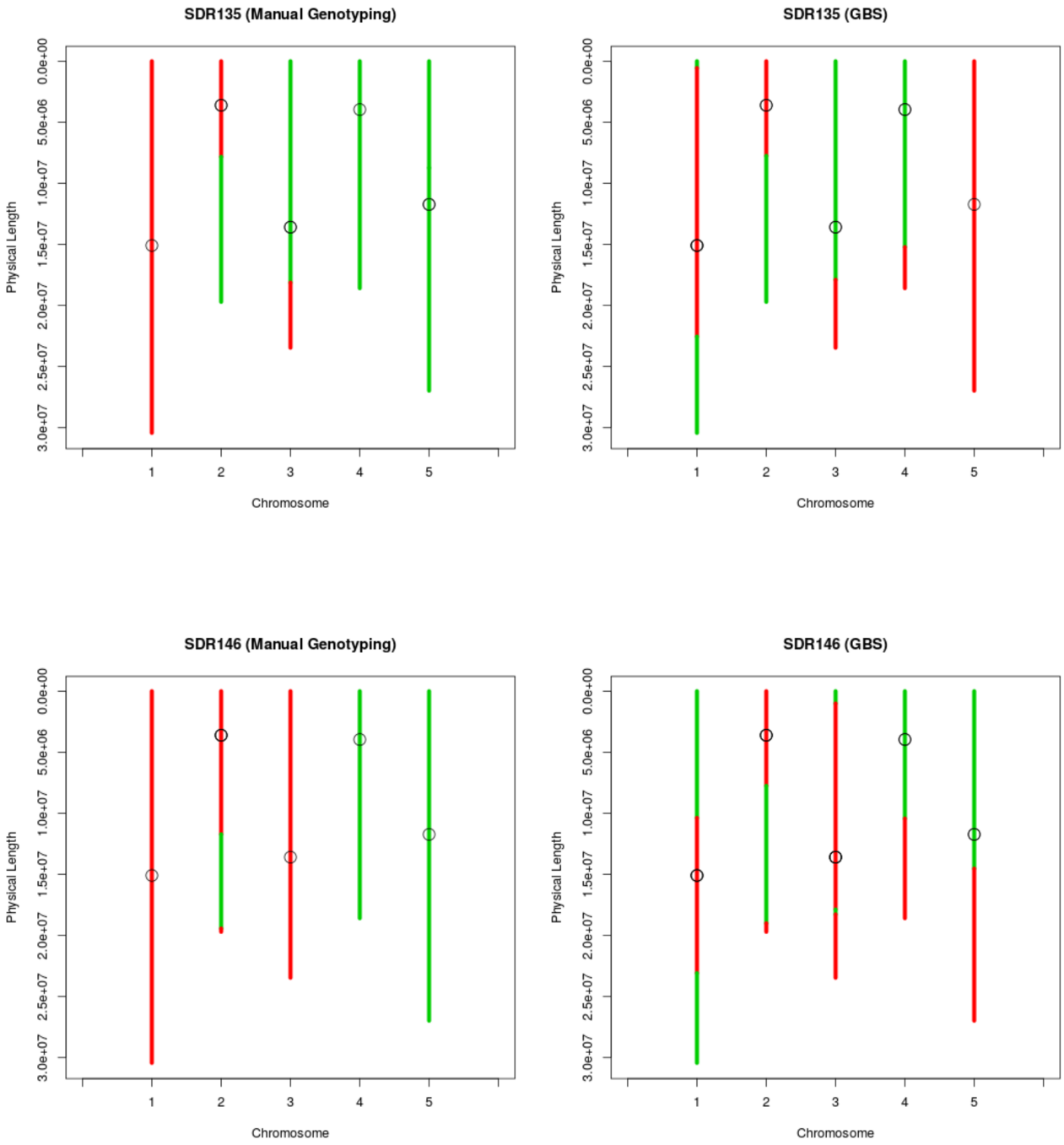

Figure 3.12: Manual and GBS genotyping for the 'Col+Het' group. Red=Col/Col sequence, Green=Col/Ler sequence, Blue=Ler/Ler sequence.

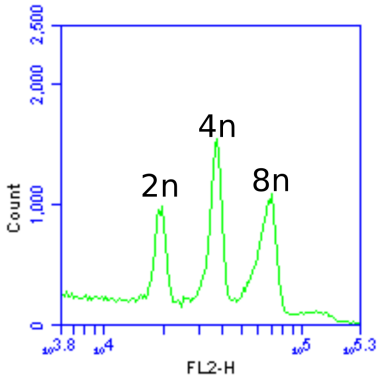

Diploid Control

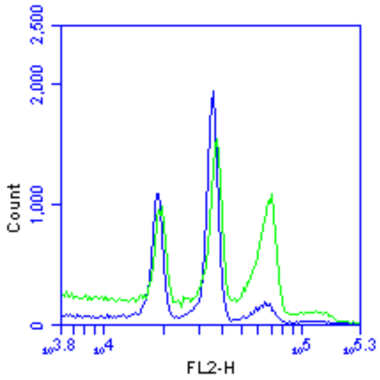

SDR002 (Diploid)

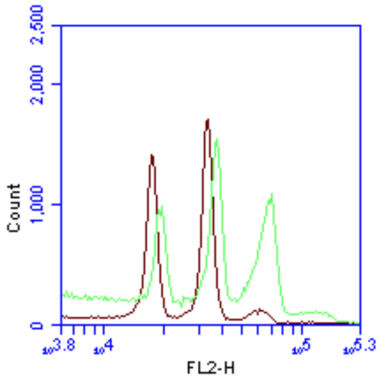

SDR004 (Diploid)

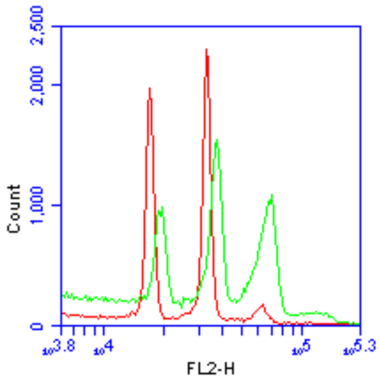

SDR009 (Diploid)

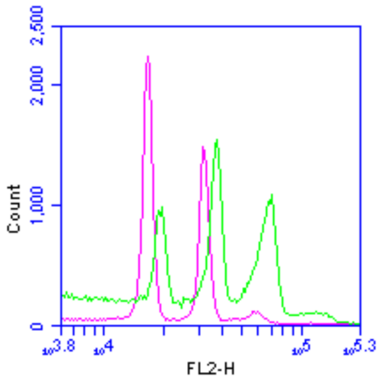

SDR010 (Diploid)

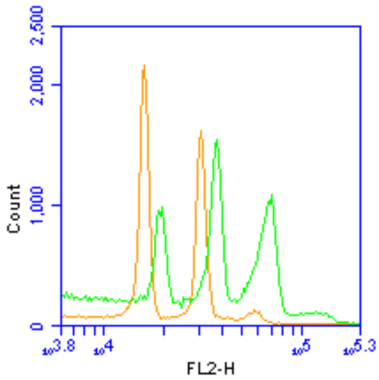

SDR011 (Diploid)

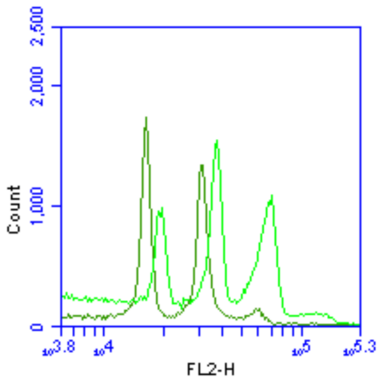

SDR015 (Diploid)

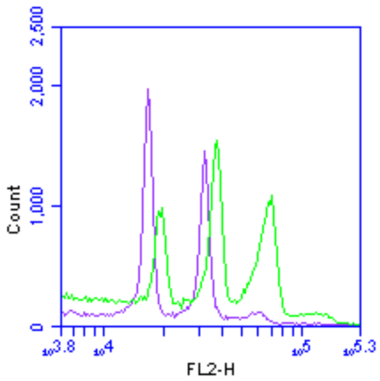

SDR017 (Diploid)

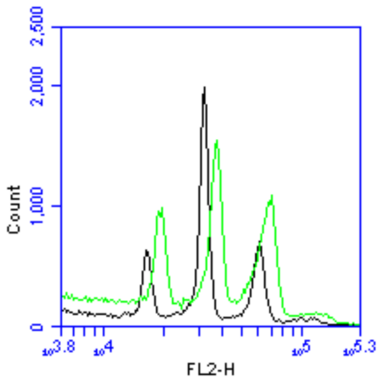

SDR021 (Diploid)

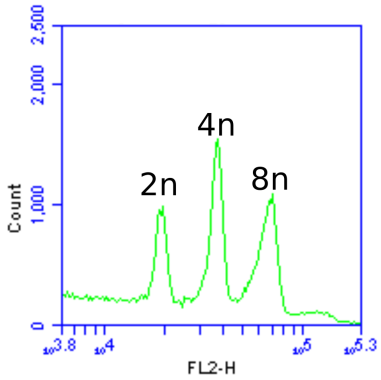

Diploid Control

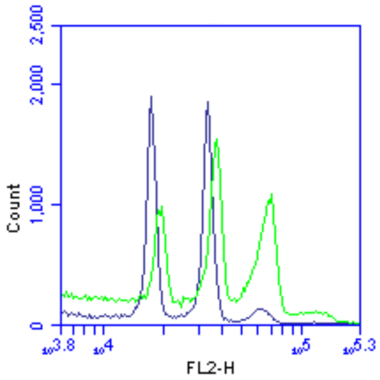

SDR023 (Diploid)

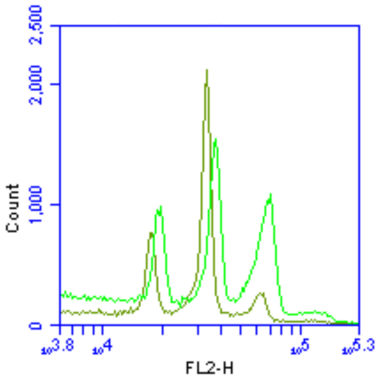

SDR031 (Diploid)

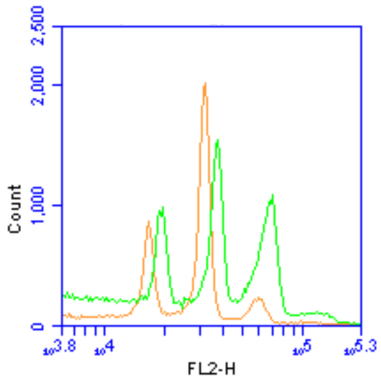

SDR036 (Diploid)

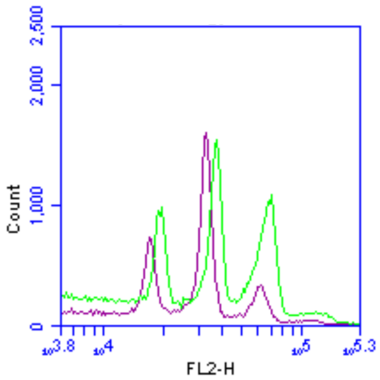

SDR040 (Diploid)

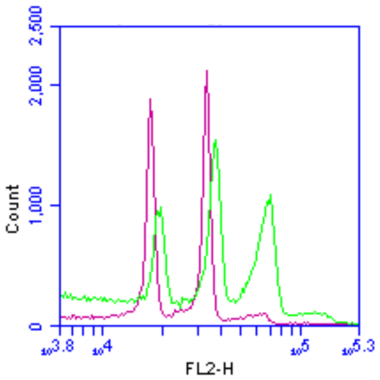

SDR051 (Diploid)

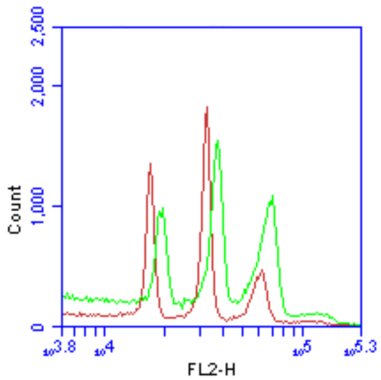

SDR052 (Diploid)

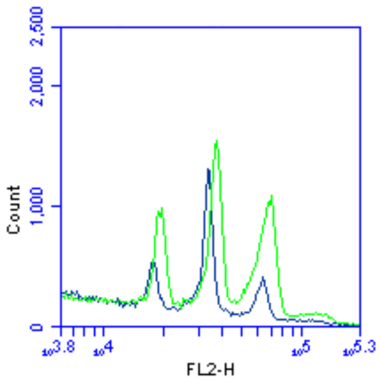

SDR066 (Diploid)

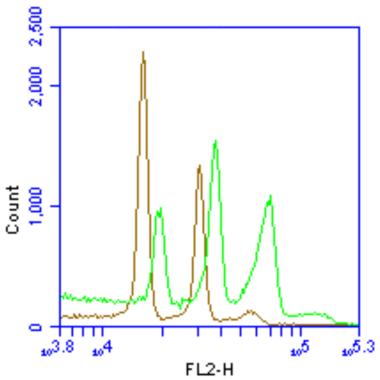

SDR121 (Diploid)

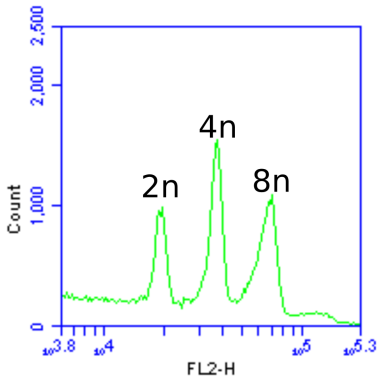

Diploid Control

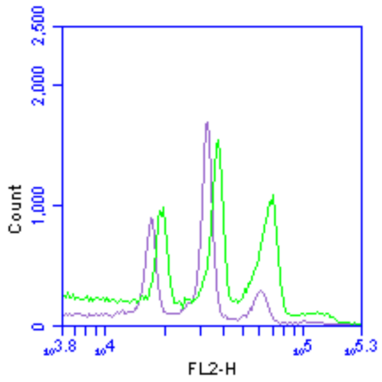

SDR126
(Diploid)

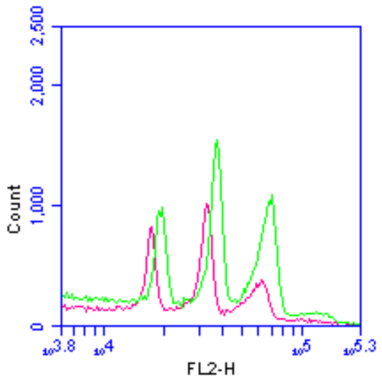

SDR0127
(Diploid)

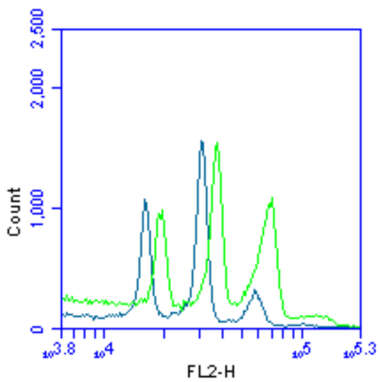

SDR135
(Diploid)

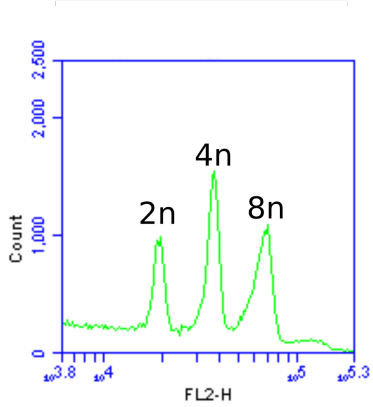

Diploid Control

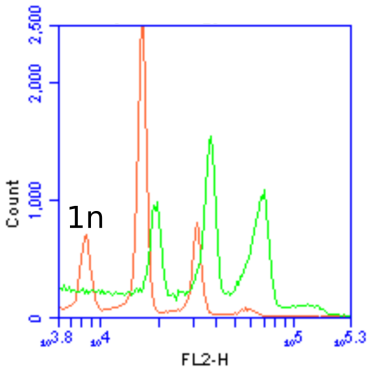

SDR070
(Haploid)

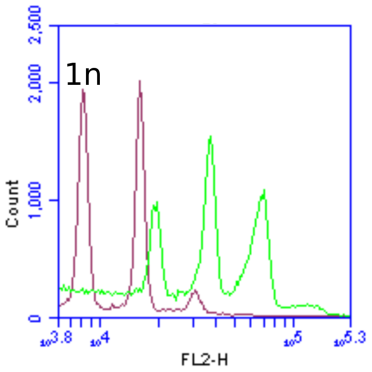

SDR078
(Haploid)

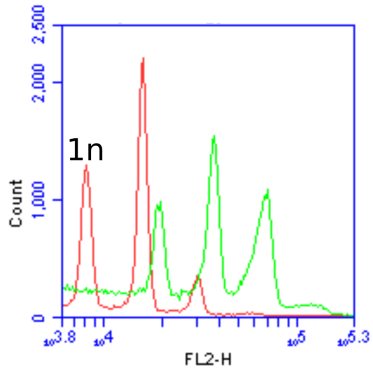

SDR101
(Haploid)

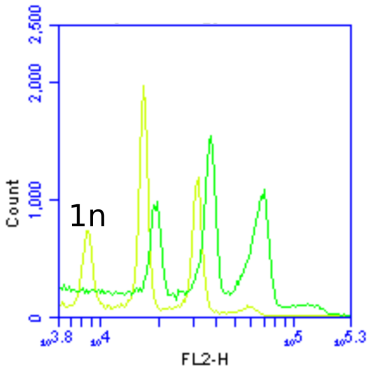

SDR153
(Haploid)

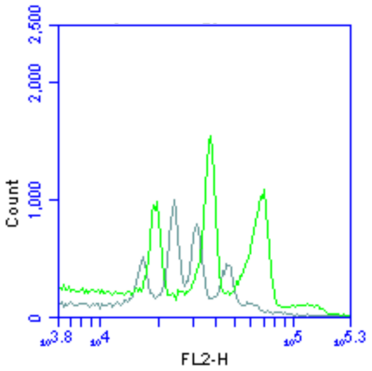

SDR146
(Aneuploid)

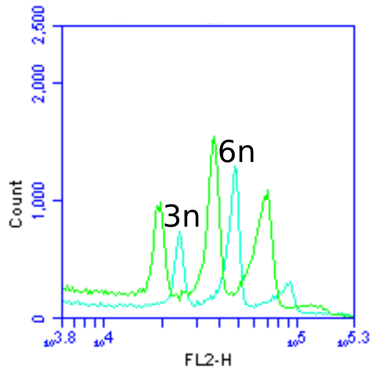

SDR067
(Triploid)

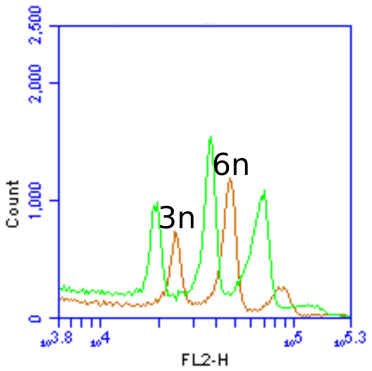

SDR163
(Triploid)

Figure 3.13: SDR population ploidy analysis via flow cytometry of propidium iodide stained nuclei. *The first (top left) graph on each page shows a diploid Col control with 2n, 4n, and 8n, peaks labelled. This control is replicated on all subsequent graphs in green as a comparison. The name of each SDR population individual, as well as its ploidy, is written beneath each graph.*

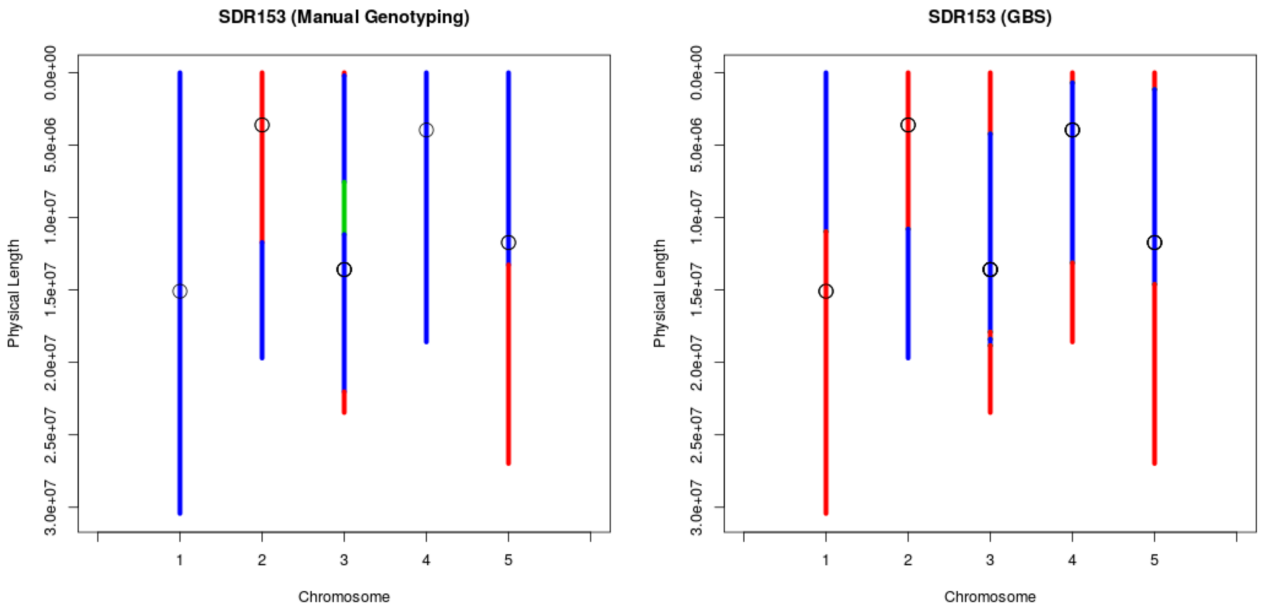

Figure 3.14: Manual and GBS genotyping for 'Col+Ler+Het' group. *Red=Col/Col sequence, Green=Col/Ler sequence, Blue=Ler/Ler sequence.*

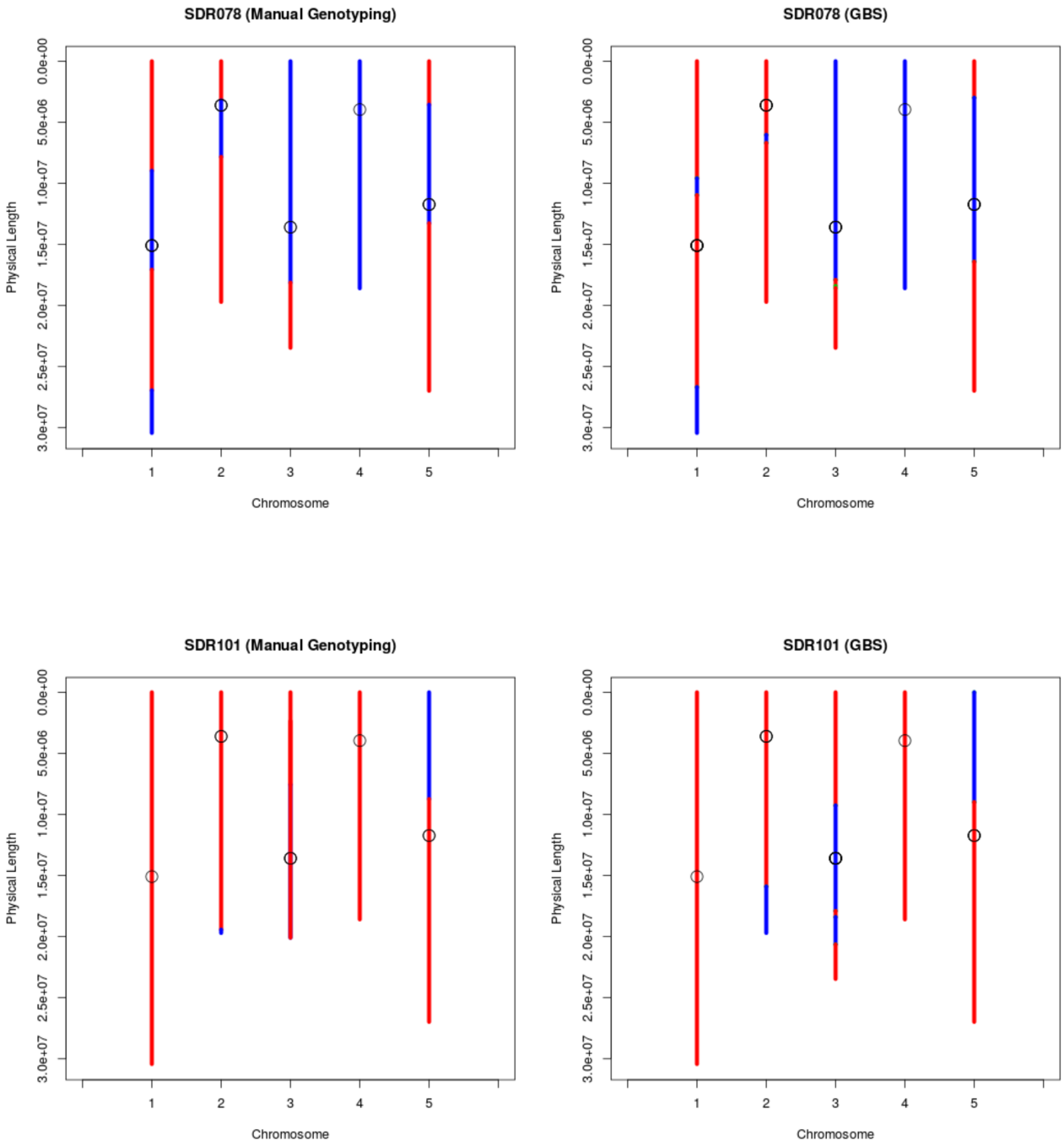

Figure 3.15: Manual and GBS genotyping for the 'Col+Ler' group. *Red=Col/Col sequence, Green=Col/Ler sequence, Blue=Ler/Ler sequence.*

3.4 Discussion

3.4.1 Expected characteristics of an SDR population

As discussed above, the SDR population created in this study was generated by crossing Col/Ler F_1 *osd1-3* KO plants as male to *GFP-tailswap* +/+ *GFP-CenH3* +/+ *cenh3* females (Figure 3.8). The anticipated offspring of this cross are diploid plants which have inherited their chromosomes uni-parentally from their paternal parent. Therefore the expected genotype of true SDR plants is as follows: *osd1-3* -/- GFP-*tailswap* -/- GFP-*CenH3* -/-; the plants should be diploid and have regions of heterozygosity on their chromosomes, accompanied by stretches of homozygous Col and Ler sequence (Figure 3.1). A further expectation is that there should be approximately equal amounts of homozygous Col and Ler regions across the population, as crossovers that generate a homozygous Col/Col region in one gamete will give rise to a corresponding homozygous Ler/Ler region of the same length in the other gamete produced in that meiosis (Figure 3.1). Previous studies crossing diploid pollen to haploid inducers have reported high levels (~74%) of aneuploid and mixaploid offspring, resulting from these crosses (Marimuthu *et al.* 2011), potentially due to defects in chromosome segregation post-fertilisation, due to the presence of excess chromosomes in the zygote. Due to the high occurrence of these 'aberrant' ploidies they could perhaps be considered the 'true' expected result of this cross. However due to the problems in propagating these haplotypes further they are only considered briefly in this discussion.

3.4.2 Aberrant ploidys observed in the SDR population

Of the 26 individuals whose ploidy was analysed, 7 (27%) showed non-diploid ploidy (haploid, triploid or aneuploid) (Figure 3.13). This is dramatically lower than the previously reported 74% aberrant ploidy observed in SDR to haploid-inducer crosses (Marimuthu *et al.* 2011). The reasons for this discrepancy are unclear, but one obvious substantive difference between the studies is that this study uses a Col/Ler hybrid to produce diploid gametes, whereas the previous study used a Nossen (No-0)/Ler hybrid. This suggests that different genetic backgrounds may influence the prevalence of aberrant ploidy offspring in SDR populations for unknown reasons.

3.4.3 Homozygous Ler/Ler stretches are under-represented in the SDR population

One striking feature of the Col/Ler genotyping data for the SDR population is the paucity of homozygous Ler stretches. Homozygous Col/Col or Ler/Ler stretches in SDR individuals are the result of crossovers between homologous chromosomes in meiosis-I. Each crossover creates a region of homozygous Col/Col sequence between two sister chromatids, which will go on to form a diploid gamete, while simultaneously creating a homozygous Ler/Ler stretch on the homologous pair of sister chromatids, which will form the other diploid gamete (Figure 3.1). Due to the reciprocal nature of crossover the gametes of SDR mutants should overall produce populations containing roughly the same frequency of homozygous Col/Col and Ler/Ler sequences.

Unexpectedly, in this SDR population there is a distinct lack of homozygous Ler/Ler stretches (Figure 3.10). Indeed, while there are many individuals which display only homozygous Col/Col and heterozygous stretches (‘Col+Het’), there are none that display only homozygous Ler/Ler and heterozygous stretches (‘Ler+Het’). However, there are some examples in the SDR population of plants having having Col/Col, Ler/Ler and Col/Ler heterozygous regions (e.g. SDR126 and 127). There are also 5 individuals displaying homozygous Col/Col and Ler/Ler stretches (The ‘Col+Ler’ group and SDR153). However with the exception of the possibly misgenotyped SDR167 all of these plants are haploid (Figure 3.13), a detail which is discussed further below.

There are a several explanations for the under-representation of Ler/Ler sequence, which are not mutually exclusive. First, there could be a bias in the viability of SDR gametes. Gametes comprising Het+Col sequence may be more likely to reach maturity or more likely to be able to successfully fertilise the eggs of haploid inducers than gametes containing Het+Ler sequence (Figure 3.16A). Second, there could be bias in chromosome dynamics post-fertilisation. A large number of the SDR population are heterozygous for *osd1-3* and/or the GFP-tailswap transgene. This means that they are not true SDR plants, but instead hybrids of the genetic material of the diploid SDR pollen and the haploid-inducer egg. It could therefore be possible that chromosomes with Ler sequence are dis-favoured compared to haploid-inducer chromosomes post-fertilisation (Figure 3.16B). Third, there could be bias in the seed

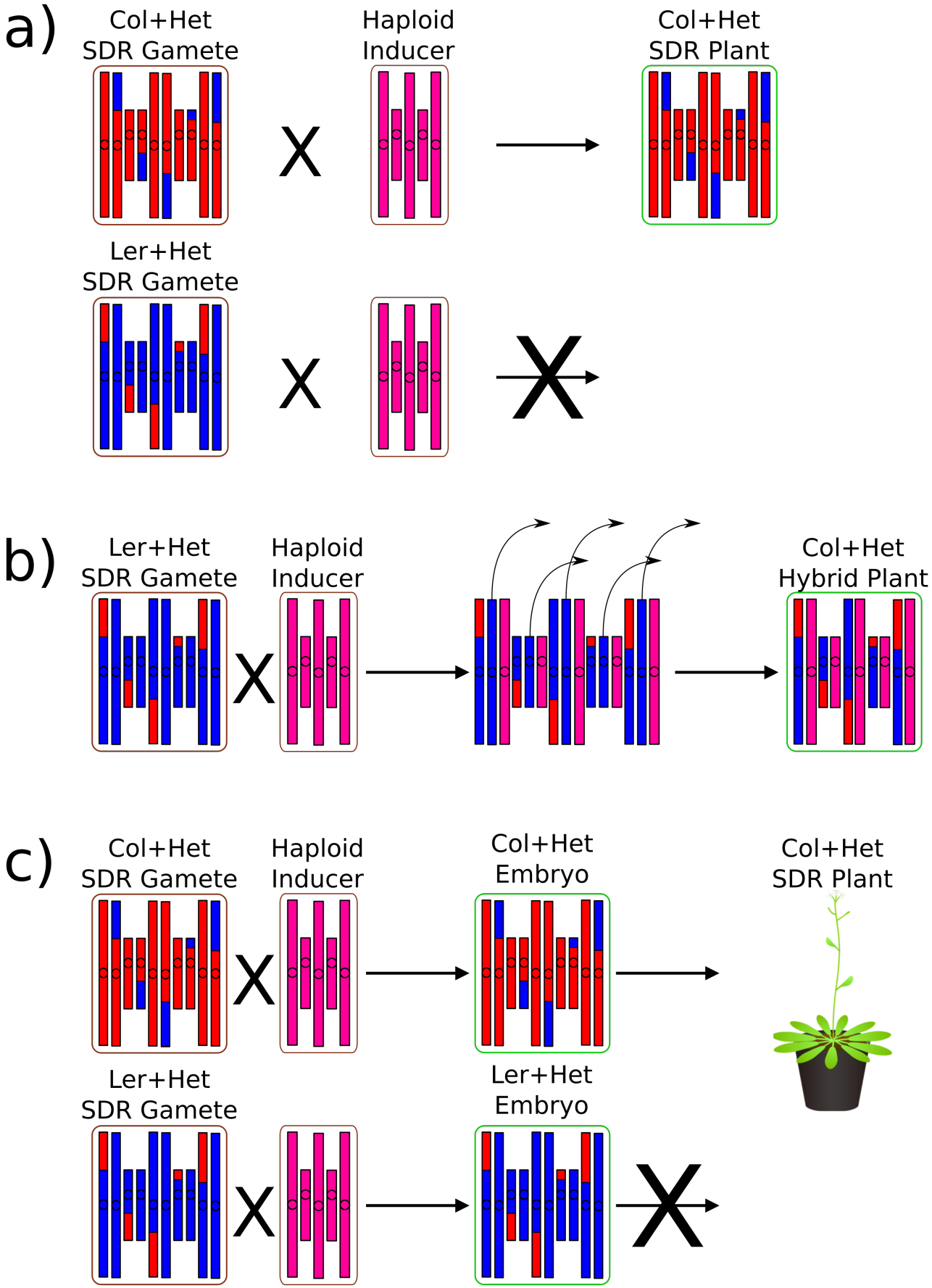
a)
Col+Het
SDR Gamete
Haploid
Inducer
Col+Het
SDR Plant
Ler+Het
SDR Gamete
b)
Ler+Het
SDR Gamete
Haploid
Inducer
Col+Het
Hybrid Plant
c)
Col+Het
SDR Gamete
Haploid
Inducer
Col+Het
Embryo
Col+Het
SDR Plant
Ler+Het
SDR Gamete
Ler+Het
Embryo

Figure 3.16: Models explaining the under-representation of Ler sequence in the SDR population. *Red=Col/Col sequence, Blue=Ler/Ler sequence, Pink=Haploid inducer sequence (the haploid-inducer line was in a Col/Col background, but a different colour is used such that true SDR and hybrid plants can be differentiated).* ***a)*** *Bias in the viability of SDR gametes. Gametes containing mainly Ler sequence either do not survive to maturity or, once mature are unable to undergo fertilisation.* ***b)*** *Bias in chromosome dynamics post-fertilisation. After fertilisation chromosomes comprised solely of Ler sequence are lost leading to the generation of a Col+Het hybrid plant.* ***c)*** *Bias in seed viability. Embryos containing mainly Ler sequence fail to grow to maturity leading to under-representation in the final SDR population.*

viability of SDR plants containing Het+Ler sequence. For example, once generated Het+Ler seeds may fail to reach maturity, either because they do not successfully germinate or after germination fail to grow normally (Figure 3.16C).

3.4.4 *OSD1*, *GFP-Tailswap* and *GFP-CenH3* genotypes

In this section, I provide hypotheses of the origin of the obtained genotypic classes obtained in the SDR population.

3.4.4.1 All-Col plants

The largest group of individuals classified according to genotype in the SDR population was those that were completely homozygous for Col/Col along all chromosomes (Figure 3.10). Of this 'all-Col' group only one individual was a homozygous mutant for *osd1-3*, while 79.5% were WT and 19.3% were heterozygous. The simplest explanation for the origins of the WT individuals is that they were not produced by a cross between SDR diploid pollen and a haploid-inducer egg, but were instead produced by the haploid-inducer self-fertilizing (Figure 3.17B). This is essentially a contamination scenario, which suggests that some percentage of the SDR population is the result of selfing of the GEM line. While this argument can explain the existence of wild type *OSD1* plants, which posses the *GFP-tailswap* and *GFP-CenH3* transgenes and were diploid, it does not account for individuals like SDR026, 029, and 031 which are wild type for *OSD1*, but possess heterozygous *GFP-tailswap* (e.g. SDR026, SDR029), or do not possess *GFP-tailswap* at all (e.g. SDR031), as these plants must be a hybrid of SDR and haploid-inducer genetic material (Figure 3.17C). The 'all-Col' plants which are heterozygous for *osd1-3* are similarly difficult to explain simply in terms of contamination of the SDR population. In order to possess an *osd1-3 +/-* genotype, diploid pollen from an SDR mutant must have undergone fertilisation with the haploid-inducer GEM line (which is wild type for *OSD1*), and then given rise to a diploid plant with a heterozygous *osd1-3* genotype. This suggests that after fertilisation one of the chromosome sets given to the zygote by the diploid pollen was eliminated, instead of the chromosome set donated by the haploid-inducer egg cell (Figure 3.17C).

3.4.4.2 ‘Col+Het’ plants

The next largest group by genotyping data is that which has stretches of Col/Ler heterozygous sequence alternating with stretches of homozygous Col/Col sequence, but no homozygous Ler/Ler sequence (Figure 3.10). This ‘Col+Het’ group has only 3 plants, which have the expected *osd1-3* homozygous genotype. However, in contrast to the ‘all-Col’ group a much larger number of plants (48.4%) in this group have a heterozygous *osd1-3* genotype, while the remaining 40.6% are wild type for *OSD1*.

Unlike the ‘all-Col’ group, the individuals in the ‘Col+Het’ group, which are not homozygous for *osd1-3* cannot be explained by aberrant selfing of the GEM line. This is because they display some Col/Ler heterozygous sequence and must therefore have chromosomes which have at least some Ler sequence. The only possible origin of this Ler sequence is from the diploid SDR pollen used in the cross. A possible explanation of the origin of ‘Col+Het’ plants which are heterozygous for *osd1-3* is that after fertilisation, one chromosome set from the diploid SDR pollen was lost while the other chromosome set was preserved, along with a chromosome set from the haploid-inducer egg (Figure 3.17D). This is supported by the fact that 61% of ‘Col+Het’ plants that were heterozygous for *osd1-3* are also heterozygous for the *GFP-tailswap* transgene, suggesting that they are hybrids of SDR and haploid-inducer genetic material.

3.4.4.3 ‘Col+Ler’ plants

Only four individuals displayed homozygous Col/Col and Ler/Ler sequence with no intervening Col/Ler heterozygous sequence (Figure 3.10). However, SDR153 should probably also be included in this group, as GBS data confirms it as a ‘Col+Ler’ plant, even though manual PCR genotyping suggested it had some heterozygous sequence on chromosome 3 (Figure 3.14). Because of the small size of this ‘Col+Ler’ group it is difficult to draw firm conclusions from it. However, it is relatively certain that these plants were true ‘Col+Ler’ plants, as two of them had their genotyping verified by GBS (Figure 3.15). With the exception of SDR167 which may actually be an ‘all-Col’ plant, all of the ‘Col+Ler’ group were confirmed as haploids (Figure 3.13). This means that they possess one set of paternal

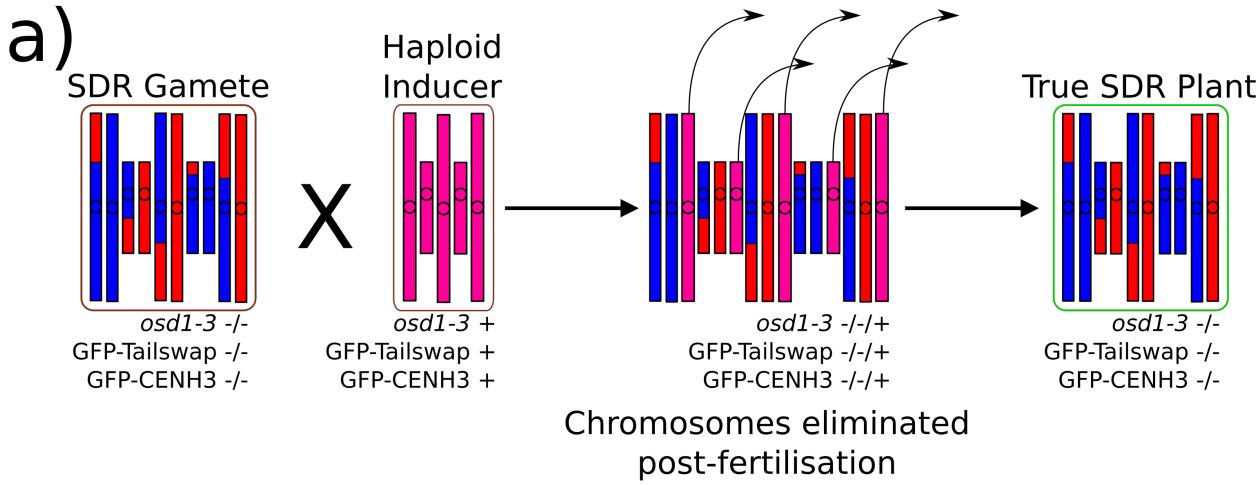
a)
SDR Gamete
Haploid Inducer
True SDR Plant
X
osd1-3 -/-
GFP-Tailswap -/-
GFP-CENH3 -/-
osd1-3 +
GFP-Tailswap +
GFP-CENH3 +
osd1-3 -/-/+
GFP-Tailswap -/-/+
GFP-CENH3 -/-/+
osd1-3 -/-
GFP-Tailswap -/-
GFP-CENH3 -/-
Chromosomes eliminated post-fertilisation

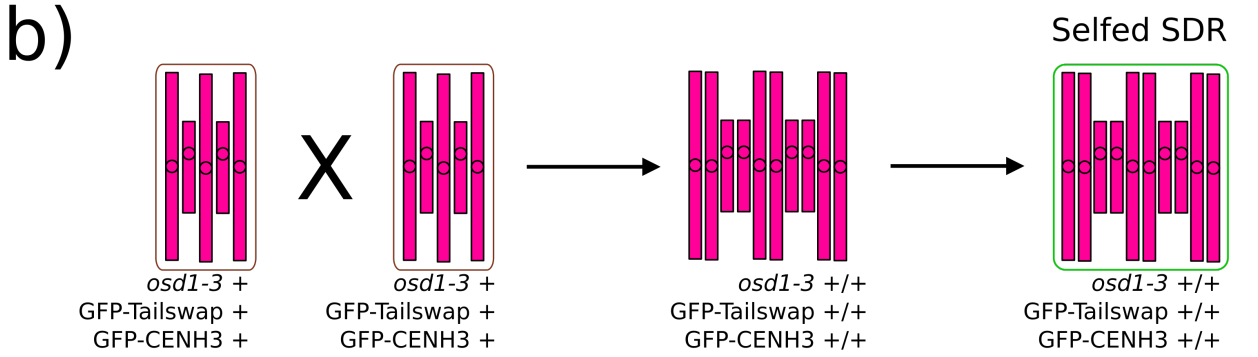
b)
Selfed SDR
X
osd1-3 +
GFP-Tailswap +
GFP-CENH3 +
osd1-3 +
GFP-Tailswap +
GFP-CENH3 +
osd1-3 +/+
GFP-Tailswap +/+
GFP-CENH3 +/+
osd1-3 +/+
GFP-Tailswap +/+
GFP-CENH3 +/+

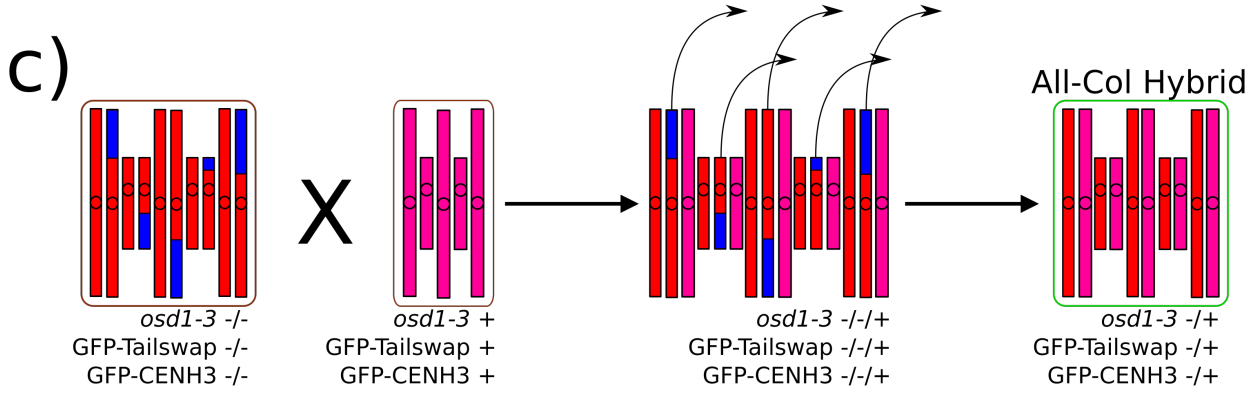
c)
All-Col Hybrid
X
osd1-3 -/-
GFP-Tailswap -/-
GFP-CENH3 -/-
osd1-3 +
GFP-Tailswap +
GFP-CENH3 +
osd1-3 -/-/+
GFP-Tailswap -/-/+
GFP-CENH3 -/-/+
osd1-3 -/+
GFP-Tailswap -/+
GFP-CENH3 -/+

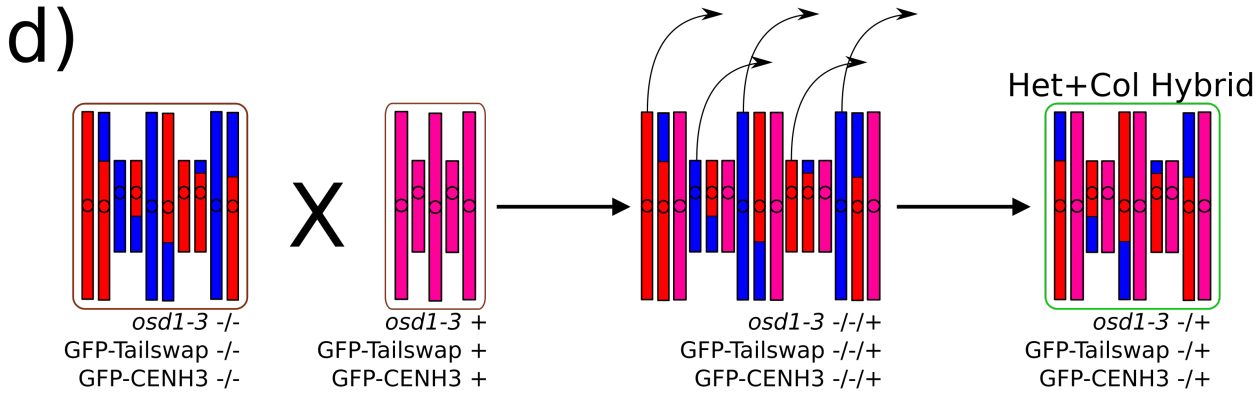
d)
X
Het+Col Hybrid
osd1-3 -/-
GFP-Tailswap -/-
GFP-CENH3 -/-
osd1-3 +
GFP-Tailswap +
GFP-CENH3 +
osd1-3 -/-/+
GFP-Tailswap -/-/+
GFP-CENH3 -/-/+
osd1-3 -/+
GFP-Tailswap -/+
GFP-CENH3 -/+

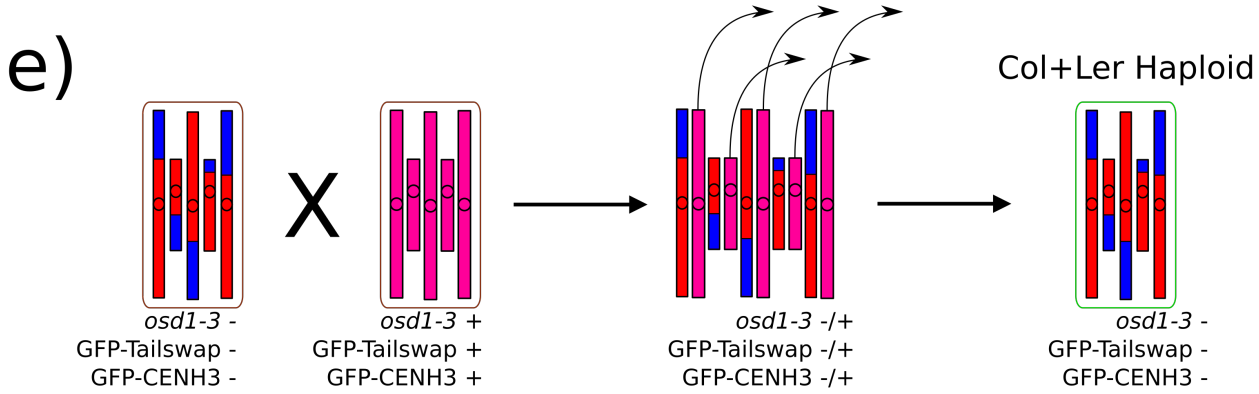
e)
X
Col+Ler Haploid
osd1-3 -
GFP-Tailswap -
GFP-CENH3 -
osd1-3 +
GFP-Tailswap +
GFP-CENH3 +
osd1-3 -/+
GFP-Tailswap -/+
GFP-CENH3 -/+
osd1-3 -
GFP-Tailswap -
GFP-CENH3 -

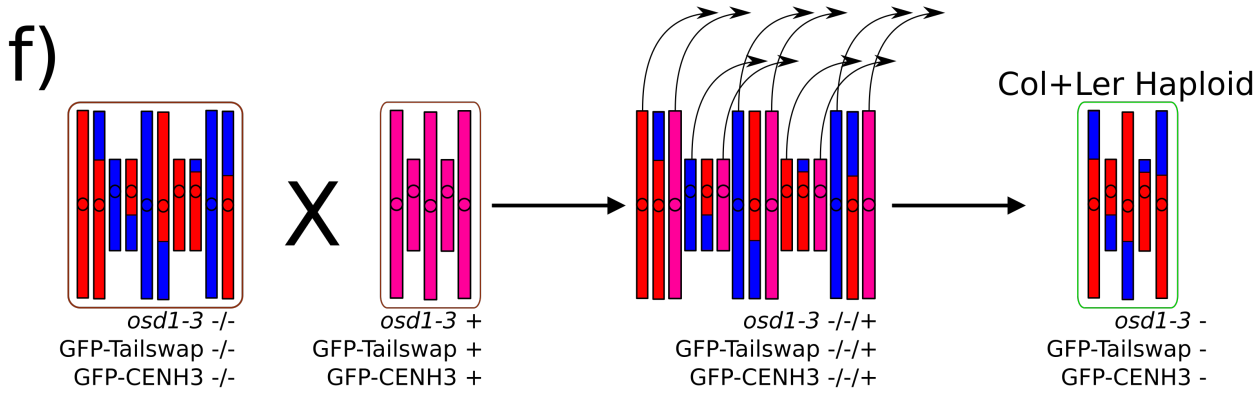
f)
X
Col+Ler Haploid
osd1-3 -/-
GFP-Tailswap -/-
GFP-CENH3 -/-
osd1-3 +
GFP-Tailswap +
GFP-CENH3 +
osd1-3 -/-/+
GFP-Tailswap -/-/+
GFP-CENH3 -/-/+
osd1-3 -
GFP-Tailswap -
GFP-CENH3 -

Figure 3.17: Models explaining the various genotypes seen in the SDR population.
Red=Col/Col sequence, Blue=Ler/Ler sequence, Pink=Haploid inducer sequence (The haploid-inducer line was in Col/Col background, but a different colour is used so that true SDR and hybrid plants can be differentiated). **a)** Expected SDR inheritance. An SDR gamete and a haploid-inducer gamete undergo fertilisation. The haploid inducer chromosomes are lost generating a true SDR plant. **b)** SDR self-fertilization. Two haploid inducer gametes undergo fertilisation leading to an 'all-Col' selfed plant (N.B. While haploid-inducer chromosomes are lost when crossed to non-haploid-inducer gametes, they are not lost during selfing). **c)** All-Col hybrid. Post-fertilisation chromosomes containing Col and Ler sequence are lost while the all-Col chromosomes from the SDR gamete and the haploid-inducer gamete remain, giving rise to an all-Col hybrid plant. **d)** Het+Col hybrid. Similar to the all-Col hybrid, following fertilisation one set of chromosomes is lost, this time chromosomes possessing all-Col or all-Ler sequence, giving rise to a Het+Col hybrid. **e)** Col+Ler haploid. A haploid SDR gamete fertilises a haploid-inducer gamete whose chromosomes are lost, giving rise to a haploid Col-Ler plant. **f)** Alternate haploid Col+Ler. A diploid SDR gamete fertilises a haploid-inducer gamete. One set of chromosomes from the SDR gamete and the chromosomes of the haploid-inducer gamete are lost, giving rise to a Col+Ler haploid plant.

chromosomes, which have undergone meiosis-I. There are two mutually exclusive explanations of how plants with this ploidy could arise; (i) the paternal SDR plant was producing some amount of haploid pollen, which when crossed with the haploid-inducer GEM line and gave rise to a haploid plant (Figure 3.17E), or (ii) alternatively, diploid pollen was produced as expected however, one set of paternal chromosomes present in the SDR pollen was lost along with the haploid-inducer chromosomes post-fertilisation leaving only one set of chromosomes in the resulting plant (Figure 3.17F).

3.4.4.4 'Col+Ler+Het' plants

This represents another group that is too small to draw reliable conclusions that contained all possible combinations of Col/Col and Ler/Ler homozygous and Col/Ler heterozygous sequence. According to the manual genotyping data there were 12 individuals with this profile, however 8 of these individuals only tested positive for homozygous Ler/Ler genotype at a single marker meaning there is a good chance they were incorrectly genotyped. Interestingly, the only two plants which show the correct genotype profile to be considered true SDR plants (SDR126, and 127) come from this 'Col+Ler+Het' group (Figure 3.10).

3.4.5 Conclusions

Producing this SDR population has demonstrated the variety of outcomes that crossing SDR mutants to haploid inducer lines is capable of producing. It is highly likely that at least two true SDR plants, which inherited their genetic material uniparentally and contained stretches of homozygous sequence, with residual regions of heterozygosity generated by crossovers, were created. However, it appears that a high number of hybrid plants which inherited genetic material from both parents and yet retained diploid ploidy were also created, as well as individuals which managed to reach maturity even though they had aberrant ploidy, or which even displayed aneuploidy.

4 Chapter 4: Directing meiotic recombination via TAL fusion proteins

4.1 Abstract

During meiosis, a minority of the DNA double strand breaks (DSBs) created by SPO11 mature into crossovers. For example, in wild-type Arabidopsis around 10 of the ~150 DSBs generated during meiosis become crossovers. Although some elements of crossover placement are understood this knowledge has not yet allowed for precise control of meiotic crossover location. In this study TALENs comprising a TAL DNA-targeting domain and a *Fok*I nuclease domain were expressed from meiotic promoters in an attempt to direct crossovers by controlling the location of meiotic DNA DSBs. Data is presented that shows that *FokI*-derived DSBs may not be competent to enter meiotic repair pathways that use SPO11-derived DSBs as substrates.

4.2 Introduction

4.2.1 Meiotic crossovers are essential for fertility in plants

Meiotic crossovers are an essential feature of plant meiosis where they serve two main purposes. The first is to physically link homologous chromosomes during meiosis-I (Nicklas & Koch 1969; Ault & Nicklas 1989; Lacefield & Murray 2007) (Figure 4.1). By creating a physical link between homologous chromosomes, evident cytologically as chiasmata, crossovers ensure that when the meiotic spindle fibres begin to contract during anaphase of meiosis-I, tension is generated along these fibres. This tension is essential for the stability of spindle fibres and therefore for correct segregation of chromosomes during meiosis (Nicklas & Koch 1969; Ault & Nicklas 1989; Lacefield & Murray 2007). The second role of crossovers is to recombine genetic variation located on the same chromosome, allowing for the generation of novel allelic combinations, and therefore novel phenotypes, in sexually reproducing organisms (Villeneuve & Hillers 2001). Due to crossovers, organisms reproducing via meiosis pass on to their offspring chromosomes that are a mosaic of the maternal and paternal chromosomes which they themselves inherited

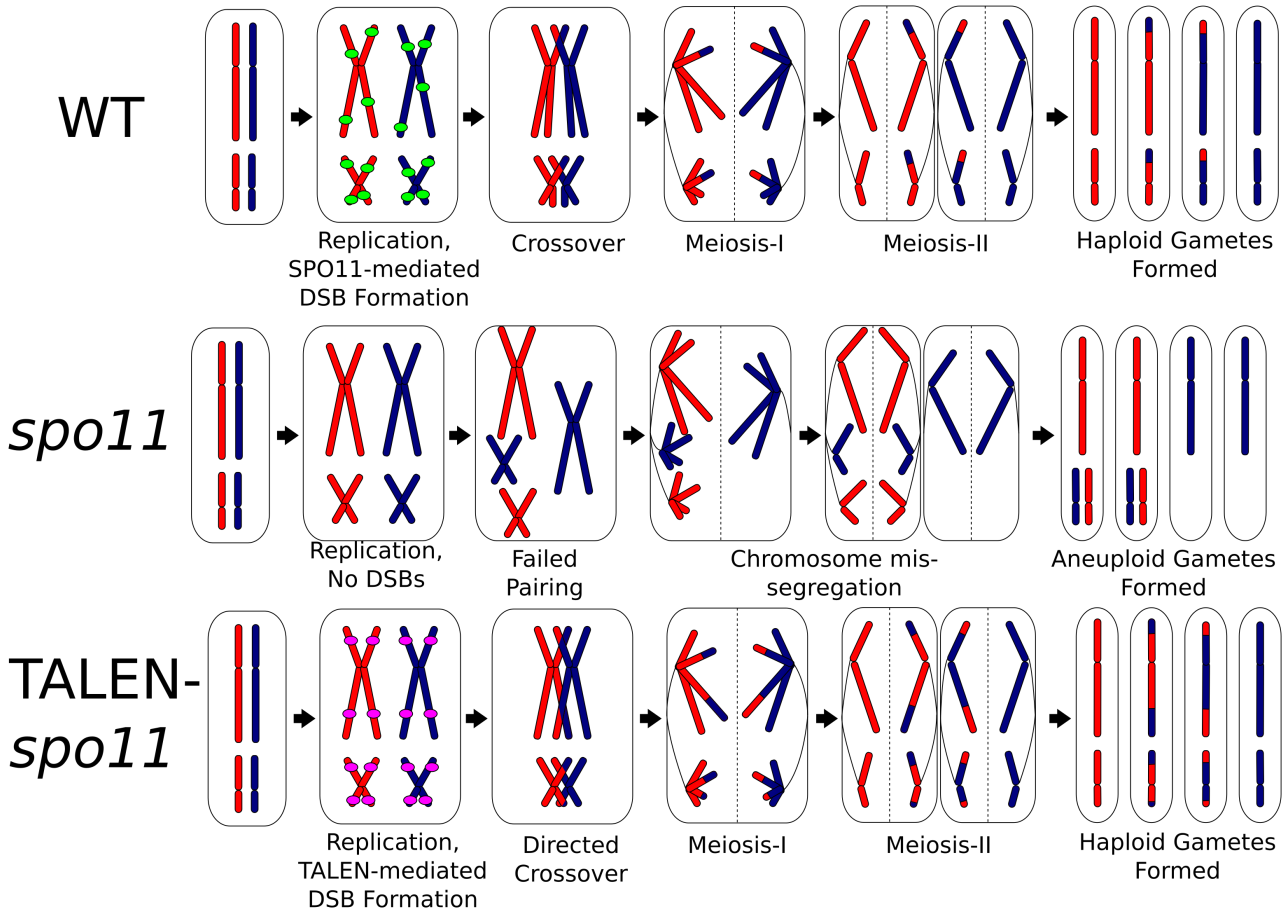

Figure 4.1: Schematic of wild type, spo11 and putative TALEN-spo11 meiosis. *In wild type meiosis SPO11 creates DSBs which can be repaired as crossovers, which ensures correct segregation of chromosomes during meiosis-I. In spo11 meiosis DSBs fail to form leading to an absence of pairing and homologue missegregation during meiosis-I and meiosis-II, ultimately leading to a high incidence of anueploid gametes and infertility. We predicted that in TALEN-spo11 meiosis the action of TALENs during meiosis would create targeted DSBs capable of undergoing crossover. This would correct the missegregation of chromosomes observed in spo11 mutants, leading to normal haploid gamete formation and therefore a recovery of fertility.*

(Morgan 1916; Creighton & McClintock 1931). It has been proposed that recombination allows deleterious mutations to be purged and beneficial mutations to be combined along chromosomes with greater efficiency than would be possible through clonal reproduction (Muller 1932; Felsenstein 1976; Barton 2009). It should also be noted that crossovers play vitally important roles in human agriculture, as current crop breeding programmes rely on crossovers to combine favourable traits and generate better adapted plant and animal breeds for farming.

At the chromosome scale, *Arabidopsis* crossovers increase in density along the chromosome from telomere to pericentromere, while the centromere is crossover-suppressed (Copenhaver *et al.* 1998; Salomé *et al.* 2012; Choi *et al.* 2013; Mézard *et al.* 2015). At the fine-scale, *Arabidopsis* crossovers preferentially occur at gene promoters and terminators within euchromatin (Yelina *et al.* 2012; Drouaud *et al.* 2013). Euchromatin is characterised by a decondensed cytological state, enrichment of gene-associated histone modifications such as H3K4^{me3} and the histone variant H2A.Z, as well as regions of low nucleosome density in gene promoters and terminators (Choi *et al.* 2013). These features are known to promote accurate and productive RNA polymerase II transcription at genes (Venters & Pugh 2010). Crossover sites are also typically DNA hypomethylated (Mirouze *et al.* 2012; Yelina *et al.* 2012), and acquisition of DNA methylation and H3K9^{me2} at hotspots is sufficient to silence crossover recombination (Yelina *et al.* 2012). Specific DNA sequence motifs are also highly correlated with elevated crossover rates, including AT-rich motifs, CCN and CCT repeats (Horton *et al.* 2012; Choi *et al.* 2013b; Wijnker *et al.* 2013; Shilo *et al.* 2015).

4.2.2 SPO11 creates DSBs that initiate crossover repair

Crossover formation during meiosis is a complex process that is described in further detail in the Introduction chapter. Briefly, during meiosis the SPO11 transesterase creates DNA double strand breaks (DSBs) along the chromosomes (Keeney *et al.* 1997) which are resected to create 3’-overhanging single-strand DNA (ssDNA) (Sun *et al.* 1991). The ssDNA is bound by the RAD51 and DMC1 recombinases, which then preferentially invade a homologous chromosome. Depending on how such interhomolog invasion sites are further processed and

repaired, either a crossover or non-crossover event occurs (Lake & Hawley 2015). Crossovers involve the reciprocal exchange of a section of chromosome with the corresponding section of the homologous partner's chromosome. Non-crossovers involve a much smaller amount of sequence exchange between partners due to *de novo* synthesis that occurs following homolog invasion. This can result in gene conversion and 3:1 patterns of inheritance of markers through meiosis (Lake & Hawley 2015). Crossover locations can be determined by inheritance of genetic markers, as parental markers will switch linkage phase from one parent to another across the site of crossovers.

In *Arabidopsis* there are two non-redundant meiotic SPO11 homologues; SPO11-1 and SPO11-2, which appear to act together as a heterodimer to catalyse DSB formation (Stacey *et al.* 2006; Vrielynck *et al.* 2016). The SPO11-1/SPO11-2 subunits have structural similarities to the 'A' subunits of archeal topoisomerase VI (TopoVI) (Vrielynck *et al.* 2016). Indeed, recent work has characterised a structural homolog of the TopoVIB subunit, named meiotic topoisomerase VIB-like (MTOPVIB), which is required for SPO11-1/SPO11-2 heterodimerisation and meiotic DSB formation (Vrielynck *et al.* 2016). SPO11-1/SPO11-2 are thought to generate approximately 100-200 DSBs throughout the *Arabidopsis* genome during meiosis, based on counts of RAD51, DMC1 and γ-H2AX DSB-associated foci (Chelysheva *et al.* 2005; Sanchez-Moran *et al.* 2007; Ferdous *et al.* 2012; Choi *et al.* 2013). A fraction of these DSBs go on to mature into ~10 crossovers per meiosis (Sanchez-Moran *et al.* 2002; López *et al.* 2012), while the remainder are thought to be repaired either via the non-crossover repair pathway, or using the sister chromatid. In both *spo11-1* and *spo11-2* mutants DSBs fail to form, meaning crossovers do not occur. As a consequence, homologous chromosomes segregate randomly at meiosis-I, which results in mostly aneuploid, infertile gametes (Grelon *et al.* 2001; Stacey *et al.* 2006). In *C. elegans* DSBs produced by γ-irradiation have been found to recover the *spo11* infertility phenotype (Dernburg *et al.* 1998). Additionally, in *Arabidopsis*, DSBs generated by cisplatin treatment gave rise to partial recovery of *spo11-1* infertility. At low cisplatin concentrations partial pairing and synapsis of homologous chromosomes was observed in DAPI-stained pachytene and metaphase-I nuclei, however this did not recover the infertility phenotype and higher concentrations of cisplatin led to chromosome fragmentation (Sanchez-Moran *et al.* 2007). These studies indicate that at least in these scenarios DSBs generated from sources other than SPO11 are competent to enter

meiotic crossover repair pathways. This project sought to generate non-SPO11 dependent DSBs during Arabidopsis meiosis in an attempt to direct the formation of meiotic recombination events and crossover formation.

4.2.3 TALENs generate site-directed DNA double strand breaks

Transcription activation-like effector (TALE) proteins were discovered in the plant pathogen *Xanthomonas campestris* (Bonas *et al.* 1989). TALE proteins contain a DNA binding domain that consists of multiple repeats of a 34 residue sequence, each repeat binding a single DNA base (Moscou & Bogdanove 2009). The identity of the 12th and 13th amino acid residues vary from repeat to repeat (Moscou & Bogdanove 2009; Cong *et al.* 2012). These hyper-variable residues are termed the repeat variable diresidue (RVD) and determine the specificity of binding for a particular repeat to a DNA base. The correspondence between RVD and DNA-base target is as follows: NI=A, HD=C, NG=T, NK=G, NN=R (G or A), NS=N (A, T, C or G) (Moscou & Bogdanove 2009; Cong *et al.* 2012; Miller *et al.* 2015). The DNA targeting domain of TALEs can be fused to a nuclease domain to generate a TAL endonuclease (TALEN). TALENs are capable of making directed DNA DSBs and in *Arabidopsis* a TALEN designed to target an intron of the *ADH1* (*ALCOHOL DEHYDROGENASE 1*) gene was found to generate numerous deletion mutants in *Arabidopsis* protoplasts, when expressed under the control of a strong *35S* promoter. This is believed to reflect the TALEN generating DSBs which were then repaired by the error-prone non-homologous end joining (NHEJ) pathway (Cermak *et al.* 2011). There are two major pathways in eukaryotes for repairing non-meiotic DSBs, termed homology directed repair (HDR) and NHEJ. HDR repairs DSBs by using a template (usually a sister chromatid) in order to determine what sequence needs to be restored to a DSB. In contrast, NHEJ ligates broken ends rapidly, but without using a template, meaning that bases are occasionally added or lost during the process (Mimitou & Symington 2009). The activity of TALENs to generate DSBs in *Arabidopsis* was further confirmed by another study which used a similar approach to Cermak *et al.* (2011) to generate heritable NHEJ mutants of five *Arabidopsis* genes in transformed plants (Christian *et al.* 2013).

4.2.4 Project aim: Use TALENs to generate directed meiotic DSBs in a *spo11-1* mutant

The aim of this project was to harness the ability of TALENs to make site-directed DNA DSBs in order to target recombination in an Arabidopsis *spo11-1* mutant. It was assumed that in the absence of endogenous DSBs generated by SPO11-1, the TALEN-generated DSBs would be channelled into the endogenous interhomolog repair pathway, thereby generating directed crossovers (Figure 4.1). TALENs were designed which contained varying numbers of the degenerately binding NS repeat variable diresidue (RVD). The aim of this was to introduce target site degeneracy into the TALEN, as the NS RVD is capable of binding to all DNA bases (Moscou & Bogdanove 2009). TALENs were placed under the control of meiotic promoters and transformed into *spo11-1-3*+/- plants. T_1 and T_2 *spo11-1-3* homozygous individuals were then screened for recovery of fertility. Additionally, *spo11-1* and *spo11-2* mutants were exposed to X-ray radiation to investigate whether exogenously supplied DSBs were competent to restore fertility.

4.3 Results

4.3.1 TALEN design

A TALEN consists of a TAL-effector DNA-targeting domain fused to a nuclease domain (Christian *et al.* 2010). In order to confer site-specificity to targeted DSBs, two TALENs (termed a TALEN pair) were used together per construct. The two TALENs are designed to target DNA sequences that are separated by a short spacer, usually 15-25 bp, following published successful designs (Cermak *et al.* 2011; Christian *et al.* 2013). This spacer is designed in order to allow paired *FokI* nuclease domains to dimerise between the TAL binding sequence, allowing a DSB to form. In order for a DSB to be made the two TALENs must therefore bind to their respective target sites on the DNA and dimerise their *FokI* nuclease domains (Cermak *et al.* 2011). As our project required generating TALENs with multiple binding sites throughout the *Arabidopsis* genome, in order to mimic the 100-200 DSBs generated by SPO11 during wild type meiosis, there was the possibility that one of the TALEN pairs could bind two DNA sites located close together and generate a DSB as a homodimer. In order to prevent this we used TALENs with a heterodimeric *FokI* nuclease domain (Doyon *et al.* 2011). This meant that DSBs would only be generated at sites where

both TALENs of a pair had bound to adjacent target sequences (Figure 4.2).

Four TALEN pairs were designed based on those previously validated in *Arabidopsis* (Christian *et al.* 2013). In this previous study seven TALEN pairs were generated that targeting five *Arabidopsis* genes and were transformed under the control of an estrogen-inducible promoter. The efficiency of NHEJ-mediated mutant generation was measured using a PCR test which relied on the destruction of a restriction site from the spacer region between the target sites of the TALEN pairs. The seven TALEN pairs varied in efficiency of mutation generation, ranging from 2% to 14% (Figure 4.3). The four TALEN pairs used in this study are adapted from the most efficient pairs tested in (Christian *et al.* 2013); ADH1, NATA2a, NATA2b and TT4 which displayed efficiencies of 14, 9, 11 and 5.5% respectively.

In order to create TALENs which could replicate some of the behaviour of SPO11, it was necessary to modify previously verified TALEN designs. This is because the previous designs had been optimised to target a single site in the Arabidopsis genome and generate a DSB at this site (Christian *et al.* 2013). However, during normal meiosis each of the five chromosomes of Arabidopsis undergoes crossover(s), meaning it is necessary to create a TALEN capable of making at least one DSB on every chromosome. In reality the required number of DSBs per chromosome is likely higher as SPO11 is known to make 100-200 DSBs throughout the Arabidopsis genome during meiosis (Mercier *et al.* 2005; Sanchez-Moran *et al.* 2007; Ferdous *et al.* 2012; Choi *et al.* 2013). Therefore, in order to increase the number of potential target sites in the *Arabidopsis* genome that each TALEN pair could bind, some of the RVDs in the original TALEN pairs were exchanged for degenerate NS RVD TAL repeats (Figure 4.4) (Cong *et al.* 2012; Miller *et al.* 2015). In order to predict the number of target sites that these adapted TALENs possessed, the TALE-NT software suite was used (Doyle *et al.* 2012). TALE-NT is a tool that predicts TALEN binding sites based on a scoring matrix for RVD binding developed by observing the base-binding preferences of RVDs in natural TAL-effectors (Doyle *et al.* 2012). The output of TALE-NT is a list of target sites for a given TALEN RVD sequence with scores for each site. The score represents the likelihood of TALEN binding at that particular site, with lower scores indicating a higher likelihood of binding. The TALEN pairs designed for this study had a range of target sites, as predicted by TALE-NT (Doyle *et al.* 2012), ranging from 74 to ~243,000 (Figure 4.5). The TALENs were

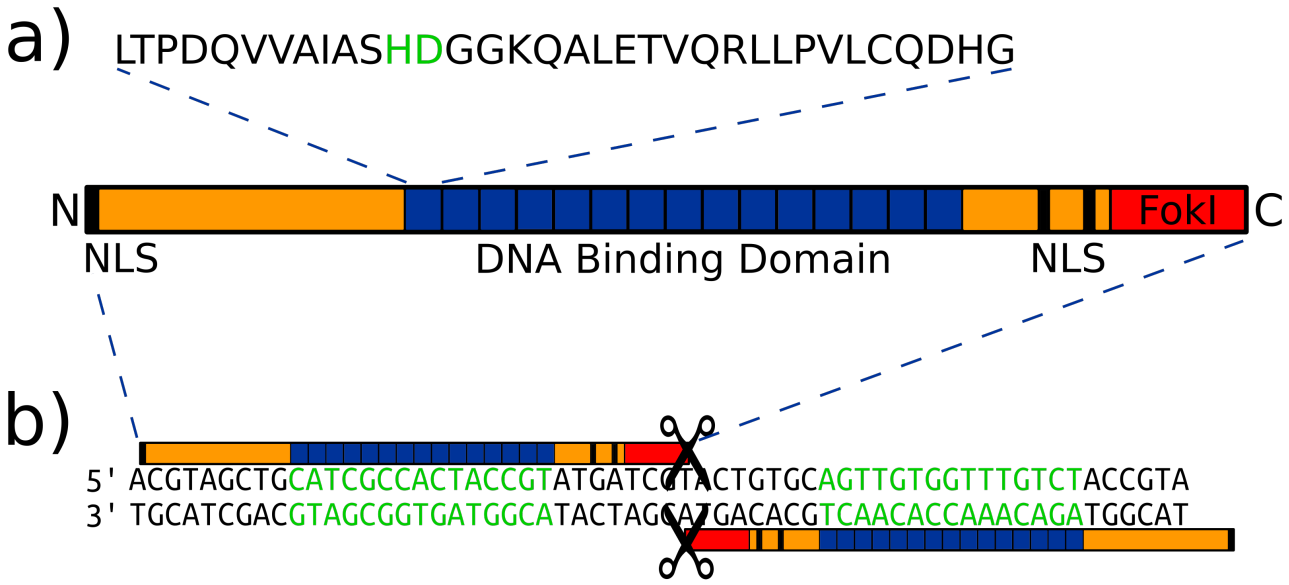

Figure 4.2: Schematic of TALEN protein structure and binding. a) *TALENs consist of a FokI nuclease domain (red) and a DNA binding domain (blue) with nuclear localisation signals (black bars labelled NLS) at the N- and C-termini. The DNA binding domain contains an array of TAL repeats of a 34 amino-acid sequence (printed above the TALEN). The amino-acids at the 12th and 13th positions (highlighted in green) are termed the repeat variable diresidue (RVD) and determine the DNA base binding specificity of a given repeat. In this case the 'HD' RVD specifies binding to cytosine.* ***b)*** *TALEN binding and DSB activity. When two TALENs bind to adjacent target sequences (highlighted in green) separated by 15-25 base pairs, the two FokI nuclease domains of the TALENs heterodimerise and generate a DNA double strand break (DSB).*

TALEN Target	Expression method	T_1 Somatic indel efficiency	T_2 mutant progeny efficiency	Study
ADH1	XVE	5 – 42%	3.8%	(Christian et al. 2013)
ADH1	35S	10 – 60%	N.A.	‘’
TT4	XVE	6 – 7%	0%	‘’
MAPKKK1	XVE	5%	0%	‘’
DSK2Ba	XVE	3 – 9%	0%	‘’
DSK2Bb	XVE	2.5 – 7%	0%	‘’
NATA2a	XVE	2.5 – 28%	0%	‘’
NATA2a	35S	N.A.	0%	‘’
NATA2b	XVE	4 – 27%	0%	‘’
NATA2b	35S	2 – 73%	2.1%	‘’

Figure 4.3: Previous TALEN designs. *Summary of the target, expression method and mutation efficiency of previously published TALENs in Arabidopsis.*

TALEN Name	RVD Sequence
ADH1	Left: HD HD NN NN NI NG NN HD NG HD HD NG HD NG NG Right: NI NN NI HD NI NI NI HD HD NI HD NI NI HD NG
ADH1_8 (A8)	Left: HD HD NN NN NS NS NS HD NS HD HD NS HD NG NS Right: NI NN NI HD NS NS NS HD HD NS HD NS NS HD NG
NATA2a	Left: HD NN NN HD HD NI HD HD HD NI NI NG NN NG NG Right: NN NN NN NI HD NI NG HD NN NN NI HD NN NN NG NN NG NG
NATA2a_3 (N3)	Left: HD NN NN HD HD NS HD HD HD NI NS NG NN NS NG Right: NN NN NN NS HD NI NS HD NN NN NS HD NN NN NS NN NG NG
NATA2a_4 (N4)	Left: HD NN NN HD HD NS HD HD HD NS NS NS NN NS NS Right: NN NN NN NS HD NS NS HD NN NN NS HD NN NN NS NN NS NS
TT4	Left: NN NG HD NN NG HD NG NG HD NG NN HD NI HD NG Right: NI NN NG HD NI NN HD NI HD HD NI NN NN HD NI NG
TT4_3 (T3)	Left: NN NS HD NN NS HD NG NG HD NG NN HD NS HD NG Right: NI NN NG HD NS NN HD NI HD HD NS NN NN HD NS NG

Figure 4.4: TALEN RVD sequence design. *Each TALEN pair consists of a left and right TALEN with a sequence of RVDs that determines its binding specificity. This table shows the RVD sequence of TALEN pairs which have been successful in other studies (Christian et al. 2013) and were therefore used as templates to create degenerate TALENs in this study (names highlighted in red), as well as the TALENs that were generated specifically for this study (names in black). The abbreviated names of the constructs used in this study are shown in brackets. The degenerate NS RVDs which were substituted in are highlighted in green.*

cloned under the control of the *SPO11-1* (Hartung *et al.* 2007) and *DMC1* (Klimyuk & Jones 1997) promoters (Figure 4.6), as these have been used previously to generate constructs which express specifically in meiotic cells (Klimyuk & Jones 1997; Siddiqi *et al.* 2000; Hartung *et al.* 2007). Both members of the TALEN pair were cloned into the pZHY013 entry vector, which allows TALENs to be put under the control of the same promoter in a T2A-linked polycistronic message (Figure 4.7). Following translation of the TALEN message the T2A sequence separating the TALENs self-cleaves, generating two free TALENs (Zhang *et al.* 2013).

4.3.2 Transformation into heterozygote *spo11-1-3* plants and screening of T_1 and T_2 generations for complementation of fertility.

TALEN constructs could not be transformed in *spo11-1-3* homozygotes, as these plants are infertile (Grelon *et al.* 2001; Stacey *et al.* 2006). Instead, TALEN constructs were transformed into *spo11-1-3* +/- plants. The resulting T_1 seeds were grown on selective plates and genotyped for the *spo11-1-3* mutation. The seed of T_1 *spo11-1* homozygotes was collected and counted to determine if there was any restoration of fertility compared to *spo11-1* (Figure 4.8). In total 14 individuals each containing a different TALEN were screened. Because of the low number of T_1 *spo11-1-3* homozygote individuals, T_1 plants heterozygous for *spo11-1-3* were allowed to self-fertilise in order to generate T_2 *spo11*-1 homozygote plants. The T_2 plants were grown on selective plates and genotyped for *spo11-1-3* in exactly the same way as the T_1 plants were. This yielded 30 individuals containing one of the 14 TALENs tested. Plants that survived selection and were homozygous for *spo11-1-3* were allowed to set seed, which was counted in order to determine if there was any restoration of fertility (Figure 4.8). Due to the large number of T_2 plants that were genotyped for *spo11-1-3* it is possible to determine the segregation ratio. While a ratio of 1:2:1 was expected for homozygous, heterozygous and wild-type genotypes respectively, the actual ratio was 47% *spo11-1/spo11-1*, 38% *SPO11-1/spo11-1* and 15% *SPO11-1/SPO11-1*. This result is most likely explained by the wild type PCR assay incorrectly leading to some heterozygous plants being mis-genotyped as *spo11-1/spo11-1* homozygous. This is supported by the fact that the few putative *spo11-1* homozygous plants which displayed high seed counts were confirmed to be heterozygous when re-genotyped. Ultimately, all the T_1 and T_2 plants which were confirmed homozygous

for *spo11-1-3* and possessed a TALEN transgene failed to show significant recovery of the *spo11-1-3* infertility phenotype (Figure 4.8)

4.3.3 Validating expression of the TALEN constructs

In order to determine whether the TALEN constructs were being expressed, protein and RNA samples were prepared from meiotic stage buds. The buds used for this experiment were between 0.39 mm and 0.5 mm, as this has previously been shown to be the stage at which meiosis-I occurs (Smyth *et al.* 1990; Stronghill & Hasenkampf 2007). Buds within this size range were collected and then pooled in order to provide sufficient tissue for protein and RNA extraction. Protein extracts were used in western blots using HA antibodies and appeared to show low levels of TALEN expression (Figure 4.7B). The western clearly shows bands which range from 90-100kDa. This is close to the predicted size of a TALEN with 15 RVDs (102 kDa). TALENs under the control of the '112' and '201' *DMC1* promoters are larger than those under the '1' *DMC1* promoter due to the fact that these promoter sequences incorporate the first two exons of *DMC1* into the TALEN construct (Figure 4.9B) (Klimyuk & Jones 1997). The western also shows a non-specific band at ~50kDa (Figure 4.9B). This is unlikely to be TALEN related due to its small size and its appearance in wild-type controls (Figure 4.9B). To confirm expression at the RNA level, the extracted RNA was used to generate cDNA, which was used to perform PCR with primers that would amplify a 275 bp fragment of the TALEN, in order to confirm RNA expression. The test confirmed TALEN expression, as a DNA fragment of the correct size was amplified from TALEN T_2 Bud cDNA, but was not observed in untransformed Col (Figure 4.7C). Therefore, the TALENs did appear to be expressed at both the RNA and protein level, which rules out failure to express as the reason for *spo11-1-3* non-complementation in tested lines. While no significant recovery of fertility was observed in TALEN *spo11-1-3* plants, some of the T_2 plants showed unusual patterns of growth and development (Figure 4.9A). The general features were as follows; many TALEN lines displayed small leaves which were curled instead of flat; the plants also displayed a greater number of leaves which caused the rosette of these plants to form a clump rather than lying flat. The plants also displayed late bolting and flowering and in some cases didn't flower at all. These phenotypes are similar to those observed in plants hypersensitive to DNA damaging agents (Bundock & Hooykaas 2002) and interestingly appeared more often in plant lines

which had TALENs containing the 'N4' TAL array. It is difficult to interpret the abnormal growth phenotypes displayed in some T_2 plants because no systematic classification of them was undertaken. However, coupled with the strong evidence that TALENs were being expressed it seems possible that TALEN action may have been responsible for the phenotypes. The simplest explanation would be that TALENs caused genomic changes via their ability to create DSBs. Presumably, these DSBs entered alternative, mutagenic repair pathways such as NHEJ, thus generating the observed developmental phenotypes.

4.3.4 Investigating complementation of *spo11-1* using irradiation

As DSBs generated by TALENs did not appear to restore fertility in *spo11-1* mutants, despite being expressed, it was decided to test if exogenously generated DSBs could recover fertility in these mutants as observed in other species (Dernburg *et al.* 1998). In order to do this *spo11-1-3* and *spo11-2* mutants were exposed to x-ray radiation at doses of 1, 4 and 8 grays in a Faxitron CellRad X-ray irradiator. This machine continuously exposes a sample to radiation until the full dose of radiation has been administered, as measured by a sensor on the sample staging platform. For this reason, higher radiation doses require samples to be in the machine for longer, as more time is required before the sample has been exposed to its full dose. For example, a 1 gray dose required approximately 30 seconds to administer, while the 4 and 8 gray doses required approximately 2 and 4 minutes to administer respectively. The *dmc1* mutant was used as negative control, as this mutation causes meiosis to arrest downstream of the *spo11-1* mutation and therefore should not be rescued by exogenous DSBs (Couteau *et al.* 1999). Col-0 was used as a positive control in order to ensure that the X-ray doses weren't so high that they disrupted meiosis and fertility. Siliques from irradiated *spo11-1* and *spo11-2* did not show increased fertility when compared to mutants not exposed to radiation (Figure 4.10). The implications of these findings are discussed below.

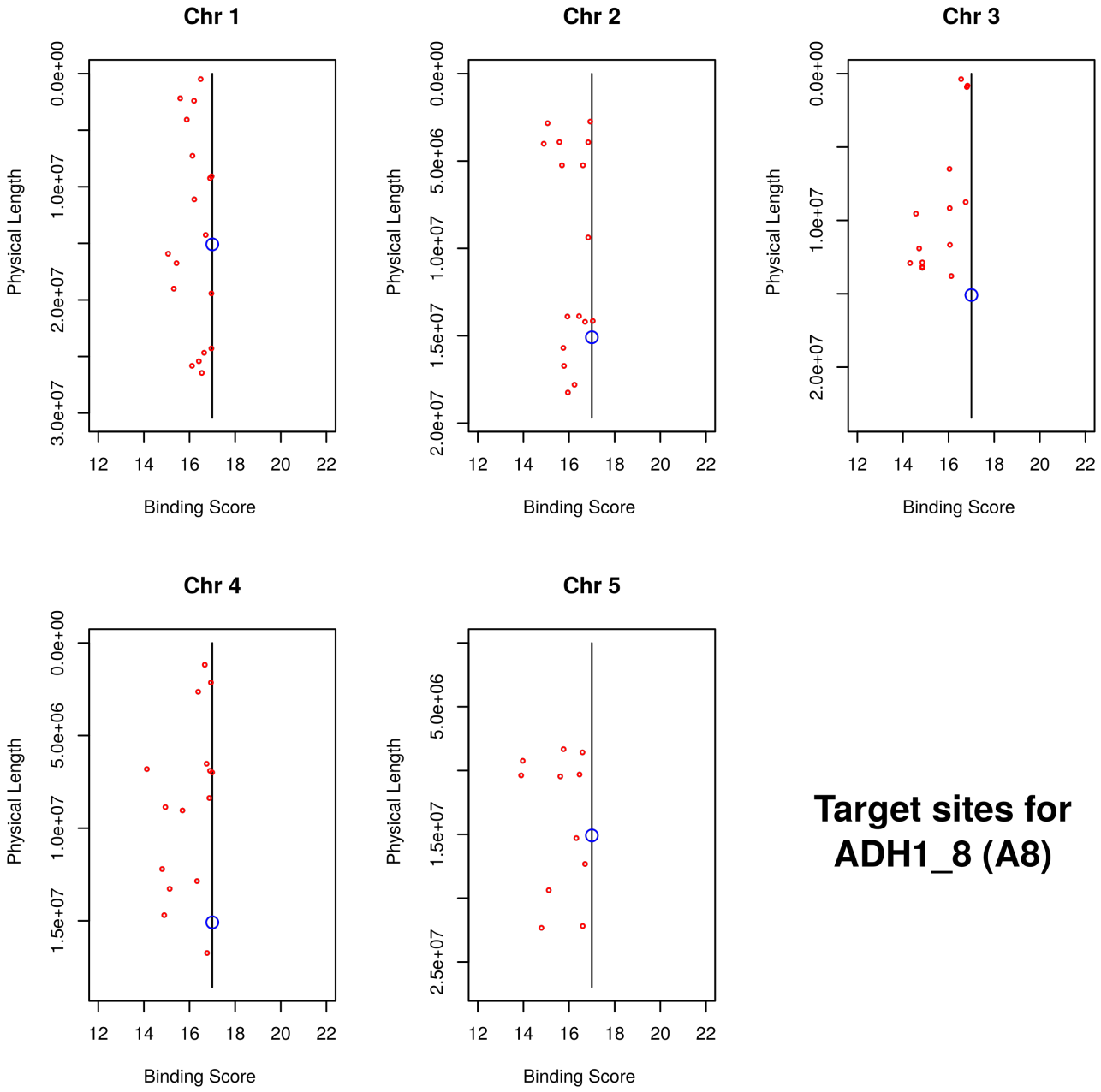
Chr 1
Chr 2
Chr 3
Chr 4
Chr 5
Physical Length
Binding Score
Target sites for
ADH1_8 (A8)

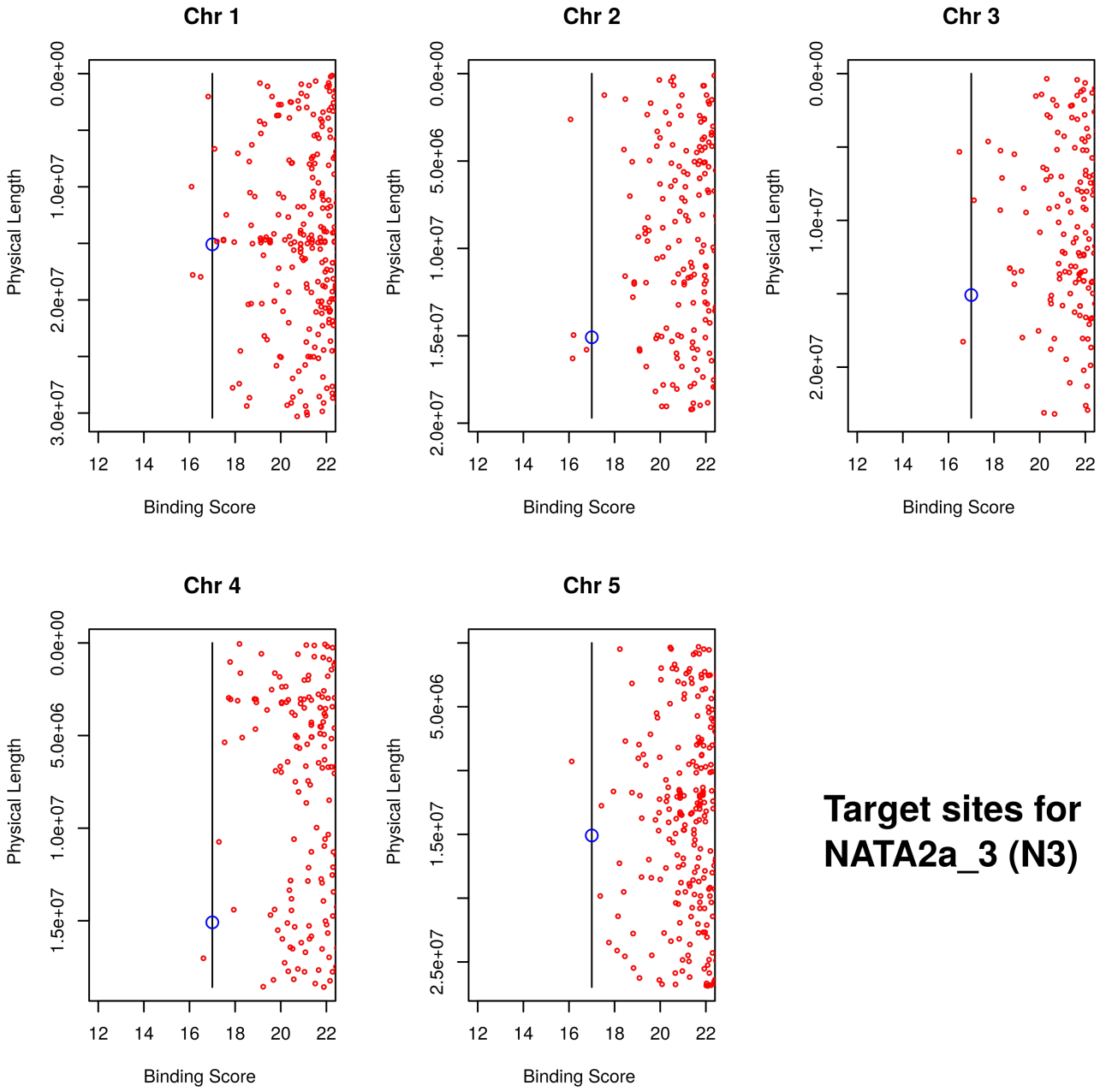
Chr 1
Chr 2
Chr 3
Chr 4
Chr 5
Physical Length
Binding Score
Target sites for NATA2a_3 (N3)

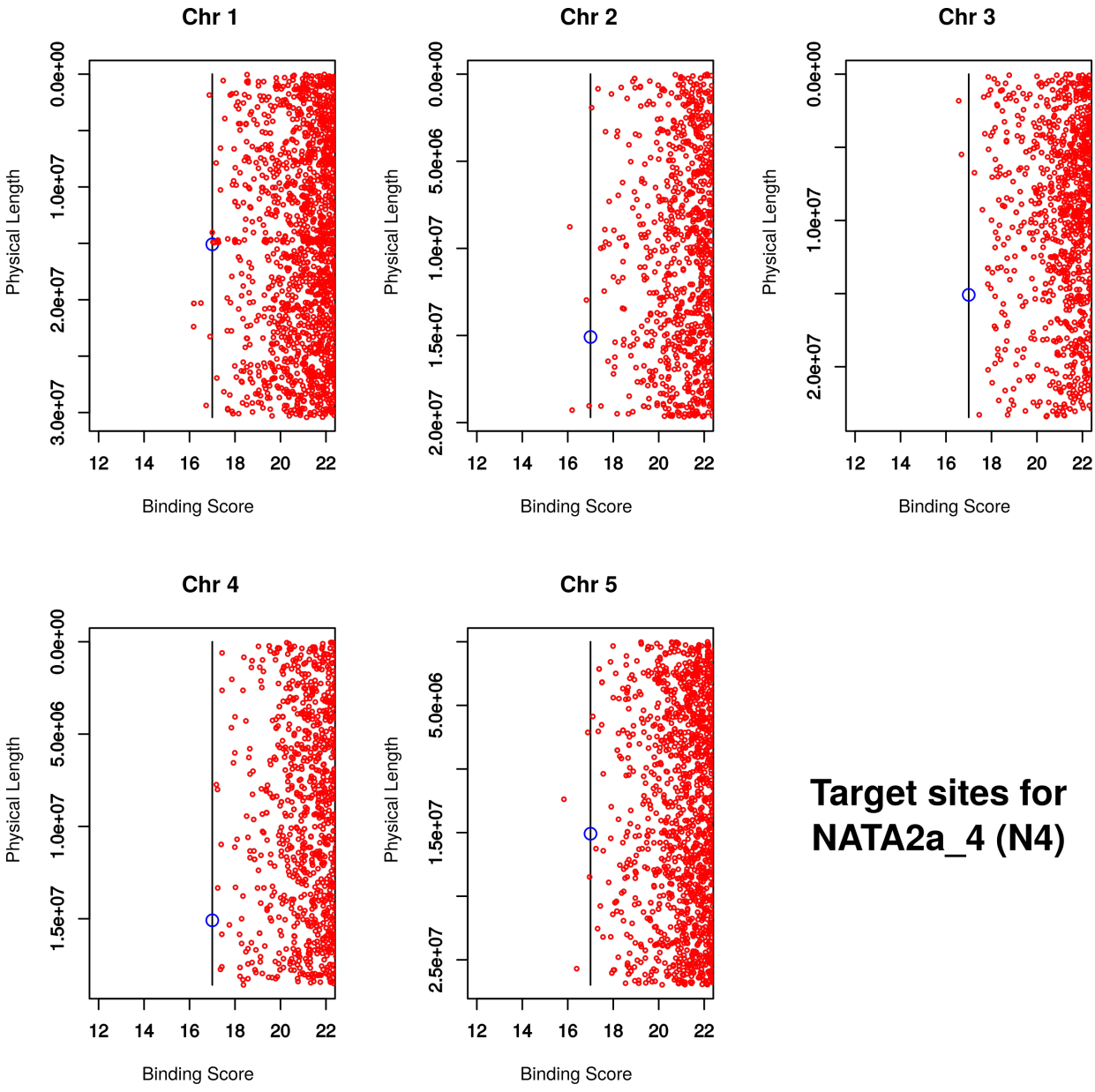
Chr 1
Chr 2
Chr 3
Chr 4
Chr 5
Physical Length
Binding Score
Target sites for
NATA2a_4 (N4)

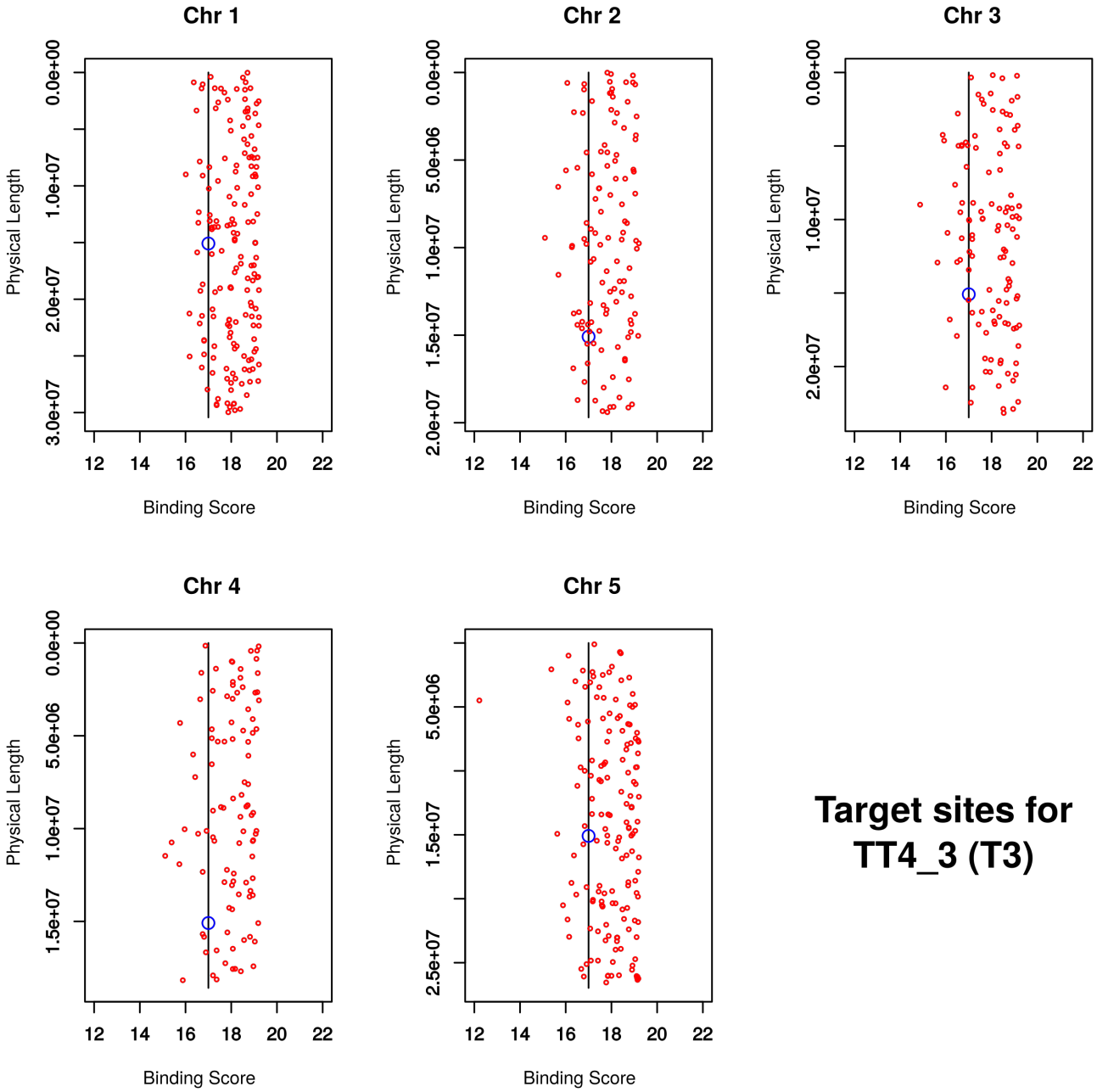

Figure 4.5: Predicted target sites of degenerate TALEN pairs*: These graphs were generated using the TALE-NT TALEN target site predictor (Doyle et al. 2012). This software gives target site locations (y-axis) as well as a 'Binding Score' which indicates the predicted strength of binding at a given target site (x-axis). A lower score indicates stronger binding.*

Promoter Name	Promoter Origin	TAIR 10 Coordinates
1	***DMC1*** promoter from Col	8103269-8100860 bp
19	***SPO11-1*** promoter from Col (Hartung et al. 2007)	4235225-4234408 bp
101	***SPO11-1*** promoter from Col with translational fusion (Promoter includes first three codons of SPO11)	4235225-4234417 bp
112	***DMC1*** promoter from Col with translational fusion (Promoter includes first two exons of DMC1 (Klimyuk & Jones 1997))	8103269-8100729 bp
201	***DMC1*** promoter from Ler	8,100,764 - 8,103,263

Figure 4.6: Names and details of the promoters used in this study. *N.B. coordinates for Ler DMC1 promoter are from SALK 1,001 genomes Ler-0 sequencing*

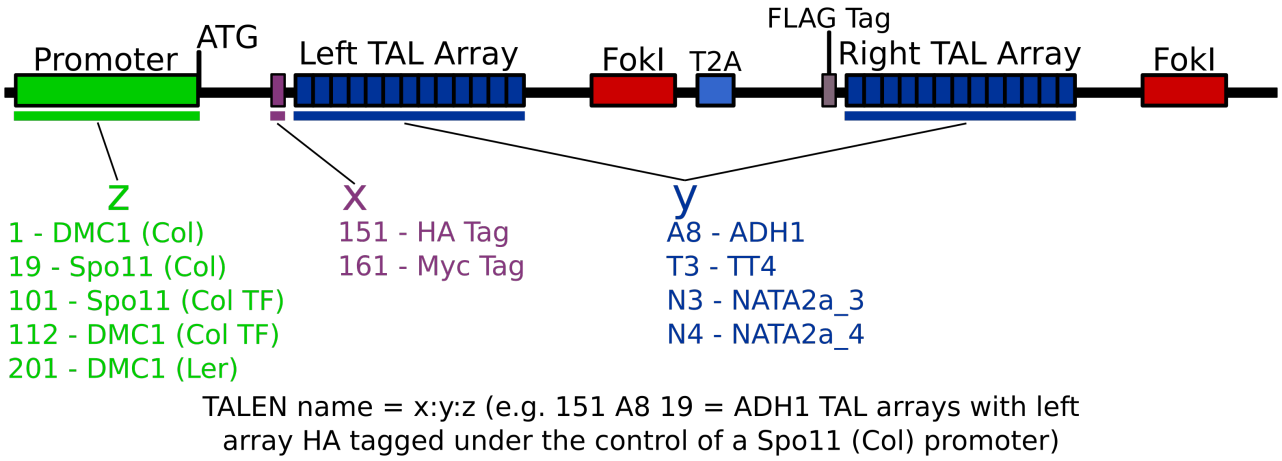

Figure 4.7: Schematic of TALEN construct and explanation of naming convention. *The final binary vectors transformed into Arabidopsis contained a promoter (green box), a left and right TAL array (dark blue boxes), a left and right FokI (red boxes) and a T2A self-cleaving sequence (light blue box). Both the left and right TAL arrays were tagged with an epitope tag (FLAG tag for the right array and a variable tag for the left array, purple boxes). The name of each TALEN was created by combining codes for the left-array epitope tag (purple text), the TAL array (blue text) and the promoter identity (green text) an explanation of the naming convention is included below the schematic (black text).*

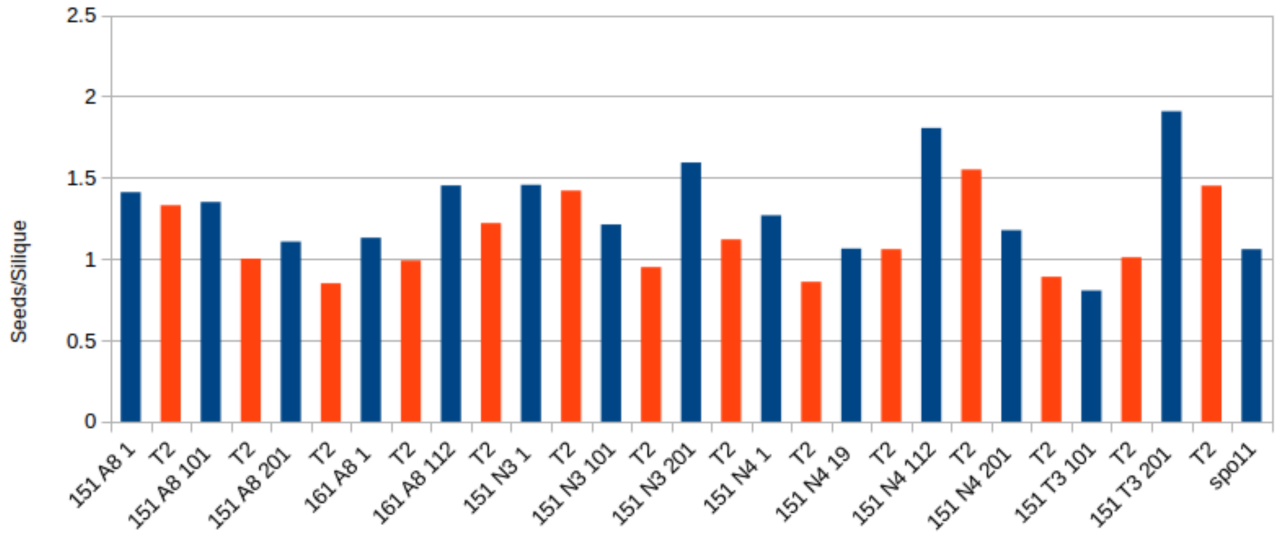

Figure 4.8: Seeds per silique for all TALEN lines in T_1 and T_2 generations: *Blue bars show the seeds/silique in the T_1 generation for a given line, while red bars show the seeds/silique in the corresponding T_2 generation. A spo11 control is shown on the far right.*

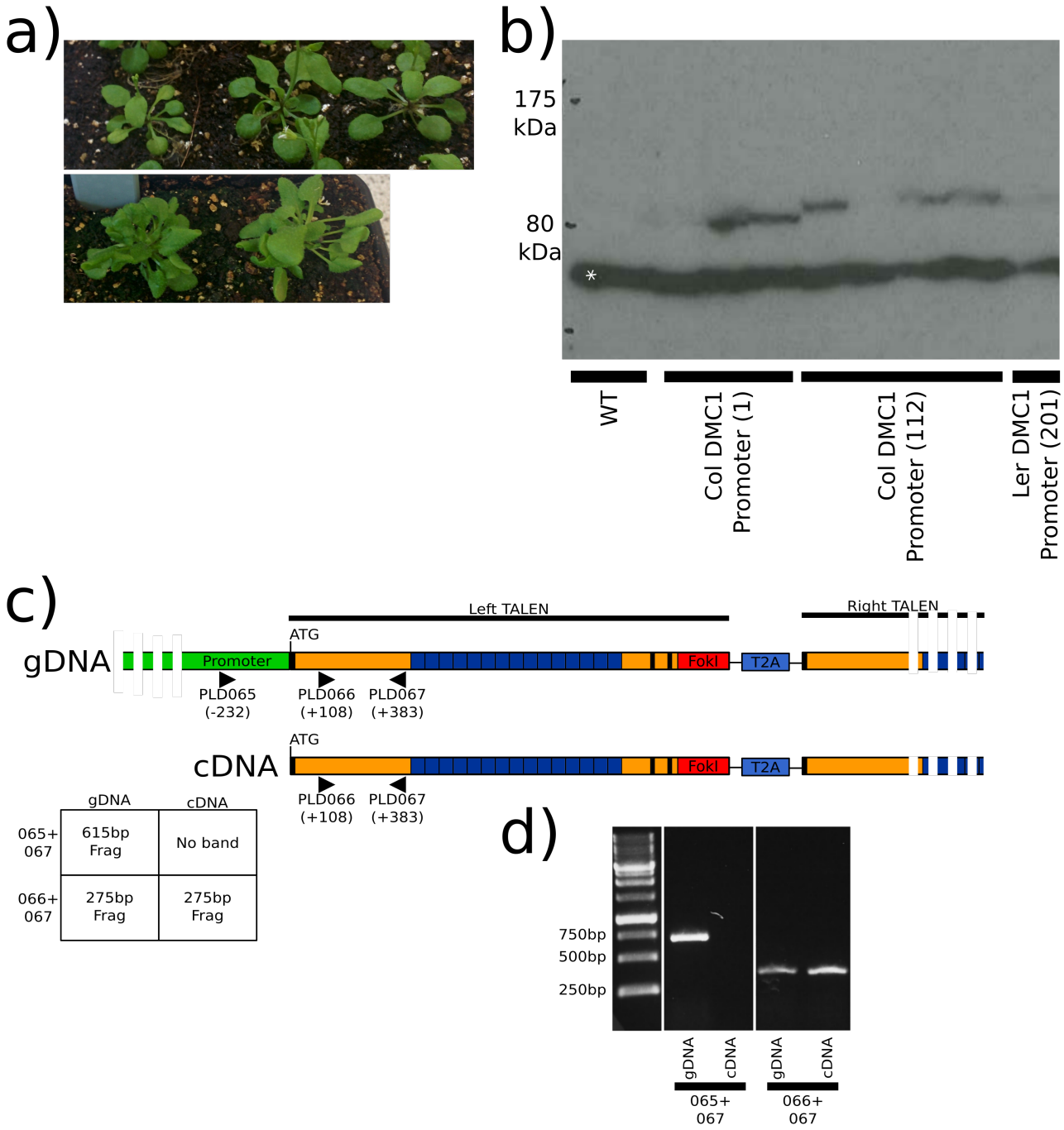
a)
b)
175 kDa
80 kDa
*
WT
Col DMC1 Promoter (1)
Col DMC1 Promoter (112)
Ler DMC1 Promoter (201)
c)
Left TALEN
Right TALEN
gDNA
ATG
Promoter
FokI
T2A
PLD065 (-232)
PLD066 (+108)
PLD067 (+383)
cDNA
ATG
FokI
T2A
PLD066 (+108)
PLD067 (+383)
gDNA
cDNA
065+ 067
615bp Frag
No band
066+ 067
275bp Frag
275bp Frag
d)
750bp
500bp
250bp
gDNA
cDNA
gDNA
cDNA
065+ 067
066+ 067

Figure 4.9: TALEN T_2 phenotypes. a) *Pictures of untransformed Col-0 (top) and TALEN line 151 N4 201 T_2 seedlings at equivalent stages (bottom).* ***b)*** *Anti-HA western of protein samples prepared from meiotic buds of T_2 plants (courtesy of Dr Nataliya Elina). Different lines were under the control of different promoters (labelled). A non-specific band (50 kDa) which featured in all samples, including negative controls, is marked with an asterix. As expected, the TALEN bands in lines under the control of the DMC1 promoter '112' are larger due to this promoter incorporating the first two exons of DMC1 into the TALEN.* ***c)*** *Schematic of the PCR test used to determine if TALEN T-DNAs had been successfully transformed and were being expressed at the level of RNA. Primer positions are shown using black triangles and primer position relative to the start codon of the TALEN is shown in brackets. In gDNA the PLD065 and PLD067 primers should give a 615 bp fragment which is not seen in cDNA. The inset table shows outcomes and expected band sizes for test.* ***d)*** *Result of PCR test of a 151 N4 201 line T_2 plant.*

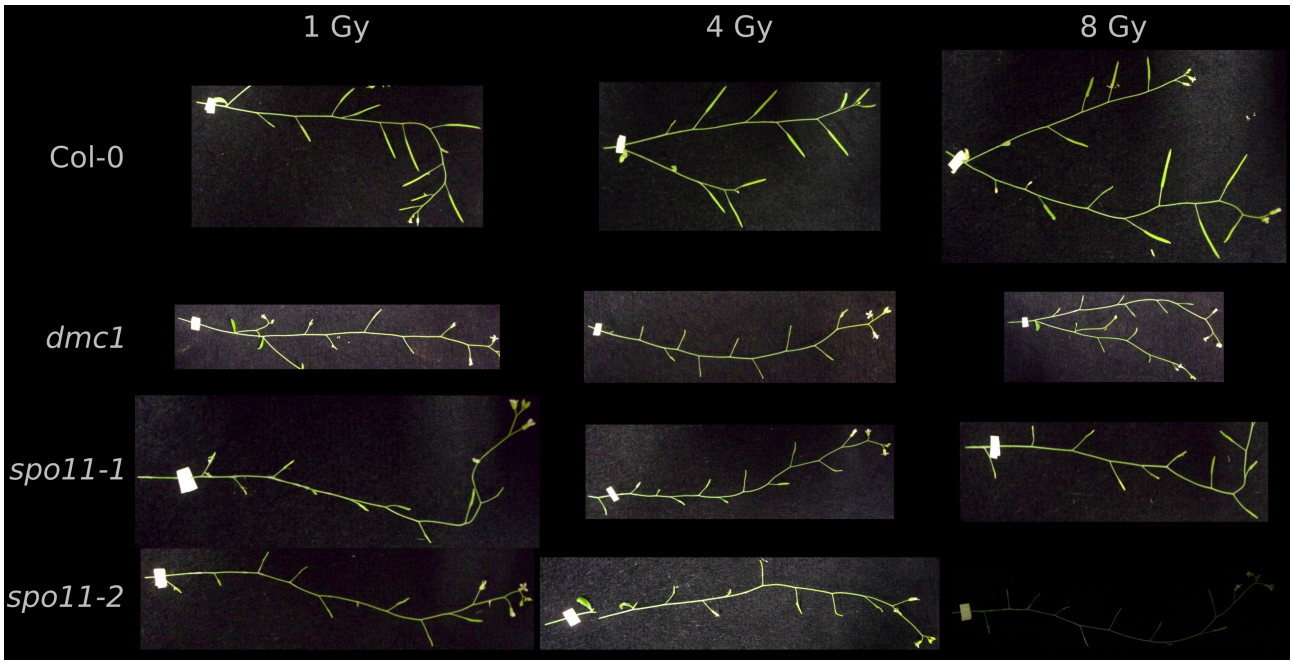

Figure 4.10: Effects of X-ray radiation on spo11 mutants.

4.4 Discussion

From the above results it appears that TALENs are incapable of recovering the fertility of *spo11-1* mutants. This cannot simply be explained by lack of expression of the TALENs constructs, as this was confirmed by western blot and reverse-transcriptase PCR analysis (Figure 4.6). However, there are a variety of possible technical and mechanistic explanations that could account for the failure of the TALEN constructs to complement *spo11-1* infertility, which are considered below.

First, TALENs, once expressed, may be incapable of generating DSBs or incapable of making them in sufficient numbers to efficiently undergo meiotic recombination and generate crossovers. While TALENs have been confirmed to create DSBs in *Arabidopsis* (Cermak *et al.* 2011; Christian *et al.* 2013; Forner *et al.* 2015), it is possible that by introducing multiple NS RVDs, in order to increase the number of potential target sites, the affinity of TALEN binding was reduced to the point that the TALENs were rendered ineffective. Some evidence for this conclusion is provided by the fact that TALE-NT gives scores between 12-22 for the target sites of the TALENs containing NS RVDs used in this study (Figure 4.3). However, it gives much lower scores (meaning greater likelihood of binding) to the TALENs without NS RVDs that have been verified in other studies. For example, the ADH1 TALEN pair from (Christian *et al.* 2013) is given scores of 4.97 and 3.26 for its left and right constituent parts respectively (Doyle *et al.* 2012). A degree of scepticism regarding these scores is necessary because they are generated based on statistical analysis of which RVDs are observed binding certain DNA bases in natural TAL-effectors (Doyle *et al.* 2012), and therefore may not apply to the TALEN constructs used in this and previous studies. However, it seem that the addition of NS RVDs causes a destabilisation of TALEN binding and that excess NS RVDs may inhibit a TALENs ability to bind DNA. While this is the simplest explanation of the findings above, it is somewhat contradicted by the fact that specific T_2 lines showed developmental phenotypes suggestive of genomic damage (see below for further discussion).

An alternative explanation could be that the TALENs were expressed at the wrong level, time or place. Previous work placing a GUS reporter system under the control of the *DMC1* promoter showed strong expression in the stages of flower development where meiosis takes

place (Klimyuk & Jones 1997). Hence, it would be difficult to explain a non-meiotic profile of expression in TALENs under the control of the same promoter. Relatedly, *SPO11-1* cDNA under the control of the *SPO11-1* promoter has previously been used to rescue *spo11-1* mutant infertility (Hartung *et al.* 2007), implying that this promoter is sufficient to drive endogenous SPO11-1 expression with the required level and timing. Since the TALENs in this experiment are designed to substitute for the activity of SPO11-1, placing them under the control of this promoter seems logical. Similar to *DMC1*, it would be difficult to explain a non-meiotic expression profile of constructs under the *SPO11-1* promoter. A complicating factor is the fact that work in budding yeast shows that the SPO11 complex that makes DSBs is not solely regulated by the promoters of its constituent genes, but is also constrained by the action of the ATM/ATR complex. As the number of DSBs in a cell increases during meiosis, the ATM/ATR complex phosphorylates the SPO11-DSB complex, reducing the rate of DSB formation, meaning that the DSB action of SPO11 is likely suppressed for at least part of the time it is expressed (Carballo *et al.* 2013). It seems unlikely that TALENs would be subject to this feedback regulation, suggesting that when they are expressed under the control of a *SPO11-1* promoter they may have a longer period of time to create DSBs than native SPO11-1. Therefore, while it seems that TALENs should have been expressed at the right time and location, it is possible that they were not expressed at the right level, at least in the plants that were observed. Because of the high number of different TALEN lines and the challenge to obtaining T_1 plants that were homozygous for *spo11-1-3*, only a few plants were tested per line for recovery of fertility. It is therefore possible that some TALEN constructs are capable of recovering fertility, but that not enough independent transformants were observed to find individuals with sufficiently high expression level.

Another explanation is that although TALENs were expressed and made DSBs at the correct time, the DSBs that were generated were not viable substrate for the interhomolog repair pathway that generates crossovers. SPO11 enzymes generate DSBs through a complex mechanism whereby it dimerises (or heterodimerizes in the case of SPO11-1 and SPO11-2) and complexes with MPTOPVIB (Stacey *et al.* 2006; Vrielynck *et al.* 2016). This complex then binds the DNA and performs nucleophilic attack on both DNA strands, with SPO11 becoming covalently bound to DNA target sites at a tyrosine residue, generating a DSB (Keeney *et al.* 1997; Robert *et al.* 2016). A second nuclease complex (MRN/MRX) then nicks

the DNA downstream of the SPO11-DSB site, releasing SPO11 bound to short DNA oligonucleotides (Neale *et al.* 2005; Milman *et al.* 2009; Rothenberg *et al.* 2009; Garcia *et al.* 2011; Lange *et al.* 2011). Resection then occurs at the SPO11 DSB site to generate regions of single stranded DNA, 10s-100s of nucleotides in length, which can then participate in strand invasion (Thomas Robert *et al.* 2016). In contrast, *FokI* generates DSBs via an S_N2 nucleophilic attack on the phosphodiester bond of DNA (Wah *et al.* 1997; Kovall & Matthews 1999) (Figure 4.11). An important difference is that the S_N2 reaction mechanism does not generate a persistent, covalent link between the nuclease and DNA backbone (Kovall & Matthews 1999). Hence, there are important molecular differences between DSBs generated by SPO11 and *FokI*. It is also possible that the SPO11 complex may interact with additional recombination factors that channel DSBs into the meiotic interhomolog repair pathway, which may not occur efficiently with *FokI*-derived DSBs. Crossover in wild type plants takes place in the context of the meiotic chromosome axis, which SPO11 has been shown to interact with (Panizza *et al.* 2011). *FokI* generated DSBs are unlikely to interact with the axis in the same way, and therefore this may underlie inefficient channelling into interhomolog recombination. It is also important to consider the other proteins which interact with SPO11 in order to generate DSBs. There are currently seven proteins known to be required for correct meiotic DSB formation in plants (in addition to SPO11-1). These are SPO11-2 , PRD1, PRD2, PRD3 and PRD4, DFO and MTOPVIB (Stacey *et al.* 2006; De Muyt *et al.* 2007; De Muyt *et al.* 2009; Zhang *et al.* 2012; Vrielynck *et al.* 2016). SPO11-1 is known to complex with SPO11-2, PRD1 and MPTOPVIB and these interactions are important for DSB formation (Stacey *et al.* 2006; De Muyt *et al.* 2007; Vrielynck *et al.* 2016). None of these interactions are likely to take place between *FokI* nuclease and the respective proteins. If it is the case that these proteins do more than aid SPO11-1 in its catalysis of a DSB, for example, if they prepare a DSB site for crossover, then even if TALENs were producing DSBs in sufficient numbers to restore fertility they may not be expected to recover the *spo11-1-3* phenotype. It seems reasonable that these differences in the biochemical and steric properties of the DSBs may make downstream processing of *FokI*-generated DSBs into meiotic interhomolog recombination inefficient or impossible. If this is the case then the DSBs are presumably repaired via NHEJ. The explanation that DSBs alone are insufficient to recover fertility in *spo11-1* mutants is made more attractive by the fact that some TALEN lines showed phenotypes consistent with DNA damage in addition to the fact that DSBs provided

exogenously by radiation also failed to recover *spo11-1* fertility (discussed below).

While TALEN introduction did not recover *spo11-1* infertility, it does seem to have given rise to abnormal growth phenotypes in many of the plants analysed in the T_2 generation. It is possible that these phenotypes are due to the introduction of foreign DNA during the process of transformation and have nothing to do with the nuclease activity of TALENs. For example, if the TALEN T-DNA was inserted into an region of a chromosome leading to the disruption of an important developmental gene, a T_1 plant heterozygous for *spo11-1-3* would likely grow normally as it would be able to rely on the alternative copy of the gene carried on the homologous chromosome. However, upon selfing to generate *spo11-1-3* knock-outs, plants could be generated which possessed the TALEN T-DNA on both chromosomes leading to the abnormal growth phenotypes that were observed in this experiment. Although this explanation merits some consideration it seems unlikely that this could have occurred at the frequency necessary to explain all of the lines which displayed abnormal growth in this study.

It therefore seems likely that these phenotypes arose due to the action of TALENs on the genome of T_1 plants. Either the TALENs were expressed outside of meiosis giving rise to DSBs that were repaired by the somatic repair mechanisms of the plant, or they were expressed during meiosis, but the DSBs generated were unable to give rise to crossovers, and so were repaired via an alternative, mutagenic pathway. In either case it is likely that the non-homologous end joining (NHEJ) pathway was responsible for DSB repair. Somatic NHEJ repair is well documented in Arabidopsis (Charbonnel *et al.* 2010; Christian *et al.* 2013; Tan *et al.* 2015), and experiments confirming NHEJ activity during meiosis in mice (Couëdel *et al.* 2004), have led to the assumption that NHEJ also occurs in plant meiosis (Abe *et al.* 2009; Roy 2014). Therefore it seems highly probable that DSBs generated somatically or during meiosis have the chance of being channelled into NHEJ repair. The inability of radiation-generated DSBs to recover *spo11-1* and *spo11-2* fertility was unexpected, given that a similar method has been shown to restore fertility in *spo11* mutants in *C. elegans* (Dernburg *et al.* 1998). However, there are two major differences between the Dernburg experiment and the one reported here. The first is the species used - *C. elegans* has been used extensively as a model species to study meiosis however there is a critical difference between its meiosis and that of plants. Homoloogous chromosomes in *C. elegans* are able to synapse even in the

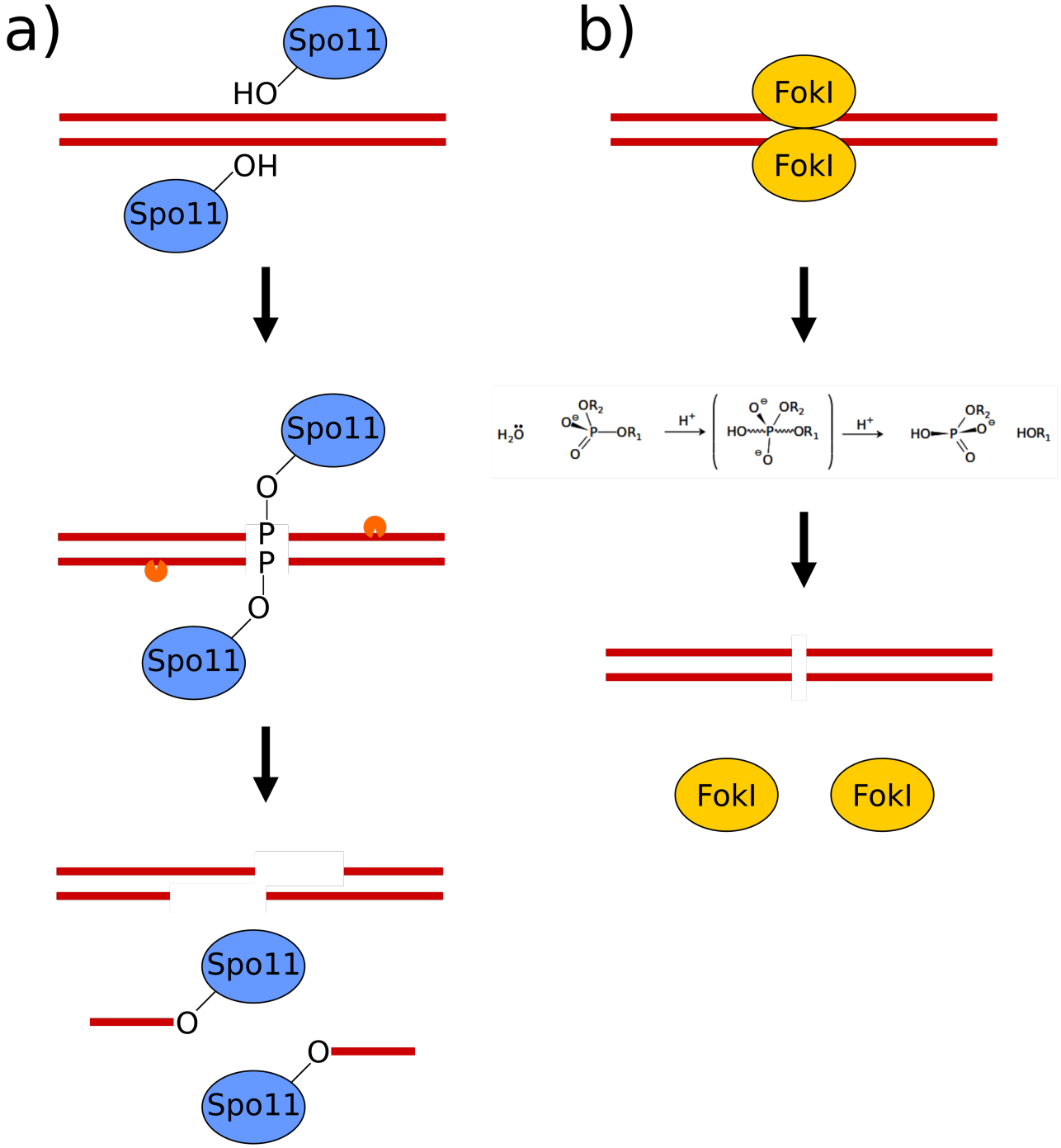
a)
Spo11
HO
OH
Spo11
Spo11
O
P
P
O
Spo11
Spo11
O
Spo11
O
b)
FokI
FokI
$H_2\ddot{O}$
OR_2
$O^{\ominus}$
P
OR_1
H^+
$O^{\ominus}$
OR_2
HO
P
OR_1
$^{\ominus}O$
H^+
HO
P
OR_2
$O^{\ominus}$
O
HOR_1
FokI
FokI

Figure 4.11: Mechanism of SPO11 and FokI DSB formation. a) *SPO11 DSB mechanism: Two SPO11 monomers (blue ovals) dimerise and form covalent bonds via a tyrosine residue (green oval) with backbone phosphates of DNA generating a DSB. The MRN/MRX complex (orange circles) then generates a single-strand break in order to release the SPO11-oligonucleotide complexes, generating a staggered DSB.* ***b)*** *FokI DSB mechanism: Two FokI monomers dimerise and bind DNA. Next, each monomer activates a water molecule to perform a one-step S_N2 attack on a backbone phosphate of DNA. FokI monomers then disassociate leaving behind a DSB.*

absence of DSBs, for example in *spo11* mutants (Dernburg *et al.* 1998). This is made possible by pairing centres (PCs) present on each of the six *C. elegans* chromosomes (Voelkel-Meiman *et al.* 2015), which consist of several hundred repeats of a 12 bp sequence motif (Phillips *et al.* 2009). This means that meiotic DSBs in *C. elegans* are only required as substrate for crossovers. It is possible that this means there are less stringent requirements for meiotic DSBs in *C. elegans* than in *Arabidopsis*, where in addition to being the substrate for crossovers, DSBs are also essential for pairing and synapsis (Pradillo *et al.* 2007). The second difference between the Dernburg experiment and the experiment reported here was the type and dose of radiation. The *C. elegans* individuals were irradiated with gamma radiation at a dose of 15 grays (Dernburg *et al.* 1998), while the Arabidopsis experiments used X-ray radiation and a maximum dose of 8 grays. However, there are reasons to believe that this difference is relatively superficial. The Dernburg experiment used gamma radiation because a previous experiment had shown an increase of genetic distance in a map interval when *C. elegans* was exposed to gamma radiation (Kim & Rose 1987). X-rays are similarly known to cause DSBs in *Arabidopsis* (Shirley *et al.* 1992), so the difference in type of radiation seems unlikely to matter. It seems more likely that the dose was either too low or administered too quickly. The Dernburg experiment does not report how long it took to administer 15 grays of radiation. However, due to the efficiency of the machine used in this experiment it only took around 4 minutes to administer the maximum dose of 8 grays to the *spo11-1-3* plants. It is possible that DSBs are generated during X-ray irradiation that are capable of recovering *spo11-1-3* infertility but that 4 minutes is too short a window, either because there are too few DSBs created, or because there are too few cells at the right stage of meiosis to be influenced from the DSBs. This would lead to an insufficient number of crossover-compentent DSBs in meiotic cells, meaning that no detectable recovery of fertility would be observed.

Another important element to consider is the fact that DSBs generated in *Arabidopsis* by cisplatin are capable of partially recovering the *spo11-1* phenotype (Sanchez-Moran *et al.* 2007). Cisplatin generates DSBs indirectly by creating interstrand crosslinks which are then resolved via some combination of nucleotide excision repair, homologous recombination and trans-lesion synthesis (Noll *et al.* 2006). During homologous recombination repair of cisplatin-induced DNA damage, DSBs are created endogenously which are presumably responsible for the partial recovery of the *spo11-1* phenotype (Sanchez-Moran *et al.* 2007). In

contrast, X-rays create DSBs, as well as other types of DNA damage, directly by inducing oxidation of the sugar-phosphate backbone of DNA (Schipler & Iliakis 2013). It is possible that this direct method of generating lesions creates DSBs that are incapable of acting as substrate for meiotic recombination, compared to the DSBs generated by cisplatin which are created by the cells own DNA damage processing pathways (Noll *et al.* 2006).

In conclusion, TALENs were expressed in *spo11* mutant Arabidopsis plants and some circumstantial evidence of DSB generation was observed in the form of abnormal growth phenotypes. However, this was not sufficient to recover the infertility phenotype of the *spo11* mutant, a fact which could be explained by many non-mutually exclusive mechanisms.

5 Chapter 5: Discussion

5.1 Generation and potential uses of an *Arabidopsis thaliana* second division restitution population

5.1.1 Haploid-inducer and SDR lines can be combined in order to generate true SDR and hybrid plants

A major aim of this project was to create an SDR population by manipulating the properties of haploid-inducer and SDR mutant lines. Although a large population of SDR plants was not created, the principal of using GEM haploid-inducer lines in conjunction with *osd1-3* mutants to generate SDR plants has been validated. At least two individuals were observed which displayed all the expected genotypes of true SDR plants. In addition to these plants a large number of hybrid plants which displayed some combination of haploid-inducer and SDR-mutant genetic material, sometimes with non-diploid ploidy, were also observed. This confirms that genome elimination is just one of multiple stable outcomes of a haploid-inducer x SDR-mutant cross. Therefore, while this strategy can be used to obtain SDR genotypes, it is unlikely to be efficient enough in the context of crop breeding programmes or experimental genetics without further modifications.

5.1.2 Refining production of SDR populations

In the future it would be desirable to be able to generate true SDR plants with greater efficiency than was achieved in this project. There are a number of possible avenues that could be explored in order to achieve this. Perhaps the simplest approach would be to use a haploid-inducer whose chromosomes were more reliably eliminated post-fertilisation. A number of lines with haploid-inducer properties have been developed in Arabidopsis which fall into two broad categories. The first consists of plants with modified native CenH3 e.g. the *cenh3* L130F point mutant (Karimi-Ashtiyani *et al.* 2015), other point mutations (Britt & Kuppu 2016) and the SeedGFP-HI line (Ravi *et al.* 2014). The second consists of plants with complete or partial non-native CenH3, e.g. the *cenh3* mutants in (Maheshwari *et al.* 2015) rescued by CenH3 from *L. oleraceum* and *B. rapa*. The GEM line used in this study falls into the first category, as it consists of a *cenh3-1* null mutant rescued by GFP-CenH3 and

GFP-tailswap CenH3, which are both modified *Arabidopsis* CenH3 proteins. While all of the above lines have been confirmed as haploid-inducers, only GEM has had its efficiency tested when used in conjunction with diploid pollen (Marimuthu *et al.* 2011). As these lines show differences in phenotype (See Figure 5.1), it is possible that one of the other lines may be more efficient at accepting diploid pollen and generating SDR plants. Therefore testing the ability of other haploid-inducer lines to accept diploid pollen and generate SDR plants may prove a fruitful avenue for increasing SDR generation efficiency.

Equally, it would also be useful to test the various *Arabidopsis* SDR mutants (i.e. mutant backgrounds that generate unreduced diploid pollen, see figure 5.2) to see if they produce SDR offspring more efficiently. In addition to the *osd1-3* mutant used in this study, *tam* (d'Erfurth *et al.* 2010) and *ps1* (Erfurth *et al.* 2008) mutants have been found to generate SDR diploid pollen, although whether *ps1* produces SDR or first division restitution gametes or a mixture of both is unclear (De Storme & Geelen 2011). The *osd1-3* mutant was chosen for this study because it solely produces diploid pollen grains (d'Erfurth *et al.* 2009), whereas the *ps1* mutant produces ~70% diploid pollen (Erfurth *et al.* 2008), and the *tam* mutant 89% (d'Erfurth *et al.* 2010). Therefore, if either *ps1* or *tam* mutants were used there would have to be a screening step which removed haploid plants generated from haploid pollen from the final SDR population. While there is no direct evidence that these different mutants would generate SDR plants at a greater frequency, the fact that they produce diploid pollen at different frequencies suggests they may behave differently when crossed to a haploid-inducer line. In addition to this, the mechanism of diploid pollen production varies between the mutants. In *osd1-3* and *tam* mutants the production of diploid pollen is hypothesised to occur due to a failure to increase CDK levels at the end of meiosis-I leading to premature exit from meiosis (d'Erfurth *et al.* 2010), while in *ps1* mutants diploid gametes are thought to arise due to defective spindle orientation (Erfurth *et al.* 2008). Therefore these mutants may behave differently than *osd1-3* when crossed to haploid-inducers.

Another promising approach to increasing the efficiency of SDR offspring production is the use of NHEJ mutants such as *lig4*. Recent work investigating the shattered chromosomes produced when haploid-inducers are crossed to wild-type plants made the discovery that crossing an SDR mutant to a plant homozygous for the *lig4* mutant doubled the number of

Line name	Haploid induction efficiency	Tested with SDR gametes?	Reference
GEM	80%	Yes, produces diploid offspring with *osd1*, *dyad* and *MiMe* mutants	(Marimuthu *et al.* 2011)
SeedGFP-HI	91% (If GFP selection is used otherwise 72%)	No	(Ravi *et al.* 2014)
cenh3 L130F point mutant	15%	No	(Karimi-Ashtiyani *et al.* 2015)

Figure 5.1: Comparison of various haploid-inducer lines

Mutant name	Phenotype	Reference
osd1	Produces diploid male and female gametes due to inability of mutant to inhibit APC/C activity.	(Cromer *et al.* 2012)
tam	An A-type cyclin which produces diploid gametes due to a failure to enter meiosis-II, presumably due to disruption of Cyclin-CDK activity.	(d'Erfurth *et al.* 2010)
ps1	Produces diploid male gametes, but haploid female gametes, resulting from abnormal orientation of spindles at meiosis-II	(Erfurth *et al.* 2008)

Figure 5.2: Comparison of various SDR lines

haploid progeny (Tan *et al.* 2015). This increase came at the expense of both aneuploid and diploid offspring, which led the authors of the study to conclude that NHEJ is involved in resolving the chromosome mis-segregation that occurs when a haploid-inducer is crossed to a wild type plant and that this resolution has two outcomes; (i) the formation of a aneuploid plant or (ii) the formation of a diploid plant. In the absence of the NHEJ pathway, they suggest that mis-segregated chromosomes enter a degradative pathway initiated by endonucleolytic breaks leading to increased haploid progeny formation (Tan *et al.* 2015). Intriguingly, only the female parent required the *lig4-2* mutation in order for this effect to manifest (Tan *et al.* 2015). While there is no guarantee that the *lig4* mutant would work in the same way when diploid pollen is being used in the cross, the similarities are significant enough to at least warrant an attempt at this approach. This could be accomplished by crossing an *osd1-3 lig4-2* double mutant to a GEM line haploid inducer with the *lig4-2* mutation (See Figure 5.3).

5.1.3 SDR/Haploid-inducer hybrids

Although the generation of plants which were hybrids of genetic material from SDR mutants and haploid-inducer lines was not the desired outcome of this project. It should be noted that with a different genetic setup these plants may be an interesting subject of study in themselves. Crosses between SDR mutants and haploid-inducer lines could be manipulated such that diploid, triploid, tetraploid and mixaploid plants with genetic material from up to four ecotypes could be generated in a single generation. This could be accomplished by crossing F_1 hybrid SDR mutants (such as the Col/Ler *osd1-3* mutants used in this study) to F_1 hybrid haploid-inducer lines. Based on the results of this study there seem to be at least four outcomes that could be expected from this cross; (i) Meiosis in the SDR mutant could produce diploid pollen that was homozygous, with regions of heterozygosity. Following the cross the haploid inducer could work as intended, leading to the loss of its own chromosome and generating a diploid plant containing only genetic material from the SDR mutant parent (i.e. a true SDR plant). (ii) Haploid plants could be generated whose chromosomes contained a mosaic of Col and Ler sequence from the SDR mutant parent but none from the haploid inducer parent. This outcome is suggested by the individuals in this study which were haploid and whose chromosomes switched from Col to Ler homozygous stretches (e.g. SDR070 and

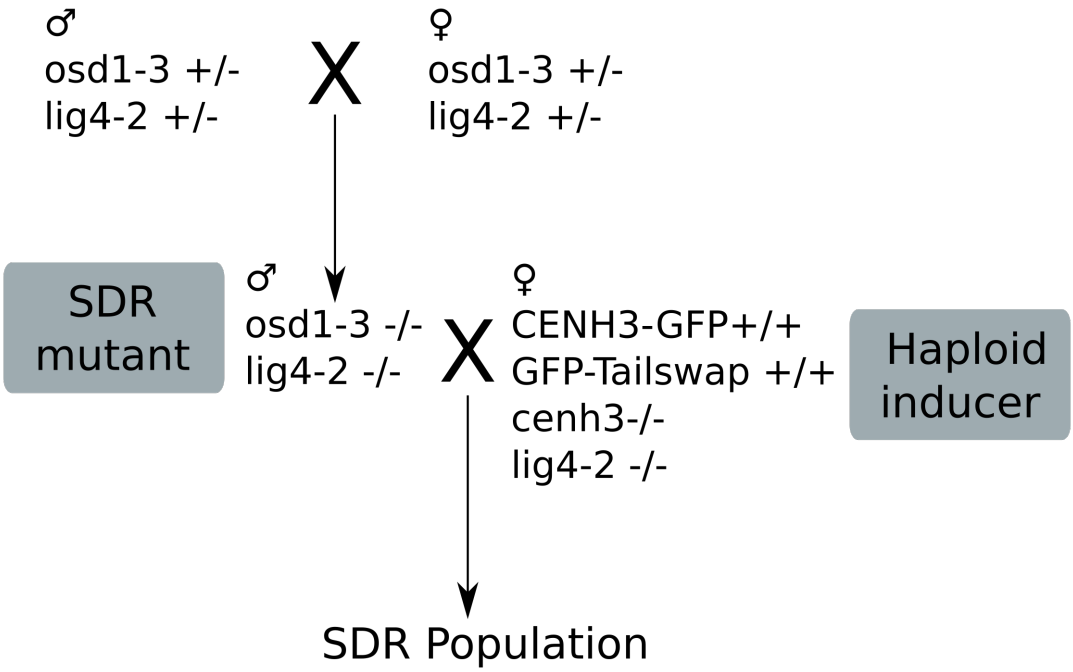

Figure 5.3: Crossing scheme to produce SDR population using the lig4-2 mutant.

SDR 078), suggesting the genetic material originated from the F_1 hybrid SDR mutant parent. (iii) Triploid plants could be generated which contained either two chromosomes from the SDR mutant parent and one from the haploid-inducer parent or one chromosome from the SDR mutant parent, and two from the haploid-inducer parent. This outcome is suggested by the triploid plants in this study (SDR067 and SDR163) which tested heterozygous at some markers and Col at others, suggesting they had some Ler genetic material from the SDR parent and Col genetic material from both its SDR mutant parent and its haploid-inducer parent. Unfortunately, the exact dynamics of inheritance are difficult to establish because the haploid-inducer parent was in a homozygous Col background. Using two F_1 hybrids as suggested above would allow the inheritance to be better understood. (iv) Aneuploid plants could also be generated such as SDR146.

5.1.4 Uses of SDR populations

Second division restitution has likely played a major role in the evolution of plants (Thompson 1995; Comai 2005). Most obviously through its potential to generate polyploid plants (Mason *et al.* 2015). However, the properties of SDR mutants have not been utilised in crop species, with the exception of the MiMe genotype, which exploits the *osd1* mutant to generate artificial apomictic *Oryza sativa* plants (d'Erfurth *et al.* 2009; Mieulet *et al.* 2016). The ability to use SDR mutants to generate high numbers of siblings which are mainly homozygous, but with small and varying regions of heterozygosity should prove useful in both pure science; for example during attempts to understand and dissect complex epistatic traits, as well as applied science breeding programs. In addition to this the SDR/haploid-inducer hybrids characterised in this study provide a novel way of combining up to 4 genotypes in a single generation.

5.2 Directing meiotic recombination via TAL fusion proteins

5.2.1 TALENs were expressed in *spo11-1-3* mutants

The main aim of this project was to introduce directed DSBs into a *spo11-1-3* mutant defective for crossovers via TALENS. This was expected to recover the infertility phenotype

of *spo11-1-3* by providing initiating DSBs for crossover formation at specific loci of choice. Fourteen TALEN lines, with a wide variety of putative target sites, were created and transformed into *spo11-1-3.* Expression of TALENs was confirmed by western blot and RT-PCR experiments, however, no significant recovery of infertility was observed in any of the lines which reached flowering. However, some plants did display phenotypes reminiscent of extreme DNA damage, which were potentially caused by TALEN-generated DSBs being repaired by the error-prone NHEJ pathway. In some plants growth was stunted to such an extent that plants never flowered, meaning it was impossible to assay the fertility of the plant.

There are currently three major technologies that may allow the creation of directed DSBs and therefore could conceivably be used in efforts to generate directed crossovers. These are, (I) zinc-finger nucleases (ZFNs), (ii) TALENs and (iii) the CRISPR/Cas9 system. Of these three, TALENs and CRISPR/Cas9 seem the most promising. ZFNs are created by generating a DNA binding domain via the combination of binding domains of multiple zinc fingers and then fusing this custom binding domain to the *FokI* nuclease (Smith *et al.* 2000). While ZFNs have been used to target DSBs in *Arabidopsis* (Lloyd *et al.* 2005; Zhang *et al.* 2010), tobacco (Cai *et al.* 2009) and maize (Kumar *et al.* 2015), the design process is laborious and somewhat unpredictable, as it relies on the idiosyncratic interactions between various zinc-finger transcription factor DNA binding domains (Smith *et al.* 2000). This presents a challenge to implement these systems in the targeted direction of DSBs.

CRISPR/Cas9 seems promising because of its well-understood targeting requirements. The CRISPR/Cas9 system comprises two components; the Cas9 nuclease which makes DSBs and a single guide RNA (sgRNA) which is complementary to the target sequence and guides the Cas9 nuclease to the desired cut site (Cong *et al.* 2013; Feng *et al.* 2014). One restriction to CRISPR targeting is the requirement that the Cas9 nuclease must recognise and bind the ‘protospacer adjacent motif’ (PAM) in order to generate DSBs (Sternberg *et al.* 2014). However, unlike TALENs where a new TALEN must be created for every new target site, CRISPR/Cas9 systems simply require a new sgRNA which can be created using commercially produced primers and fewer vectors than required for TALEN cloning (Jinek *et al.* 2012; Gaj *et al.* 2013). In addition to this, when used in mutagenesis studies CRISPR/Cas9 has shown higher efficiencies than TALENs suggesting it is more efficient at creating DSBs at

its target sites (Ma *et al.* 2016).

However, in spite of these facts, TALENs retain one advantage over CRISPR/Cas9. This is that degeneracy can be built into the DNA targeting domain of TALENs through the use of the 'NS' RVD (Moscou & Bogdanove 2009; Boch *et al.* 2009; Rogers *et al.* 2015). This allows TALENs to be produced with a wide range of theoretical target sites in any given genome. In contrast, in order to generate a CRISPR/Cas9 system that generates DSBs at multiple loci it is necessary to multiplex many sgRNAs. In plants, at least one crossover per chromosome (the obligate crossover) is required in order to ensure correct chromosome segregation at meiosis-I. A minimum requirement of any system which sought to direct crossover would be the ability to provide the minimum number of DSBs necessary in order to ensure the formation of one crossover per chromosome. The exact number of DSBs required per meiosis is unclear. In wild type *Arabidopsis* approximately 200 DSBs are made during meiosis (Chelysheva *et al.* 2005; Sanchez-Moran *et al.* 2007; Ferdous *et al.* 2012; Choi *et al.* 2013). However, in yeast, hypomorphic *spo11* mutants which produce less DSBs are capable of generating a crossover on each chromosome, due to a phenomena known as crossover homoeostasis (Martini *et al.* 2006)). While it is unclear how many DSBs are strictly necessary to ensure at least one crossover per chromosome, it seems likely that any crossover targeting system would have to make multiple DSBs on each chromosome. The current highest number of sgRNAs to be multiplexed in one-step is 30 (Vad-Nielsen *et al.* 2016). It may be the case that 30 DSB loci are sufficient to recover the *spo11-1-3* loss of crossover, but this would presumably only be the case if the target sites were effectively distributed across all chromosomes. Alternatively, 30 sgRNAs with multiple off-target sites could be used to generate a greater number of DSBs than sgRNAs. However, the ease at which TALENs can be produced with a range of target sites from 1-1,000,00 means that they likely posses an edge over CRISPR/Cas9 in efforts to direct crossovers. An important caveat to this point is that in order to generate TALENs with multiple target sites the NS RVD must be used and introduction of many RVDs likely deceases the affinity of a TALEN for its target sites meaning there is a balance to be struck between the number of target sites and the binding affinity of the TALEN.

5.2.2 Increasing the effectiveness of TALENs

There are a number of modifications that could be made to the TALENs used in this study in order to increase their effectiveness at directing crossover. One approach which could prove fruitful is the testing of different meiotic promoters. Both the *DMC1* and *SPO11-1* promoters used in this study were chosen because published reports showing expression during meiosis (Klimyuk & Jones 1997; Shingu *et al.* 2010). However it is possible that these were not the ideal promoters to use. For example, in *S. cerevisiae* the activity of native SPO11 is known to be regulated by ATM/ATR kinase activity, which serves to down-regulate SPO11 DSB formation (Carballo *et al.* 2013). This suggests that the TALEN constructs under the control of the *SPO11-1* promoter in this study may possess different expression and/or activity levels to native SPO11, once post-translational control is taken into account. This could explain the apparent DNA-damaging qualities of the TALENs observed in this study. The ideal promoter would be one known to promote high expression specifically during the DSB-forming stage of prophase-I and known to control a gene primarily regulated through its promoter-controlled expression.

Another strategy for improving the efficacy of TALENs would be to modify the nuclease domain of the TALENs. The TALENs in this study used two *FokI* nucelase domains which had been modified such that they needed to heterodimerise in order to generate a DSB, as opposed to native *FokI* which homodimerises (Miller *et al.* 2007; Szczepek *et al.* 2007). These domains could be replaced with SPO11-1 and SPO11-2 nuclease domains. Fortunately, SPO11-1 and SPO11-2 already act as heterodimers so no modification would need to be made in order to ensure DSBs were only made at sites where left and right TALENs had bound in close proximity (Shingu *et al.* 2010). With TALENs possessing SPO11 nuclease domains it is possible that the DSBs would have a greater chance of being channelled into the crossover repair pathway.

There was some evidence that DSBs generated by the TALENs used in this study were being directed down the NHEJ repair pathway instead of being channelled into crossovers. This presents an alternative way to increase crossover efficiency without the need to make modifications to the TALENs used. It has been shown that disabling the NHEJ pathway in

mice leads to an accumulation of meiotic DSBs (Couëdel *et al.* 2004). Therefore using NHEJ mutants in plants expressing TALENs may halt repair of DSBs via NHEJ and instead channel DSBs into the crossover pathway. This approach is complicated by the fact that in *Arabidopsis, lig4* and *ku80* NHEJ mutants were found to repair somatic DSBs quickly due to an independent DSB repair pathway (Kozak *et al.* 2009). While there is no direct evidence this alternative pathway functions during meiosis, it is at least formally possible that instead of channelling DSBs into the crossover pathway, expressing TALENs in an NHEJ mutant would simply channel them into this alternative DSB repair pathway. However, this could perhaps be countered by using a *lig4 xrcc1* double mutant which has both pathways disabled (Charbonnel *et al.* 2010).

A final tool that would greatly aid in the creation of crossover-directing TALENs would be a high-throughput *in vivo* assay of TALEN target sites. There have been numerous *in vivo* assays of TALEN binding sites (Cermak *et al.* 2011; Huang *et al.* 2011; Forsyth *et al.* 2016; Budhagatapalli *et al.* 2016). These usually consist of a reporter gene whose expression is restrained by the presence of a stop codon flanked by TALEN binding sites. When TALENs capable of binding to these sites are introduced they mutate the stop codon and so restore expression of the reporter gene. These approaches have the disadvantage that only one pair of target sites can be evaluated at a time, meaning it would be challenging to evaluate the hundreds of putative target sites possessed by a degenerate TALEN. An alternative *in vitro* approach to validating high-numbers of TALEN target sites has been demonstrated recently (Guilinger *et al.* 2014). This approach incubates preselection libraries of 10^{12} DNA sequences with TALENs. Cleaved sequences are then captured via adaptor ligation and sequenced. As the preselection library is large enough to contain all possible combinations of DNA sequence this offers a way to comprehensively assay TALEN target sites *in vitro*. While this seems a promising way to determine the true binding specificities of a given TALEN, because it is an *in vitro* technique there is no guarantee that the binding observed in this test will be mirrored in meiotic cells. For example, there is evidence from *S. cerevisiae* and *S. pombe* to suggest that chromatin structure plays a large role in which sites native SPO11 is capable of binding and generating DSBs (Prieler *et al.* 2005; Lorenz *et al.* 2006; Miyoshi *et al.* 2012), and TALENs would presumably be subject to some or all of the same limitations.

5.2.3 Uses of directed crossover

Directing crossover is likely to have both pure science applications, such as allowing a greater understanding of the events of meiosis, as well as applied science applications, such as allowing the breakage of linkage groups during crop breeding. This project has laid the groundwork for these efforts, devising a way to design TALENs with multiple target sites which are suitable for directing crossover. It is likely that a few straightforward modifications to the protocols detailed in this study will allow the successful direction of crossover in the near future.

Chapter 6: References

Abe, K. et al., 2009. Inefficient double-strand DNA break repair is associated with increased fasciation in Arabidopsis BRCA2 mutants. *Journal of Experimental Botany*, 60(9), pp.2751–2761.

Acquaviva, L. et al., 2013. Spp1 at the crossroads of H3K4me3 regulation and meiotic recombination. *Epigenetics : official journal of the DNA Methylation Society*, 8(4), pp.355–360.

Aklilu, B.B., Soderquist, R.S. & Culligan, K.M., 2014. Genetic analysis of the Replication Protein A large subunit family in Arabidopsis reveals unique and overlapping roles in DNA repair, meiosis and DNA replication. *Nucleic Acids Research*, 42(5), pp.3104–3118.

Alonso, J.M., 2003. Genome-Wide Insertional Mutagenesis of Arabidopsis thaliana. *Science*, 301(5633), pp.653–657. Available at: http://www.sciencemag.org/content/301/5633/653.short%5Cnhttp://www.ncbi.nlm.nih.gov/pubmed/12893945%5Cnhttp://www.sciencemag.org/cgi/doi/10.1126/science.1086391.

An, X.J., Deng, Z.Y. & Wang, T., 2011. OsSpo11-4, a rice homologue of the archaeal topVIA protein, mediates double-strand DNA cleavage and interacts with OsTopVIB. *PLoS ONE*, 6(5).

Anderson, L.K. et al., 2014. Combined fluorescent and electron microscopic imaging unveils the specific properties of two classes of meiotic crossovers. *Proceedings of the National Academy of Sciences of the United States of America*, 111(37), pp.13415–20. Available at: http://www.pnas.org/content/111/37/13415.abstract.

Anugrahwati, D.R. et al., 2008. Isolation of wheat-rye 1RS recombinants that break the linkage between the stem rust resistance gene SrR and secalin. *Genome*, 51(5), pp.341–349.

Armstrong, S.J., Franklin, F.C. & Jones, G.H., 2001. Nucleolus-associated telomere clustering and pairing precede meiotic chromosome synapsis in Arabidopsis thaliana. *Journal of Cell Science*, 114(Pt 23), pp.4207–4217. Available at: http://eutils.ncbi.nlm.nih.gov/entrez/eutils/elink.fcgi?dbfrom=pubmed&id=11739653&retmode=ref&cmd=prlinks%5Cnpapers3://publication/uuid/A28AE7C9-4143-4E0D-BF7F-025719432A5B.

Armstrong, S.J., Franklin, F.C.H. & Jones, G.H., 2003. A meiotic time-course for Arabidopsis thaliana. *Sexual Plant Reproduction*, 16(3), pp.141–149.

Ault, J.G. & Nicklas, R.B., 1989. Tension, microtubule rearrangements, and the proper distribution of chromosomes in mitosis. *Chromosoma*, 98(1), pp.33–9. Available at: http://www.ncbi.nlm.nih.gov/pubmed/2766878 [Accessed August 31, 2016].

Azumi, Y. et al., 2002. Homolog interaction during meiotic prophase I in Arabidopsis requires the SOLO DANCERS gene encoding a novel cyclin-like protein. *The EMBO Journal*, 21(12), p.3081 LP-3095. Available at: http://emboj.embopress.org/content/21/12/3081.abstract.

Barton, N.H., 2009. Why Sex and Recombination ? GENETIC VARIANCE IF THERE ARE. , LXXIV.

Baudat, F. et al., 2000. Chromosome synapsis defects and sexually dimorphic meiotic progression in mice lacking Spo11. *Mol Cell*, 6(5), pp.989–998. Available at: http://www.ncbi.nlm.nih.gov/entrez/query.fcgi?cmd=Retrieve&db=PubMed&dopt=Citation&list_uids=11106739.

Baudat, F. et al., 2010. PRDM9 is a major determinant of meiotic recombination hotspots in humans and mice. *Science (New York, N.Y.)*, 327(5967), pp.836–40. Available at: http://www.ncbi.nlm.nih.gov/pubmed/20044539 [Accessed May 23, 2014].

Bauknecht, M. & Kobbe, D., 2014. AtGEN1 and AtSEND1, two paralogs in Arabidopsis, possess holliday junction resolvase activity. *Plant physiology*, 166(1), pp.202–16. Available at: http://www.pubmedcentral.nih.gov/articlerender.fcgi?artid=4149707&tool=pmcentrez&rendertype=abstract.

Berchowitz, L.E. et al., 2007. The role of AtMUS81 in interference-insensitive crossovers in A. thaliana. *PLoS Genetics*, 3(8), pp.1355–1364.

Berchowitz, L.E. & Copenhaver, G.P., 2010. Genetic interference: don’t stand so close to me. *Current genomics*, 11(2), pp.91–102. Available at: http://www.pubmedcentral.nih.gov/articlerender.fcgi?artid=2874225&tool=pmcentrez&rendertype=abstract.

Bergerat, a et al., 1997. An atypical topoisomerase II from Archaea with implications for meiotic recombination. *Nature*, 386, pp.414–417.

Bishop, D.K. et al., 1992. DMC1: a meiosis-specific yeast homolog of E. coli recA required for recombination, synaptonemal complex formation, and cell cycle progression. *Cell*, 69(3), pp.439–56. Available at: http://www.ncbi.nlm.nih.gov/pubmed/1581960 [Accessed August 31, 2016].

Bishop, D.K., 1994. RecA homologs Dmc1 and Rad51 interact to form multiple nuclear complexes prior to meiotic chromosome synapsis. *Cell*, 79(6), pp.1081–1092. Available at: http://dx.doi.org/10.1016/0092-8674(94)90038-8.

Blitzblau, H.G. et al., 2007. Mapping of Meiotic Single-Stranded DNA Reveals Double-Strand-Break Hotspots near Centromeres and Telomeres. *Current Biology*, 17(23), pp.2003–2012.

Boateng, K.A. et al., 2013. Homologous Pairing Preceding SPO11 Mediated Double Strand Breaks in Mice. , 24(2), pp.196–205.

Boch, J. et al., 2009. Breaking the code of DNA binding specificity of TAL-type III effectors. *Science (New York, N.Y.)*, 326(5959), pp.1509–12. Available at: http://www.ncbi.nlm.nih.gov/pubmed/19933107 [Accessed July 14, 2014].

Bonas, U., Stall, R.E. & Staskawicz, B., 1989. Genetic and structural characterization of the avirulence gene avrBs3 from Xanthomonas campestris pv. vesicatoria. *Molecular & general genetics : MGG*, 218(1), pp.127–36. Available at: http://www.ncbi.nlm.nih.gov/pubmed/2550761 [Accessed August 31, 2016].

Börner, G.V., Kleckner, N. & Hunter, N., 2004. Crossover/noncrossover differentiation, synaptonemal complex formation, and regulatory surveillance at the leptotene/zygotene transition of meiosis. *Cell*, 117(1), pp.29–45. Available at: http://www.ncbi.nlm.nih.gov/pubmed/15066280.

Bovill, W.D. et al., 2009. Whole genome approaches to identify early meiotic gene candidates in cereals. *Functional and Integrative Genomics*, 9(2), pp.219–229.

Britt, A.B. & Kuppu, S., 2016. Cenh3: An Emerging Player in Haploid Induction Technology. *Frontiers in plant science*, 7(April), p.357. Available at: http://journal.frontiersin.org/article/10.3389/fpls.2016.00357%5Cnhttp://www.ncbi.nlm.nih.gov/pubmed/27148276%5Cnhttp://www.pubmedcentral.nih.gov/articlerender.fcgi?artid=PMC4828581.

Brownfield, L. & Köhler, C., 2011. Unreduced gamete formation in plants: mechanisms and prospects. *Journal of experimental botany*, 62(5), pp.1659–68. Available at: http://www.ncbi.nlm.nih.gov/pubmed/21109579 [Accessed October 16, 2013].

Budhagatapalli, N. et al., 2016. A simple test for the cleavage activity of customized endonucleases in plants. *Plant methods*, 12(December), p.18. Available at: /pmc/articles/PMC4784412/?report=abstract.

Bulankova, P. et al., 2013. Identification of Arabidopsis Meiotic Cyclins Reveals Functional Diversification among Plant Cyclin Genes. *PLoS Genetics*, 9(5).

Bundock, P. & Hooykaas, P., 2002. Severe developmental defects, hypersensitivity to DNA-damaging agents, and lengthened telomeres in Arabidopsis MRE11 mutants. *The Plant cell*, 14(10), pp.2451–62.

Cai, C.Q. et al., 2009. Targeted transgene integration in plant cells using designed zinc finger nucleases. , pp.699–709.

Cai, X. et al., 2003. The Arabidopsis SYN1 cohesin protein is required for sister chromatid arm cohesion and homologous chromosome pairing. *Journal of cell science*, 116(Pt 14), pp.2999–3007. Available at: http://jcs.biologists.org/content/116/14/2999.full.

Carballo, J. a et al., 2013. Budding yeast ATM/ATR control meiotic double-strand break (DSB) levels by down-regulating Rec114, an essential component of the DSB-machinery. *PLoS*

genetics, 9(6), p.e1003545. Available at: http://www.pubmedcentral.nih.gov/articlerender.fcgi?artid=3694840&tool=pmcentrez&rendertype=abstract [Accessed June 4, 2014].

Cermak, T. et al., 2011. Efficient design and assembly of custom TALEN and other TAL effector-based constructs for DNA targeting. *Nucleic acids research*, 39(12), p.e82. Available at: http://www.pubmedcentral.nih.gov/articlerender.fcgi?artid=3130291&tool=pmcentrez&rendertype=abstract [Accessed November 8, 2013].

Cervantes, M.D., Farah, J.A. & Smith, G.R., 2000. Meiotic DNA breaks associated with recombination in S. pombe. *Molecular Cell*, 5(5), pp.883–888.

Charbonnel, C., Gallego, M.E. & White, C.I., 2010. Xrcc1-dependent and Ku-dependent DNA double-strand break repair kinetics in Arabidopsis plants. *Plant Journal*, 64, pp.280–290.

Chelysheva, L. et al., 2010. An easy protocol for studying chromatin and recombination protein dynamics during Arabidopsisthaliana meiosis: Immunodetection of cohesins, histones and MLH1. *Cytogenetic and Genome Research*, 129(1–3), pp.143–153.

Chelysheva, L. et al., 2005a. AtREC8 and AtSCC3 are essential to the monopolar orientation of the kinetochores during meiosis. *Journal of cell science*, 118(Pt 20), pp.4621–32. Available at: http://www.ncbi.nlm.nih.gov/pubmed/16176934 [Accessed August 31, 2016].

Chelysheva, L. et al., 2005b. AtREC8 and AtSCC3 are essential to the monopolar orientation of the kinetochores during meiosis. *Journal of cell science*, 118(Pt 20), pp.4621–32. Available at: http://www.ncbi.nlm.nih.gov/pubmed/16176934 [Accessed July 14, 2014].

Chelysheva, L. et al., 2012. The Arabidopsis HEI10 is a new ZMM protein related to Zip3. *PLoS genetics*, 8(7), p.e1002799. Available at: http://www.pubmedcentral.nih.gov/articlerender.fcgi?artid=3405992&tool=pmcentrez&rendertype=abstract [Accessed July 14, 2014].

Chelysheva, L. et al., 2007. Zip4/Spo22 is required for class I CO formation but not for synapsis completion in Arabidopsis thaliana. *PLoS Genetics*, 3(5), pp.802–813.

Choi, K. et al., 2013a. Arabidopsis meiotic crossover hot spots overlap with H2A.Z nucleosomes at gene promoters. *Nature Genetics*. Available at: http://www.nature.com/doifinder/10.1038/ng.2766 [Accessed September 24, 2013].

Choi, K. et al., 2013b. Arabidopsis meiotic crossover hot spots overlap with H2A.Z nucleosomes at gene promoters. *Nature genetics*, 45(11), pp.1327–36. Available at: http://www.pubmedcentral.nih.gov/articlerender.fcgi?artid=3812125&tool=pmcentrez&rendertype=abstract [Accessed May 23, 2014].

Choi, K. & Henderson, I.R., 2015. Meiotic recombination hotspots - A comparative view. *Plant Journal*, 83(1), pp.52–61.

Christian, M. et al., 2013. Targeted mutagenesis of Arabidopsis thaliana using engineered TAL effector nucleases. *G3 (Bethesda, Md.)*, 3(10), pp.1697–705. Available at:

http://www.pubmedcentral.nih.gov/articlerender.fcgi?artid=3789794&tool=pmcentrez&rendertype=abstract [Accessed January 21, 2014].

Christian, M. et al., 2010. Targeting DNA double-strand breaks with TAL effector nucleases. *Genetics*, 186(2), pp.756–761.

Cloud, V. et al., 2012. Rad51 is an accessory factor for Dmc1-mediated joint molecule formation during meiosis. *Science (New York, N.Y.)*, 337(6099), pp.1222–5. Available at: http://www.ncbi.nlm.nih.gov/pubmed/22955832 [Accessed May 6, 2014].

Clough, S.J. & Bent, a F., 1998. Floral dip: a simplified method for Agrobacterium-mediated transformation of Arabidopsis thaliana. *The Plant journal : for cell and molecular biology*, 16(6), pp.735–43. Available at: http://www.ncbi.nlm.nih.gov/pubmed/10069079.

Comai, L., 2005. The advantages and disadvantages of being polyploid. *Nature reviews. Genetics*, 6(11), pp.836–46. Available at: http://www.ncbi.nlm.nih.gov/pubmed/16304599 [Accessed July 10, 2014].

Cong, L. et al., 2012. Comprehensive interrogation of natural TALE DNA-binding modules and transcriptional repressor domains. *Nature communications*, 3, p.968. Available at: http://www.pubmedcentral.nih.gov/articlerender.fcgi?artid=3556390&tool=pmcentrez&rendertype=abstract [Accessed November 12, 2013].

Cong, L. et al., 2013. Multiplex Genome Engineering Using CRISPR/Cas Systems. *Science*, 339(February), pp.819–822.

Cooper, K.F. & Strich, R., 2011. Meiotic control of the APC/C: similarities & differences from mitosis. *Cell division*, 6(1), p.16. Available at: http://www.ncbi.nlm.nih.gov/pubmed/21806783.

Cooper, T.J. et al., 2014. Homeostatic regulation of meiotic DSB formation by ATM/ATR. *Experimental Cell Research*, 329(1), pp.124–131. Available at: http://dx.doi.org/10.1016/j.yexcr.2014.07.016.

Cooper, T.J., Garcia, V. & Neale, M.J., 2016. Meiotic DSB patterning: A multifaceted process. *Cell Cycle*, 15(1), pp.13–21. Available at: http://dx.doi.org/10.1080/15384101.2015.1093709.

Copenhaver, G.P., Browne, W.E. & Preuss, D., 1998. Assaying genome-wide recombination and centromere functions with Arabidopsis tetrads. *Proceedings of the National Academy of Sciences of the United States of America*, 95(1), pp.247–252.

Copenhaver, G.P., Housworth, E.A. & Stahl, F.W., 2002. Crossover interference in arabidopsis. *Genetics*, 160(4), pp.1631–1639.

Couëdel, C. et al., 2004. Collaboration of homologous recombination and nonhomologous end-joining factors for the survival and integrity of mice and cells. *Genes and Development*, 18(11), pp.1293–1304.

Couteau, F. et al., 1999. Random chromosome segregation without meiotic arrest in both male and female meiocytes of a dmc1 mutant of Arabidopsis. *The Plant cell*, 11(9), pp.1623–34. Available at: http://www.pubmedcentral.nih.gov/articlerender.fcgi?artid=144309&tool=pmcentrez&rendertype=abstract.

Creighton, H.B. & McClintock, B., 1931. A Correlation of Cytological and Genetical Crossing-Over in Zea Mays. *Proceedings of the National Academy of Sciences of the United States of America*, 17(8), pp.492–7. Available at: http://www.ncbi.nlm.nih.gov/pubmed/16587654 [Accessed August 31, 2016].

Crismani, W., Girard, C., Froger, N., et al., 2012. FANCM limits meiotic crossovers. *Science (New York, N.Y.)*, 336(6088), pp.1588–90. Available at: http://www.ncbi.nlm.nih.gov/pubmed/22723424 [Accessed May 23, 2014].

Crismani, W., Girard, C. & Mercier, R., 2012. Tinkering with meiosis. *Journal of experimental botany*, 63(2), pp.695–709. Available at: http://www.pubmedcentral.nih.gov/articlerender.fcgi?artid=3254685&tool=pmcentrez&rendertype=abstract [Accessed May 23, 2014].

Cromer, L. et al., 2013. Centromeric cohesion is protected twice at meiosis, by SHUGOSHINs at anaphase i and by PATRONUS at interkinesis. *Current Biology*, 23(21), pp.2090–2099. Available at: http://dx.doi.org/10.1016/j.cub.2013.08.036.

Cromer, L. et al., 2012. OSD1 promotes meiotic progression via APC/C inhibition and forms a regulatory network with TDM and CYCA1;2/TAM. *PLoS genetics*, 8(7), p.e1002865. Available at: http://www.pubmedcentral.nih.gov/articlerender.fcgi?artid=3406007&tool=pmcentrez&rendertype=abstract [Accessed October 14, 2013].

Cromie, G.A. et al., 2007. A discrete class of intergenic DNA dictates meiotic DNA break hotspots in fission yeast. *PLoS Genetics*, 3(8), pp.1496–1507.

d'Erfurth, I. et al., 2010. The cyclin-A CYCA1;2/TAM is required for the meiosis I to meiosis II transition and cooperates with OSD1 for the prophase to first meiotic division transition. *PLoS genetics*, 6(6), p.e1000989. Available at: http://www.pubmedcentral.nih.gov/articlerender.fcgi?artid=2887465&tool=pmcentrez&rendertype=abstract [Accessed October 10, 2013].

d'Erfurth, I. et al., 2009. Turning meiosis into mitosis. *PLoS biology*, 7(6), p.e1000124. Available at: http://www.pubmedcentral.nih.gov/articlerender.fcgi?artid=2685454&tool=pmcentrez&rendertype=abstract [Accessed September 24, 2013].

Deng, Z.-Y. & Wang, T., 2007. OsDMC1 is required for homologous pairing in Oryza sativa. *Plant molecular biology*, 65(1–2), pp.31–42. Available at: http://www.ncbi.nlm.nih.gov/pubmed/17562186 [Accessed September 26, 2013].

Dernburg, a F. et al., 1998. Meiotic recombination in C. elegans initiates by a conserved mechanism and is dispensable for homologous chromosome synapsis. *Cell*, 94(3), pp.387–98. Available at: http://www.ncbi.nlm.nih.gov/pubmed/9708740.

Dissmeyer, N. et al., 2007. T-loop phosphorylation of Arabidopsis CDKA;1 is required for its function and can be partially substituted by an aspartate residue. *The Plant cell*, 19(3), pp.972–85. Available at: http://www.plantcell.org/content/19/3/972.full.

Doyle, E.L. et al., 2012. TAL Effector-Nucleotide Targeter (TALE-NT) 2.0: Tools for TAL effector design and target prediction. *Nucleic Acids Research*, 40(W1), pp.117–122.

Doyon, Y. et al., 2011. Enhancing zinc-finger-nuclease activity with improved obligate heterodimeric architectures. *Nature methods*, 8(1), pp.74–79.

Dray, E. et al., 2006. Interaction between Arabidopsis Brca2 and its partners Rad51, Dmc1, and Dss1. *Plant physiology*, 140(3), pp.1059–1069.

Drouaud, J. et al., 2013. Contrasted patterns of crossover and non-crossover at Arabidopsis thaliana meiotic recombination hotspots. *PLoS genetics*, 9(11), p.e1003922. Available at: http://www.pubmedcentral.nih.gov/articlerender.fcgi?artid=3828143&tool=pmcentrez&rendertype=abstract [Accessed May 23, 2014].

Durbarry, A., Vizir, I. & Twell, D., 2005. Male germ line development in Arabidopsis. duo pollen mutants reveal gametophytic regulators of generative cell cycle progression. *Plant physiology*, 137(1), pp.297–307.

Emmanuel, E. et al., 2006. The role of AtMSH2 in homologous recombination in Arabidopsis thaliana. *EMBO reports*, 7(1), pp.100–5. Available at: http://www.scopus.com/inward/record.url?eid=2-s2.0-33646185177&partnerID=tZOtx3y1.

Erfurth, I. et al., 2008. Mutations in AtPS1 (Arabidopsis thaliana Parallel Spindle 1) Lead to the Production of Diploid Pollen Grains. , 4(11), pp.1–9.

Esch, E. et al., 2007. Using crossover breakpoints in recombinant inbred lines to identify quantitative trait loci controlling the global recombination frequency. *Genetics*, 177(3), pp.1851–1858.

Esposito, M.S. & Esposito, R.E., 1969. the Genetic Control of Sporulation in Saccharomyces. *Genetics*, 61, pp.79–89.

Fachinetti, D. et al., 2013. A two-step mechanism for epigenetic specification of centromere identity and function. *Nature Cell Biology*, 15(9), pp.1056–1066. Available at: http://www.nature.com/doifinder/10.1038/ncb2805 [Accessed August 25, 2016].

Fan, Q.Q. et al., 1997. Competition between adjacent meiotic recombination hotspots in the yeast Saccharomyces cerevisiae. *Genetics*, 145(3), pp.661–670.

Fanning, E., Klimovich, V. & Nager, A.R., 2006. A dynamic model for replication protein A (RPA) function in DNA processing pathways. *Nucleic Acids Research*, 34(15), pp.4126–4137.

Felsenstein, J., 1976. The evolutionary advantage of recombination. II. Individual selection for recombination. *Genetics*, 83(4), pp.845–859.

Feng, Z. et al., 2014. Multigeneration analysis reveals the inheritance, specificity, and patterns of CRISPR/Cas-induced gene modifications in Arabidopsis. *Proc Natl Acad Sci U S A*, 111(12), pp.4632–4637. Available at: http://www.ncbi.nlm.nih.gov/pubmed/24550464%5Cnhttp://www.ncbi.nlm.nih.gov/pmc/articles/PMC3970504/pdf/pnas.201400822.pdf.

Ferdous, M. et al., 2012. Inter-homolog crossing-over and synapsis in Arabidopsis meiosis are dependent on the chromosome axis protein AtASY3. *PLoS genetics*, 8(2), p.e1002507. Available at: http://www.pubmedcentral.nih.gov/articlerender.fcgi?artid=3271061&tool=pmcentrez&rendertype=abstract [Accessed July 14, 2014].

Forner, J. et al., 2015. Germline-transmitted genome editing in Arabidopsis thaliana using TAL-effector-nucleases. *PLoS ONE*, 10(3), pp.1–15.

Forsyth, A. et al., 2016. Transcription Activator-Like Effector Nucleases (TALEN)-Mediated Targeted DNA Insertion in Potato Plants. *Frontiers in Plant Science*, 7, p.1572. Available at: http://www.ncbi.nlm.nih.gov/pmc/articles/PMC5078815/.

Foss, E. et al., 1993. Chiasma interference as a function of genetic distance. *Genetics*, 133(3), pp.681–691.

Foss, E.J. & Stahl, F.W., 1995. A test of a counting model for chiasma interference. *Genetics*, 139(3), pp.1201–1209.

Fowler, K.R. et al., 2014. Evolutionarily diverse determinants of meiotic DNA break and recombination landscapes across the genome. *Genome Research*, 24(10), pp.1650–1664.

Francis, K.E. et al., 2007. Pollen tetrad-based visual assay for meiotic recombination in Arabidopsis. *Proceedings of the National Academy of Sciences of the United States of America*, 104(10), pp.3913–8. Available at: http://www.pubmedcentral.nih.gov/articlerender.fcgi?artid=1805420&tool=pmcentrez&rendertype=abstract.

Fujitani, Y., Mori, S. & Kobayashi, I., 2002. A reaction-diffusion model for interference in meiotic crossing over. *Genetics*, 161(1), pp.365–372.

Fukuda, T. et al., 2008. Targeted induction of meiotic double-strand breaks reveals chromosomal domain-dependent regulation of Spo11 and interactions among potential sites of meiotic recombination. *Nucleic Acids Research*, 36(3), pp.984–997.

Gaj, T., Gersbach, C.A. & Barbas III, C.F., 2013. ZFN, TALEN, and CRISPR/Cas-based methods for genome engineering. *Trends in Biotechnology*, 31(7), pp.397–405. Available at: file://www.sciencedirect.com/science/article/pii/S0167779913000875.

Galbraith, D.W., Harkins, K.R. & Knapp, S., 1991. Systemic Endopolyploidy in Arabidopsis thaliana. *Plant physiology*, 96(3), pp.985–9. Available at:

http://www.ncbi.nlm.nih.gov/pubmed/16668285%5Cnhttp://www.pubmedcentral.nih.gov/articlerender.fcgi?artid=PMC1080875.

Garcia, V. et al., 2011. Bidirectional resection of DNA double-strand breaks by Mre11 and Exo1. *Nature*, 479(7372), pp.241–244. Available at: http://dx.doi.org/10.1038/nature10515.

Garcia, V. et al., 2015. Tel1(ATM)-mediated interference suppresses clustered meiotic double-strand-break formation. *Nature*, 520, pp.114–118. Available at: http://dx.doi.org/10.1038/nature13993.

Geuting, V. et al., 2009. Two distinct MUS81-EME1 complexes from Arabidopsis process Holliday junctions. *Plant physiology*, 150(2), pp.1062–71. Available at: http://www.plantphysiol.org/content/150/2/1062.short.

Girard, C. et al., 2015. AAA-ATPase FIDGETIN-LIKE 1 and Helicase FANCM Antagonize Meiotic Crossovers by Distinct Mechanisms. *PLoS Genetics*, 11(7), pp.1–22.

Girard, C. et al., 2014. FANCM-associated proteins MHF1 and MHF2, but not the other Fanconi anemia factors, limit meiotic crossovers. *Nucleic Acids Research*, 42(14), pp.9087–9095.

Gray, S. et al., 2013. Positive regulation of meiotic {DNA} double-strand break formation by activation of the {DNA} damage checkpoint kinase {Mec1(ATR).}. *Open Biol*, 3(7), p.130019.

Grelon, M. et al., 2001. AtSPO11-1 is necessary for efficient meiotic recombination in plants. *The EMBO journal*, 20(3), pp.589–600. Available at: http://www.pubmedcentral.nih.gov/articlerender.fcgi?artid=133473&tool=pmcentrez&rendertype=abstract.

Gruber, S., Haering, C.H. & Nasmyth, K., 2003. Chromosomal cohesin forms a ring. *Cell*, 112(6), pp.765–77. Available at: http://www.ncbi.nlm.nih.gov/pubmed/12654244.

Guilinger, J.P. et al., 2014. Broad specificity profiling of TALENs results in engineered nucleases with improved DNA-cleavage specificity. *Nature methods*, 11(4), pp.429–35. Available at: http://dx.doi.org/10.1038/nmeth.2845.

Gutiérrez-Caballero, C., Cebollero, L.R. & Pendás, A.M., 2017. Shugoshins: from protectors of cohesion to versatile adaptors at the centromere. *Trends in Genetics*, 28(7), pp.351–360. Available at: http://dx.doi.org/10.1016/j.tig.2012.03.003.

Haering, C.H. et al., 2008. The cohesin ring concatenates sister DNA molecules. *Nature*, 454(7202), pp.297–301. Available at: http://www.ncbi.nlm.nih.gov/pubmed/18596691.

Hamant, O. et al., 2005. A REC8-dependent plant shugoshin is required for maintenance of centromeric cohesion during meiosis and has no mitotic functions. *Current Biology*, 15(10), pp.948–954.

Han, Y.W. & Mizuuchi, K., 2010. Phage Mu Transposition Immunity: Protein Pattern Formation along DNA by a Diffusion-Ratchet Mechanism. *Molecular Cell*, 39(1), pp.48–58. Available at: http://dx.doi.org/10.1016/j.molcel.2010.06.013.

Hartung, F. et al., 2002. Not Present in Other Eukaryotes Is Indispensable for Cell Proliferation of Plants. , 12(2), pp.1787–1791.

Hartung, F. et al., 2007. The Catalytically Active Tyrosine Residues of Both SPO11-1 and SPO11-2 Are Required for Meiotic Double-Strand Break Induction in *Arabidopsis*. *The Plant Cell*, 19(10), pp.3090–3099. Available at: http://www.plantcell.org/lookup/doi/10.1105/tpc.107.054817 [Accessed August 11, 2016].

Hartung, F. & Puchta, H., 2000. Molecular characterisation of two paralogous SPO11 homologues in Arabidopsis thaliana. *Nucleic acids research*, 28(7), pp.1548–54. Available at: http://www.pubmedcentral.nih.gov/articlerender.fcgi?artid=102794&tool=pmcentrez&rendertype=abstract.

Hartung, F. & Puchta, H., 2001. Molecular characterization of homologues of both subunits A (SPO11) and B of the archaebacterial topoisomerase 6 in plants. *Gene*, 271(1), pp.81–86.

Heyman, J. et al., 2011. Arabidopsis ULTRAVIOLET-B-INSENSITIVE4 maintains cell division activity by temporal inhibition of the anaphase-promoting complex/cyclosome. *The Plant cell*, 23(12), pp.4394–410. Available at: http://www.pubmedcentral.nih.gov/articlerender.fcgi?artid=3269873&tool=pmcentrez&rendertype=abstract [Accessed November 1, 2013].

Higgins, J.D. et al., 2004. The Arabidopsis MutS homolog AtMSH4 functions at an early step in recombination : evidence for two classes of recombination in Arabidopsis. , (Keeney 2001), pp.2557–2570.

Higgins, J.D. et al., 2005. The Arabidopsis synaptonemal complex protein ZYP1 is required for chromosome synapsis and normal fidelity of crossing over. , pp.2488–2500.

Holliday, R., 1964. A mechanism for gene conversion in fungi. *Genetical research*, 5(1964), pp.282–304.

Horton, M.W. et al., 2012. Genome-wide patterns of genetic variation in worldwide Arabidopsis thaliana accessions from the RegMap panel. *Nature Publishing Group*, 44(2), pp.212–216. Available at: http://dx.doi.org/10.1038/ng.1042.

Hosouchi, T. et al., 2002. Physical Map-Based Sizes of the Centromeric Regions of Arabidopsis thaliana Chromosomes 1, 2, and 3. *DNA Research*, 9(4), pp.117–121. Available at: http://dnaresearch.oxfordjournals.org/cgi/doi/10.1093/dnares/9.4.117 [Accessed August 25, 2016].

Howard, A. & Pelc, S.R., 1953. Synthesis of Desoxyribonucleic Acid in Normal and Irradiated Cells and Its Relation to Chromosome Breakage. *International Journal of Radiation Biology*

and Related Studies in Physics, Chemistry and Medicine, 49(2), pp.207–218. Available at: http://dx.doi.org/10.1080/09553008514552501.

Huang, P. et al., 2011. Heritable gene targeting in zebrafish using customized TALENs. *Nature biotechnology*, 29(8), pp.699–700. Available at: http://dx.doi.org/10.1038/nbt.1939.

Hultén, M. a, 2011. On the origin of crossover interference: A chromosome oscillatory movement (COM) model. *Molecular Cytogenetics*, 4(1), p.10. Available at: http://www.molecularcytogenetics.org/content/4/1/10.

Hunter, N. & Kleckner, N., 2001. The Single-End Invasion. *Cell*, 106(1), pp.59–70. Available at: http://www.sciencedirect.com/science/article/pii/S0092867401004305.

Da Ines, O., Degroote, F., Amiard, S., et al., 2013. Effects of XRCC2 and RAD51B mutations on somatic and meiotic recombination in Arabidopsis thaliana. *Plant Journal*, 74(6), pp.959–970.

Da Ines, O., Degroote, F., Goubely, C., et al., 2013. Meiotic Recombination in Arabidopsis Is Catalysed by DMC1, with RAD51 Playing a Supporting Role F. C. H. Franklin, ed. *PLoS Genetics*, 9(9), p.e1003787. Available at: http://dx.plos.org/10.1371/journal.pgen.1003787 [Accessed September 30, 2013].

Ingouff, M. et al., 2010. Zygotic resetting of the HISTONE 3 variant repertoire participates in epigenetic reprogramming in arabidopsis. *Current Biology*, 20(23), pp.2137–2143.

Irniger, S. et al., 1995. Genes involved in sister chromatid separation are needed for b-type cyclin proteolysis in budding yeast. *Cell*, 81(2), pp.269–277.

Iwata, E. et al., 2011. GIGAS CELL1, a novel negative regulator of the anaphase-promoting complex/cyclosome, is required for proper mitotic progression and cell fate determination in Arabidopsis. *The Plant cell*, 23(12), pp.4382–93. Available at: http://www.pubmedcentral.nih.gov/articlerender.fcgi?artid=3269872&tool=pmcentrez&rendertype=abstract.

Jackson, N. et al., 2006. Reduced meiotic crossovers and delayed prophase I progression in AtMLH3-deficient Arabidopsis. *The EMBO Journal*, 25(6), pp.1315–1323. Available at: http://emboj.embopress.org/content/25/6/1315.abstract%5Cnhttp://emboj.embopress.org/cgi/doi/10.1038/sj.emboj.7600992.

Jia, L., Kim, S. & Yu, H., 2013. Tracking spindle checkpoint signals from kinetochores to APC/C. *Trends in Biochemical Sciences*, 38(6), pp.302–311. Available at: http://dx.doi.org/10.1016/j.tibs.2013.03.004.

Jinek, M. et al., 2012. A Programmable Dual-RNA – Guided DNA Endonuclease in Adaptice Bacterial Immunity. *Science (New York, N.Y.)*, 337(August), pp.816–822. Available at: http://science.sciencemag.org/content/337/6096/816.abstract.

Karimi-Ashtiyani, R. et al., 2015. Point mutation impairs centromeric CENH3 loading and induces haploid plants. *Proceedings of the National Academy of Sciences of the United States of America*, 112(36), p.1504333112-. Available at: http://www.pnas.org/content/early/2015/08/19/1504333112.

Keeney, S., Giroux, C.N. & Kleckner, N., 1997. Meiosis-Specific DNA Double-Strand Breaks Are Catalyzed by Spo11, a Member of a Widely Conserved Protein Family. *Cell*, 88(3), pp.375–384.

Keightley, P.D. & Eyre-Walker, A., 2000. Deleterious mutations and the evolution of sex. *Science*, 290(5490), pp.331–333.

Kerrebrock, A.W. et al., 1995. Mei-S332, a drosophila protein required for sister-chromatid cohesion, can localize to meiotic centromere regions. *Cell*, 83(2), pp.247–256.

Kim, J.S. & Rose, A.M., 1987. The effect of gamma radiation on recombination frequency in Caenorhabditis elegans. *Genome*, 29(3), pp.457–462.

King, J.S. & Mortimer, R.K., 1990. A polymerization model of chiasma interference and corresponding computer simulation. *Genetics*, 126(4), pp.1127–1138.

King, R.W. et al., 1995. A 20s complex containing CDC27 and CDC16 catalyzes the mitosis-specific conjugation of ubiquitin to cyclin B. *Cell*, 81(2), pp.279–288.

Kitajima, T.S. et al., 2003. Rec8 cleavage by separase is required for meiotic nuclear divisions in fission yeast. *EMBO Journal*, 22(20), pp.5643–5653.

Kitajima, T.S., Kawashima, S. a & Watanabe, Y., 2004. The conserved kinetochore protein shugoshin protects centromeric cohesion during meiosis. *Nature*, 427(6974), pp.510–517.

Kleckner, N. et al., 2004. A mechanical basis for chromosome function. *Proceedings of the National Academy of Sciences of the United States of America*, 101(34), pp.12592–7. Available at: http://www.pubmedcentral.nih.gov/articlerender.fcgi?artid=515102&tool=pmcentrez&rendertype=abstract.

Kleckner, N.E. et al., 2012. Correction for Zhang et al., Meiotic double-strand breaks occur once per pair of (sister) chromatids and, via Mec1/ATR and Tel1/ATM, once per quartet of chromatids. *Proceedings of the National Academy of Sciences*, 109(4), pp.1353–1353. Available at: http://www.pnas.org/cgi/doi/10.1073/pnas.1120345109 [Accessed July 2, 2014].

Klein, F. et al., 1999. A central role for cohesins in sister chromatid cohesion, formation of axial elements, and recombination during yeast meiosis. *Cell*, 98(1), pp.91–103. Available at: http://www.ncbi.nlm.nih.gov/pubmed/10412984.

Klimyuk, V.I. & Jones, J.D., 1997. AtDMC1, the Arabidopsis homologue of the yeast DMC1 gene: characterization, transposon-induced allelic variation and meiosis-associated expression. *The*

Plant journal : for cell and molecular biology, 11(1), pp.1–14. Available at: http://www.ncbi.nlm.nih.gov/pubmed/9025299.

Knoll, A. et al., 2012. The Fanconi anemia ortholog FANCM ensures ordered homologous recombination in both somatic and meiotic cells in Arabidopsis. *The Plant cell*, 24(4), pp.1448–64. Available at: http://www.pubmedcentral.nih.gov/articlerender.fcgi?artid=3398556&tool=pmcentrez&rendertype=abstract [Accessed July 10, 2014].

Koncz, C. et al., 1992. T-DNA insertional mutagenesis in Arabidopsis. *Plant Molecular Biology*, 20(5), pp.963–976.

Kondrashov, A.S., 1988. Deleterious mutations and the evolution of sexual reproduction. *Nature*, 336(6198), pp.435–440.

Kovall, R.A. & Matthews, B.W., 1999. Type II restriction endonucleases: Structural, functional and evolutionary relationships. *Current Opinion in Chemical Biology*, 3(5), pp.578–583.

Kozak, J. et al., 2009. Rapid repair of DNA double strand breaks in Arabidopsis thaliana is dependent on proteins involved in chromosome structure maintenance. *DNA Repair*, 8(3), pp.413–419.

Kudo, N.R. et al., 2009. Role of cleavage by separase of the Rec8 kleisin subunit of cohesin during mammalian meiosis I. *Journal of cell science*, 122(Pt 15), pp.2686–2698.

Kumar, S. et al., 2015. A modular gene targeting system for sequential transgene stacking in plants. *Journal of Biotechnology*, 207, pp.12–20. Available at: http://dx.doi.org/10.1016/j.jbiotec.2015.04.006.

Kumekawa, N. et al., 2001. The size and sequence organization of the centromeric region of Arabidopsis thaliana chromosome 4. *DNA research : an international journal for rapid publication of reports on genes and genomes*, 8(6), pp.285–90. Available at: http://www.ncbi.nlm.nih.gov/pubmed/11853315 [Accessed August 25, 2016].

Kumekawa, N. et al., 2000. The size and sequence organization of the centromeric region of arabidopsis thaliana chromosome 5. *DNA research : an international journal for rapid publication of reports on genes and genomes*, 7(6), pp.315–321.

Kurzbauer, M.-T. et al., 2012. The recombinases DMC1 and RAD51 are functionally and spatially separated during meiosis in Arabidopsis. *The Plant cell*, 24(5), pp.2058–70. Available at: http://www.pubmedcentral.nih.gov/articlerender.fcgi?artid=3442587&tool=pmcentrez&rendertype=abstract [Accessed April 29, 2014].

Lacefield, S. & Murray, A.W., 2007. The spindle checkpoint rescues the meiotic segregation of chromosomes whose crossovers are far from the centromere. *Nature genetics*, 39(10), pp.1273–1277.

Lake, C.M. & Hawley, R.S., 2015. Becoming a crossover-competent DSB. *Seminars in Cell and Developmental Biology*, 54, pp.117–125. Available at: http://dx.doi.org/10.1016/j.semcdb.2016.01.008.

Lam, W.S., Yang, X. & Makaroff, C. a, 2005. Characterization of Arabidopsis thaliana SMC1 and SMC3: evidence that AtSMC3 may function beyond chromosome cohesion. *Journal of cell science*, 118(Pt 14), pp.3037–3048.

Lange, J. et al., 2011. ATM controls meiotic double-strand-break formation. *Nature*, 479(7372), pp.237–40. Available at: http://www.pubmedcentral.nih.gov/articlerender.fcgi?artid=3213282&tool=pmcentrez&rendertype=abstract [Accessed May 5, 2014].

Lara-Gonzalez, P., Westhorpe, F.G. & Taylor, S.S., 2012. The spindle assembly checkpoint. *Current Biology*, 22(22), pp.R966–R980. Available at: http://dx.doi.org/10.1016/j.cub.2012.10.006.

Lee, J. et al., 2008. Unified mode of centromeric protection by shugoshin in mammalian oocytes and somatic cells. *Nature cell biology*, 10(1), pp.42–52. Available at: http://www.ncbi.nlm.nih.gov/pubmed/18084284.

Lhuissier, F.G.P. et al., 2007. The Mismatch Repair Protein MLH1 Marks a Subset of Strongly Interfering Crossovers in Tomato. *the Plant Cell Online*, 19(3), pp.862–876. Available at: http://www.plantcell.org/cgi/doi/10.1105/tpc.106.049106.

Lin, E.H.B. et al., 2014. Population targeting and durability of multimorbidity colloborative care management. *American Journal of Managed Care*, 20(11), pp.887–893.

Liu, C.M. et al., 2002. Condensin and cohesin knockouts in Arabidopsis exhibit a titan seed phenotype. *Plant Journal*, 29(4), pp.405–415.

Liu, H. et al., 2002. mei-P22 encodes a chromosome-associated protein required for the initiation of meiotic recombination in Drosophila melanogaster. *Genetics*, 162(1), pp.245–258.

Liu, S.T. et al., 2006. Mapping the assembly pathways that specify formation of the trilaminar kinetochore plates in human cells. *Journal of Cell Biology*, 175(1), pp.41–53.

Liu, Z. & Makaroff, C.A., 2006. Arabidopsis Separase AESP Is Essential for Embryo Development and the Release of Cohesin during Meiosis. *Plant Cell*, 18(5), pp.1213–1225. Available at: http://www.plantcell.org/cgi/doi/10.1105/tpc.105.036913%5Cnhttp://www.plantcell.org/cgi/content/abstract/18/5/1213.

Lloyd, A. et al., 2005. Targeted mutagenesis using zinc-finger nucleases in Arabidopsis.

López, E. et al., 2012. Looking for natural variation in chiasma frequency in Arabidopsis thaliana. *Journal of Experimental Botany*, 63(2), pp.887–894.

Lorenz, A. et al., 2006. Meiotic recombination proteins localize to linear elements in Schizosaccharomyces pombe. *Chromosoma*, 115(4), pp.330–340.

De los Santos, T. et al., 2003. The MUS81/MMS4 endonuclease acts independently of double-holliday junction resolution to promote a distinct subset of crossovers during meiosis in budding yeast. *Genetics*, 164(1), pp.81–94.

Luo, Q. et al., 2013. The role of OsMSH5 in crossover formation during rice meiosis. *Molecular Plant*, 6(3), pp.729–742. Available at: http://dx.doi.org/10.1093/mp/sss145.

Ma, X. et al., 2016. CRISPR/Cas9 platforms for genome editing in plants: developments and applications. *Molecular Plant*, 9(April), pp.1–32. Available at: http://dx.doi.org/10.1016/j.molp.2016.04.009.

Macaisne, N. et al., 2008. SHOC1, an XPF Endonuclease-Related Protein, Is Essential for the Formation of Class I Meiotic Crossovers. *Current Biology*, 18(18), pp.1432–1437.

Macaisne, N., Vignard, J. & Mercier, R., 2011. SHOC1 and PTD form an XPF-ERCC1-like complex that is required for formation of class I crossovers. *Journal of Cell Science*, 124(16), pp.2687–2691. Available at: http://jcs.biologists.org/cgi/doi/10.1242/jcs.088229.

Macqueen, A.J., 2002. mechanisms stabilize homolog pairing during meiotic prophase in C . elegans. , pp.2428–2442.

MacQueen, A.J. et al., 2005. Chromosome sites play dual roles to establish homologous synapsis during meiosis in C. elegans. *Cell*, 123(6), pp.1037–1050.

Magnard, J. et al., 2001. The Arabidopsis Gene Tardy Asynchronous Meiosis Is Required for the Normal Pace and Synchrony of Cell Division during Male Meiosis. *Plant physiology*, 127(November), pp.1157–1166.

Maheshwari, S. et al., 2015. Naturally Occurring Differences in CENH3 Affect Chromosome Segregation in Zygotic Mitosis of Hybrids. *PLoS genetics*, 11(1), p.e1004970. Available at: http://www.ncbi.nlm.nih.gov/pubmed/25622028 [Accessed January 29, 2015].

Marimuthu, M.P.A., Jolivet, S., Ravi, M., Pereira, L., Davda, J.N., Cromer, L., Wang, L., Nogué, F., Chan, S.W.L., et al., 2011. Synthetic clonal reproduction through seeds. *Science (New York, N.Y.)*, 331(6019), p.876. Available at: http://www.ncbi.nlm.nih.gov/pubmed/21330535 [Accessed August 11, 2016].

Marimuthu, M.P.A., Jolivet, S., Ravi, M., Pereira, L., Davda, J.N., Cromer, L., Wang, L., Nogué, F. & Chan, S.W.L., 2011. Synthetic Clonal ReproductionThrough Seeds. *Science*, 331, p.876.

Martinez-Perez, E. & Villeneuve, A.M., 2005. HTP-1-dependent constraints coordinate homolog pairing and synapsis and promote chiasma formation during C. elegans meiosis. *Genes and Development*, 19(22), pp.2727–2743.

Martini, E. et al., 2006. Crossover homeostasis in yeast meiosis. *Cell*, 126(2), pp.285–95. Available at: http://www.pubmedcentral.nih.gov/articlerender.fcgi?artid=1949389&tool=pmcentrez&rendertype=abstract [Accessed October 23, 2013].

Mason, A.S. et al., 2015. Unreduced gametes: meiotic mishap or evolutionary mechanism? *Trends in Genetics*, 31(1), pp.5–10. Available at: http://linkinghub.elsevier.com/retrieve/pii/S0168952514001590 [Accessed August 24, 2016].

Masson, J.Y. & West, S.C., 2001. The Rad51 and Dmc1 recombinases: A non-identical twin relationship. *Trends in Biochemical Sciences*, 26(2), pp.131–136.

de Massy, B., 2013. Initiation of meiotic recombination: how and where? Conservation and specificities among eukaryotes. *Annual review of genetics*, 47, pp.563–99. Available at: http://www.ncbi.nlm.nih.gov/pubmed/24050176 [Accessed February 24, 2014].

McKim, K.S. et al., 1998. Meiotic synapsis in the absence of recombination. *Science*, 279(5352), pp.876–878.

McKinley, K.L. & Cheeseman, I.M., 2016. The molecular basis for centromere identity and function. *Nat Rev Mol Cell Biol*, 17(1), pp.16–29. Available at: http://dx.doi.org/10.1038/nrm.2015.5%5Cn10.1038/nrm.2015.5.

Mercier, R. et al., 2015a. The Molecular Biology of Meiosis in Plants. *Annual Review of Plant Biology*, 66(1), pp.297–327. Available at: http://www.annualreviews.org/doi/10.1146/annurev-arplant-050213-035923.

Mercier, R. et al., 2015b. The Molecular Biology of Meiosis in Plants. *Annual Review of Plant Biology*, 66(1), p.141210140145001–. Available at: http://www.annualreviews.org/doi/abs/10.1146/annurev-arplant-050213-035923.

Mercier, R. et al., 2005. Two meiotic crossover classes cohabit in Arabidopsis: one is dependent on MER3,whereas the other one is not. *Current biology : CB*, 15(8), pp.692–701. Available at: http://www.ncbi.nlm.nih.gov/pubmed/15854901 [Accessed May 22, 2014].

Meselson, M.S. & Radding, C.M., 1975. A general model for genetic recombination. *Proceedings of the National Academy of Sciences of the United States of America*, 72(1), pp.358–361.

Mézard, C., Tagliaro Jahns, M. & Grelon, M., 2015. Where to cross? New insights into the location of meiotic crossovers. *Trends in Genetics*, 31(7), pp.1–9.

Mieulet, D. et al., 2016. Turning rice meiosis into mitosis. *Cell Research*, pp.1–13. Available at: http://www.nature.com/doifinder/10.1038/cr.2016.117.

Miller, J.C. et al., 2007. An improved zinc-finger nuclease architecture for highly specific genome editing. *Nature biotechnology*, 25(7), pp.778–85. Available at: http://www.ncbi.nlm.nih.gov/pubmed/17603475.

Miller, J.C. et al., 2015. Improved specificity of TALE-based genome editing using an expanded RVD repertoire. *Nature Methods*, 12(5), pp.465–471. Available at: http://www.nature.com/doifinder/10.1038/nmeth.3330.

Milman, N., Higuchi, E. & Smith, G.R., 2009. Meiotic DNA double-strand break repair requires two nucleases, MRN and Ctp1, to produce a single size class of Rec12 (Spo11)-oligonucleotide complexes. *Molecular and Cellular Biology*, 29(22), pp.5998–6005. Available at: http://eutils.ncbi.nlm.nih.gov/entrez/eutils/elink.fcgi?dbfrom=pubmed&id=19752195&retmode=ref&cmd=prlinks%5Cnpapers3://publication/doi/10.1128/MCB.01127-09.

Mimitou, E.P. & Symington, L.S., 2009. DNA end resection: many nucleases make light work. *DNA repair*, 8(9), pp.983–95. Available at: http://www.pubmedcentral.nih.gov/articlerender.fcgi?artid=2760233&tool=pmcentrez&rendertype=abstract [Accessed May 9, 2014].

Mirouze, M. et al., 2012. Loss of DNA methylation affects the recombination landscape in Arabidopsis. *Proceedings of the National Academy of Sciences*, 109(15), pp.5880–5885. Available at: http://www.pnas.org/cgi/doi/10.1073/pnas.1120841109 [Accessed August 30, 2016].

Miyoshi, T. et al., 2012. A Central Coupler for Recombination Initiation Linking Chromosome Architecture to S Phase Checkpoint. *Molecular Cell*, 47(5), pp.722–733. Available at: http://dx.doi.org/10.1016/j.molcel.2012.06.023.

Morgan, T.H., 1916. A Critique of the Theory of Evolution.

Moscou, M.J. & Bogdanove, A.J., 2009. A simple cipher governs DNA recognition by TAL effectors. *Science (New York, N.Y.)*, 326(5959), p.1501. Available at: http://science.sciencemag.org/content/326/5959/1501.abstract.

Muller, H.J., 1932. Some Genetic Aspects of Sex. *Source: The American Naturalist*, 66(703), pp.118–138. Available at: http://www.jstor.org/stable/2456922 [Accessed August 31, 2016].

De Muyt, A. et al., 2009. A high throughput genetic screen identifies new early meiotic recombination functions in Arabidopsis thaliana. *PLoS genetics*, 5(9), p.e1000654. Available at: http://www.pubmedcentral.nih.gov/articlerender.fcgi?artid=2735182&tool=pmcentrez&rendertype=abstract [Accessed May 3, 2014].

De Muyt, A. et al., 2007. AtPRD1 is required for meiotic double strand break formation in Arabidopsis thaliana. *The EMBO journal*, 26(18), pp.4126–37. Available at: http://www.pubmedcentral.nih.gov/articlerender.fcgi?artid=2230667&tool=pmcentrez&rendertype=abstract [Accessed May 22, 2014].

Myers, S. et al., 2010. Drive against hotspot motifs in primates implicates the PRDM9 gene in meiotic recombination. *Science (New York, N.Y.)*, 327(5967), pp.876–9. Available at: http://science.sciencemag.org/content/327/5967/876.abstract.

Nagaki, K. et al., 2003. Chromatin immunoprecipitation reveals that the 180-bp satellite repeat is the key functional DNA element of Arabidopsis thaliana centromeres. *Genetics*, 163(3), pp.1221–1225.

Nasmyth, K., 1996. At the heart of the budding yeast cell cycle. *Trends in genetics*, 12(10), pp.405–412.

Nasmyth, K., 2001. Disseminating the genome: joining, resolving, and separating sister chromatids during mitosis and meiosis. *Annual Review of Genetics*, 35, pp.673–745.

Neale, M.J., Pan, J. & Keeney, S., 2005. Endonucleolytic processing of covalent protein-linked DNA double-strand breaks. *Nature*, 436(7053), pp.1053–7. Available at: http://dx.doi.org/10.1038/nature03872.

Nicklas, R.B. & Koch, C.A., 1969. Chromosome micromanipulation. 3. Spindle fiber tension and the reorientation of mal-oriented chromosomes. *The Journal of cell biology*, 43(1), pp.40–50. Available at: http://www.ncbi.nlm.nih.gov/pubmed/5824068 [Accessed August 31, 2016].

Nishino, T. et al., 2005. Structural and functional analyses of an archaeal XPF/Rad1/Mus81 nuclease: Asymmetric DNA binding and cleavage mechanisms. *Structure*, 13(8), pp.1183–1192.

Niu, B. et al., 2015. Arabidopsis Cell Division Cycle 20.1 Is Required for Normal Meiotic Spindle Assembly and Chromosome Segregation. *The Plant cell*, 27(12), pp.3367–82. Available at: http://www.plantcell.org/content/early/2015/12/15/tpc.15.00834.abstract.

Noll, D.M., Mason, T.M. & Miller, P.S., 2006. Formation and Repair of Interstrand Cross-Links in DNA. *Chemical reviews*, 106(2), pp.277–301. Available at: http://www.ncbi.nlm.nih.gov/pmc/articles/PMC2505341/.

Nowack, M.K. et al., 2012. Genetic Framework of Cyclin-Dependent Kinase Function in Arabidopsis. *Developmental Cell*, 22(5), pp.1030–1040. Available at: http://dx.doi.org/10.1016/j.devcel.2012.02.015.

Nurse, P., 2000. A long twentieth century of the cell cycle and beyond. *Cell*, 100(1), pp.71–78.

Oa, W. et al., 2010. Meiotic Progression in Arabidopsis Is Governed by Complex Regulatory Interactions between SMG7, TDM1, and the Meiosis I–Specific Cyclin TAM.

Palmer, D.K. et al., 1991. Purification of the centromere-specific protein CENP-A and demonstration that it is a distinctive histone. *Proceedings of the National Academy of Sciences of the United States of America*, 88(9), pp.3734–8. Available at: http://www.ncbi.nlm.nih.gov/pubmed/2023923 [Accessed August 25, 2016].

Panizza, S. et al., 2011. Spo11-accessory proteins link double-strand break sites to the chromosome axis in early meiotic recombination. *Cell*, 146(3), pp.372–83. Available at: http://www.ncbi.nlm.nih.gov/pubmed/21816273 [Accessed July 17, 2014].

Parvanov, E.D., Petkov, P.M. & Paigen, K., 2010. Prdm9 controls activation of mammalian recombination hotspots. *Science (New York, N.Y.)*, 327(5967), p.835. Available at: http://www.pubmedcentral.nih.gov/articlerender.fcgi?artid=2821451&tool=pmcentrez&rendertype=abstract.

Pesin, J.A. & Orr-Weaver, T.L., 2008. Regulation of APC/C activators in mitosis and meiosis. *Annual review of cell and developmental biology*, 24, pp.475–99. Available at: http://www.pubmedcentral.nih.gov/articlerender.fcgi?artid=4070676&tool=pmcentrez&rendertype=abstract.

Phillips, C.M. et al., 2009. Identification of chromosome sequence motifs that mediate meiotic pairing and synapsis in C. elegans. *Nature Cell Biology*, 11(8), pp.934-U66.

Pines, J., 1995. Cyclins and cyclin-dependent kinases: a biochemical view. *Biochemical Journal*, 308(Pt 3), pp.697–711.

Ponticelli, A.S. & Smith, G.R., 1989. Meiotic recombination-deficient mutants of Schizosaccharomyces pombe. *Genetics*, 123(1), pp.45–54.

Pradillo, M. et al., 2007. An analysis of univalent segregation in meiotic mutants of Arabidopsis thaliana: a possible role for synaptonemal complex. *Genetics*, 175(2), pp.505–11. Available at: http://www.pubmedcentral.nih.gov/articlerender.fcgi?artid=1800621&tool=pmcentrez&rendertype=abstract [Accessed July 17, 2014].

Prieler, S. et al., 2005. The control of Spo11 ' s interaction with meiotic recombination hotspots. *Genes & development*, 19, pp.255–269.

Puizina, J. et al., 2004. Mre11 Deficiency in Arabidopsis Is Associated with Chromosomal Instability in Somatic Cells and Spo11-Dependent Genome Fragmentation during Meiosis. , 16(August), pp.1968–1978.

Ravi, M. et al., 2014. A haploid genetics toolbox for Arabidopsis thaliana. *Nature Communications*, 5, p.5334. Available at: http://www.nature.com/doifinder/10.1038/ncomms6334 [Accessed August 25, 2016].

Ravi, M. & Chan, S.W.L., 2010a. Haploid plants produced by centromere-mediated genome elimination. *Nature*, 464(7288), pp.615–618.

Ravi, M. & Chan, S.W.L., 2010b. Haploid plants produced by centromere-mediated genome elimination. *Nature*, 464(7288), pp.615–8. Available at: http://www.ncbi.nlm.nih.gov/pubmed/20336146 [Accessed May 6, 2014].

Ravi, M. & Chan, S.W.L., 2010c. Haploid plants produced by centromere-mediated genome elimination. *Nature*, 464(7288), pp.615–8. Available at: http://www.ncbi.nlm.nih.gov/pubmed/20336146 [Accessed September 25, 2013].

Recker, J., Knoll, A. & Puchta, H., 2014. The Arabidopsis thaliana homolog of the helicase RTEL1 plays multiple roles in preserving genome stability. *Plant Cell*, 26(12), pp.4889–4902. Available at: http://www.ncbi.nlm.nih.gov/pubmed/25516598.

Reeder, S.H. et al., 2016. A Ploidy-Sensitive Mechanism Regulates Aperture Formation on the Arabidopsis Pollen Surface and Guides Localization of the Aperture Factor INP1. *PLoS Genetics*, 12(5), pp.1–24.

Régnier, V. et al., 2005. CENP-A Is Required for Accurate Chromosome Segregation and Sustained Kinetochore Association of BubR1. *MOLECULAR AND CELLULAR BIOLOGY*, 25(10), pp.3967–3981.

Riehs, N. et al., 2008. Arabidopsis SMG7 protein is required for exit from meiosis. *Journal of cell science*, 121, pp.2208–2216.

RILEY, R. & CHAPMAN, V., 1958. Genetic Control of the Cytologically Diploid Behaviour of Hexaploid Wheat. *Nature*, 182(4637), pp.713–715. Available at: http://dx.doi.org/10.1038/182713a0.

Robert, T. et al., 2016. A new light on the meiotic DSB catalytic complex. *Seminars in Cell & Developmental Biology*, 54, pp.165–176. Available at: http://www.sciencedirect.com/science/article/pii/S1084952116300659.

Robert, T. et al., 2016. The TopoVIB-Like protein family is required for meiotic DNA double-strand break formation. *Science*, 351(6276), p.943 LP-949. Available at: http://science.sciencemag.org/content/351/6276/943.abstract.

Robine, N. et al., 2007. Genome-wide redistribution of meiotic double-strand breaks in Saccharomyces cerevisiae. *Molecular and cellular biology*, 27(5), pp.1868–80. Available at: http://mcb.asm.org/cgi/doi/10.1128/MCB.02063-06%5Cnhttp://www.pubmedcentral.nih.gov/articlerender.fcgi?artid=1820458&tool=pmcentrez&rendertype=abstract.

Roeder, G.S. & Bailis, J.M., 2000. The pachytene checkpoint. *Trends in Genetics*, 16(9), pp.395–403. Available at: http://dx.doi.org/10.1016/S0168-9525(00)02080-1.

Rogers, J.M. et al., 2015. Context influences on TALE-DNA binding revealed by quantitative profiling. *Nature communications*, 6(May), p.7440. Available at: http://www.nature.com/ncomms/2015/150611/ncomms8440/abs/ncomms8440.html.

Ronceret, A. & Vielle-Calzada, J.-P., 2015. Meiosis, unreduced gametes, and parthenogenesis: implications for engineering clonal seed formation in crops. *Plant Reproduction*, pp.91–102. Available at: http://link.springer.com/10.1007/s00497-015-0262-6.

Ross, K.J., Fransz, P. & Jones, G.H., 1996. A light microscopic atlas of meiosis in Arabidopsis thaliana. *Chromosome research : an international journal on the molecular, supramolecular and evolutionary aspects of chromosome biology*, 4(May), pp.507–516.

Rothenberg, M., Kohli, J. & Ludin, K., 2009. Ctp1 and the MRN-complex are required for endonucleolytic Rec12 removal with release of a single class of oligonucleotides in fission yeast. *PLoS Genetics*, 5(11).

Roy, S., 2014. Maintenance of genome stability in plants: repairing DNA double strand breaks and chromatin structure stability. *Frontiers in plant science*, 5(September), p.487. Available at: http://journal.frontiersin.org/article/10.3389/fpls.2014.00487/abstract.

Salomé, P. et al., 2012. The recombination landscape in Arabidopsis thaliana F 2 populations. *Heredity*, 108(November 2011), pp.447–45595.

Sanchez-moran, E. et al., 2007. ASY1 mediates AtDMC1-dependent interhomolog recombination during meiosis in Arabidopsis. , 1, pp.2220–2233.

Sanchez-Moran, E. et al., 2002. Variation in chiasma frequency among eight accessions of Arabidopsis thaliana. *Genetics*, 162(3), pp.1415–1422.

Schipler, A. & Iliakis, G., 2013. DNA double-strand-break complexity levels and their possible contributions to the probability for error-prone processing and repair pathway choice. *Nucleic Acids Research*, 41(16), pp.7589–7605.

Schubert, V. et al., 2009. Cohesin gene defects may impair sister chromatid alignment and genome stability in Arabidopsis thaliana. *Chromosoma*, 118(5), pp.591–605.

Séguéla-Arnaud, M. et al., 2015. Multiple mechanisms limit meiotic crossovers: TOP3α and two BLM homologs antagonize crossovers in parallel to FANCM. *Proceedings of the National Academy of Sciences of the United States of America*, 112(15), pp.4713–8. Available at: http://www.ncbi.nlm.nih.gov/pubmed/25825745%5Cnhttp://www.pubmedcentral.nih.gov/articlerender.fcgi?artid=PMC4403193.

Shen, Y. et al., 2012. ZIP4 in homologous chromosome synapsis and crossover formation in rice meiosis. *Journal of cell science*, 125(Pt 11), pp.2581–91. Available at: http://www.ncbi.nlm.nih.gov/pubmed/22393242.

Sheridan, S.D. et al., 2008. A comparative analysis of Dmc1 and Rad51 nucleoprotein filaments. *Nucleic Acids Research*, 36(12), pp.4057–4066.

Shilo, S. et al., 2015. DNA Crossover Motifs Associated with Epigenetic Modifications Delineate Open Chromatin Regions in Arabidopsis. *The Plant Cell*, 27(9), p.tpc.15.00391. Available at: http://www.plantcell.org/content/27/9/2427.short.

Shingu, Y. et al., 2010. A DNA-binding surface of SPO11-1, an Arabidopsis SPO11 orthologue required for normal meiosis. *FEBS Journal*, 277(10), pp.2360–2374.

Shinohara, A., Ogawa, H. & Ogawa, T., 1992. Rad51 protein involved in repair and recombination in S. cerevisiae is a RecA-like protein. *Cell*, 69(3), pp.457–470. Available at: http://dx.doi.org/10.1016/0092-8674(92)90447-K.

Shirley, B.W., Hanley, S. & Goodman, H.M., 1992. Effects of ionizing radiation on a plant genome: analysis of two Arabidopsis transparent testa mutations. *Plant Cell*, 4(3), pp.333–347.

Siaud, N. et al., 2004. Brca2 is involved in meiosis in Arabidopsis thaliana as suggested by its interaction with Dmc1. *The EMBO journal*, 23(6), pp.1392–401. Available at: http://www.pubmedcentral.nih.gov/articlerender.fcgi?artid=381417&tool=pmcentrez&rendertype=abstract [Accessed February 24, 2014].

Siddiqi, I. et al., 2000. The dyad gene is required for progression through female meiosis in Arabidopsis. *Development (Cambridge, England)*, 127(1), pp.197–207.

Smagulova, F. et al., 2011. Genome-wide analysis reveals novel molecular features of mouse recombination hotspots. *Nature*, 472(7343), pp.375–378. Available at: http://dx.doi.org/10.1038/nature09869.

Smith, J. et al., 2000. Requirements for double-strand cleavage by chimeric restriction enzymes with zinc finger DNA-recognition domains. , 28(17), pp.3361–3369.

Smith, J.M. & Maynard-Smith, J., 1978. *The evolution of sex*, Cambridge Univ Press.

Smyth, D.R., Bowman, J.L. & Meyerowitz, E.M., 1990. Early flower development in Arabidopsis. *Plant Cell*, 2(8), pp.755–767. Available at: http://www.ncbi.nlm.nih.gov/pubmed/2152125.

Sommermeyer, V. et al., 2013. Spp1, a Member of the Set1 Complex, Promotes Meiotic DSB Formation in Promoters by Tethering Histone H3K4 Methylation Sites to Chromosome Axes. *Molecular Cell*, 49(1), pp.43–54.

Stacey, N.J. et al., 2006. Arabidopsis SPO11-2 functions with SPO11-1 in meiotic recombination. *The Plant journal : for cell and molecular biology*, 48(2), pp.206–16. Available at: http://www.ncbi.nlm.nih.gov/pubmed/17018031 [Accessed May 21, 2014].

Stern, B. & Nurse, P., 1996. A quantitative model for the cdc2 control of S phase and mitosis in fission yeast. *Trends in Genetics*, 12(9), pp.345–350.

Sternberg, S.H. et al., 2014. DNA interrogation by the CRISPR RNA-guided endonuclease Cas9. *Nature*, 507(7490), pp.62–67. Available at: http://www.ncbi.nlm.nih.gov/pubmed/24476820%5Cnhttp://www.nature.com/nature/journal/v507/n7490/pdf/nature13011.pdf.

Stoop-Myer, C. & Amon, A., 1999. Meiosis: Rec8 is the reason for cohesion. *Nature cell biology*, 1(September), pp.E125–E127.

Storlazzi, A. et al., 2003. Meiotic double-strand breaks at the interface of chromosome movement, chromosome remodeling, and reductional division. *Genes and Development*, 17(21), pp.2675–2687.

De Storme, N. & Geelen, D., 2013. Sexual polyploidization in plants - cytological mechanisms and molecular regulation. *New Phytologist*, 198(3), pp.670–684.

De Storme, N. & Geelen, D., 2011. The Arabidopsis mutant jason produces unreduced first division restitution male gametes through a parallel/fused spindle mechanism in meiosis II. *Plant physiology*, 155(3), pp.1403–15. Available at: http://www.pubmedcentral.nih.gov/articlerender.fcgi?artid=3046594&tool=pmcentrez&rendertype=abstract [Accessed August 28, 2014].

Stronghill, P.E. & Hasenkampf, C.A., 2007. Analysis of substage associations in prophase I of meiosis in floral buds of wild-type Arabidopsis thaliana (Brassicaceae). *American Journal of Botany*, 94(12), pp.2063–2067.

Sturtevant, A.H., 1915. The behavior of the chromosomes as studied through linkage. *Zeitschrift f?? r Induktive Abstammungs- und Vererbungslehre*, 13(1), pp.234–287.

Sugimoto-Shirasu, K. et al., 2002. DNA topoisomerase VI is essential for endoreduplication in Arabidopsis. *Current Biology*, 12(20), pp.1782–1786.

Sullivan, K.F., Hechenberger, M. & Masri, K., 1994. Human CENP-A contains a histone H3 related histone fold domain that is required for targeting to the centromere. *The Journal of cell biology*, 127(3), pp.581–92. Available at: http://www.ncbi.nlm.nih.gov/pubmed/7962047 [Accessed August 25, 2016].

Sun, H., Treco, D. & Szostak, J.W., 1991. Extensive 3'-overhanging, single-stranded DNA associated with the meiosis-specific double-strand breaks at the ARG4 recombination initiation site. *Cell*, 64(6), pp.1155–61. Available at: http://www.ncbi.nlm.nih.gov/pubmed/2004421 [Accessed August 31, 2016].

Szczepek, M. et al., 2007. Structure-based redesign of the dimerization interface reduces the toxicity of zinc-finger nucleases. *Nature biotechnology*, 25(7), pp.786–93. Available at: http://www.ncbi.nlm.nih.gov/pubmed/17603476.

Szostak, J.W. et al., 1983. The double-strand-break repair model for recombination. *Cell*, 33(1), pp.25–35.

Tan, E.H. et al., 2015. Catastrophic chromosomal restructuring during genome elimination in plants. *eLife*, 4, p.e06516. Available at: http://elifesciences.org/content/early/2015/05/15/eLife.06516.abstract.

Thompson, J.D., 1995. Tansley Review No . 78 Gametes with the somatic chromosome number : mechanisms of their formation and role in the evolution of autopolyploid plants AND. , (78), pp.1–22.

Uanschou, C. et al., 2007. A novel plant gene essential for meiosis is related to the human CtIP and the yeast COM1/SAE2 gene. *The EMBO journal*, 26(24), pp.5061–70. Available at: http://www.pubmedcentral.nih.gov/articlerender.fcgi?artid=2140101&tool=pmcentrez&rendertype=abstract [Accessed July 14, 2014].

Uanschou, C. et al., 2013. Sufficient amounts of functional HOP2/MND1 complex promote interhomolog DNA repair but are dispensable for intersister DNA repair during meiosis in Arabidopsis. *Plant Cell*, 25(12), pp.4924–4940. Available at: http://www.ncbi.nlm.nih.gov/pubmed/24363313.

Vad-Nielsen, J. et al., 2016. Golden Gate Assembly of CRISPR gRNA expression array for simultaneously targeting multiple genes. *Cellular and Molecular Life Sciences*, 73(22), pp.4315–4325.

Vandepoele, K. et al., 2002. Genome-wide analysis of core cell cycle genes in Arabidopsis. *Plant Cell*, 14(4), pp.903–916. Available at: http://www.ncbi.nlm.nih.gov/entrez/query.fcgi?cmd=Retrieve&db=PubMed&dopt=Citation&list_uids=11971144.

Vecchiarelli, A.G., Hwang, L.C. & Mizuuchi, K., 2013. Cell-free study of F plasmid partition provides evidence for cargo transport by a diffusion-ratchet mechanism. *Proc Natl Acad Sci U S A*, 110(15), pp.E1390-7. Available at: http://www.ncbi.nlm.nih.gov/pubmed/23479605.

Venters, B.J. & Pugh, B.F., 2010. How eukaryotic genes are transcribed. *Critical Review*, 44(Pol II), pp.117–141.

Villeneuve, A.M. & Hillers, K.J., 2001. Whence Meiosis ? Minireview. , 106, pp.647–650.

Voelkel-Meiman, K. et al., 2015. Separable Crossover-Promoting and Crossover-Constraining Aspects of Zip1 Activity during Budding Yeast Meiosis. *PLOS Genetics*, 11(6), p.e1005335. Available at: http://dx.plos.org/10.1371/journal.pgen.1005335.

Vrielynck, N. et al., 2016. A DNA topoisomerase VI–like complex initiates meiotic recombination. *Science*, 351(6276), p.939 LP-943. Available at: http://science.sciencemag.org/content/351/6276/939.abstract.

Wah, D.A. et al., 1997. Structure of the multimodular endonuclease FokI bound to DNA. *Nature*, 388(6637), pp.97–100. Available at: http://www.ncbi.nlm.nih.gov/pubmed/9214510%5Cnhttp://www.nature.com/nature/journal/v388/n6637/pdf/388097a0.pdf.

Wang, G. et al., 2004. Genome-Wide Analysis of the Cyclin Family in Arabidopsis and Comparative Phylogenetic Analysis of Plant Cyclin-Like Proteins 1 [w]. , 135(June), pp.1084–1099.

Wang, K. et al., 2009. MER3 is required for normal meiotic crossover formation, but not for presynaptic alignment in rice. *Journal of cell science*, 122(Pt 12), pp.2055–63. Available at: http://www.ncbi.nlm.nih.gov/pubmed/19470578.

Wang, K. et al., 2012. The role of rice HEI10 in the formation of meiotic crossovers. *PLoS Genetics*, 8(7).

Wang, M. et al., 2011. OsSGO1 maintains synaptonemal complex stabilization in addition to protecting centromeric cohesion during rice meiosis. *Plant Journal*, 67(4), pp.583–594.

Wang, T.-F., Kleckner, N. & Hunter, N., 1999. Functional specificity of MutL homologs in yeast: Evidence for three Mlh1-based heterocomplexes with distinct roles during meiosis in recombination and mismatch correction. *Proceedings of the National Academy of Sciences*, 96, pp.13914–13919. Available at: http://www.pnas.org/content/96/24/13914.abstract.

Wang, Y. et al., 2004. Progression through meiosis I and meiosis II in Arabidopsis anthers is regulated by an A-type cyclin predominately expressed in prophase I. *Plant physiology*, 136(4), pp.4127–35. Available at: http://www.pubmedcentral.nih.gov/articlerender.fcgi?artid=535843&tool=pmcentrez&rendertype=abstract.

Watanabe, Y., 2012. Geometry and force behind kinetochore orientation: lessons from meiosis. *Nat Rev Mol Cell Biol*, 13(6), pp.370–382. Available at: http://dx.doi.org/10.1038/nrm3349.

Watanabe, Y. & Nurse, P., 1999. Cohesin Rec8 is required for reductional chromosome segregation at meiosis. *Nature*, 400(6743), pp.461–4. Available at: http://dx.doi.org/10.1038/22774.

Watts, A., Kumar, V. & Bhat, S.R., 2016. Centromeric histone H3 protein: from basic study to plant breeding applications. *Journal of Plant Biochemistry and Biotechnology*. Available at: http://link.springer.com/10.1007/s13562-016-0368-4.

Weigel, D. & Mott, R., 2009. The 1001 genomes project for Arabidopsis thaliana. *Genome biology*, 10(5), p.107. Available at: http://genomebiology.com/2009/10/5/107.

Weismann, A., 1893. *The Germ-Plasm: A Theory of Heredity, Translated by W. Newton Parker and Harriet Rönnfeldt*, Elibron. com.

Wijeratne, A.J. et al., 2005. The Arabidopsis thaliana PARTING DANCERS Gene Encoding a Novel Protein Is Required for Normal Meiotic Homologous Recombination. *Genetics*, 125(2), pp.351–369.

Wijnker, E. et al., 2013. The genomic landscape of meiotic crossovers and gene conversions in Arabidopsis thaliana. *eLife*, 2013(2), pp.1–22.

Wijnker, E. & Schnittger, A., 2013a. Control of the meiotic cell division program in plants. *Plant Reproduction*, 26(3), pp.143–158. Available at: http://link.springer.com/10.1007/s00497-013-0223-x [Accessed August 24, 2016].

Wijnker, E. & Schnittger, A., 2013b. Control of the meiotic cell division program in plants. *Plant Reproduction*, 26(3), pp.143–158.

Wijnker, E. & Schnittger, A., 2013c. Control of the meiotic cell division program in plants. *Plant Reproduction*, 26(3), pp.143–158.

Wold, M.S., 1997. Replication protein A: A Heterotrimeric, Single-Stranded DNA-Binding Protein Required for Eukaryotic DNA Metabolism. *Annual Review of Biochemistry*, 66, pp.61–92.

Wu, S. et al., 2010. A conditional mutation in Arabidopsis thaliana separase induces chromosome non-disjunction, aberrant morphogenesis and cyclin B1;1 stability. *Development (Cambridge, England)*, 137, pp.953–961.

Xu, Z. et al., 2010. Structure and function of the PP2A-shugoshin interaction Zheng. *Structure*, 35(4), pp.426–441.

Yandeau-Nelson, M.D., Nikolau, B.J. & Schnable, P.S., 2006. Effects of trans-acting genetic modifiers on meiotic recombination across the a1-sh2 interval of maize. *Genetics*, 174(1), pp.101–112.

Yang, X. et al., 2009. Arabidopsis separase functions beyond the removal of sister chromatid cohesion during meiosis. *Plant Physiol*, 151(1), pp.323–333. Available at: http://www.ncbi.nlm.nih.gov/pubmed/19592426.

Yang, X. et al., 2011. The radially swollen 4 separase mutation of arabidopsis thaliana blocks chromosome disjunction and disrupts the radial microtubule system in meiocytes. *PLoS ONE*, 6(4).

Yao, Y. & Dai, W., 2012. Shugoshins function as a guardian for chromosomal stability in nuclear division. *Cell Cycle*, 11(14), pp.2631–2642.

Yelina, N.E. et al., 2012. Epigenetic remodeling of meiotic crossover frequency in Arabidopsis thaliana DNA methyltransferase mutants. *PLoS genetics*, 8(8), p.e1002844. Available at: http://www.pubmedcentral.nih.gov/articlerender.fcgi?artid=3410864&tool=pmcentrez&rendertype=abstract [Accessed May 23, 2014].

Yokobayashi, S., Yamamoto, M. & Watanabe, Y., 2003. Cohesins determine the attachment manner of kinetochores to spindle microtubules at meiosis I in fission yeast. *Molecular and cellular biology*, 23(11), pp.3965–73. Available at: http://www.pubmedcentral.nih.gov/articlerender.fcgi?artid=155229&tool=pmcentrez&rendertype=abstract.

Zakharyevich, K. et al., 2012. Delineation of joint molecule resolution pathways in meiosis identifies a crossover-specific resolvase. *Cell*, 149(2), pp.334–347. Available at: http://dx.doi.org/10.1016/j.cell.2012.03.023.

Zamariola, L. et al., 2014. SHUGOSHINs and PATRONUS protect meiotic centromere cohesion in Arabidopsis thaliana. *Plant Journal*, 77(5), pp.782–794.

Zhang, C. et al., 2012. The Arabidopsis thaliana DSB formation (AtDFO) gene is required for meiotic double-strand break formation. *The Plant journal : for cell and molecular biology*, 72(2), pp.271–81. Available at: http://www.ncbi.nlm.nih.gov/pubmed/22694475 [Accessed May 22, 2014].

Zhang, F. et al., 2010. High frequency targeted mutagenesis in Arabidopsis thaliana using zinc fi nger nucleases. *Proceedings of the National Academy of Sciences of the United States of America*, 107, pp.12028–12033.

Zhang, L. et al., 2014. Crossover Patterning by the Beam-Film Model: Analysis and Implications. *PLoS Genetics*, 10(1).

Zhang, Y. et al., 2013. Transcription activator-like effector nucleases enable efficient plant genome engineering. *Plant physiology*, 161(1), pp.20–7. Available at: http://www.pubmedcentral.nih.gov/articlerender.fcgi?artid=3532252&tool=pmcentrez&rendertype=abstract [Accessed January 22, 2014].